

Liu, Yi-Chia (2014) Understanding chronic inflammatory diseases in the human lung: the cystic fibrosis and idiopathic pulmonary fibrosis paradigms. PhD thesis, University of Nottingham.

**Access from the University of Nottingham repository:**

[http://eprints.nottingham.ac.uk/27807/1/LiuYC\\_thesis\\_final.pdf](http://eprints.nottingham.ac.uk/27807/1/LiuYC_thesis_final.pdf)

**Copyright and reuse:**

The Nottingham ePrints service makes this work by researchers of the University of Nottingham available open access under the following conditions.

- Copyright and all moral rights to the version of the paper presented here belong to the individual author(s) and/or other copyright owners.
- To the extent reasonable and practicable the material made available in Nottingham ePrints has been checked for eligibility before being made available.
- Copies of full items can be used for personal research or study, educational, or not-for-profit purposes without prior permission or charge provided that the authors, title and full bibliographic details are credited, a hyperlink and/or URL is given for the original metadata page and the content is not changed in any way.
- Quotations or similar reproductions must be sufficiently acknowledged.

Please see our full end user licence at:

[http://eprints.nottingham.ac.uk/end\\_user\\_agreement.pdf](http://eprints.nottingham.ac.uk/end_user_agreement.pdf)

**A note on versions:**

The version presented here may differ from the published version or from the version of record. If you wish to cite this item you are advised to consult the publisher's version. Please see the repository url above for details on accessing the published version and note that access may require a subscription.

For more information, please contact [eprints@nottingham.ac.uk](mailto:eprints@nottingham.ac.uk)

**UNDERSTANDING CHRONIC INFLAMMATORY  
DISEASES IN THE HUMAN LUNG:  
THE CYSTIC FIBROSIS AND IDIOPATHIC  
PULMONARY FIBROSIS PARADIGMS**

YI-CHIA LIU, MSc.

Thesis submitted to the University of Nottingham for  
the degree of Doctor of Philosophy

DECEMBER 2014

# ABSTRACT

---

Chronic inflammation is a persistent inflammatory condition ultimately leading to tissue destruction. The human lung is constantly exposed to foreign irritants and microbes thus effective immune regulation is essential to maintain lung homeostasis. The chronic infection of the cystic fibrosis (CF) lung with *Pseudomonas aeruginosa* strongly correlates with the decline of pulmonary function and mortality. *Pseudomonas* alkyl-quinolone signal (PQS), generated through the 2-alkyl-4-quinolones (AQs) system, is a diffusible signal for cell-to-cell communication controlling the production of virulence factors in a population density dependent manner. PQS has been detected in the lung of CF patients and the amount was proportionate to *P. aeruginosa* colonisation. PQS molecules have also been demonstrated to inhibit pro-inflammatory signalling. However, how PQS influences the recognition of *P. aeruginosa* by the human lung is unknown. Towards this aim the contribution of PQS to the interaction of *P. aeruginosa* with human bronchial epithelial cells (HBECs) was characterised using a PQS-deficient mutant  $\Delta pqsA_L$  in comparison with its isogenic wild type (WT).  $\Delta pqsA_L$  did not produce AQs and pyocyanin; displayed reduced rhamnolipid synthesis and fragile biofilms suggesting an attenuated phenotype. However, the pathogenesis of WT and  $\Delta pqsA_L$  upon infection of HBEC did not differ in bacterial growth, actin degradation, junction protein disruption, and pro-inflammatory activation in HBECs. Further, despite PQS being highly secreted by a CF isolate LESB58, preliminary data showed that LESB58 was less cytotoxic than the laboratory

WT strain. Our results suggest that PQS does not alter *P. aeruginosa* pathogenicity during infection of HBECs.

Idiopathic pulmonary fibrosis (IPF) is a progressive pro-fibrotic disease characterised by heterogeneous pathological patterns caused by scarring that leads to destruction of lung architecture and high mortality. Despite the fact that inflammation is considered secondary to the IPF pathogenesis, emerging evidence suggests that dysregulated immunological events could cause the failure of tissue healing. Systemic immune responses of patients with IPF and age- and sex-matched healthy donors were determined by quantifying cytokines produced by peripheral blood mononuclear cells (PBMCs) upon an array of stimuli. Cytokine production in the cases was also correlated with their survival. The results showed that PBMCs in patients with IPF were less likely to produce IL-17A, IL-10 and IL-13 than healthy controls (IL-17A: OR 0.14, 95% CI 0.003; IL-10: OR 0.3, 95% CI 0.03; IL-13: OR 0.27; 95% CI 0.018). Patients with lower levels of IFN- $\gamma$ , IL-17A, IL-13 production by PBMCs had a four to six-fold increased risk of death (IFN- $\gamma$ : HR 4.31, 95% CI 0.0176; IL-17A: HR 4.60, 95% CI 0.0138; IL-13: HR 6.13, 95% CI 0.0052).

This study contributes to a better understanding of the role of PQS in the pathogenesis of *P. aeruginosa* and identified cytokine production by immune cells as a novel prognosis marker in IPF.



# ACKNOWLEDGEMENT

---

I would like to thank Dr. Luisa Martínez-Pomares for her supervision, advice and continuous support. I would also like to express my gratitude to my co-supervisors Professor Miguel Cámara and Professor Paul Williams in Pseudomonas study; Dr. Andrew Fogarty, Professor Richard Hubbard, and Dr. Vidya Navaratnam in IPF study. I appreciated Dr. Ola Negm and Dr. Paddy Tighe for the protein microarray experiment and Dr. Cynthia Bosquillon for helping with differentiated airway epithelial cell culture. The intellectual discussions with you were the most enjoyable moments during PhD.

Colleagues and friends, Jean Dubern, Sonali Singh, Darryl Jackson, Denise Christie, Matthew Fletcher, Davy Chang, Jeni Lockett, Lee Wheldon, Nigel Holladay, James Lazenby, Alex Tarr, Patrick McClure, Robyn Bates, Ye Chen, Hazel Silistre; clinical scientists and research nurse in the city hospital Helen Bailey, Garry Meakin and Susan Ledger; lab members Tamanna, Farah, Raed, Sirina, Mohammad. This study would not be possible without your support, scientific discussion and laughter.

I would like to dedicate this thesis to my grandfather and my late grandmother, for their unconditional love encourages me to carry on my research. I appreciated my parents for their support that made this PhD study possible. A particular thanks to my partner, your love and humour carried me through the unbearable lightness and madness during my writing of the thesis.

# TABLE OF CONTENTS

---

List of Figures .....	v
List of Tables.....	ix
List of Abbreviations .....	x
1. GENERAL INTRODUCTION.....	1
1.1. HUMAN RESPIRATORY SYSTEM.....	2
1.1.1. Lung structure and function .....	2
1.1.2. The innate immunity in the lung .....	7
1.1.3. The adaptive immunity in the lung .....	18
1.1.4. Pathogenesis of pulmonary inflammatory diseases .....	19
1.2. Cystic fibrosis.....	32
1.2.1. Aetiology and pathophysiology of cystic fibrosis.....	32
1.2.2. Airway inflammation in cystic fibrosis.....	33
1.2.3. Respiratory infections in cystic fibrosis.....	39
1.3. Aims and objectives .....	44
2. GENERATION AND CHARACTERISATION OF A PSEUDOMONAS AERUGINOSA MUTANT DEFICIENT IN ALKYL-QUINOLONE PRODUCTION .....	45
2.1. INTRODUCTION.....	45
2.1.1. Quorum-sensing.....	46
2.1.2. Quorum-sensing in <i>Pseudomonas aeruginosa</i> .....	49
2.1.3. The impact of alkyl-quinolones on <i>P. aeruginosa</i> pathogenesis .....	56
2.1.4. Generation of a <i>pqsA</i> mutant in PAO1 Lausanne .....	64
2.2. HYPOTHESIS.....	66
2.3. AIM .....	66
2.4. MATERIALS AND METHODS .....	67
2.4.1. Bacterial strains, plasmids and culture condition.....	67
2.4.2. Generation of a <i>pqsA</i> in-frame deletion mutant in PAO1-L .....	67
2.4.3. Phenotypic characterisation of <i>ΔpqsA<sub>L</sub></i> .....	74
2.5. RESULTS.....	78
2.5.1. Generation of the <i>ΔpqsA<sub>L</sub></i> mutant.....	78
2.5.2. Phenotypic characterisation of <i>ΔpqsA<sub>L</sub></i> in comparison with <i>ΔpqsA<sub>N</sub></i> .....	82
2.6. DISCUSSION .....	91
2.6.1. <i>ΔpqsA<sub>L</sub></i> mutant was compromised in the production of several virulence factors.....	91

2.6.2. Phenotype differences between PAO1-L and PAO1-N might due to the 58 kb deletion in PAO1-N and SNPs in PAO1-N subline.....	93
2.7. SUMMARY .....	97
3. ESTABLISHMENT AND CHARACTERIZATION OF AN in vitro infection model to study the interaction of <i>Pseudomonas aeruginosa</i> with differentiated HUMAN BRONCHIAL EPITHELIAL cells.....	98
3.1. INTRODUCTION.....	98
3.2. HYPOTHESIS.....	104
3.3. AIM .....	104
3.4. MATERIALS AND METHODS .....	105
3.4.1. Calu-3 cell culture and differentiation .....	105
3.4.2. Assessment of Calu-3 cell differentiation.....	106
3.4.3. <i>Pseudomonas aeruginosa</i> culture .....	110
3.4.4. PAO1-L infection of differentiated Calu-3 cells.....	110
3.4.5. Statistical analysis .....	112
3.5. RESULTS.....	113
3.5.1. Characterisation of Calu-3 cells differentiation at air-liquid interface ...	113
3.5.2. Optimisation of <i>P. aeruginosa</i> inoculum.....	123
3.5.3. Assessment of the suitability of differentiated Calu-3 monolayers to model PAO1-L infection.....	130
3.6. DISCUSSION .....	132
3.6.1. Successful generation of differentiated human bronchial epithelium cultures at air-liquid interface .....	132
3.6.2. Variation of <i>P. aeruginosa</i> inoculum occurred at high cell density.....	135
3.7. SUMMARY .....	138
4. The impact of alkyl-quinolone quorum sensing on the interaction of <i>Pseudomonas aeruginosa</i> with bronchial epithelium and phagocytes .....	139
4.1. INTRODUCTION.....	139
4.2. HYPOTHESIS.....	143
4.3. AIM .....	143
4.4. MATERIALS AND METHODS .....	144
4.4.1. Bacterial strains and culture conditions .....	144
4.4.2. Infection of differentiated Calu-3 cells with <i>P. aeruginosa</i> .....	144
4.4.3. Assessment of the expression of proinflammatory cytokines and chemokines by diffCalu-3 cells in response to <i>P. aeruginosa</i> infection.....	145
4.4.4. Immunofluorescence staining and confocal laser scanning microscopy	151
4.4.5. Microarray analysis of signalling pathways activation .....	151

4.4.6. Cytotoxicity.....	152
4.4.7. Measurement of reactive oxygen species (ROS) production by neutrophils in response to PAO1-L.....	153
4.4.8. Extraction of quorum-sensing signaling molecules and LC-MS analysis .....	155
4.4.9. In vitro infection of macrophages with PAO1-L WT and $\Delta pqsA_L$ .....	156
4.4.10. Statistical analysis .....	158
4.5. RESULTS.....	159
4.5.1. Effect of PQS on <i>P. aeruginosa</i> colonisation, invasion and growth on differentiated Calu-3 cells.....	159
4.5.2. Induction of pro-inflammatory cytokines in diffCalu-3 cells in response to PAO1-L WT and $\Delta pqsA_L$ .....	168
4.5.3. Similar activation of innate signalling pathways in diffCalu-3 cells upon <i>P.</i> <i>aeruginosa</i> PAO1-L WT and $\Delta pqsA_L$ infection .....	176
4.5.4. Assessment of <i>P. aeruginosa</i> -mediated cytotoxicity in response to WT and $\Delta pqsA_L$ infection.....	179
4.5.5. WT and $\Delta pqsA_L$ disrupted tight junctions and abrogated barrier function .....	183
4.5.6. Analysis of the interaction of WT and $\Delta pqsA_L$ with differentiated Calu-3 cells at low MOI.....	185
4.5.7. Analysis of the potential role of PQS in modulating ROS production by human neutrophils in response to PAO1-L.....	188
4.6. DISCUSSION .....	193
4.7. SUMMARY .....	206
5. THE INTERACTION BETWEEN PSEUDOMONAS AERUGINOSA STRAIN LESB58 AND HUMAN BRONCHIAL EPITHELIUM.....	207
5.1. INTRODUCTION.....	207
5.2. HYPOTHESIS.....	210
5.3. AIM .....	210
5.4. MATERIALS AND METHODS .....	211
5.4.1. Phenotypic characterisation of LESB58 .....	211
5.4.2. Infection of diffCalu-3 cells with PAO1-L and LESB58.....	211
5.4.3. Assessment of pathogenesis of LESB58 on diffCalu-3 cells in comparison with PAO1-L.....	211
5.5. RESULTS.....	212
5.5.1. Phenotypic characterisation of LESB58 in comparison with PAO1 laboratory strains.....	212

5.5.2. Reduced translocation of LESB58 upon infection of diffCalu-3 cells....	215
5.5.3. LESB58 induced a lower pro-inflammatory response upon infection of diffCalu-3 cells compared to PAO1-L .....	217
5.5.4. LESB58 was less cytotoxic than PAO1-L upon infection of diffCalu-3 cells .....	219
5.6. DISCUSSION .....	222
5.7. SUMMARY .....	229
6. SYSTEMIC IMMUNE RESPONSES IN IDIOPATHIC PULMONARY FIBROSIS.....	230
6.1. INTRODUCTION.....	230
6.1.1. Pathogenesis and molecular mechanisms of IPF .....	231
6.1.2. The immunology of IPF.....	234
6.1.3. Rationale of experimental design.....	235
6.2. HYPOTHESIS.....	238
6.3. AIM .....	238
6.4. MATERIALS AND METHODS .....	239
6.4.1. Study design.....	239
6.4.2. Study populations.....	239
6.4.3. Determination the levels of IFN- $\gamma$ , IL-17A, IL-10, and IL-13 in peripheral blood mononuclear cells (PBMCs) supernatant by multiplex immunoassays ..	239
6.4.4. Statistical analysis .....	241
6.5. RESULTS.....	243
6.5.1. Optimisation of PBMCs stimulation.....	243
6.5.2. Comparison of the cytokine profile between IPF patients and healthy donors.....	244
6.5.3. Case-control study: the association between IPF and the cytokine production .....	249
6.5.4. Assessing the association between IPF and the production of IL-10 and IL-13 in PBMCs upon PMA and PHA stimulation in the total population (66 patients and 66 healthy controls) .....	258
6.5.5. Correlation between the levels of cytokine production and survival in the IPF cohort .....	264
6.6. DISCUSSION .....	269
6.7. SUMMARY .....	276
7. GENERAL DISCUSSION AND FUTURE PERSPECTIVES .....	277
REFERENCES.....	292

# LIST OF FIGURES

---

Figure 1.1	Structure of the human lung. ....	3
Figure 1.2	Cellular composition in the human lower and distal respiratory tract.....	6
Figure 1.3	Epithelial cell junctions. ....	8
Figure 1.4	Schematic view of innate immunity in the respiratory epithelial cells.....	17
Figure 1.5	Inflammatory cascade of asthma and COPD.....	27
Figure 1.6	Proposed pro-inflammatory and pro-fibrotic cascade in the initiation and maintenance of pulmonary fibrosis. ....	31
Figure 1.7	Comparison of airway surface liquid topography between normal and CF bronchial epithelial cells.....	35
Figure 1.8	Proposed model of CFTR structure.....	36
Figure 2.1	General mechanism of quorum sensing autoinduction in Gram-negative bacteria. ....	48
Figure 2.2	Interactions between the two AHL QS systems in <i>P. aeruginosa</i> and their regulation in virulence.....	50
Figure 2.3	Biosynthesis, autoinduction, and virulence regulation by alkyl-quinolones in <i>P. aeruginosa</i> . ....	54
Figure 2.4	Integration of quorum-sensing networks in <i>P. aeruginosa</i> . ....	55
Figure 2.5	Strategy to generate a <i>pqsA</i> in-frame deletion in PAO1-L.....	73
Figure 2.6	Nucleotide sequencing confirmed that an in-frame deletion was generated by joining first 12 nucleotides and the last 15 nucleotides of the <i>pqsA</i> gene. ....	79
Figure 2.7	$\Delta pqsA_L$ mutants were deficient in the production of pyocyanin and alkyl-quinolones. ....	81
Figure 2.8	Similar growth of <i>P. aeruginosa</i> PAO1-L (WT) and $\Delta pqsA_L$ in LB and X-vivo 15 media under aerated conditions.....	83
Figure 2.9	Similar growth of <i>P. aeruginosa</i> PAO1-L, PAO1-N and their isogenic <i>pqsA</i> mutants in LB and X-vivo 15 under static conditions.....	83
Figure 2.10	Mutation in <i>pqsA</i> rendered PAO1-L AQ-negative.....	85
Figure 2.11	Lack of pyocyanin synthesis upon mutation of <i>pqsA</i> in PAO1-L and PAO1-N.....	86
Figure 2.12	The <i>pqsA</i> mutation decreased rhamnolipids production in $\Delta pqsA_L$ but not in PAO1-N. ....	88
Figure 2.13	Motility was increased in $\Delta pqsA_L$ and $\Delta pqsA_N$ mutants compared with their WT parental strains. ....	89

Figure 2.14 $\Delta pqsA_L$ and $\Delta pqsA_N$ formed fragile and immature biofilms compared with PAO1-L and PAO1-N. ....	90
Figure 3.1 Schematic of the in vitro respiratory epithelium model for <i>P. aeruginosa</i> infection.....	103
Figure 3.2 Morphology of undifferentiated Calu-3 cells at confluency in a T-75 flask. ....	114
Figure 3.3 Detection of cilia and mucin expression in one week-old Calu-3 cells cultured in DMEM at ALI.....	116
Figure 3.4 Calu-3 cells grown on polyester inserts for up to 21 days differentiated into a pseudostratified monolayer and expressed mucins at the apical surface. ....	117
Figure 3.6 Calu-3 cells at ALI for 21 days exhibited microvilli at their apical surface. ....	119
Figure 3.5 Extensive mucin accumulation in Calu-3 cells when seeded on transwell inserts without coating. ....	119
Figure 3.7 Transepithelial electrical resistance of Calu-3 cells ALI cultures in both in DMEM and MEM. ....	121
Figure 3.8 Localisation of the tight junction protein ZO-1 in Calu-3 cells cultured in ALI for 21 days. ....	122
Figure 3.9 <i>P. aeruginosa</i> PAO1-L growth rate was comparable in LB, DMEM and MEM but the final cell density was lower in MEM.....	125
Figure 3.10 Lack of correlation between experimental and expected CFU in high density inocula. ....	127
Figure 3.11 Lack of correlation between actual and expected CFU in high density inocula for WT PAO1-L and $\Delta pqsA_L$ .....	128
Figure 3.12 Reliable bacterial counting was achieved when inocula for MOI 50 were prepared.....	129
Figure 3.13 WT and $\Delta pqsA_L$ inocula were comparable and achieved consistency at MOI 50.....	129
Figure 3.14 Detection of PAO1-L at the bottom chamber of differentiated Calu-3 cultures at 6 hpi. ....	131
Figure 4.1 Visualisation of differentiated Calu-3 cells infected with PAO1-L WT and $\Delta pqsA_L$ by scanning electron microscopy. ....	161
Figure 4.2 Invasion of WT and $\Delta pqsA_L$ in differentiated Calu-3 cells occurred at 3 hpi whilst epithelium maintained its integrity. ....	165
Figure 4.3 Substantial accumulation of WT and $\Delta pqsA_L$ associated to extracellular DNA in infected Calu-3 cells cultures. ....	166

Figure 4.4 The majority of PAO1-L WT and $\Delta pqsA_L$ remained cell-associated at 6 hpi during infection of diffCalu-3. ....	167
Figure 4.5 Consistent $C_q$ values of reference genes in uninfected diffCalu-3 cells in two independent experiments. ....	170
Figure 4.6 Induction of pro-inflammatory cytokines, GM-CSF, IL-8, TNF- $\alpha$ , IL-17c, and IL-6 in Calu-3 cells in response to WT and $\Delta pqsA_L$ . ....	172
Figure 4.7 Infection on Calu-3 cells with WT and $\Delta pqsA_L$ induced the secretion of proinflammatory cytokines at 2 and 6 hpi. ....	175
Figure 4.8 Low levels of GM-CSF secretion was not due to the accumulation in the cytoplasmic compartment. ....	176
Figure 4.9 A small induction of mitogen activated protein kinase, NF- $\kappa$ B, serine/threonine AKT and IRF7 signaling pathways in Calu-3 cells in response to WT and $\Delta pqsA_L$ infection. ....	178
Figure 4.10 Actin normalisation is essential for interpretation of signaling data. ....	178
Figure 4.11 WT and $\Delta pqsA_L$ induced actin degradation on differentiated Calu-3 cells. ....	181
Figure 4.12 <i>P. aeruginosa</i> PAO1-L WT and $\Delta pqsA_L$ induced actin and HSP90 degradation, but did not affect NUP98 levels. ....	181
Figure 4.13 Calu-3 cell death during the course of infection with WT and $\Delta pqsA_L$ . ....	183
Figure 4.14 PQS was not essential for PAO1-L on epithelial barrier destruction and tight junction disruption. ....	184
Figure 4.15 Both WT and $\Delta pqsA_L$ breached the epithelial barrier at 6 hpi at MOI 0.5 but the epithelium restrained PA growth till 12 hpi. ....	187
Figure 4.16 Effect of PQS on ROS production by human neutrophils. ....	190
Figure 4.17 Donor dependent variability in ROS production by human neutrophils. ....	192
Figure 4.18 PQS, HHQ and QNO were detectable in MEM only and the basal medium from Calu-3 cells infected with WT, but not $\Delta pqsA_L$ . ....	196
Figure 4.19 WT and $\Delta pqsA_L$ produced comparable amounts of C4-HSL and 3-oxo-C12-HSL in MEM and in the basal medium of diff Calu-3 cells after infection. ....	196
Figure 4.20 Equivalent growth of WT and $\Delta pqsA_L$ on M-CSF primed macrophages. ....	197
Figure 4.21 TLR protein expression in bronchial airway epithelial cells. ....	203
Figure 5.1 LESB58 produced high amounts of PQS and pyocyanin compared to PAO1 strains, despite reaching lower cell density in culture. ....	213
Figure 5.2 LESB58 produces low levels of rhamnolipids and is non-motile. ....	214



Figure 5.3	LESB58 remained mainly cell-associated upon infection of diffCalu-3 cells. ....	216
Figure 5.4	Induction of pro-inflammatory cytokines and chemokines by diffCalu-3 cells upon Wt and LESB58 infection. ....	218
Figure 5.5	Calu-3 cells actin, HSP90 and NUP98 remained intact upon LESB58 infection at 6 hpi. ....	220
Figure 5.6	The barrier function of Calu-3 cells was maintained after LESB58 infection compared to PAO1-L infection. ....	221
Figure 6.1	Dysregulation in wound healing contributes to pulmonary fibrosis. ....	233
Figure 6.2	The levels of cytokines, IFN- $\gamma$ , IL-17A, IL-10 and IL-13 secreted by PBMCs in response to PPD, HDM and PAO1-L lysates were mostly dose dependent. ....	247
Figure 6.3	Levels of IFN- $\gamma$ , IL-17A, IL-10 and IL-13 in PBMCs from healthy donors (HD) and IPF patients (IPF) in response to a panel of stimuli. ....	248
Figure 6.4	Summary of OR assessing the association between IPF and IFN- $\gamma$ production in PBMCs in response to a panel of stimuli. ....	252
Figure 6.5	Summary of OR assessing the association between IPF and IL-17A production in PBMCs in response to a panel of stimuli. ....	254
Figure 6.6	Summary of OR assessing the association between IPF and IL-10 production by PBMCs in response to a panel of stimuli. ....	255
Figure 6.7	Summary of OR assessing the association between IPF and IL-13 production in PBMCs in response to a panel of stimuli. ....	257
Figure 6.8	Mean of the IL-10 and IL-13 production in PBMCs from 68 IPF patients (IPF) upon PMA stimulation was higher than that of 66 healthy donors (HD) and the trend of lower IL-10 production in PBMCs of IPF patients. ....	259
Figure 6.9	A summary plot illustrates the association between IPF and the induced production of IL-10 in response to PMA and PHA from the whole population in this study. ....	262
Figure 6.10	A summary of odds ratios quantifying the association between IPF and IL-13 production in response to a panel of stimulation. ....	263
Figure 6.11	Survival plot of IPF patients with high and low levels of IL-17A in PBMCs upon PMA, SEB, HDM and PA extract stimulation. ....	266
Figure 6.12	Survival of IPF patients with high and low levels of IL-13 in PBMCs upon HDM and PA extract stimulation. ....	267
Figure 6.13	Survival of IPF patients with high and low levels of IFN- $\gamma$ in PBMCs upon SEB, HDM and PA extract stimulation. ....	268

# LIST OF TABLES

---

Table 2.1	Bacterial strains and plasmids used in this study.....	68
Table 2.2	Primer sequences for <i>ΔpqsA<sub>L</sub></i> mutant generation.....	71
Table 2.3	<i>pqsA</i> gene nucleotide sequence along with its 800 bp upstream and downstream sequence.....	72
Table 2.4	Phenotype summary of PAO1-L, PAO1-N and their correspondent <i>pqsA</i> mutants. ....	93
Table 3.1	Summary of morphological characteristics and barrier function of commonly used in vitro human bronchial epithelial cell models.....	103
Table 4.1	Primers used for qPCR .....	148
Table 4.2	Summary of the averages of bacterial colony forming units of inocula, PA only controls, transmigrated and cell-associated bacteria at 6 hpi. ....	167
Table 4.3	Brief description of references genes tested using qPCR .....	169
Table 4.4	HPRT C <sub>T</sub> values in diffCalu-3 cells collected after exposure to <i>P. aeruginosa</i> infection at MOI 50 for 2 hpi and uninfected control .....	170
Table 5.1	Summary of the average number of bacteria ± standard deviation for Wt and LESB58 in each compartment at 6 hpi of diffCalu-3 .....	216
Table 6.1	Significant cytokine production difference between treatments or between the cases and healthy donors .....	245
Table 6.2	Demographic characteristics of controls and IPF patients from the first part of the population in this study .....	251
Table 6.3	The association between IFN-γ secretion and IPF.....	252
Table 6.4	The association between the production of IL-17A and IPF .....	254
Table 6.5	The association between the production of IL-10 and IPF.....	255
Table 6.6	The association between induced production of IL-13 and IPF .....	257
Table 6.7	Demographics containing the whole population of incident cases of IPF and healthy controls in this study.....	261
Table 6.8	The association between PMA and PHA induced production of IL-10 and IPF in the whole population in this study.....	262
Table 6.9	The association between PMA and PHA induced production of IL-13 and IPF in the whole population in this study.....	263
Table 6.10	Significant Cox regression correlations between individual cytokine production and survival in the IPF cohort.....	265
Table 6.11	Summary of ORs with significance differences .....	271

# LIST OF ABBREVIATIONS

---

3-oxo-C12	N-(3-oxo-dodecanoyl)-homoserine lactone
AFU	arbitrary fluorescence unit
AHL	acyl-homoserine lactone
ANOVA	analysis of variance
AQs	2-alkyl-4-quinolones
ASL	air-surface liquid
BMP4	bone morphogenetic protein 4
bp	base pair
C4-HSL	butyl-homoserine lactone
CCL	chemokine (C-C motif) ligand
CF	cystic fibrosis
CFTR	cystic fibrosis transmembrane conductance regulator
CFU	colony forming unit
COPD	chronic obstructive pulmonary disease
C <sub>q</sub>	quantification cycle
DAPI	4',6-diamidino-2-phenylindole hydrochloride
diffCalu-3	differentiated Calu-3
dLN	draining lymph nodes
DMEM	Dulbecco's modified Eagle's medium (DMEM)/ Nutrient Mixture F-12 Hams (1:1)
EDTA	ethylenediaminetetraacetic acid
EMT	epithelial-mesenchymal transition
ETA	exotoxin A
ER	endoplasmic reticulum
ERK	extracellular-signal-regulated kinase

FCS	foetal calf serum
FITC	fluorescein isothiocyanate
FVC	forced vital capacity
GM-CSF	granulocyte macrophage colony-stimulating factor
GNB2L1	guanine nucleotide-binding protein $\beta$ -peptide 2-like-1
GSH	glutathione
HDM	house dust mite
HHQ	2-heptyl-4(1H)-quinolone
HIP-1	hypoxia-inducible factor 1
HKGs	housekeeping genes
hpi	hour post infection
HPRT	hypoxanthine-guanine phosphoribosyl transferase
HRP	horse-reddish peroxidase
HSP90	heat-shock protein 90
ICOS	inducible T cell co-stimulator
IGHMBP2	immunoglobulin mu binding protein 2
IL	interleukin
ILCs	innate lymphoid cells
ILC2	type 2 innate lymphoid cells
ILD	Interstitial lung disease
IRF	interferon-regulatory factor
ITK	IL2-inducible T-cell kinase
KL-6	Krebs von den lungen-6 antigen
LasB	elastase B
LB broth	Luria-Bertani broth
LCC	liquid covered culture
LCK	lymphocyte-specific protein tyrosine kinase

LC-MS/MS	liquid chromatography mass/mass spectrometry
LDH	lactate dehydrogenase
LESB58	Liverpool epidemic strain B58
LPS	lipopolysaccharide
LTA	lipoteichoic acid
MAPKs	mitogen-activated protein kinases
M-CSF	macrophage colony-stimulating factor
MCP-1	monocyte chemotactic protein-1
MDA5	melanoma differentiation-associated gene 5
MDCK cells	Madin-Darby canine kidney cells
MEM	minimum essential medium $\alpha$ containing GlutaMAX™ I
MIP-1 $\alpha$	macrophage inflammatory protein 1 $\alpha$
miR	microRNA
MOI	multiplicity of infection
NF- $\kappa$ B	nuclear factor kappa-light-chain-enhancer of activated B cells
NUP98	nucleoporin 98kDa
OR	odds ratio
PA	<i>Pseudomonas aeruginosa</i>
PAO1-L	<i>Pseudomonas aeruginosa</i> PAO1 obtained from Lausanne
PAO1-N	<i>Pseudomonas aeruginosa</i> PAO1 obtained from Nottingham
PHA	phytohaemoagglutinin
PI	propidium iodide
PI3K	phosphatidylinositol 3-kinase
PIP <sub>3</sub>	phosphatidylinositol 3,4,5- triphosphate
PMA	12-O-phorbol-myristic-13-acetate
PPD	protein purified derivative from tuberculosis

PQS	Pseudomonas quinolone signal
PQS (molecule)	2-heptyl-3-hydroxy-4(1H)-quinolone
$\Delta$ pqsA <sub>L</sub>	pqsA gene deletion mutant in PAO1 Lausanne subline
$\Delta$ pqsA <sub>N</sub>	pqsA gene deletion mutant in PAO1 Nottingham subline
PRRs	pattern-recognition receptors
QNO	2-heptyl-4-hydroxyquinoline N-oxide
qPCR	quantitative real-time PCR
QS	quorum-sensing
RE	rhamnolipids equivalent
RIG-1	Retinoic acid-inducible gene I
rpm	revolutions per minute
SNP	single nucleotide polymorphism
TEER	transepithelial electrical resistance
TFP	type-IV pili
TLC	total lung capacity
TLco	diffusing capacity calculated from the concentrations of CO inspired and exhaled
TLR	toll-like receptor
TNF- $\alpha$	tumour necrosis factor-alpha
Tregs	regulatory T cells
TSLP	thymic stromal lymphopoietin
UPR	unfolded protein response

# 1. GENERAL INTRODUCTION

---

The lung is a dynamic organ that constitutes one of the largest interfaces between the body and the external environment and is constantly exposed to microorganisms and particulate irritants (Suzuki et al., 2008). In particular the lung epithelium acts as a key orchestrator of the pulmonary immune response. The aim of this study was to extend the understanding of the immune mechanisms of human pulmonary diseases by focusing on two chronic fibrotic diseases: cystic fibrosis (CF) and idiopathic pulmonary fibrosis (IPF). In order to contextualise and justify the present study, this general introduction briefly reviews the main features of the human respiratory system including anatomy, immunology and pathology, and introduces two fibrotic pulmonary diseases: (1) CF focusing on the innate response of airway epithelium upon bacterial infection and (2) IPF when the emphasis will be placed on systemic immune responses and their association with disease.

## **1.1. HUMAN RESPIRATORY SYSTEM**










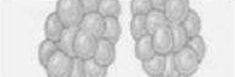
### **1.1.1. Lung structure and function**

Humans have two lungs; a right lung consisting of three lobes and a left lung slightly smaller and consisting of two lobes. The primary function of the lung is gas exchange to obtain O<sub>2</sub> for the use of body cells and to eliminate CO<sub>2</sub> (Sherwood, 2007). The air passes through the nasal, larynx and pharynx down into the conducting zone branching from trachea, bronchi to terminal bronchioles (see structure in Fig. 1.1) where the conditioning process takes place. This conditioning process involves warming and humidifying of incoming air and removal of particulate materials. The respiratory zone, also called lung parenchyma, comprises alveolar air spaces, alveolar epithelium and the pulmonary capillaries where gas exchange occurs (Berube et al., 2010, Ross et al., 2010). The human adult lung has approximately 200 million alveoli with an internal surface area of 75 m<sup>2</sup> hence it is a tremendous platform easily accessed by foreign bodies. For this, the lung has evolved effective innate defense mechanisms that constantly protect airways against bacterial and other types of intrusions (Knowles and Boucher, 2002, Sherwood, 2007).

The wall of bronchi contains five layers: (1) mucosa, which consists in a layer of pseudostratified epithelium that lies on the basement membrane lamina propria; (2) submucosa, a relatively loose connective tissue where glands and adipose tissue are present in the larger bronchi (Fig. 1.2B); (3) muscularis, a continuous layer of smooth muscle in the larger bronchi. Muscle contraction maintains the shape of the airway; (4) cartilage layer and (5) adventica, the



moderately dense connective tissue that connects with adjacent structures, such as pulmonary artery and lung parenchyma.

	Anatomy	Structure	Generation (Z)
Conducting zone		Larynx	N/A
		Trachea	0
		Primary bronchi	1
		Secondary bronchi	2
		Tertiary bronchi	3
		Small bronchi	4
		Bronchioles	5
		Terminal bronchioles	6-16
Respiratory zone		Respiratory bronchioles	17-19
		Alveolar sacs	23

**Figure 1.1 Structure of the human lung.**

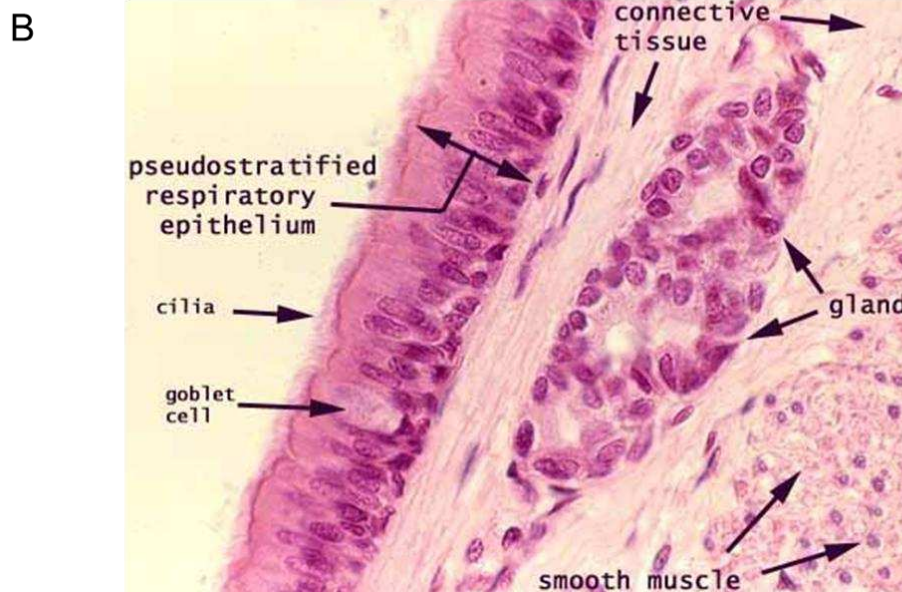
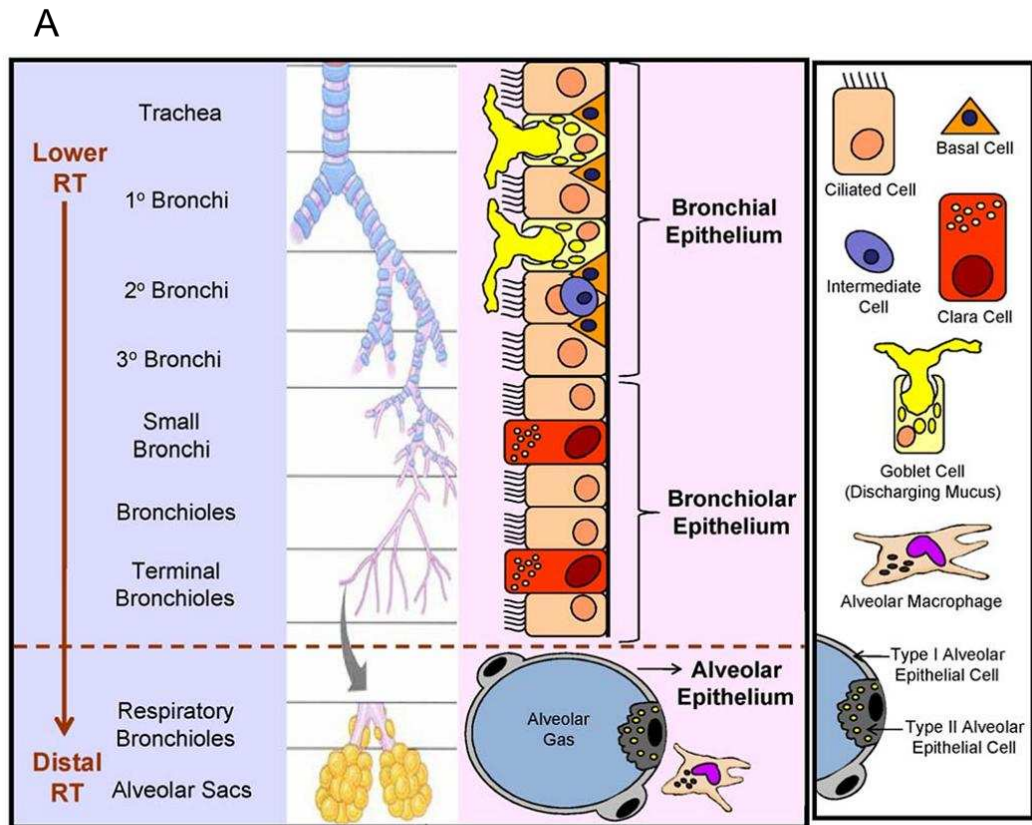
Schematic presentation of the respiratory branches in the human lung. The conducting zone consists of the trachea, bronchi, and terminal bronchioles. In this area air passes through but no gaseous exchange takes place. The respiratory zone consists of respiratory bronchioles, the alveolar ducts and alveolar sacs where gas exchange occurs between the lung and pulmonary capillaries. From the larynx, the branching starts dividing from the trachea into two primary bronchi and up to 23 generations (Z) to the alveolar sacs. Figure adopted from (Berube et al., 2010).

The bronchial epithelium is approximately 25-40  $\mu\text{m}$  thick and is made up of various differentiated epithelial cell types including ciliated cells, mucin-

producing goblet cells, secretory club cells (Clara cells were renamed as club cells in 2013 (Irwin et al., 2013)) and basal cells that form a heterogeneous pseudostratified columnar epithelium (Fig. 1.2). The ciliated columnar cell is the most abundant cell type in the bronchial epithelium. It displays a characteristic pseudostratified columnar appearance with each cell carrying approximately 250 cilia at the apical surface, interspersed with microvilli that projects to the respiratory lumen. The motile cilia beat with the aid of mucus, traps noxious inhaled particles and propel them out of the lung (Shah et al., 2009). This movement is termed the mucociliary clearance and protects the lung by facilitating the removal of small particles or infectious pathogens prior infection is established or further damage occurs (Mall, 2008, Ross et al., 2010). Goblet cells secrete mucins and are the second most numerous cell types in the bronchial epithelium. Like ciliated cells, goblet cells span the full depth of the epithelium and also project microvilli to increase surface area for mucus secretion. Their cytoplasm is occupied mostly by mucinogen granules that accumulate near the apical side. The mucins, secreted by goblet cells and from mucus glands, make up the mucus layer which covers the luminal surface and protects the epithelium from dehydration by saturation of inhaled air with water, and potential damage from inhaled particles (Ross et al., 2010, Boucherat et al., 2013). Club cells are cuboidal non-ciliated cells located in human terminal bronchioles and secrete glycosaminoglycans, club cell secretory protein uteroglobin, and surfactant by apocrine secretion to protect the bronchial lining (Reynolds and Malkinson, 2010). Club cells are also facultative progenitor cells and are capable of self-renewal and restoring terminally differentiated cells such as ciliated cells. Thus, this unique feature of

the maintenance and repair of lung epithelium suggests that an intervention that stabilises the club cell pool could be used for the treatment of chronic lung diseases (Reynolds and Malkinson, 2010). Basal cells are undifferentiated epithelial cells that extend into the respiratory lumen and are located adjacent to the basement membrane. They are able to differentiate and replenish ciliated and goblet cells (Ross et al., 2010).

The alveolar epithelium is composed of type I (95% of the coverage) and type II alveolar cells (less than 5%) and occasional brush cells (Ross et al., 2010). The direct contact with air and continuous exposure to particles and microbial pathogens makes the alveolar surface vulnerable. Type I alveolar cells (also named type I pneumocytes) are squamous cells that line the alveolar surface by joining adjacent cells through occluding junctions. Type I alveolar cells are terminally differentiated. Type II alveolar cells (also named type II pneumocytes) are secretory cells rich in phospholipids, neutral lipids and able to produce surfactant. Type II alveolar cells are also the progenitor cells for type I alveolar cells (Barkauskas et al., 2013a). One proposed theory of idiopathic pulmonary fibrosis (IPF) aetiology is a defect of type II alveolar cells to differentiate into type I alveolar cells; aberrant epithelial cell function could result from continuous apoptosis of type I pneumocytes and proliferation of type II pneumocytes eventually leading to irreversible fibroblast foci (Hoo and Whyte, 2012).



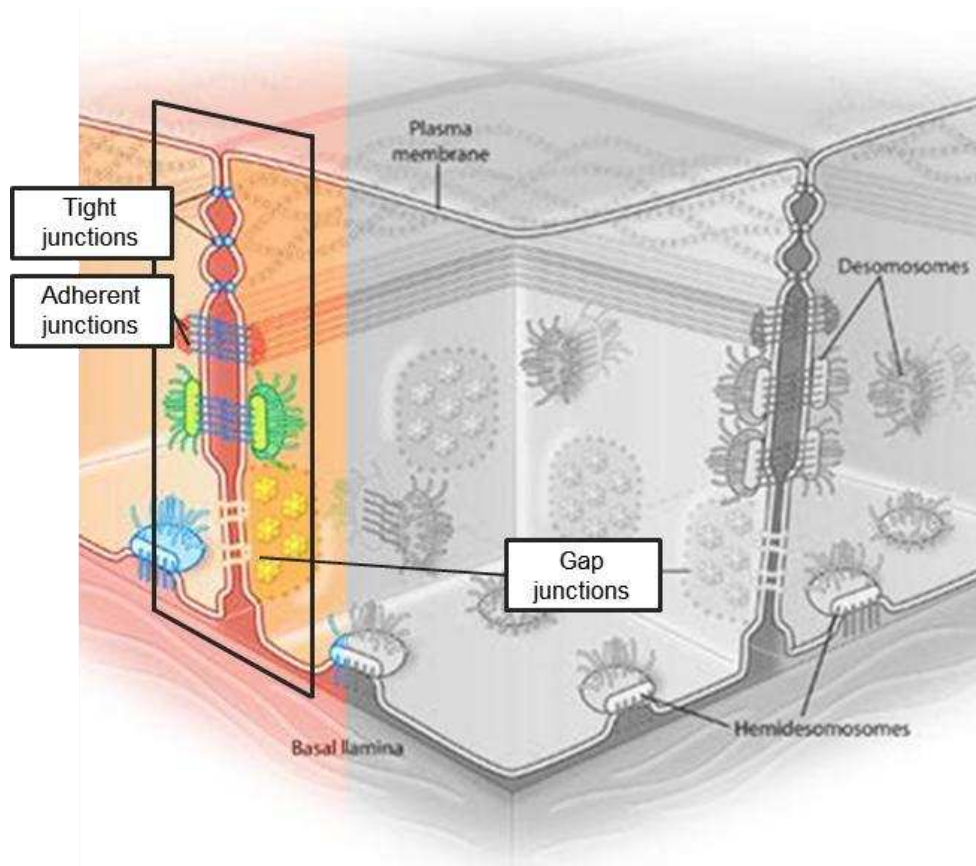
**Figure 1.2 Cellular composition in the human lower and distal respiratory tract.**

A. The lower respiratory tract (RT) is comprised of trachea, bronchi (primary, secondary, tertiary and small which are defined by the number of dividing branches 1 to 4), bronchioles and terminal bronchioles. The lower RT is covered with bronchial/ bronchiolar epithelium comprised of ciliated cells, club (Clara) cells, basal cells, and goblet cells. Respiratory bronchioles and alveolar sacs, which belong to the distal RT, are composed by alveolar epithelium containing type I, II alveolar cells and alveolar macrophages. Figure adopted from (Berube et al., 2010). B. Cross-section of bronchial tissue stained with haematoxylin and eosin. Image taken from <http://www.siumed.edu/>.

## **1.1.2. The innate immunity in the lung**

### 1.1.2.1. Cells and their functions in the airway epithelium

The airway epithelium plays an essential role in innate immunity to xenobiotics. In addition to gas exchange, airway epithelium participates in the regulation of immune defense encompassing the passive physical barrier, active mucociliary movement and immune modulation through the secretion of chemical mediators. The mucociliary escalator is powered by the cilia that is continually beating, pushing mucus up and out from the airway into the throat. Microbial pathogens or particles ranging from 2 to 10  $\mu\text{m}$  in diameter are trapped in the sticky mucus blanket and moved up by the mucociliary escalator away from the respiratory tract (Ross et al., 2010, Widmaier et al., 2006). The mechanic movement able to expel pathogens and external irritants provides a major barrier against infection. The epithelial barrier is impermeable to foreign bodies because of the presence of the junctional complex consisting of tight junctions, anchoring junctions (desmosomes and adherens junctions), and gap junctions that tightly bind adjacent epithelial cells (Fig. 1.3) (Alberts et al., 2002). Epithelial cells are capable of triggering immune responses and killing microbial pathogens through internalisation of pathogens, secretion of cytotoxic molecules ( $\text{NO}$ ,  $\text{O}_2^-$  and  $\text{H}_2\text{O}_2$ ), anti-microbial peptides and cytokines (described in section 1.1.2.3.) (Kowalski et al., 2007). Meanwhile, epithelial cells can be activated by bacterial components and cytokines such as tumour necrosis factor-alpha ( $\text{TNF-}\alpha$ ) and interleukin 1beta ( $\text{IL-1}\beta$ ) to regulate the inflammatory response (Suzuki et al., 2008).



**Figure 1.3 Epithelial cell junctions.**

Three specialised junctions support the cellular polarity and paracellular communication of differentiated epithelium. Tight junctions (TJs) are situated closest to the apical membrane and form a continuous intercellular barrier between adjacent epithelial cells. TJs which are composed of claudins, occludins and intracellular peripheral membrane proteins called zonula occludin (ZO) proteins form a restrictive barrier preventing the flux of fluid, ions and macromolecules between the apical and basolateral side (Godfrey, 1997). Beneath the TJs lie adherent junctions (AJs) which form a belt made up by cadherin-catenin complex around the circumference of cell membrane that linked to actin and myosin filaments (Baum and Georgiou, 2011). AJs function to join adjoining cells in a calcium-dependent manner (Baum and Georgiou, 2011). Gap junctions which sit near the basolateral side allow the exchange of intracellular cytoplasm, ions and other small molecules (Alberts et al., 2002). Figure adapted and modified from (Nature.com, 2014)

---

Upon microbial infection, endothelial cells reorganise their cytoskeleton to increase vascular permeability; the expression of surface proteins intercellular adhesion molecule-1 (ICAM-1) and platelet activating factor (PAF) on activated endothelial cells are also enhanced to increase the binding of neutrophils to facilitate the downstream inflammatory response (Sherwood,

2007, Ross et al., 2010). In addition to their role as major constituents of the connective tissue structure, fibroblasts produce extracellular matrix, predominantly collagen type I and type III, to sustain the architecture of the lung (Suzuki et al., 2008). Fibroblasts are important in wound healing, and this activity is thought to be regulated by fibrocytes that reside in the tissue stroma. Following tissue injury, fibroblasts migrate to the site of damage and facilitate the healing process through the deposition of new collagen. At a healing wound, they change their actin gene expression and take on the contractile properties of smooth muscle cells that help to pull the wound margins together; these modified fibroblasts are termed myofibroblasts (Rubin and Strayer, 2008). Fibroblast secretion of matrix metalloproteases (MMPs) and cytokines induce leukocytes activation and also help shaping the inflammatory response (Andersson et al., 2008, Rubin and Strayer, 2008).

#### 1.1.2.2. Innate immune cells in the lung

Macrophages are critical players in the initiation of inflammation and can promote chronic inflammation in some circumstances (Rubin and Strayer, 2008). Alveolar macrophages are the major resident myeloid-derived cells in the lung. They are located on the luminal side of the lung and exert highly phagocytic function to facilitate protection of the host against infections. Alveolar macrophage activation is tightly controlled by soluble mediators in the lumen and the close cell-cell binding with bronchial/alveolar epithelial cells to limit unwanted inflammatory responses (Hussell and Bell, 2014). Current research indicated that the negative regulation of macrophage activation is controlled via the binding of IL-10 to IL-10R expressed by alveolar

macrophages that triggers Janus Kinase 1 (JAK1)-signal transducer and activator of transcription 3 (STAT3) resulting in the expression of suppressor of cytokine signalling 3 (SOCS3) and the microRNA miR-146b. The ligation of the ligand CD200 at type II alveolar epithelial cells with CD200 receptor (CD200R) in alveolar macrophage also inhibits the extracellular signal-regulated kinase (ERK), p38 mitogen-activated protein kinase (MAPK) and JUN N-terminal kinase (JNK) inflammatory pathways. Binding of latent TGF- $\beta$  by  $\alpha$ v $\beta$ 6 integrin on the bronchial or inflamed alveolar epithelial cells induces a conformational change in TGF- $\beta$  that facilitates access of the TGF- $\beta$  receptor (TGF- $\beta$ R) resulting in inhibition of pro-inflammatory signalling (Hussell and Bell, 2014). A subset of alveolar macrophages was found to remain immunosuppressive upon endotoxin induced inflammation through the physical contact with alveolar epithelial cells at gap junctions. The connexion 43 expressing gap junction protein knock-out alveolar macrophages in mice recruit higher amounts of neutrophils and secrete pro-inflammatory cytokines indicating that the activation of alveolar macrophages is tightly controlled through their intercommunication with alveolar epithelium to repress inflammation (Westphalen et al., 2014). Alveolar macrophages have a M2-like (alternatively activated macrophages), a phenotype associated with the resolution of many lung inflammatory conditions but that can also promote fibrotic disease through the production of TGF- $\beta$ , CCL18 and platelet-derived growth factor (PDGF). Despite that fact that alveolar macrophages produce higher levels of IL-13 in asthma patients and that the expression of CD163 is also higher on alveolar macrophages from patients with IPF, which activation pattern of alveolar macrophages promote healing or aggravate tissue damage



either transiently or chronically is still unclear and disputable (Alber et al., 2012, Hussell and Bell, 2014).

Neutrophils are phagocytes with potent anti-microbial capabilities. During pulmonary microbial infection, neutrophils migrate out of the pulmonary capillaries into the air spaces. The combination of degranulation through the release of proteases (neutrophil elastase, cathepsin G, lactoferrin, myeloperoxidase, etc.) and the oxidative response (the production of superoxide  $\text{H}_2\text{O}_2$  by NADPH oxidase) result in efficient microbial killing in the phagolysosome. Neutrophils are not only the hallmark of acute inflammation but dysregulated function of neutrophils or neutropenia predispose patients to chronic pulmonary inflammation (Rubin and Strayer, 2008).

Mast cells are ubiquitous in the airways and lung parenchyma (Suzuki et al., 2008). Mast cells are involved in the response to parasitic infections and in mediating allergic responses. Aggregation of the IgE receptor Fc $\epsilon$ RI by binding to multivalent IgE-coated antigens causes rapid degranulation of mast cells, resulting in the release of various mediators such as histamine, prostaglandins and leukotrienes together with an array of proteases and cytokines/chemokines that cause immediate airway inflammation and the symptoms of asthma (Moiseeva and Bradding, 2011). Activated mast cells have been shown to produce inflammatory cytokines TNF- $\alpha$ , IL-1 $\beta$ , and IL-6 to promote acute inflammation in the rat lung after intratracheal instillation of *P. aeruginosa* LPS (Le et al., 2012). In addition, human cord blood-derived mast cells were also implicated in neutrophil recruitment via secretion of IL-1 $\alpha$  and IL-1 $\beta$  upon activation with *P. aeruginosa* culture supernatants (Lin et al., 2002).

Eosinophils act to eliminate parasitic infections and are effector cells responsive to allergic responses (Suzuki et al., 2008). Eosinophil granules contain four different granule cationic proteins: eosinophil peroxidase, eosinophil cationic protein, eosinophil-derived neurotoxin and a major basic protein that is toxic to parasites and causes epithelial cell necrosis. Eosinophils secrete lipid mediators such as leukotriene C4 and platelet-activating factor in response to allergic inflammation that may result in dysfunction and injury to other cells (Rubin and Strayer, 2008).

#### 1.1.2.3. Soluble immune mediators in the lung

##### Airway surface liquid and its anti-microbial properties

Airway surface liquid (ASL) is composed mainly of mucin glycoproteins and anti-microbial molecules including  $\beta$ -defensins, lactoferrin, and lysozyme. These anti-microbial molecules that can be secreted by neutrophils and macrophages in addition to epithelial cells ASL have anti-microbial properties and are effective at pH ranging from 6.5 to 7.3. Lysozyme hydrolyses peptidoglycan is the major component of Gram-positive bacterial membranes. Defensins are peptides containing 6 cysteines and 3 intramolecular disulphide bonds.  $\alpha$  and  $\beta$  forms are expressed by humans. Epithelial cells mainly express 6  $\beta$ -defensins (hBD-1 to 6) whereas  $\alpha$  defensins 1-4 are produced by neutrophils in the airways. Recruited neutrophils to the site of inflammation by microbial products secrete defensins and thereby induce airway epithelial cells to produce more IL-8, TNF- $\alpha$ , and IL-1 $\beta$  to recruit additional neutrophils (van Wetering et al., 2002). In addition to anti-microbial activities, defensins enhance airway epithelial cells bacterial binding, cytotoxicity, and cytokine

production. Lactoferrin is an iron-binding protein that directly damages bacterial membranes resulting in the release of lipopolysaccharides (LPS) and interferes with the binding of LPS to LPS binding protein. As a result, lactoferrin prevents host cells from activation by bacterial LPS. Cathelicidin LL-37 works synergistically with lysozyme and lactoferrin is secreted by airway epithelial cells and mast cells. LL-37 exerts chemotaxis for leukocytes, ligation of LPS, and induction of cytokine and chemokine expression by epithelial cells and promotion of epithelial wound healing (Suzuki et al., 2008).

#### Complement components

Complement proteins circulate in the blood in an inactive form in the absence of infection. In the presence of pulmonary infections, complement proteins extruding from the plasma to airways are involved in the inflammatory response against bacterial infection via opsonisation to facilitate leukocyte phagocytosis (Murphy, 2011). Complement activation can be triggered through three pathways: classical pathway that is initiated by the interaction of C1q (a component of C1 complex) with pathogen surface or with antibodies to the antigens bound bacterial surfaces; alternative pathway, the spontaneous hydrolysis of C3 binding to factor proteins triggered by microorganism-derived products, such as endotoxin, zymosan, polysaccharides; lectin pathway is triggered by the recognition and binding of mannose-binding lectin and ficolins to mannose groups on the pathogen surfaces. Complement C3a and C5a are anaphylatoxins that stimulate smooth muscle contraction and promote vascular permeability neutrophil recruitment into the lung and microbial killing (Rubin and Strayer, 2008, Suzuki et al., 2008).

## Surfactant proteins

Pulmonary surfactant is essential to reduce the air-liquid surface tension of the lung (Pattle, 1955) and functions in various aspects of pulmonary host defence (Wright, 2005). The majority of surfactant is composed of phospholipids and about 10% of surfactant consists of proteins with four surfactant proteins defined: surfactant protein A (SP-A), SP-B, SP-C and SP-D. SP-A and SP-D along with mannose-binding lectin (MBL) belong to the family of collectins which opsonise pathogens including a variety of bacteria, viruses, fungi, allergens and apoptotic cells and thereby enhance the uptake of these cells and particles by phagocytes (Crouch and Wright, 2001, Holmskov et al., 2003). Distinctive roles have been ascribed to surfactant proteins. SP-A inhibits the maturation of dendritic cells (DCs), whereas SP-D promotes the uptake and presentation of antigen by DCs (Lipscomb and Masten, 2002). Studies also indicated that the binding of SP-A and SP-D to T cells inhibits T-cell proliferation (Lambrecht et al., 1999, Wright, 2005). The above evidence suggests that surfactant proteins bridge innate and adaptive immunity. Surfactant proteins also negatively regulate alveolar macrophage activation. SP-A and SP-D prevent pro-inflammatory response through nuclear factor  $\kappa$  light-chain enhancer of activated B cells (NF- $\kappa$ B) activation in alveolar macrophages by blocking the interaction of TLR2, TLR4 and its co-receptors MD2 and CD14 with their correspondent ligands (Hussell and Bell, 2014). Binding of SP-A and SP-D to signal-regulatory protein- $\alpha$  (SIRP $\alpha$ ) on the surface of alveolar macrophages recruits SH2 domain-containing protein tyrosine phosphatase 1 (SHP1) that inhibits phagocytosis (Hussell and Bell, 2014).

## Induced inflammatory mediators

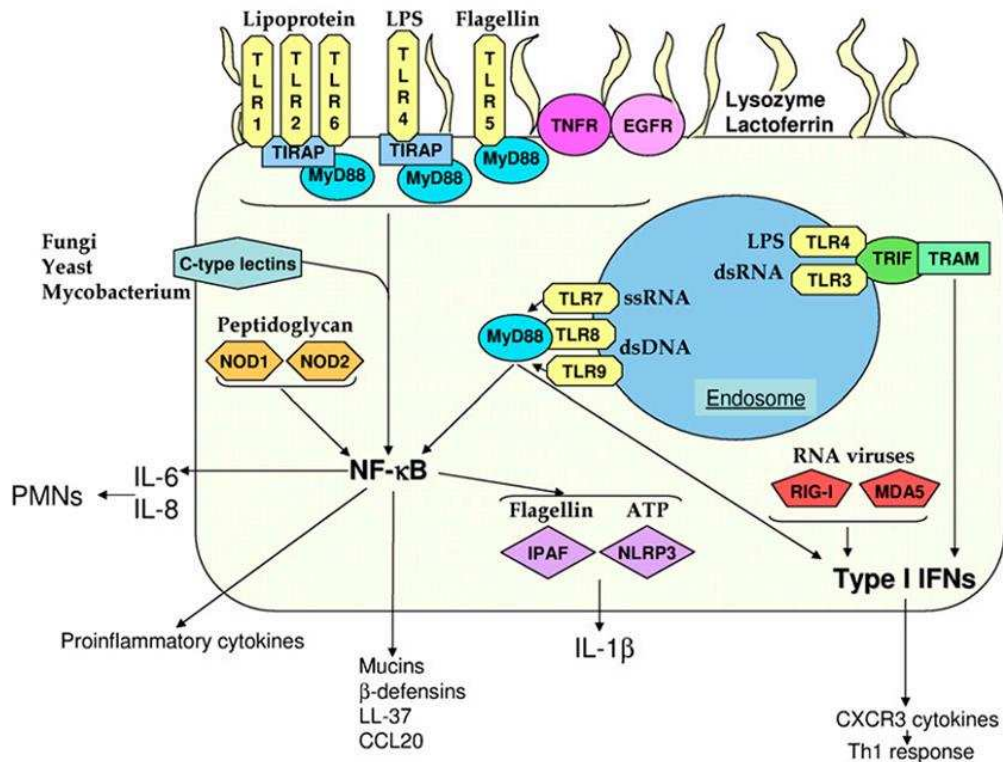
Activation of receptors in the airway epithelial cells leads to the secretion of an array of cytokines/chemokines and growth factors that recruit leukocytes and lymphocytes to the site of infection (Parker and Prince, 2011). Cytokines can be categorised as pro-inflammatory and anti-inflammatory. TNF- $\alpha$ , IL-6, IL-1 $\beta$  and the growth factor granulocyte macrophage colony-stimulating factor (GM-CSF), chemokines IL-8, monocyte chemotactic protein-1 (MCP-1), T-cell-specific CXC chemokines, IFN-induced protein of 10 kDa (IP-10) are among the well-known pro-inflammatory mediators produced by airway epithelial cells and haematopoietic cells that participate in acute inflammatory response (Parker and Prince, 2011). Major anti-inflammatory cytokines include IL-10, transforming growth factor-beta (TGF- $\beta$ ), soluble cytokine receptors/receptor antagonist sIL-1ra. Secretion of IL-10 and TGF- $\beta$  by alveolar macrophages and epithelial cells down-regulates the inflammatory response by T cells, NK cells and monocytes (Stow et al., 2009).

### 1.1.2.4. Pattern recognition receptors on the airway epithelium

The innate immune response is the first line of host defence and is responsible for immediate recognition and control of a broad range of microbial infections. The sensing of infections relies on innate pattern recognition receptors (PRRs) which include surface transmembrane Toll-like receptors (TLRs) and cytosolic receptors retinoic acid-inducible gene I like (RIG-I-like) receptors, nucleotide-binding oligomerisation domain-like (NOD-like) receptors and C-type lectin receptors that recognise highly conserved microbial structures (Takeuchi and Akira, 2010, Tam et al., 2011). Ligand-receptor binding triggers intracellular

signalling and a major component of mucosal immunity involves the activation of NF- $\kappa$ B, activator protein 1, IFN regulatory factors (IRFs), MAPKs leading to recruitment and activation of neutrophils and other immune cells in the airways (Parker and Prince, 2011). So far, human airway epithelial cells have been documented to express all ten TLRs mRNA but the predominant TLR genes expressed are TLR2 to TLR6 (Kato and Schleimer, 2007, Hallstrand et al., 2014). TLR2, which forms heterodimers with TLR1 or TLR6, recognises lipoprotein, peptidoglycan and lipoteichoic acid (LTA) in Gram-positive bacteria (Kato and Schleimer, 2007). Interaction of airway epithelium with *P. aeruginosa* involves TLR2, -4, and -5 (Zhang et al., 2005). *P. aeruginosa* infection induces the expression of TLR2 on airway epithelial cells and the binding of TLR2 regulates the function of gap junction through Ca<sup>2+</sup> signalling (Martin and Prince, 2008). The flagellum of *P. aeruginosa* is recognised by TLR5 and asialoGM1 and induces mobilization of these receptors to the surface of the cell (McNamara et al., 2006, Zhang et al., 2005). TLR3 recognises viral double-stranded RNA (dsRNA) and a synthetic analogue of dsRNA, polyinosine-polycytidylic acid. TLR4 recognizes LPS which is present in Gram-negative bacteria and a protein that mediates membrane fusion from respiratory syncytial virus, although TLR4 remains largely cytosolic thus less responsive, in airway epithelial cells (Gomez and Prince, 2008). Two cytoplasmic RNA helicases, melanoma differentiation-associated gene 5 (MDA5) and (RIG-I) are expressed in airway epithelial cells that are responsive to viral dsRNA recognition independent of TLR3 (Kato and Schleimer, 2007). NOD-1 and NOD-2 which recognise peptidoglycan-derived

peptides,  $\gamma$ -D-glutamyl-mesodiaminopimelic acid and muramyl dipeptide respectively, are also expressed in airway epithelial cells (Opitz et al., 2004).



**Figure 1.4 Schematic view of innate immunity in the respiratory epithelial cells.**

Airway epithelial cells express transmembrane surface receptors (TLR1-6) and intracellular receptors (endosomal receptors TLR3, 4, 7-9 and cytosolic receptors RIG-I, MDA5, NOD1,2, IL-1 $\beta$ -converting enzyme protease activating factor (IRAF) and NOD-like receptor pyrin domain (NLRP3)). The secretion of anti-microbial peptides and cytokines after the activation of signalling results from the ligation of receptor-ligand. Figure adapted from (Parker and Prince, 2011).

### **1.1.3. The adaptive immunity in the lung**

Soluble antigens have limited access to lung draining lymph nodes (dLN) through passive mechanisms (Hulbert et al., 1989) at early time points following intranasal challenge and it is unlikely that particulate antigens such as non-invasive bacteria gain free access to the pulmonary lymphatics. However, the adaptive immunity is developed in the lung dLN following transport of antigens, such as microbial pathogens and inhaled foreign irritants, by antigen presenting cells to this site (Kirby et al., 2009). CCR7-dependent migration of pulmonary dendritic cells is once thought to be the only mechanism in antigen presentation transported from the lungs to dLN (Legge and Braciale, 2003). In fact, in addition to the immunoregulatory function, alveolar macrophages also contribute to the antigen acquisition, patrol at alveolar spaces and constitutively migrate to the dLN to orchestrate immune responses (Kirby et al., 2009, Murphy, 2011). Effective and efficient immune defence follows the binding of antigen presented by antigen presenting cells to T-cell receptor on T lymphocytes and B-cell receptor on B lymphocytes at the site of inter cortex and subcapsular sinuses in the lymph nodes, respectively (Kirby et al., 2009). The secretion of antibodies by antibody-producing plasma cells which differentiated from B lymphocytes provides an additional layer of protection of the epithelial barrier against a wide range of different pathogens after pulmonary infection and inflammation. Antibodies bind to pathogens therefore facilitates antibody-dependent cell-mediated cytotoxicity in the lung parenchyma (Murphy, 2011). After encountering with antigens, T cells proliferate and differentiate into functional effector T lymphocytes. CD8+ cytotoxic T cells are responsible for clearance of intracellular pathogens such



as viruses. CD4<sup>+</sup> helper T cells (Th cells) signal the function of antibody-producing B cells and produce pro-inflammatory cytokines (IFN- $\gamma$ , TNF- $\alpha$ ) that influence the macrophage phagocytic capacity against bacteria, viruses, and intracellular parasites. Th2 T cells, another subset of CD4<sup>+</sup> T cells which secrete IL-4, IL-5, IL-9 and IL-13, promote the activation of eosinophils, basophils, and mast cells to facilitate the control of parasite infections. Th1 and Th2 responses counteract each other to maintain a fine balance (Murphy, 2011). A dysregulated T-cell response could lead to chronic inflammatory diseases such as asthma and chronic bronchitis (described further in section 1.1.4.2.). IL-17-producing T cells such as Th17,  $\gamma\delta$ T cells and natural killer cells (NK cells) are protective against some bacterial infections through the recruitment and activation of neutrophils (Nembrini et al., 2009). The airway epithelium bridges the innate and adaptive immune responses through the secretion of cytokines such as IL-25 (also known as IL-17E), IL-33 and thymic stromal lymphopietin (TSLP) that are considered upstream of Th2 cytokines IL-4, IL-5 and IL-13 in allergic inflammation such as asthma (Parker and Prince, 2011).

#### **1.1.4. Pathogenesis of pulmonary inflammatory diseases**

Respiratory tract diseases are diseases that affect the nasal passages, the bronchi and the distal alveoli of the lung. Regulation of lung inflammation is tightly controlled by cellular and molecular mechanisms for efficient orchestration of pro-inflammatory responses upon stimulation. These responses need to be proportionate to the type of stimulation and lead to the elimination of intruders/irritants. Balance is achieved through an anti-inflammatory inflammatory response characterised by the cytokines IL-10 and TGF- $\beta$ ,

leading to airway remodelling and restoration of tissue homeostasis. Current concepts in the pathogenesis of acute inflammatory diseases are covered in the following sections and include infectious diseases such as bronchitis and pneumonia, and chronic inflammatory diseases such as asthma and chronic obstructive pulmonary disease (COPD). Two unconventional chronic inflammatory diseases in the lung: cystic fibrosis in which inflammation is propagated by chronic infections and idiopathic pulmonary fibrosis (IPF) in which the inflammatory response is considered secondary to disease progression was also discussed.

#### 1.1.4.1. Respiratory tract infections

Upper respiratory tract is inhabited normal microbial flora but the lower respiratory tract remains sterile. Many microbial pathogens preferentially infect the peripheral airways, bronchi and bronchioles leading to bronchiolitis and bronchiectasis, such as in the case of adenovirus, respiratory syncytial virus (RSV) and measles infection. These infectious agents cause acute extensive inflammation of bronchioles caused by extravasation of inflammatory cells and congestion of the mucosa with subsequent healing by fibrosis. Non-obstructive bronchiectasis usually results from respiratory infections or defects in the defence mechanisms that protect the airways from infection. Bronchiectasis displays irreversible abnormal dilation of bronchi with thickening of the bronchial walls and fibrosis of the pulmonary parenchyma along with exaggerated inflammation that is vulnerable to infective exacerbations. Pneumonia is an acute lung inflammatory disease caused mainly by bacterial and viral infections in the lower respiratory tract that leads to alveolar filling

with exudate in the lung parenchyma. Nosocomial pneumonia is usually initiated by the infections at the upper airways of hospitalised patients. The transmission routes of pathogens leading to nosocomial pneumonia could be through 1) ventilator devices and feeding tubes termed mechanical injuries, 2) healthcare personnel that facilitate the transmission of *Pseudomonas* spp., and *Acinetobacter* spp. and 3) antibiotics resistant strains such as methicillin-resistant *Staphylococcus aureus* (MRSA). *Pseudomonas* pneumonia is commonly seen in nosocomial infections and the chronic airway infection progressing to bronchiectasis, gas trapping, and hypoxaemia that lead to pulmonary insufficiency (O'Sullivan and Freedman, 2009). In this case, hospitalised patients with exposed wounds, immunosuppressed patients undergoing chemotherapies, patients treated with broad-spectrum of antibiotics and suffering from acquired immunodeficiency syndrome (AIDS) with T cell dysfunction are vulnerable to opportunistic pneumonia that could lead to systemic inflammation, shock or even sepsis (Rubin and Strayer, 2008).

The acute inflammation induced by bacterial infection and successful resolution to restore tissue homeostasis involves multiple cellular components (non-haemopoietic and haemopoietic cells) and molecular mediators. Taking *S. pneumoniae* infection as example, the entry of *S. pneumoniae* to the distal alveoli is recognised by PRRs including TLRs on epithelial cells and alveolar macrophages, and macrophage receptor with collagenous structure (MARCO) expressed on alveolar macrophages. Low dose *S. pneumoniae* infection can be contained by epithelial cells, resident alveolar macrophages and the release of protective mediators such as IL-1, TNF- $\alpha$ , SP-D and anti-microbial peptides without the infiltration of neutrophils. At high doses of infection, neutrophils

are recruited by chemoattractants to enhance the phagocytosis of the pathogen. In the transition phase of inflammation, neutrophils under the action of pro-resolving signals start undergoing apoptosis followed by efferocytosis by alveolar macrophages. During efferocytosis, macrophage phenotypes switch from M1 to M2-like phenotype producing anti-inflammatory molecules (such as IL-10 and TGF- $\beta$ ) and pro-resolving mediators to promote tissue repair and resolution. M2 macrophages then further switch to M resolution (Mres) phenotype, which display reduced phagocytosis but produce anti-fibrotic and anti-oxidant proteins that limit tissue damage and fibrosis. Such events of increased production of pro-resolving mediators (such as lipoxin, resolvins, protectins), anti-inflammatory and anti-fibrotic agents by resolution macrophage (Mres), and lymph node drainage or apoptosis of macrophage close the inflammatory process and restore tissue homeostasis. Chronic infection is usually rare in immunocompetent individuals, but in cystic fibrosis patients which are immunocompromised in epithelial barrier function are predisposed to recurrent pulmonary infections (van der Poll and Opal, 2009, Alessandri et al., 2013). Section 1.2 describes in detail cystic fibrosis aetiology, pathology, and explores intrinsic and exogenous factors in chronic airway inflammation and respiratory infections.

#### 1.1.4.2. Chronic inflammatory lung diseases

Different phases of acute inflammatory processes are meticulously on-check for successful resolution. A successful resolution is attributed to 1) abrogation of chemokine signalling that blocks continued neutrophil tissue influx; 2) neutrophil apoptosis that attracts monocytes and macrophages to induce their

clearance; 3) clearance of apoptotic neutrophils promoted by a transition of a pro-inflammatory to an anti-inflammatory macrophage phenotype which is also a prerequisite for macrophages to return to their tissue homeostatic state; 4) migration of macrophages and dendritic cells from the site of inflammation after efferocytosis; 5) the aid of suppressive immune cells and the adaptive immune response; 6) induction of tissue repair to return to homeostasis without scarring (Michlewska et al., 2009, Ortega-Gomez et al., 2013). However, an extended or dysregulated inflammatory response may lead to chronic inflammation in which persistent injury prevents the restoration of tissue integrity and function (Ortega-Gomez et al., 2013). This section introduces the mechanisms of pathogenesis of two well-recognised chronic inflammatory lung diseases, asthma and chronic obstructive pulmonary disease (COPD). This led us to address the current view of how interstitial pulmonary fibrosis could also be propagated by inflammatory response which is regulated by macrophages (Lech and Anders, 2013, Hussell and Bell, 2014) and T lymphocytes (Wynn, 2004, Kotsianidis et al., 2009, Gilani et al., 2010) and is distinct from the above conventional mechanisms.

## Asthma

Asthma, a life-long disease that usually starts during childhood; it is characterised by recurrent, reversible bronchial obstruction and usually associated with bronchial hyper-responsiveness and chronic airway inflammation. Asthma is marked by a Th2-cell-dependent, IgE-mediated allergic disease and asthmatic patients are more likely to be sensitised to aeroallergens. The pathology of asthma is characterised by mucus-cell

hyperplasia. The secretion of CCL20 from epithelial cells recruits dendritic cells via binding to the receptor CCR6. The activated dendritic cells thereby induce naïve T cells to differentiate into Th2 cells. The infiltrated T cells further interact with B cells, eosinophils, and mast cells to promote allergic inflammation (Martinez and Vercelli, 2013). The Th2-centric paradigm of this disease is also related to the capacity of regulatory T cells to control Th2 responses (van Oosterhout and Bloksma, 2005, Robinson, 2009). Airway remodelling contributes to the development and progression of the disease. In severe cases, airway obstruction attributed to mucus-cell hyperplasia, thickened subepithelial basement membrane, increased smooth-muscle mass and the undergoing airways fibrosis are in combination with increased deposition of fibroblast and myofibroblast proliferation. Asthma has a strong genetic component termed asthma-related loci, and the genes for CHI3L1, IL6R, IL-33, SMAD3, ORMDL3-GSDMB, and IL2RB, etc. have been identified in genome-wide association studies. However, only ORMDL3-GSDMB was repeatedly found between studies indicating that a polygenetic component is strongly involved in the genetics of asthma. The innate immune component is responsible for the initiation and promotion of this Th2-mediated disease. The release of IL-25, IL-33, TSLP by damaged airway epithelium upon allergens, pathogens, or pollutants activates natural-killer T cells, mast cells, eosinophils, and basophils (Mjosberg et al., 2011, Klein Wolterink et al., 2012). The newly identified innate immune lineage type II innate lymphoid cells (ILC2) found in human lung tissue and peripheral blood, secrete Th2 cytokines IL-13 and IL-5 in response to airway epithelial damage that also promote adaptive Th2 responses. Repetitive stimulation of epithelial cells, smooth muscle cells and

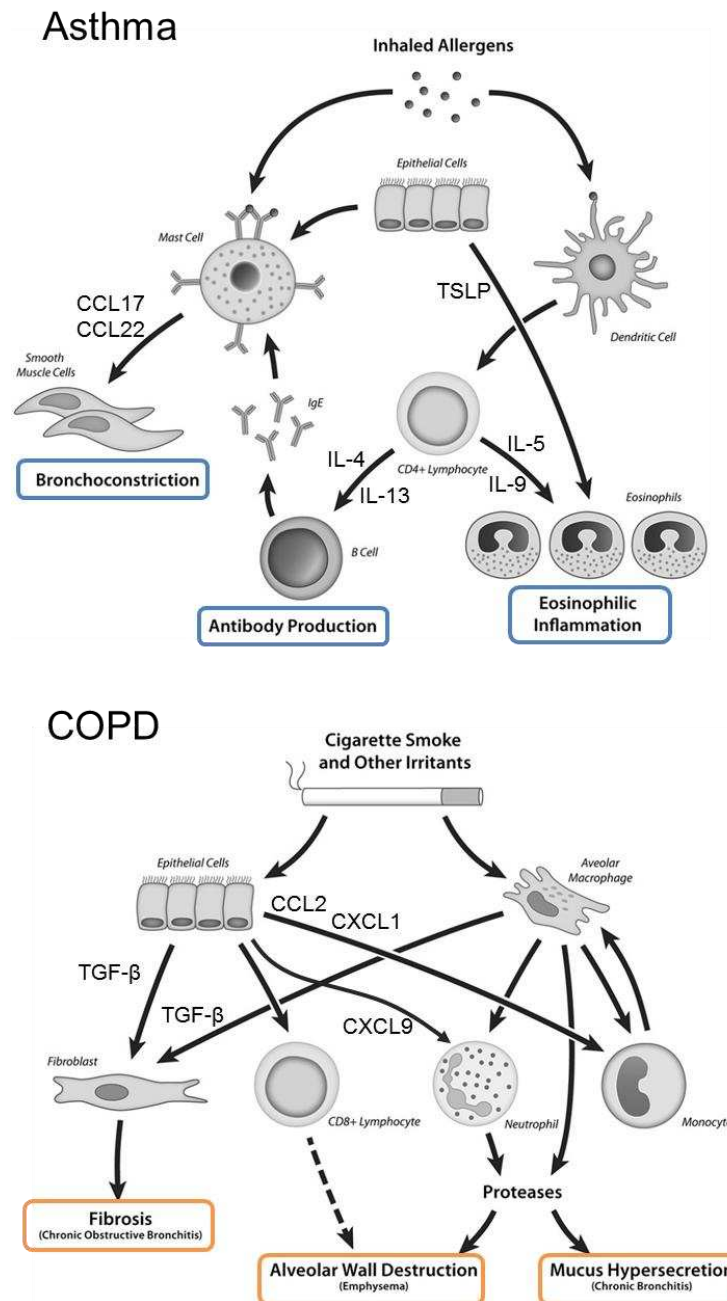
fibroblasts by Th2-derived and ILC2-derived cytokines would lead to airway hyper-responsiveness and remodelling. Inhaled corticosteroids remain to be the mainstream treatment of mild and moderate asthma (Martinez and Vercelli, 2013). Schematic inflammatory cascade of asthma is illustrated in Fig. 1.5.

### Chronic obstructive pulmonary disease

Severe end of asthma comorbidities can overlap with chronic obstructive pulmonary disease (COPD) (Martinez and Vercelli, 2013). However, COPD is defined as a preventable disease characterised by progressive airflow obstruction that is usually irreversible and the main cause is smoking tobacco (Decramer et al., 2012). Clinical manifestations of COPD include chronic bronchitis, a condition of large-airway inflammation and remodelling, and loss of elastic recoil by emphysema due to the destruction of parenchyma resulting in progressive decline of forced expiratory volume (FEV) and inadequate lung emptying on expiration (Tuder and Petrache, 2012, Decramer et al., 2012). Distinct from asthma, the cells that potentiate inflammatory response in COPD are neutrophils, macrophages, and CD8+ T cells. There is a major infiltration of neutrophils to the lung and neutrophilia is persistent throughout the progression of the disease. Increased proteinase production by neutrophils contributes to alveolar epithelial cell apoptosis leading to destruction of alveolar structures (emphysema). Proteinases also promote mucus hypersecretion resulting in increased goblet cell numbers and enlarged airway submucosal glands and narrow the small airway walls (obstructive bronchiolitis). In COPD, macrophages are increased in airway lumen, lung parenchyma and bronchoalveolar lavage fluid. Increasing evidence showed that

lung macrophages orchestrate the inflammation of COPD through the release of chemokines that attract neutrophils, monocytes and T cells and of proteases, particularly matrix metalloprotease 9 (MMP9) (Barnes, 2004). Despite the inflammation in COPD patients is aggressive, patients are refractory to corticosteroid treatment. Recent transcriptomic analysis investigating the pattern of macrophage activation demonstrated a distinct pattern in COPD patients from those in healthy smokers (Xue et al., 2014). Epigenetic regulation in COPD patients showed that glucocorticosteroid insensitivity is attributed to the nitrosylation at histone deacetylase 2 (HDAC2) in macrophages and the potential intervention to reverse the sensitivity has also been tested (Malhotra et al., 2011). A brief summary of the inflammatory cascade of COPD was also described in Fig. 1.5 in comparison with asthma.





**Figure 1.5 Inflammatory cascade of asthma and COPD.**

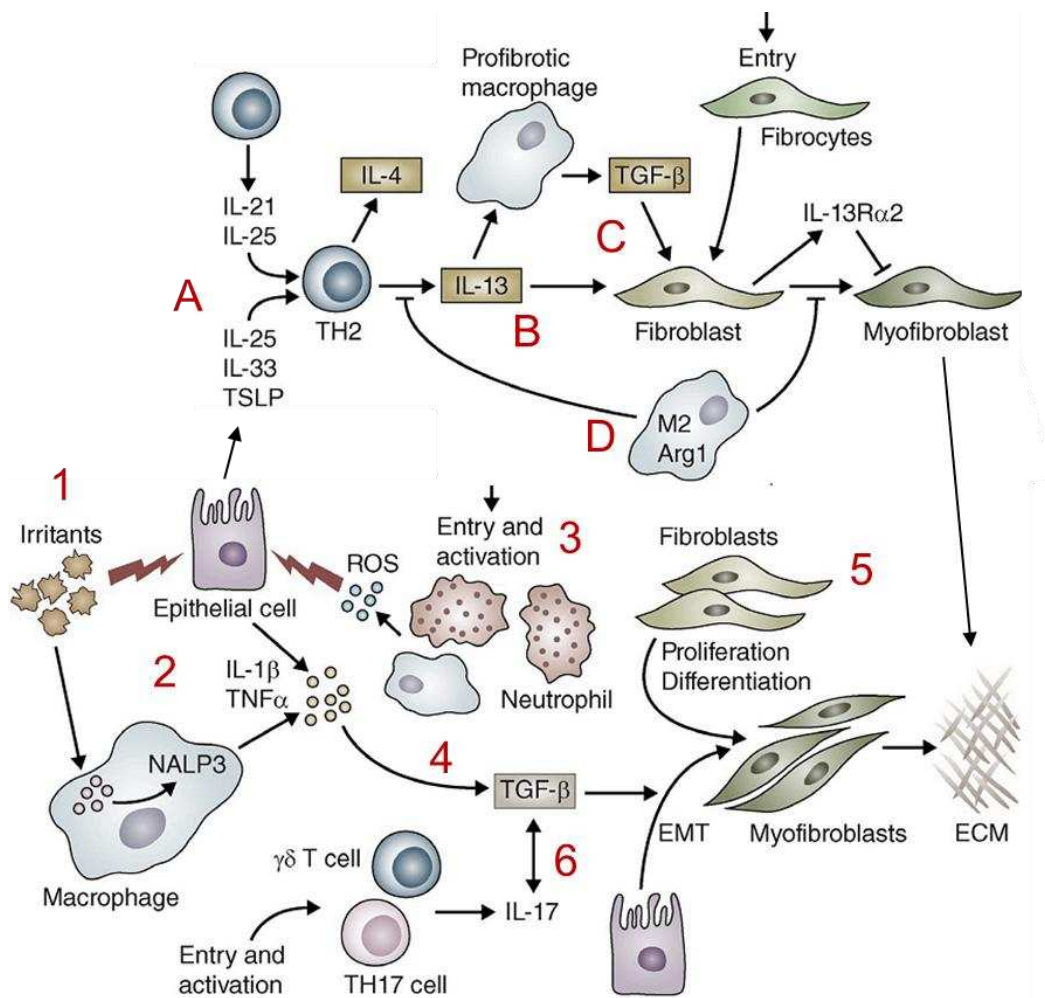
The underlying disease mechanisms between asthma and COPD were illustrated. In asthma, inhaled allergens activate mast cells by crosslinking surface-bound IgE to release histamine, leucotrienes and prostaglandin D2 as bronchoconstriction mediators. Allergens are processed by dendritic cells which conditioned with TSLP released by epithelial cells and mast cells to release CCL17 and CCL22 to act CCR4 on Th2 cells. Th2 cells act a central role in orchestrating the inflammatory response in allergy via the release of IL-4 and IL-13 to stimulate B cells to synthesise IgG and IL-5 and IL-9 to induce eosinophilic inflammation (Barnes, 2008). The inflammation in COPD in the lung is perpetuated by neutrophilia. Inhaled cigarette smoke and other irritants activate epithelial cells and macrophages to release CCL2 with CCR2 on monocytes, CXCL1 and CXCL9 to act on CCR2 to attract neutrophils and monocytes differentiation in the lung. Release of proteinases from neutrophils (mainly), alveolar macrophages and epithelial cells together cause elastin degradation, emphysema and mucus hyper-secretion. Release of TGF-β by macrophages and epithelial cells stimulates fibroblast proliferation leading to fibrosis in the distal airways. Figure adapted from (Roth, 2008).

## Interstitial lung diseases

Interstitial space is the space between the alveolar epithelium and the capillary endothelium. The thin side of capillary consists of the fused basement membranes of the epithelial and endothelial layers where gas exchange occurs, whereas the thick side governs the fluid exchange across the endothelium and is composed of type I collagen fibrils. Interstitial lung diseases (ILDs; also known as pulmonary fibrosis) result from the development of excess fibrous connective tissue in the lung and are therefore termed 'scarring of the lung.' The scarring in the lung parenchyma (alveolar tissue) or the pleura and chest wall cause the lungs to become stiffer and lose their elasticity to expand leading to dyspnoea. This is later followed by an impaired repair process of the epithelial barrier that results in extensive fibroblast proliferation, collagen deposition and destruction of lung architecture and function (Jakubzick et al., 2004, Noble et al., 2012). Reduced lung vital capacity and small resting lung volume are the characteristics of these diseases, thus they are described as restrictive pulmonary diseases (Wardlaw and Hamid, 2002, West, 2003). ILDs can be categorised as known and unknown causes. In the case of 1) autoimmune conditions (lupus, rheumatoid arthritis and sarcoidosis); 2) environmental irritants (asbestos, silica, dust, etc.); 3) chemotherapeutic drugs (bleomycin, nitrofurantoin, sulfonamides, etc.) and 4) radiation therapies, diseases are triggered by an inflammatory response with infiltration of lymphocytes and plasma cells in the lung (Wardlaw and Hamid, 2002, Rubin and Strayer, 2008, Chen and Stubbe, 2005). Cigarette smoking may increase the risk of developing ILDs and may aggravate the disease progression. Idiopathic pulmonary fibrosis (IPF) for which no causative agent is known is

the most common form of ILDs and shares the histological characteristics of usual interstitial pneumonia (UIP). Patchy dense scarring with extensive regions of honeycomb cystic change is the pathologic pattern of this disease. Interstitial fibrosis is usually temporal and heterogeneous referring to the fact that the fibrosis changes over time in the lung tissue. Fibrosis is mostly pronounced beneath the pleura and adjacent to the interlobular septa. The dense scarring fibrosis leads to the remodelling of the lung architecture and dilation of proximal bronchioles and growth of the bronchiolar epithelium into the dilated air space that could ultimately result in collapse of alveolar walls, formation of cystic space and destruction of the distal airway. Wound repair is normally accomplished by four sequential steps: 1) clotting and coagulation; 2) infiltration of neutrophils at early stage of wound healing, soon replaced by macrophages after neutrophil degranulation; 3) fibroblast migration and proliferation of myofibroblasts via epithelial-mesenchymal transition, recruitment from fibrocytes or resident fibroblasts; 4) tissue remodelling. Although the cystic spaces contain mucus, macrophages or neutrophils, the interstitial chronic inflammation is usually mild or moderate and thus the contribution of inflammation to disease is considered secondary (Thannickal et al., 2004). In this regard, intrinsic defects in the wound healing process involving epithelial cells and fibroblasts have been proposed. The fact that an active inflammatory response is not a prerequisite would partially explain the failure of anti-inflammatory medications to treat pulmonary fibrosis (Demedts et al., 2005). Despite research being focused on the mechanisms on the proliferation, activation and regulation of collagen-secreting myofibroblasts, recent studies have identified different mechanisms that suggest macrophages

and Th2 cells playing active roles in propagating the disease (Wynn, 2011, Homer et al., 2011). A schematic representation of the proposed inflammatory regulation in pulmonary fibrosis is described in detail in Fig. 1.6. The introduction of the most severe form of pulmonary fibrosis, idiopathic pulmonary fibrosis was described in chapter 6.



**Figure 1.6 Proposed pro-inflammatory and pro-fibrotic cascade in the initiation and maintenance of pulmonary fibrosis.**

(1) Irritants like silica, asbestos, and bleomycin can injure lung epithelial cells and can be detected by the Nalp3 inflammasome in macrophages. (2) These irritants stimulate the production of ROS, chemokines, and cytokines. (3) Subsequent recruitment and activation of leukocytes are induced by these inflammatory mediators could enhance the site of tissue injury, such as via ROS-expressing neutrophils that further damage epithelial cells. (4) IL-1 $\beta$  also promotes production of TGF- $\beta$ 1, an important profibrotic cytokine that triggers fibroblast proliferation and activation. (5) TGF- $\beta$  also targets epithelial cells, inducing epithelial-mesenchymal transition (EMT) and the formation of extracellular matrix (ECM)-producing myofibroblasts. (6) TGF- $\beta$ 1 further exacerbates the inflammatory response by stimulating the differentiation of Th17 cells.

Th2 cells and macrophages play distinct roles in pulmonary fibrosis. (A) After injury, epithelial cells release IL-25, IL-33, and TSLP, which facilitate the development of pro-fibrotic Th2 responses. T cells also release IL-21 and IL-25 promoting Th2 differentiation. (B) Th2 cells release IL-4 and IL-13, which promote the development of a pro-fibrotic macrophage subpopulation that secretes TGF- $\beta$ 1. (C) IL-13 can directly activate fibroblasts independently of TGF- $\beta$ 1. Th2 cytokines also trigger specific chemokines that promote the recruitment of collagen-secreting fibrocytes from the bone marrow, which amplify fibrotic responses. The resulting myofibroblasts release ECM components. (D) Th2 cytokines can also activate arginase-1 activity in M2 macrophages, which inhibit further IL-13 production and myofibroblast differentiation. IL-13 can also up-regulate the IL-13 decoy receptor in fibroblasts, which antagonizes ECM production via a negative feedback loop. Figure adapted and regenerated from (Wynn, 2011).

## 1.2. CYSTIC FIBROSIS

### 1.2.1. Aetiology and pathophysiology of cystic fibrosis

Cystic fibrosis (CF) is an autosomal recessive disorder caused by a mutation in the gene encoding cystic fibrosis transmembrane conductance regulator (CFTR) which encodes a chloride channel categorised in the family of adenosine triphosphate (ATP) binding cassette transporters (O'Sullivan and Freedman, 2009, Patrick and Thomas, 2012). The abnormal chloride conductance caused by the defect in CFTR promotes extensive absorption of  $\text{Na}^+$  and water from the lumen of the respiratory, gastrointestinal, and reproductive epithelial tracts (Kreda et al., 2012). As a result, the decreased airway surface liquid (ASL) and mucociliary escalator malfunction create an unusual thick viscous mucosal layer. For the respiratory tract in particular, subsequent pulmonary lesions can be caused by obstruction of the bronchioles that blocks the airways and leads to thickening of the bronchiole walls (bronchiectasis) and the alveoli (bronchiolitis). The plugs of mucoid material trapped in the airways favours microbial colonisation resulting in a vicious circle of phlegm retention, pathogen infections and chronic inflammation. Chronic inflammation causes lung damage that ultimately advances to the stage of irreversible fibrosis (Hauser et al., 2011, Lavoie et al., 2011, Katkin, 2014).

CFTR is a large chloride channel glycoprotein consisting of two membrane-spanning regions and a cytoplasmic regulatory R domain and is expressed primarily in epithelial cells but can also be found in leukocytes (Cohen and Prince, 2012) (Fig. 1.8). In addition to chloride transportation, CFTR also regulates the functions of other ion channels such as  $\text{Na}^+$  and  $\text{HCO}_3^-$  thus

coordinating the fluid and electrolyte absorption in the airway epithelium (Sheppard and Welsh, 1999, O'Sullivan and Freedman, 2009). Nearly 2000 mutations in the CFTR gene have been identified and are classified into 5 types of mutations: class I, lack of CFTR production; class II, protein trafficking defect with ubiquitination and degradation in the endoplasmic reticulum and Golgi body; class III, defective CFTR activation; class IV, deficient ion transport at the apical membrane; class V, splicing defect with reduced production of normal CFTR, thus cause disease by impairing CFTR translation, cellular processing, and/or chloride channel gating (O'Sullivan and Freedman, 2009, Rowe and Verkman, 2013). The most prevalent mutation  $\Delta F508$ , which accounts for two-thirds of mutated alleles in northern European and North American populations (O'Sullivan and Freedman, 2009), belongs to the class II group of mutations and causes misfolding of the CFTR protein and degradation by endosome (Ratjen, 2009). Mutation G551D causes a partially functional channel whose activity can be potentiated by potentiators. The oral therapy Ivacaftor, a potentiator that restores CFTR cAMP-dependent chloride channel activity at the cell surface has recently been proved effective to treat CF patients with mutation at G551D (Derichs, 2013).

### **1.2.2. Airway inflammation in cystic fibrosis**

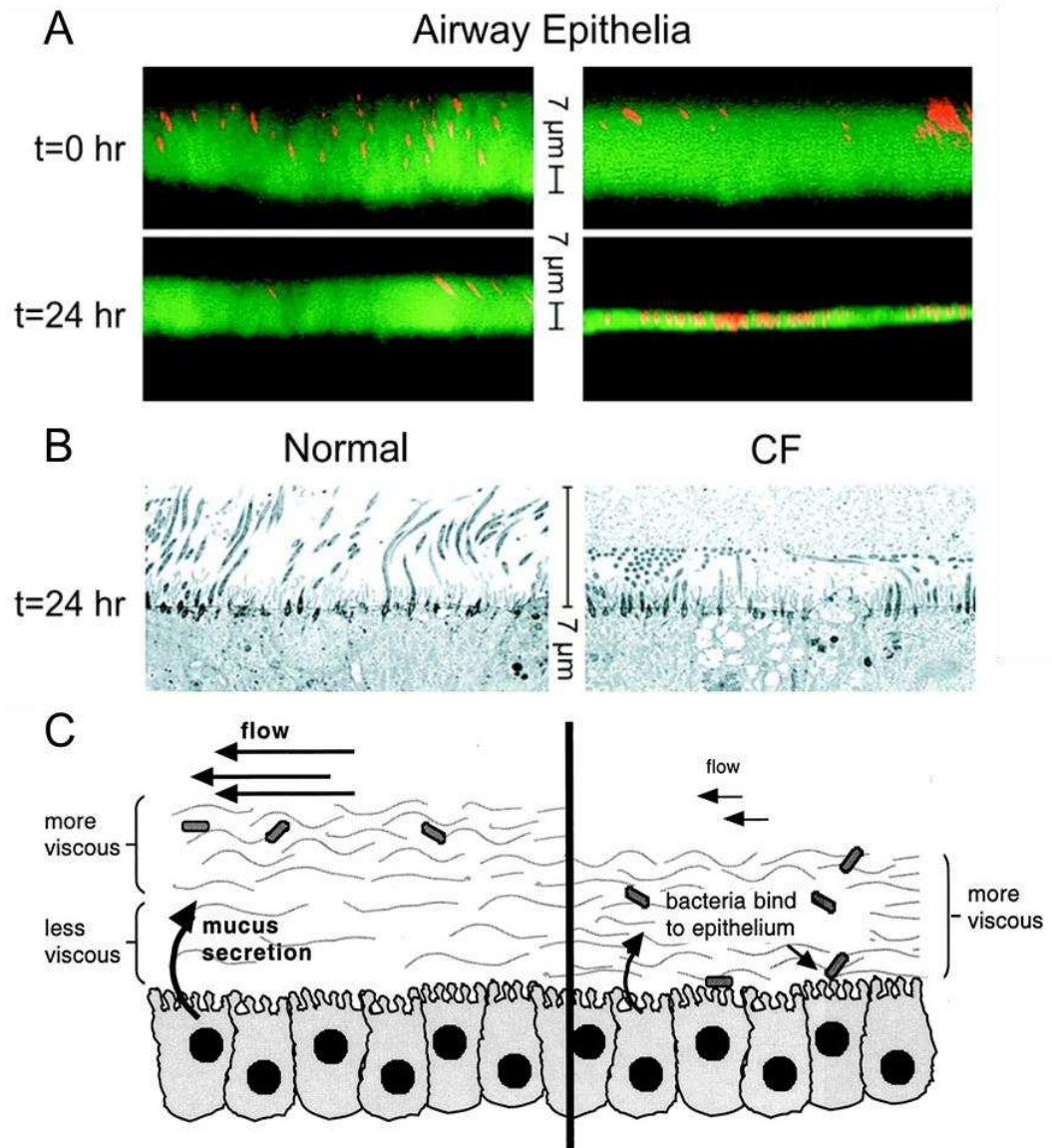
In vitro studies showed that dysfunction of CFTR predisposes airway epithelial cells to constitutive activation of proinflammatory signalling even in the absence of microbial stimulation (Cohen and Prince, 2012). Elevated endogenous activation of NF- $\kappa$ B leads to the induction of interleukin 8 (IL-8) and TNF- $\alpha$  in the airways and the recruitment of neutrophils (Cohen-

Cymerknoh et al., 2013). High levels of IL-8 correlated with the increased neutrophil count and free neutrophil elastase activity in the bronchoalveolar lavage (BAL) of most infants (Sagel et al., 2012). In addition, the accumulation of abnormally processed CFTR in the endoplasmic reticulum results in unfolded protein responses that trigger 'cell stress' and apoptosis leading to dysregulation of the epithelial cells and innate immune function in the lung, resulting in exaggerated and ineffective airway inflammation (Konstan et al., 1994, Jacquot et al., 2008, Cohen-Cymerknoh et al., 2013). The following sections provide recent insights in the development of the airway inflammatory process in CF including aspects of endogenous effects in the airway epithelium and immune cell functions.

#### 1.2.2.1. Effects of epithelial cells in CF airway inflammation

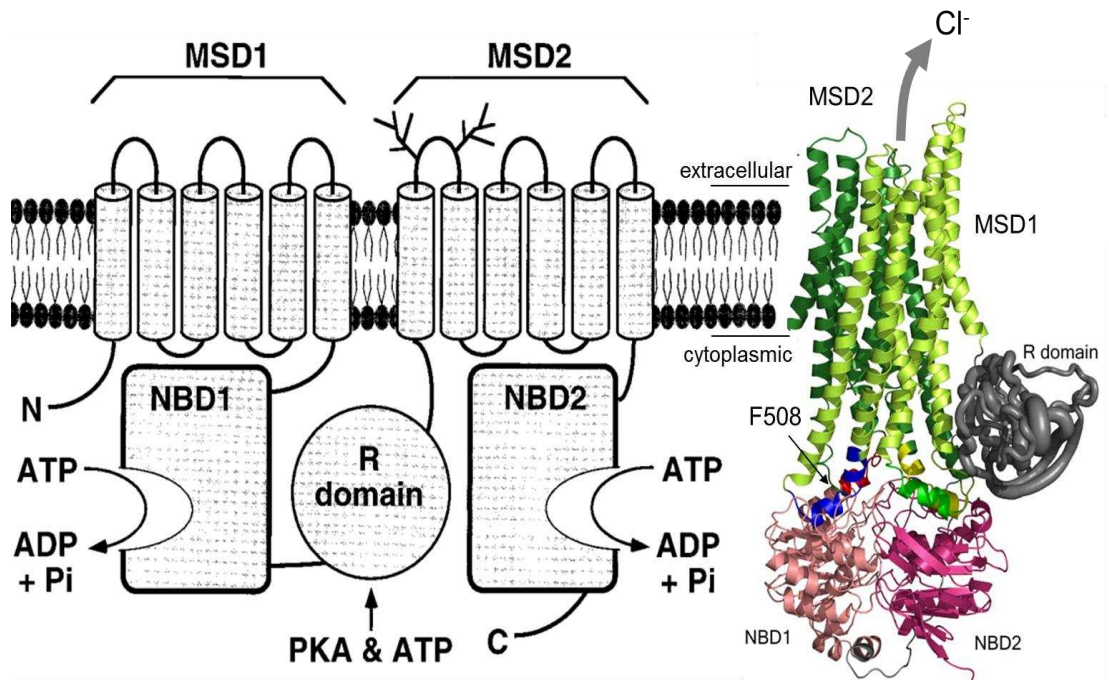
Inherent abnormal intracellular signalling pathways lead to abnormal apoptosis, cell stress and exaggerated cytokine production and propagating the inflammatory events in the CF airways. The activation of p38 and ERK/MAPKs pathways with high levels of NF- $\kappa$ B, p65 (RelA/RelB) and inhibition of I $\kappa$ B kinase, which is the primary inhibitor of NF- $\kappa$ B, was demonstrated in some CF epithelial cell lines and has been associated with altered CFTR function (Cohen-Cymerknoh et al., 2013). As mentioned above, another intrinsic proinflammatory feature in CF is the cytosolic accumulation of misfolded or unfolded CFTR proteins in the endoplasmic reticulum (ER) (Cohen-Cymerknoh et al., 2013).





**Figure 1.7 Comparison of airway surface liquid topography between normal and CF bronchial epithelial cells.**

Mucus in airway surface liquid (ASL) is compact in CF airways due to excessive absorption of  $\text{Na}^+$  ion and fluid retention. A, Confocal microscopic images show thicknesses of fluid surface layers at time 0 and 24 h after covering cultured normal (left) and CF (right) bronchial epithelial cells with dextran (Green, Oregon green-dextran; red, 1  $\mu\text{m}$  red fluorescent microsphere). 1  $\mu\text{m}$  red-bead retention was observed in the ASL below 7  $\mu\text{m}$  thick. B, Electron micrographs of tissues 24 h after applying the same fluid load above each culture of cells. The thin CF layer above and the apparently compressed cilia in the image below indicate excessive fluid absorption. C, Schematic illustration of the viscous mucus layer occupying the apical surface of the airway epithelium that causes ineffective mucociliary clearance in CF. Figure adapted from (Quinton, 2010, Matsui et al., 1998, Lyczak et al., 2002).



**Figure 1.8 Proposed model of CFTR structure.**

Theoretical CFTR is shown with a schematic presentation (black and white on the left (Sheppard and Welsh, 1999)) and a crystal structure simulation on the right (Serohijos et al., 2008). The CFTR primary structure contains two nucleotide-binding domains (NBD1 and NBD2) that control channel opening, two membrane-spanning domains (MSD1 and MSD2) each with six membrane-spanning  $\alpha$ -helix, and a regulatory region (R domain) that undergoes cAMP-dependent phosphorylation by protein kinase A (PKA) and possibly other kinases results in channel activation. Each MSD contains two cytoplasmic loops that form interfaces with the NBDs. Homologous NBD and MSD structures have been modelled (Patrick and Thomas, 2012) whereas the R domain remains largely unstructured. Phenylalanine-508 (F508) is located at the N-terminal NBD1. PKA, protein kinase A. Figure reconstructed from (Sheppard and Welsh, 1999, Serohijos et al., 2008).

The production of antioxidants such as glutathione (GSH) and thiocyanate (SCN<sup>-</sup>) as well as their trafficking to the ASL are essential in response to the oxidative damage in the airway epithelium (Rahman and MacNee, 2000). Systemic GSH secretion to the epithelial surface is significantly reduced in CF patients and in the CF mouse model; increased oxidative stress in turn leads to further induction of IL-8 gene expression (Roum et al., 1993, Bartling and

Drumm, 2009). Bactericidal components hypochlorite ( $\text{OCl}^-$ ) and  $\text{SCN}^-$  generated by airway epithelial cells eliminate bacterial infections in the airway surface. Epithelial cells with mutations in CFTR fail to secrete  $\text{SCN}^-$  and are compromised in their ability to kill bacteria (Moskwa et al., 2007).

Intracellular alkalinisation and pH reduction in the ASL are also caused by CFTR deficiency. Reduced pH in the ASL resulting in impaired antimicrobial function was demonstrated in the porcine CF lung (Pezzulo et al., 2012).

Mediators such as microRNA (miR) have also been studied in the regulation of airway inflammation in the CF lung (Tsuchiya et al., 2013). High levels of miR-155 and miR-215 in ex vivo CF epithelial cells were associated with increased production of IL-8 and pro-apoptotic pathway p53 (Tsuchiya et al., 2013), suggesting miRNA also contributes to the differential regulation of inflammation in the CF airways.

#### 1.2.2.2. The function of immune cells in CF

The influx of neutrophils is of importance for bacterial clearance during infection. However, the massive neutrophil accumulation in the CF lung does not correlate with bacterial eradication but rather causes extensive tissue damage and inflammation disproportionate to infection. This indicates that the function of neutrophils is dysregulated in CF (Cohen-Cymerknoh et al., 2013). Neutrophil elastase, shown to be present in the airway early in paediatric CF patients, induces a pro-inflammatory state of senescence in bronchial epithelial cells in vitro and correlate with the decline of lung functions (Gifford and Chalmers, 2014). Circulating neutrophils from CF patients display higher

CD64 (marker of neutrophil activation) and decreased level of TLR2 compared to neutrophils from healthy donors, and airways neutrophils from CF patients produce high levels of IL-8, are unresponsive to lipopolysaccharide (LPS) and peptidoglycan stimulation, as well as resistant to the anti-inflammatory mediator IL-10 (Petit-Bertron et al., 2008). Thus, the differential expression patterns of circulating neutrophils and airway neutrophils in CF suggest a complex neutrophilic inflammation in CF.

Alveolar macrophages in BAL were increased in paediatric CF patient (median age 3 yr) compared with non-CF in the absence of infection and were associated with elevated levels of CC chemokines including macrophage inflammatory protein (MIP-3 $\alpha$ , MIP-1 $\alpha$  and MIP-1 $\beta$ ), chemokine C-C motif ligand (CCL20), and monocyte chemoattractant protein-1 (MCP-1) (Brennan et al., 2009). The exaggerated pro-inflammatory response in CF might also derived from impaired function of peripheral macrophages where decreased expression of CD11b and TLR5, elevated production of inflammatory cytokines and deficient phagocytosis were demonstrated (Simonin-Le Jeune et al., 2013).

Dysregulated adaptive immune response was also described in CF. Studies have suggested that CFTR deficiency results in a Th2 cell bias upon *P. aeruginosa* infection (Hartl et al., 2006), although recent data showed that Th17 signalling plays a key role in response to extracellular pathogens in CF (Tan et al., 2011). IL-17 is a proinflammatory cytokine that has been implicated in mucosal neutrophil recruitment via regulating the local production of CXCR2 ligands CXCL1, CXCL6 and CXCL8 that are chemoattractants for neutrophils, together with neutrophil survival factors

granulocyte macrophage colony-stimulating factor (GM-CSF) and granulocyte colony-stimulating factor (G-CSF) from the airway epithelium (Traves and Donnelly, 2008). High levels of IL-17 and IL-23 were found in BAL of patients with CF during pulmonary exacerbations and increased numbers of IL-17 secreting cells, including Th17, nature killer (NK) T cells and  $\gamma\delta$  T cells were also found in paediatric patients in the absence of elevated IL-8. The above evidence indicates the importance of IL-17 secreting cells in the modulation of airway inflammation at early stage of CF.

### **1.2.3. Respiratory infections in cystic fibrosis**

Infections in the upper airways predispose the lower respiratory tract of CF patients to a particular subset of microbial pathogens. *Staphylococcus aureus* and *Haemophilus influenzae* are amongst the most commonly isolated pathogens in infants and paediatric patients in CF (Hauser et al., 2011). Although infections by these two pathogens are under control since antibiotic intervention was introduced, the breach of epithelial barrier by the above pathogens might therefore cultivate a colonisation niche for subsequent infections from nosocomial pathogens or even opportunistic pathogens. The prevalence of *P. aeruginosa* infection increases with age, and together with *Burkholderia cepacia* infection, is associated with rapid declines in the lung function of CF patients (Hauser et al., 2011). *B. cepacia* is highly transmissible and elicit robust inflammation in the host resulting in acute deterioration (Jones et al., 2004, Kalish et al., 2006). Around 15-20% of CF patients are colonised with *Stenotrophomonas maltophilia*, methicillin-resistant *S. aureus* (MRSA) and the colonisation is associated with the deterioration of pulmonary function

(Dasenbrook et al., 2008). Fungus *Aspergillus fumigatus* is also frequently isolated in CF patients. *A. fumigatus* usually does not cause invasive infection but rather induces intense allergic response which is known as allergic bronchopulmonary aspergillosis. This may affect up to 15% of patients with CF and the symptoms include wheezing, pulmonary infiltrates, and bronchiectasis (Stevens et al., 2003, O'Sullivan and Freedman, 2009).

#### 1.2.3.1. *Pseudomonas aeruginosa*

*P. aeruginosa* is a Gram-negative aerobic rod-shaped motile bacterium with a single or two flagella categorised in the family Pseudomonadaceae. It is environmentally ubiquitous and thrives in a wide range of ecological niches from soil, water, plants to animal tissues. *P. aeruginosa* carries a large genome size of 6.3 million base pairs that is believed to provide it with metabolic versatility and environmental adaptability (Stevens et al., 2003, Stover et al., 2000). The intrinsic low susceptibility to antibiotics of *P. aeruginosa* is attributable to the action of multidrug efflux pumps and *P. aeruginosa* is naturally resistant to penicillin and the majority of  $\beta$ -lactam antibiotics. *P. aeruginosa* is also an opportunistic pathogen that preferentially infects susceptible individuals with compromised epithelial barrier that can be caused by tracheal intubation, urinary tract catheterisation, mechanical ventilation or burn wounds (Lavoie et al., 2011, Engel and Eran, 2011). The respiratory tract infection by *P. aeruginosa* is the leading cause of mortality in patients with CF.

Consistent with the large genome size and versatile life pattern, *P. aeruginosa* exploits tightly regulatory mechanisms to control the expression of virulence determinants such as elastase, exotoxins, pyocyanin and biofilm formation.

Many of them are regulated in a cell density-dependent manner via cell-cell communication or so-called quorum-sensing (QS). Amongst the QS systems identified in *P. aeruginosa*, this thesis has focused on the investigation of the contribution of alkyl-quinolone (AQ) QS to *P. aeruginosa* pathogenesis and that will be further discussed in chapter 2.

#### 1.2.3.2. *P. aeruginosa* adaptation to the CF lung

According to the cystic fibrosis foundation annual report, half of CF patients under 18 years of age are infected with *P. aeruginosa* and the prevalence rises up to 80% of patients age above 18 (Hauser et al., 2011). The mechanisms of how *P. aeruginosa* compete with other pathogens to adapt in the CF lung is still unclear, despite theories on the initial infections of the lung epithelium by *S. aureus* and *H. influenza* cultivating a niche suitable for *P. aeruginosa* persistence (Hauser et al., 2011). Here the evidence of phenotypic changes of *P. aeruginosa* that are considered superior for adaptation in the CF lung is listed. As mentioned above, in the CF airways, the function of the mucociliary clearance, cationic antimicrobial peptides and neutrophils and macrophages are impaired and inflammatory signal transduction pathways exaggerated. This results in the chronic airway colonisation with opportunistic pathogens and leads to life-threatening lung disease. Being a ubiquitous environmental strain, it is intriguing how *P. aeruginosa* shifts its lifestyle from an environmental unobtrusive planktonic life-pattern to a biofilm-forming phenotype during infection in the host. There are several virulence factors involved either in initial attachment and invasion or in the later chronic stage.

## Early colonization

Colonisation of CF airways is mediated by the adhesion of cell appendages such as flagellum and type IV pili to host epithelial cell surfaces. Studies have demonstrated that a type IV pili-associated protein (PilY1) is required for *P. aeruginosa* adherence to mucosal epithelium and preferentially binds to the exposed basolateral cell surfaces (Heiniger et al., 2010, Bucior et al., 2012). After attachment, *P. aeruginosa* is thought to inject type III secretion proteins ExoU, S, T, and Y into the host cells. These secreted proteins were identified to have a role in activating pro-apoptotic pathways, modulating small GTPases, enhancing *P. aeruginosa* invasive capabilities by interacting with multiple eukaryotic cytoskeletal components, such as tight junctions and causing cell death as a consequence (Soong et al., 2008, Kipnis et al., 2006, Engel and Balachandran, 2009, Angus et al., 2010). In addition, *P. aeruginosa* elastases, LasA and LasB, and alkaline protease are thought to modulate host immunoregulatory proteins and damage epithelia through mitogen-activated protein kinase (MAPK) pathways, increasing IL-8 expression (Azghani, 1996).

## Late stage adaptation

The long-term persistence of *P. aeruginosa* in CF lung is characterised by the process of adaptive radiation, which causes the selection of a variety of genotype and phenotypes (Hogardt and Heesemann, 2010). The adaptability of *P. aeruginosa* confers a selective advantage to better thrive in the diverse niches and microenvironments of the inflamed and hostile CF lung. Loss-of-function mutations in genes such as *lasR*, *mucA* and *mexT* lead to a general adaptation pattern of *P. aeruginosa*. More intriguingly, several cellular



virulence factors including type II secreted elastases and pyoverdines, exotoxins S/T/Y secreted via T3SS, pyocyanin and siderophores were attenuated. The most striking clinically important feature of *P. aeruginosa* infection is the tendency of this bacterium to adjust its life style from a single cell to mucoid phenotype. This phenotypic change probably initiates the chronic infection stage and therefore, enables *P. aeruginosa* to survive in the microaerobic or even anaerobic environment in CF lungs. *P. aeruginosa* mucoid exopolysaccharide, alginate has been shown to reduce chemotaxis of neutrophils into the CF lung and by itself to inhibit activation of the complement system. Mutated mucoid *P. aeruginosa* is inherently resistant to macrophage and neutrophil phagocytosis (Matsui et al., 2006). Clinical isolates of *P. aeruginosa* from a single CF sputum sample appear morphologically diverse and include mucoid variants, non-mucoid pyomelanin producing variants, non-pigmented LPS-rough variants and small-colony variants. This high mutation rate of variants that coexist with non-mutated variants is another evidence of how *P. aeruginosa* accelerates its ecological fitness in the CF lung (Hogardt and Heesemann, 2010, Hauser et al., 2011).

### **1.3. AIMS AND OBJECTIVES**

A type of QS in *P. aeruginosa*, the Pseudomonas alkyl-quinolone QS signal (PQS) which has been detected in the CF lung, regulates virulence and has been shown to have immunomodulatory properties. However, the contribution of PQS to *P. aeruginosa* infection of human bronchial epithelium needs better characterisation. Chapters 2 to 5 aimed to increase our understanding of inflammation in the CF airways by investigating the impact of the cell density-dependent regulator of *P. aeruginosa* pathogenesis, PQS, in the interaction with human bronchial epithelial cells. The main aims of each chapter were 1) to generate a *P. aeruginosa* mutant deficient in PQS to identify the impact of PQS on the expression of virulence factors in vitro; 2) to develop an in vitro human bronchial epithelial infection model and 3) to use an in vitro airway epithelial model to investigate the role of PQS in the innate immune recognition of *P. aeruginosa* by airway epithelium; 4) to use a CF clinical isolate to assess the efficacy of the airway epithelial cell infection model retrospectively.

The aim of Chapter 6 was to understand the systemic immune response in patients with idiopathic pulmonary fibrosis. This was achieved by an exploratory study measuring cytokine production by PBMCs, which was later correlated with clinical outcomes.

## **2. GENERATION AND CHARACTERISATION OF A *PSEUDOMONAS AERUGINOSA* MUTANT DEFICIENT IN ALKYL-QUINOLONE PRODUCTION**

---

### **2.1. INTRODUCTION**

*P. aeruginosa* is an opportunistic pathogen known for its metabolic plasticity to adapt a variety of environments such as that encountered in the CF lungs and where it has evolved the ability to form biofilms which are difficult to eradicate by antibiotics (Winsor et al., 2011, Heeb et al., 2011). Antibiotics work by inhibiting bacterial cellular processes that are essential for microbial survival, thus they pose a selective pressure which results in the emergence of drug resistant mutants. The population density-dependent regulatory systems called quorum sensing are used by many bacterial pathogens to regulate the expression of virulence factors, but they are not essential for survival under most conditions. Therefore, the disruption of quorum sensing (termed ‘quorum quenching’) (QQ) is considered as an alternative to attenuate virulence without imposing the level of selective pressure posed by currently used antibiotics. (Galloway et al., 2011, Jimenez et al., 2012). *P. aeruginosa* employs a complex cell-cell communication network to coordinate the expression of a plethora of genes, many of which code for virulence determinants (Williams and Cámara, 2009). Driven by the urgent need to develop alternative therapeutic strategies (LaSarre and Federle, 2013, Galloway et al., 2011), a comprehensive

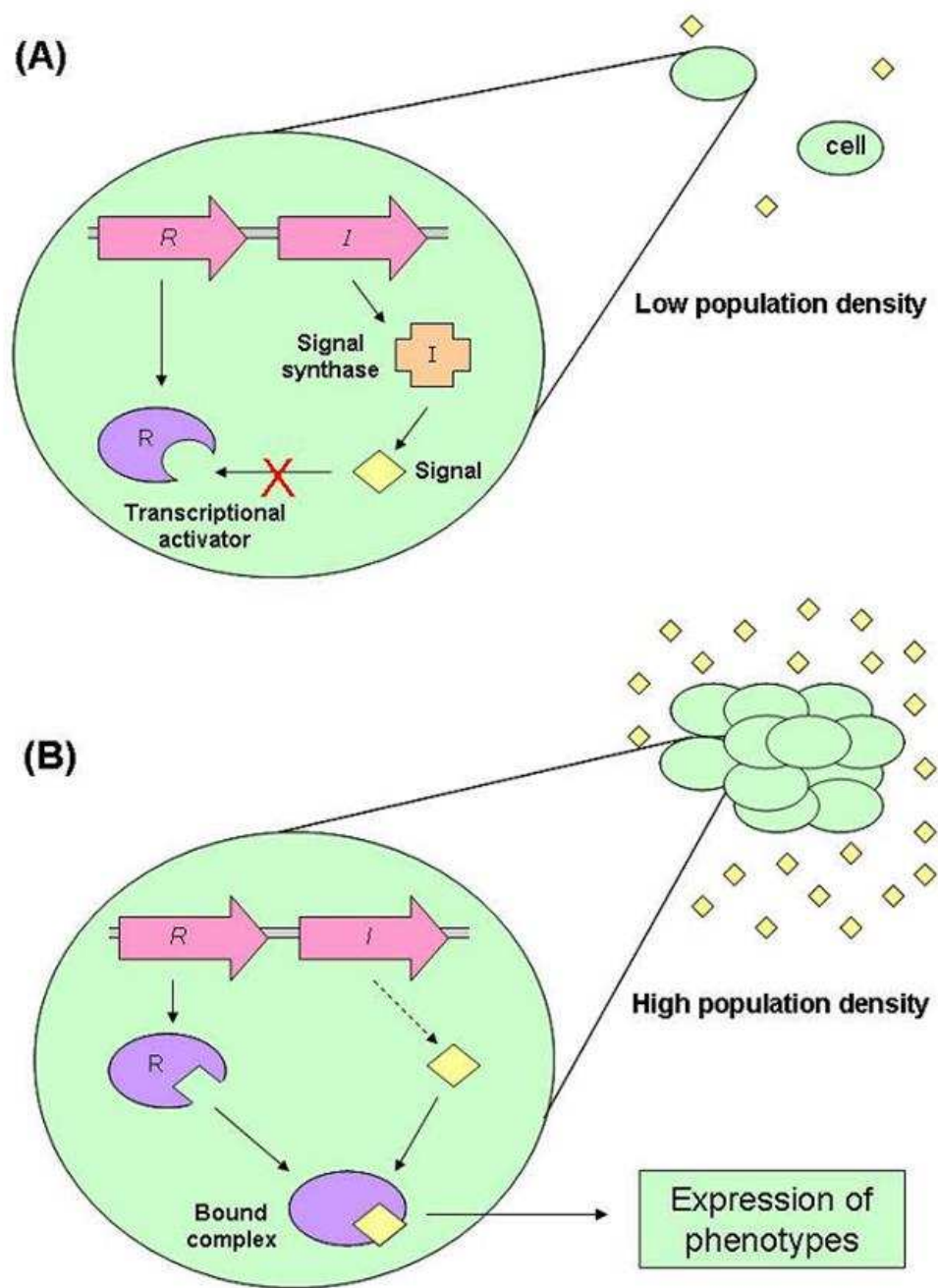
understanding on the role of QS on the interactions between *P. aeruginosa* and the human airway epithelium is paramount.

For the present chapter, the influence of QS on *P. aeruginosa* pathogenesis and its potential as a therapeutic target was further evaluated. In particular, the work focused on the alkyl-quinolone (AQ) QS system that is also known as the *Pseudomonas* quinolone signal (PQS) system. To achieve this, a mutant in blocking the AQs biosynthetic pathway for these signal molecules was constructed and its virulence was analysed. The following introduction sections will describe the QS networks in *P. aeruginosa*, their roles in virulence as well as the need for the generation of a new mutant in the PQS system.

### **2.1.1. Quorum-sensing**

Quorum-sensing (QS) is an intercellular co-operative behaviour of bacteria used to coordinate the activities of individual cells (Miller and Bassler, 2001, Heeb et al., 2011, Williams and Cámara, 2009). This signalling mechanism is based on the use of diffusible signal molecules (also known as ‘autoinducers’) which, when they reach a threshold concentration, can coordinate multiple gene expression and a change in the behaviour of the bacterial population through the activation of sensor regulatory proteins. These activated regulators are also able to induce the transcription of the genes involved in the biosynthesis of the signal molecules triggering an autoinduction feed-back loop which results in more signal generation and changes in the whole bacterial population (illustrated in Fig. 2.1). QS is responsible for the regulation of a large number of genes, for instance, around 10% of genes in the genome of *P. aeruginosa* are regulated by QS system (Williams and Cámara, 2009). The QS

signal synthase, QS signal receptor, and QS signal molecules are three essential elements of basic QS circuit machinery. The phenomena of QS was firstly described in the marine bioluminescence bacterium *Vibrio fischeri* that has been considered the paradigm of QS for the majority of Gram-negative bacteria (Nealson and Hastings, 1979). The bioluminescence was initiated with the luciferase operon (*luxICDABE*) where *luxI* encodes the autoinducer synthase that generates N-(3-oxo-hexanoyl)-L-homoserine lactone (3-oxo-C6 HSL) and *luxCDABE* codes for proteins responsible for bioluminescence production. This operon is regulated by the LuxR protein, also known as the QS transcriptional regulator/activator. Binding of 3-oxo-C6 HSL by LuxR activates the expression of the *luxICDABE* operon which in turns results in the production of more of this signal molecule, through an auto induction feedback loop, and bioluminescence (Engebrecht and Silverman, 1984). LuxI/LuxR homologues are widely spread in Gram-negative bacteria such as *Yersinia enterocolitica* (Atkinson et al., 2006), *Burkholderia pseudomallei* (Eberl, 2006), *Salmonella enterica* (Michael et al., 2001), *Vibrio harveyi*, *Vibrio cholerae* (LaSarre and Federle, 2013) and *Pseudomonas aeruginosa* (Galloway et al., 2011, Waters and Bassler, 2005) amongst many other. QS in *P. aeruginosa* will be discussed further in this chapter.



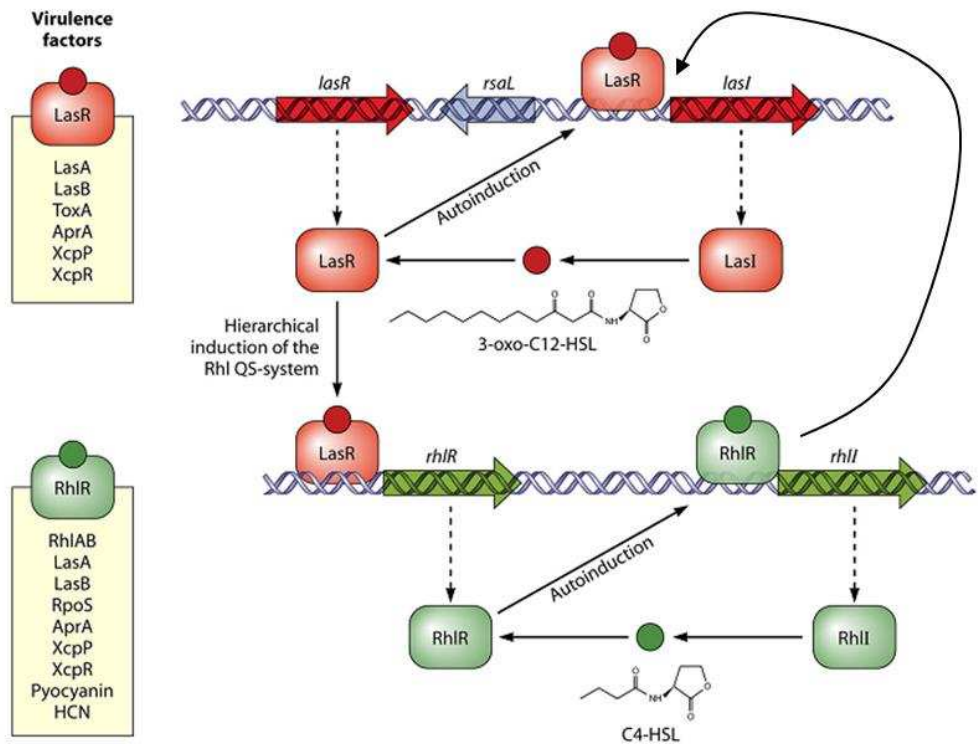
**Figure 2.1 General mechanism of quorum sensing autoinduction in Gram-negative bacteria.**

(A) At low population densities autoinducer signal concentration is low and cannot bind to the corresponding transcriptional activator protein due to unfavourable binding kinetics. (B) At higher population densities, signal concentration reaches the threshold at which it binds to the transcriptional regulatory protein inducing a conformational change. The bound complex subsequently regulates the expression of QS dependent phenotypes. R, QS transcriptional regulator (autoinducer receptor); I, autoinducer synthase. Figure adapted from (Fletcher, 2007).

## 2.1.2. Quorum-sensing in *Pseudomonas aeruginosa*

### 2.1.2.1. N-acylhomoserine lactone driven quorum-sensing in *P. aeruginosa*

Two N-acylhomoserine lactones (AHL)-based QS systems named *las* and *rhl* circuits in *P. aeruginosa* have been widely studied (Heeb et al., 2011, Lee et al., 2013, Diggle et al., 2006a). The *las* system is composed of an analogous of Lux-like synthase LasI and LuxR-like receptor, LasR. LasI mediates the synthesis of the autoinducer N-(3-oxododecanoyl)-L-homoserine lactone (3-oxo-C12-HSL). This molecule is responsible for the activation of the transcriptional regulator LasR which in turns binds to the promoter region of *lasI* ultimately resulting in the production of more 3-oxo-C12-HSL. The LasR/I QS system controls the secretion of virulence factors such as elastase, the protease LasA, alkaline protease, exotoxin A and biofilm development (Diggle et al., 2003). Similarly, the *rhl* system is composed of another LuxI/LuxR-type system termed RhlI/RhlR. RhlI mediates the synthesis of N-butanoyl-L-homoserine lactone (C4-HSL) which upon binding to RhlR activates the production of many virulence determinants including rhamnolipids, elastase, LasA protease, hydrogen cyanide, pyocyanin, and the cytotoxic lectins LecA and LecB (Williams, 2007, Cooley et al., 2008). The *las* and *rhl* systems control more than 6% of the *P. aeruginosa* genome (Schuster et al., 2003). Although it was originally thought that the LasR/I QS system work in a hierarchical way by controlling the expression of the RhlR/I system, it has now been shown that RhlR/I can function in the absence of the LasR being even able to activate *lasI* expression and a range of LasR/I controlled phenotypes (Dekimpe and Deziel, 2009) (Fig. 2.2).



**Figure 2.2 Interactions between the two AHL QS systems in *P. aeruginosa* and their regulation in virulence.**

After a threshold concentration of 3-oxo-C12-HSL is reached the 3-oxo-C12-HSL–LasR complex binds the promoter regions of multiple genes, activating or repressing their transcription. Among the genes upregulated by this complex are *lasI*, which enhances the production of 3-oxo-C12-HSL (autoinduction effect), and *rhlR*, which increases the production of the *rhl* transcriptional regulator RhIR, activating the second AHL pathway. Virulence factors regulated by correspondent receptor-ligand complex are detailed on the left. Figure adapted from (Jimenez et al., 2012).



#### 2.1.2.2. The alkyl-quinolones QS network in *P. aeruginosa*

The study of the AQs from *P. aeruginosa* as signal molecules began from their intriguing structures similar to antimicrobial quinolones (Pesci et al., 1999). The role of PQS as a QS signal molecule was first described by Pesci et al., 1999. Although PQS is not an antimicrobial, further studies unveiled that among more than 50 alkyl-quinolones found in *P. aeruginosa*, 2-heptyl-3-hydroxy-4(1H)-quinolone (PQS) and its precursor molecular 2-heptyl-4(1H)-quinolone (HHQ) can also work as QS signal that cooperates with the AHL-dependent QS system in *P. aeruginosa* (Xiao et al., 2006a, Heeb et al., 2011). Synthesis of 2-heptyl-3-hydroxy-4(1H)-quinolone (PQS) depends on the *pqsABCDE* operon. PqsA, the anthranilate co-enzyme A ligase, catalyses anthranilate that produced by *phnAB* to anthraniloyl-coenzyme A. PqsD then mediates the synthesis of 2-aminobenzoylacetate (2-ABA) from anthraniloyl-coenzyme A and malonyl-CoA, decarboxylating coupling of 2-ABA to an octanoate group of octanoic acid that linked to PqsC and PqsB to produce HHQ (Dulcey et al., 2013). HHQ can be transformed to 2-heptyl-3-hydroxy-4(1H)-quinolone (PQS) by the mono-oxygenase PqsH (Fig. 2.3) (Diggle et al., 2006a, Pesci et al., 1999). HHQ and PQS are the major AQ QS signalling molecules. PqsR, also known as MvfR, is a LysR-type transcriptional regulator, with a conserved N-terminal DNA-binding helix-turn-helix and a C-terminal co-inducer-binding domain. PqsR activates the transcription of *pqsABCDE* and possibly the *phnAB* operon when binding to PQS or HHQ and triggers the typical QS autoinducing response enhancing AQ biosynthesis (Maddocks and Oyston, 2008, Heeb et al., 2011). PQS has been shown to reach the maximal production at late logarithmic phase (Diggle et al., 2003) and its production is

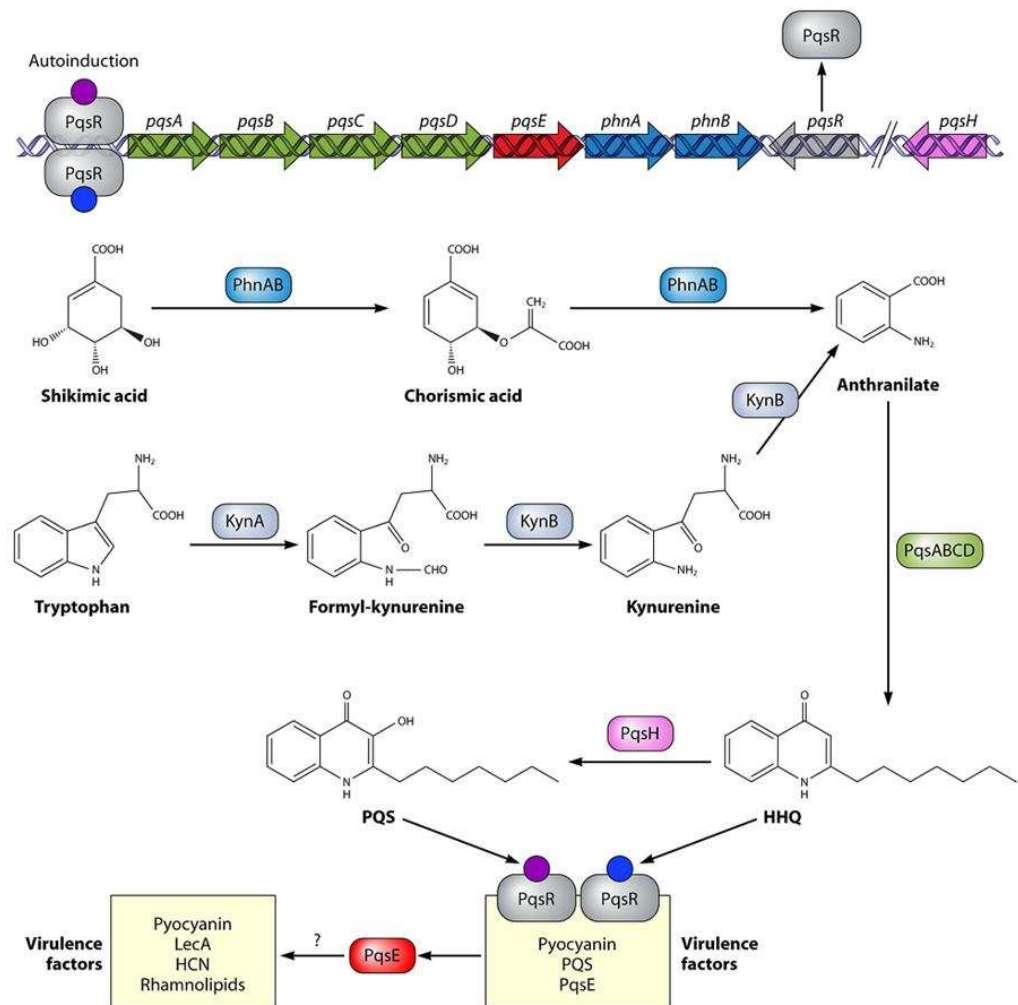
also promoted by the availability of the substrate anthranilate and presence of the aromatic amino acids tryptophan, phenylalanine and tyrosine (Palmer et al., 2005). The las QS circuit increases the expression of pqsR and pqsA as well as controlling the expression of pqsH indicating las acts as a positive regulator of PQS (Xiao et al., 2006b). However, the biosynthesis of PQS only partially relies on the las system since PQS is still produced during late stationary phase in the absence of lasR (Diggle et al., 2003). In contrast to the las QS system, the rhl system negatively regulates the PQS production (Heeb et al., 2011, Xiao et al., 2006b).

PQS is regarded as a multifunctional molecular in addition to the regulatory role in quorum-sensing (Williams and Cámara, 2009). PQS has iron-chelating properties that contributes to iron transport and it is thought to facilitate siderophore-mediated iron delivery (Diggle et al., 2007). PQS is also involved in cell autolysis at high population densities in nutrient deprived conditions (Williams and Cámara, 2009). It has been demonstrated that there is far less DNA release in a pqsA mutants than its wild-type counterpart in both planktonic and biofilm cultures (Allesen-Holm et al., 2006).

The control of virulence by the AQ systems remains a puzzle. Whilst PQS can have an impact on the expression of genes related to iron starvation, the control of most virulence factors is exerted by PqsE. Although this protein has been crystallised, this has not revealed any key information with regards to its mechanisms for controlling virulence gene expression. Virulence in a pqsA mutant has been shown to be restored by PqsE on its own to nearly wild-type levels. Furthermore, PqsE has been shown to negatively regulate the expression

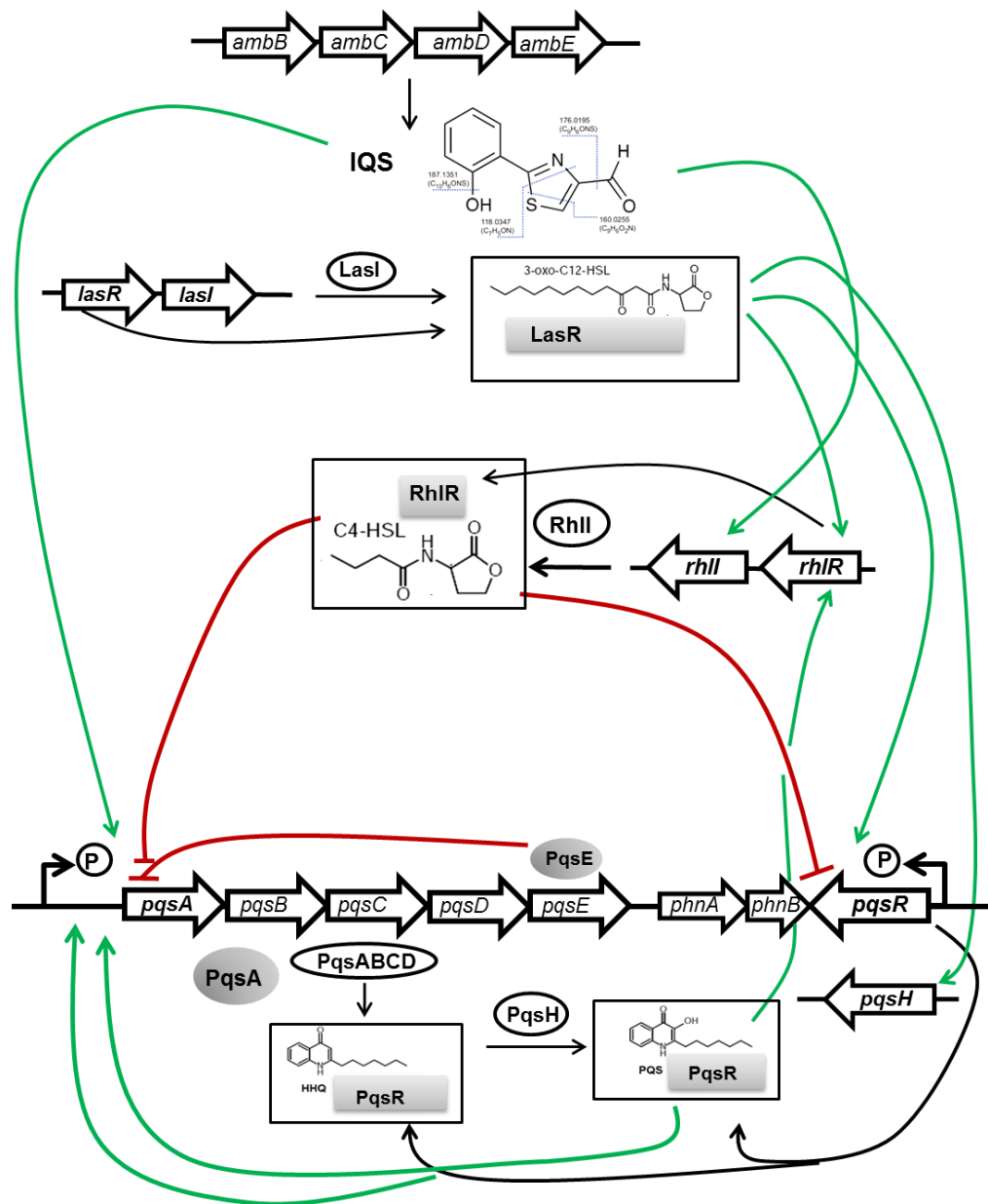
of the *pqs* operon as a way to modulate virulence (Folch et al., 2013, Rampioni et al., 2010, Hazan et al., 2010).

Recently, a new QS molecule, 2-(2-hydroxyphenyl)-thiazole-4-carbaldehyde (IQS) encoded by the *ambBCDE* operon was discovered (Fig. 2.4). IQS is induced when *P. aeruginosa* is exposed to a phosphate deprived environment (Lee et al., 2013). Under an unfavourable environment, expression of IQS overcomes the *las*-led QS circuit and promotes the expression of virulence factors. This finding may also partially explain how *P. aeruginosa* clinical isolates persist in CF respiratory infection in the absence of a functional *las* system (Winstanley and Fothergill, 2009).



**Figure 2.3 Biosynthesis, autoinduction, and virulence regulation by alkyl-quinolones in *P. aeruginosa*.**

Biosynthesis of PQS starts with the conversion (by the PqsABCD proteins) of anthranilate (originates from either the kynurenine pathway or the PhnAB anthranilate synthase) into HHQ, which is converted into PQS by the PqsH monooxygenase. Both HHQ and PQS bind the PqsR regulator, and the complex activates the transcription of the pqsABCDE and phnAB operons, increasing the levels of PQS (autoinduction) and pyocyanin production. Additionally, transcription of the PQS operon results in an increase in the levels of PqsE that increases the levels of pyocyanin, lectin, HCN, and rhamnolipids. Figure adapted from (Jimenez et al., 2012)



**Figure 2.4 Integration of quorum-sensing networks in *P. aeruginosa*.**

The best described QS systems in *P. aeruginosa* are the AHL and AQ driven systems which are closely interlinked. The expression of the *pqsABCDE* operon is up-regulated by LasI/LasR but negatively controlled by RhlI/RhIR system. PQS enhances the production of RhlI/RhIR by activating the expression the autoinducer receptor, RhIR. The above three systems work reciprocally in an intertwined manner resulting in a fine control of virulence gene expression in *P. aeruginosa*. A newly uncovered cell-cell communication signal, IQS, functionally substitutes the central *las* system when *P. aeruginosa* in under phosphate-deprived environment. Disruption of IQS biosynthesis disabled the *pqs* and *rhl* QS systems and attenuated *P. aeruginosa* virulence in vitro. Green lines denote positive regulation; red lines denote negative regulation. This QS architecture diagram was expanded from (Williams and Cámara, 2009, Lee et al., 2013).

### **2.1.3. The impact of alkyl-quinolones on *P. aeruginosa* pathogenesis**

Despite the fact that the AHL-based QS systems of *P. aeruginosa* have been shown to play a central role in the regulation of virulence and immune modulation in vitro, this situation could very much change in vivo. In the CF lung 50% of strains from late stage CF patients are deficient in lasR function (Winstanley and Fothergill, 2009). Moreover, abolishing the whole AHL QS by generating a quadruple mutation of rhlIR and lasIR exerted comparable infectivity to the wild-type strain in a mouse lung infection model (Lazenby et al., 2013), suggesting that the AHL-dependent QS might not be required for full pathogenesis in vivo and other regulatory mechanism might be involved.

PQS has been identified in sputum, bronchoalveolar lavage fluid, and mucopurulent fluid from distal airways of end-stage CF lungs removed for transplant (Collier et al., 2002) and at different stages of the disease, from asymptotic early stage to late progression, implying a potential role of PQS in coordinating virulence factors during the course of infection (Collier et al., 2002, Guina et al., 2003). An in vitro transcriptomic study investigating the physiology of *P. aeruginosa* grown in CF sputum revealed that expression of genes associated with PQS metabolism, such as those coding for the aromatic amino acid aminotransferase, 4-hydroxyphenylpyruvate dioxygenase (hpd) and pqsABCDE, was more than 10-fold induced compared to their expression in media containing glucose as carbon source (Palmer et al., 2005). In other words, the Pqs QS circuit, rather than the AHL-dependent QS may have a more dominant role in the control of virulence factors during infection of the CF lung. The above evidence suggests a pivotal role for the Pqs QS system in

orchestrating the production of virulence determinants and facilitating *P. aeruginosa* persistence in the human host.

#### 2.1.3.1. Virulence factors under the control of PQS

*P. aeruginosa* produces a wide range of virulence determinants and many of them are regulated by QS. The virulence factors chosen for discussion below are those strongly controlled by the Pqs QS system.

##### Elastase B

Elastase B (LasB) is an elastolytic metalloproteinase encoded by the *lasB* gene. Over 75% of clinical isolates of *P. aeruginosa* secrete elastase B. Previous in vitro studies have shown that LasB degrades a number of components of the innate and adaptive immune systems, including surfactant proteins, antibacterial peptides, cytokines, chemokines and immunoglobulins (Kuang et al., 2011, Singh et al., 2010). PQS positively controls the expression of the *lasB* gene and this expression increases synergistically in the presence of both PQS and C4-HSL (McKnight et al., 2000).

##### Pyocyanin

Pyocyanin acts as a redox-active toxin required for full pathogenesis of *P. aeruginosa* in animal infection models (Lau et al., 2004). *P. aeruginosa* produces high levels of pyocyanin in the CF lungs and these levels are directly correlated with the deterioration of lung function (Winstanley and Fothergill, 2009, Caldwell et al., 2009). Pyocyanin inhibits ciliary beat frequency in airway epithelial cells, induces cytotoxicity in A549 alveolar epithelial cells by

suppressing catalase activity and induces neutrophil extracellular trap (NET) formation (Rada et al., 2013, O'Malley et al., 2003). PqsE is essential for pyocyanin production via the control of phenazine biosynthetic operons. Interestingly, PqsE can control pyocyanin production in the absence of PQS (Rampioni et al., 2010, Jimenez et al., 2012).

### Rhamnolipids

Rhamnolipids are biosurfactants that enhance bacterial surface translocation and mediate the uptake and degradation of hydrophobic compounds in the surrounding environment (Noordman and Janssen, 2002). Apart from being involved in adaptation to the environment, rhamnolipids also act as innate immune-modulators in the human host. Rhamnolipids purified from *P. aeruginosa* culture supernatants inhibited the production of IL-1 $\beta$  and the antimicrobial peptide, human  $\beta$ -defensin hBD-2 from keratinocytes by affecting protein kinase C signalling (Dossel et al., 2012, Gerstel et al., 2009). Rhamnolipids were also found to initiate bacterial biofilm dispersal from a mucoid clinical strain PA17 and induce necrotic death of neutrophils (Davey et al., 2003, Jensen et al., 2007). Rhamnolipids exerted cytotoxicity and acted as heat-stable extracellular hemolysins controlled by QS during *P. aeruginosa* chronic infection (Noordman and Janssen, 2002, Johnson and Boese-Marrazzo, 1980, Wang et al., 2013, Jensen et al., 2007).

In *P. aeruginosa*, three genes linked to the rhl QS system, rhlAB and rhlC, code for the enzymes responsible for the last step of rhamnolipids synthesis (Abdel-Mawgoud et al., 2010, Reis et al., 2011). The Pqs QS system positively regulates the rhl QS system and hence promotes rhamnolipid biosynthesis in a



las QS independent manner. Additionally, due to the production of rhamnolipids occurs at late log phase which corresponds to the time point when PQS accumulates to the maximum (Reis et al., 2011), it is likely that the Pqs QS system exerts a key regulatory role over the expression of rhamnolipids.

## Biofilms

*P. aeruginosa* undergoes a phenotypic transition from planktonic cells to a biofilm state to survive to environmental stress conditions. A biofilm is a complex dynamic mixture consisting of cells surrounded by an extracellular matrix made of exopolysaccharides, secreted proteins, nucleic acids and cellular debris (Mann and Wozniak, 2012). Biofilm attachment to the surface of biomedical devices such as urinary catheters and respiratory ventilators leads to severe nosocomial infections difficult to control. It has been recognised that *P. aeruginosa* chronic persistence in the CF lung might be driven by biofilm development as biofilms are 1,000 times more resistant to antibiotics than planktonic cells (Wagner and Iglewski, 2008). Interest in the development of methods for dispersing biofilms and improved coating of medical implants is rising in order to tackle biofilm-forming pathogens that can persist long-term in the host (Hook et al., 2012, Hansch, 2012). QS contributes to biofilm development in different ways. The *psl* (polysaccharide synthesis locus) operon is essential for the initiation and maintenance of biofilms and is tightly controlled by bis-(3'-5')-cyclic dimeric guanosine monophosphate (c-di-GMP) (Wei and Ma, 2013). LasR can bind to the *psl* promoter region, suggesting that QS can regulate biofilm formation (Wei and Ma, 2013).

A key component in biofilms is the presence of extracellular DNA (e-DNA). PQS has been shown to play a key role in the release of e-DNA enhancing biofilm formation this way (Yang et al., 2009). The QS regulated lectins LecA and LecB which bind sugars from the surface of *P. aeruginosa* have been shown to also play an important role in biofilm formation (Diggle et al., 2006b, Tielker et al., 2005). Furthermore, the QS controlled rhamnolipids are required for the formation of mature biofilms and their water channels also play an important role in biofilm dispersal (Boles et al., 2005, Davey et al., 2003).

#### Type III secretion system and the transition from acute to chronic infection

Toxins translocate into host cells via a transmembrane syringe-like apparatus constituted of around 25 proteins designated as type III secretion system (T3SS). Insertion of the T3SS of Gram-negative pathogens on eukaryotic cells results in pore formation and acute cell death (Shafikhani et al., 2008). The biochemical characteristics of at least five T3SS effector proteins in *P. aeruginosa* including ExoS, ExoT, ExoU, ExoY and FliC, have been extensively studied (Diaz et al., 2011). ExoS is essential and sufficient for the induction of caspase-3-dependent cell death but it is expressed only by approximately one-third of clinical isolates. ExoU, a phospholipase, induces necrotic cell death and ExoY is an adenylate cyclase that contributes to *P. aeruginosa* virulence in a mouse model of pneumonia (Soong et al., 2008). ExoT inhibits bacterial internalization into epithelial cells through its ADP-ribosyltransferase domain activity and suppresses cell migration by altering the actin cytoskeleton. Together, T3SS exotoxins enhance *P. aeruginosa* invasive capacities by interacting with eukaryotic cytoskeletal components, including

tight junction proteins zonula occludin 1 (ZO-1), occluding and ezrin (Angus et al., 2010).

T3SS is considered to be responsible for acute infection but is lost during chronic persistence. Although there have been numerous studies trying to understand the mechanisms governing the switch between acute to chronic infection and in particular the regulation of T3SS in *P. aeruginosa*, there is still a significant gap in the knowledge of this transition. A study examined the profile of virulence factors associated with chronic infections using five sequential clinical samples isolated from a single patient who developed ventilator-acquired pneumonia. A reduction in pyoverdinin production and increased secretion of ExoU and ExoT in the latter strains indicated that *P. aeruginosa* underwent a transition from a typical chronic to an acute phenotype in this clinical context. Moreover, the authors also found that PQS production and *pqsA* gene expression were higher in strains isolated during the chronic infection; addition of the PQS inhibitor farnesol to these strains, in turn promoted ExoU secretion. These findings supported the idea of PQS playing an important role in the modulation of T3SS and hence the transition between an acute to a chronic status (Singh et al., 2010).

#### 2.1.3.2. The impact of PQS on *P. aeruginosa* virulence

The contribution of the Pqs QS system to virulence was firstly described by Cao, et al. using a *pqsR* knock-out mutant in *P. aeruginosa* PA14. *PqsR* positively regulates the expression of *phnAB* operon in this strain and the production of elastase, 3-oxo-C12, as well as PQS, thereby influencing the production of numerous virulence determinants. The *pqsR* mutant was

attenuated up to 320-fold in the *Arabidopsis* plant infection model caused a 65% reduction in mortality in a burn wound mouse disease model (Cao et al., 2001). The interaction of PqsR with the AHL QS circuit was investigated by another group showed that the effect of pqsR deficiency on pathogenesis was independent from LasRI/RhlRI (Deziel et al., 2005). This finding highlighted the importance of PQS on *P. aeruginosa* pathogenicity. Mutations in the multidrug efflux pump, such as mexI and opmD led to the inhibition of PQS production and the attenuation of *P. aeruginosa* in rat and plant infection models (Aendekerk et al., 2005). Additionally, provision of exogenous Aqs to these mutants restored virulence on plants (Aendekerk et al., 2005). In 2010, Rampioni et al. found that both pqsA and pqsE mutants in PAO1 were attenuated in plant, nematode and mouse burn wound infection models (Rampioni et al., 2010).

The QS signal molecules 3-oxo-C12-HSL, PQS and HHQ have been shown to have an important role not only in controlling the expression of virulence factors and biofilm formation in *P. aeruginosa* but also the interactions of this organism with the host (Williams and Cámara, 2009). In this chapter we will only focus on the Aqs system. PQS was shown to inhibit T cell proliferation resulting in the inhibition of interleukin-2 (IL-2) production. However, PQS did not inhibit tumour necrosis factor alpha (TNF- $\alpha$ ) release from human monocytes treated with *Escherichia coli* lipopolysaccharide as 3-oxo-C12-HSL did, suggesting that PQS has very distinct immune modulatory properties from 3-oxo-C12-HSL (Hooi et al., 2004). Both HHQ and PQS can inhibit the innate immune response in a murine model. Extracts from culture supernatants of a PA14 pqsA mutant elicited higher levels of TNF- $\alpha$  and IL-6 production by a

mouse monocyte cell line than those extracted from wild-type PA14 that contains PQS. The addition of exogenous PQS to a pqsA mutant restored this inhibitory activity on mouse monocytes and primary bronchoalveolar cells via the suppression of the signalling mediated by the innate immune regulator nuclear factor- $\kappa$ B (NF- $\kappa$ B) (Kim et al., 2010b). Apart from the interference with the NF- $\kappa$ B activation cascade, PQS extracted from *P. aeruginosa* culture supernatant was found to suppress the HIP-1 $\alpha$  protein expression in human bronchial epithelial cells (IB3-1) (Schaible et al., 2013, Legendre et al., 2012). The hypoxia-inducible factor 1 (HIP-1) is a transcriptional factor required for adaptation to cellular stress caused by low-oxygen and has been recently associated with infection and inflammation. The upregulation of HIP-1 via NF- $\kappa$ B pathway facilitates phagocytosis and enhances the innate immune activities of dendritic cell, mast cell and epithelial cells in response to microbial infection (Nizet and Johnson, 2009). These findings suggested AQS acts differently from AHLs in the inhibition of host innate immune responses.

Despite the proposed contribution of the PQS molecules themselves to the interactions of *P. aeruginosa* with the host, there is still very little known on the role these molecules play on the interaction of this organism with the human airways. Our study was thereby initiated to address this question and expand our understanding of the role AQS have in the initial recognition of *P. aeruginosa* in the human lung.

#### **2.1.4. Generation of a *pqsA* mutant in PAO1 Lausanne**

During the course of a study in our laboratory investigating the regulatory role of RsmA (a small RNA binding protein that acts as a post-transcriptional regulator controlling many phenotypes including swarming), it was discovered that a  $\Delta$ *rsmA* mutant in the PAO1-subline Nottingham (PAO1-N) was unable to swarm, whereas swarming was maintained in a *rsmA* in PAO1-subline Lausanne (PAO1-L) (Mai-Prochnow, et al., manuscript in preparation). This led to the discovery of some key genomic differences between PAO1-N and PAO1-L which revealed that PAO1-L was closer to the original PAO1 ancestor strain as this organism has been shown to evolve very quickly (Klockgether et al., 2010). The main difference between these two strains was a 58,569 base pair chromosomal deletion in PAO1-N, between bases 724103 – 780973, which was not present in PAO1-L. Amongst the genes present in this region is *toxR* (PA0707) which codes for a key regulator of exotoxin A (ETA), an important virulence factor in *P. aeruginosa*. ToxR was later shown to modulate swarming motility (Mai-Prochnow, et al., manuscript in preparation). Subsequently, genomic sequencing of PAO1-N and PAO1-L revealed the presence of a number of single nucleotide polymorphisms (SNPs) in the PAO1-N strain (Hardeep Naphra, on-going PhD thesis). Hence there was a risk that the attenuation observed in a  $\Delta$ *pqsA* constructed in PAO1-N using a mouse burn wound model of infection could in part have been influenced by these strain differences (Rampioni et al., 2010). To gain a better understanding of how PQS impacts on *P. aeruginosa* pathogenesis, a new *pqsA* in-frame deletion mutant was constructed in the PAO1-L background. The generation and characterisation of this mutant would be described in this chapter. The

effect of PQS on the interaction of *P. aeruginosa* with human bronchial epithelium was subsequently investigated and described in chapter 4.

## **2.2. HYPOTHESIS**

Previous studies using *P. aeruginosa* PQS-deficient mutants indicated that interfering with AQ biosynthesis could reduce *P. aeruginosa* virulence in plant, nematode, and mouse burn wound models. Based on the high levels of PQS detected in bronchoalveolar lavage fluids from both early and late stage CF patients, we hypothesised that PQS could potentially influence the virulence of *P. aeruginosa* interaction with human bronchial epithelial cells.

## **2.3. AIM**

To understand the impact of PQS in coordinating *P. aeruginosa* pathogenesis during the infection of the differentiated human bronchial epithelium, an AQs deficient mutant was generated by in-frame deletion of the *pqsA* gene in the PAO1-L background. This chapter includes the genotypic and phenotypic characterisation of this new mutant (termed  $\Delta pqsA_L$ ) and a comparison with a *pqsA* mutant generated previously in PAO1-N.



## **2.4. MATERIALS AND METHODS**

### **2.4.1. Bacterial strains, plasmids and culture condition**

The strains and plasmids used in this study are listed in Table 3.1. Both *E. coli* and *P. aeruginosa* strains were routinely grown in Luria broth (LB) at 37°C with 200 rpm shaking. Antibiotics were added to culture media when required: ampicillin at the concentration of 100 µg/ml was added to LB to maintain the cloning plasmid pBluescript KS II (+) in *E. coli* DH5α; tetracycline at the concentration of 25 µg/ml in LB was used to select for the suicide vector pME3087 in *E. coli* S17-1 λpir; tetracycline at 150 µg/ml was used for pME6032mCherry in *E. coli* DH5α. Antibiotics tetracycline at 20 µg/ml and carbenicillin at 2,000 µg/ml were used for the enrichment step during mutant generation to obtain tetracycline sensitive colonies.

### **2.4.2. Generation of a pqsA in-frame deletion mutant in PAO1-L**

#### 2.4.2.1. DNA manipulation

Chromosomal DNA extracted from *P. aeruginosa* was prepared using a Wizard Genomic DNA purification kit (Promega, UK) following manufacture's recommendations. Briefly, bacterial cells from 1 ml overnight culture were centrifuged for 2 min at 13,000 rpm; cell pellets underwent lysis, RNase treatment, protein precipitation and genomic DNA precipitation and rehydration.

Plasmid DNA isolation was conducted using the Qiagen Miniprep kit (Qiagen, UK) according to the manufacturer's protocol.

**Table 2.1 Bacterial strains and plasmids used in this study**

Strain/plasmid	Relevant characteristics	Reference or origin
<b>Strain</b>		
E. coli		
DH5 $\alpha$	Cloning strain; F' endA1 hsdR17 supE44 thi-1 recA1 gurA96 relA1 $\Delta$ (lacZYA-argF)U169 deoR $\lambda$ ( $\phi$ 80lacZ $\Delta$ M15)	(Grant et al., 1990)
S17- $\lambda$ pir	Conjugative strain for suicide plasmids	(Simon et al., 1983)
P. aeruginosa		
PAO1-L	Wild-type P. aeruginosa from Université de Lausanne, Switzerland	
<i>ΔpqsA<sub>L</sub></i>	pqsA mutant in PAO1-L background	This study
PAO1-N	P. aeruginosa PAO1 collection from University of Nottingham	
<i>ΔpqsA<sub>N</sub></i>	pqsA mutant in PAO1-N background	
<b>Plasmid</b>		
pBluescript-II KS+	Cloning vector; ColE1 replicon; Amp <sup>R</sup>	Agilent Technologies, US
pME3087	Suicide vector, polylinker of pMMB67, ColE1-replicon; Tc <sup>R</sup>	(Voisard et al., 2007)
pYCL1	pME3087 derivative for pqsA in-frame deletion; Tc <sup>R</sup>	This study
pME6032mCherry	pME6032 with mCherry fusion constitutively expresses red fluorescence protein	(Heeb et al., 2002)

Amp<sup>R</sup>, ampicillin resistant; Tc<sup>R</sup>, tetracyclin resistant

To identify the size of DNA fragments, DNA samples were mixed with 6x DNA loading buffer (Promega, UK) and loaded into 1% (w/v) agarose gel in 1X TAE buffer (40 mM Tris, pH 8.0, 20 mM acetic acid, and 1 mM EDTA) supplemented with ethidium bromide (Sigma-Aldrich, UK) to a final concentration of 10  $\mu$ g/ ml. The gels were run in 1X TAE buffer in a DNA electrophoresis tank at 100 volt for 20 min. DNA fragments were visualised using a UV trans-illuminator (UVP, USA). Restriction enzyme digestions and ligations were carried out by standard methods described in Molecular Cloning (Sambrook et al., 1989).

#### 2.4.2.2. Introduction of DNA to bacteria

Electro-competent cells were prepared by using overnight E. coli or P. aeruginosa cultures to start a new culture in LB to OD<sub>600</sub> 0.6-0.8. Cells were harvested by centrifugation at 10,000 x g at 4°C for 5 min and washed with

10% sterile ice-cold glycerol in H<sub>2</sub>O (Sigma-Aldrich, UK) four times. The wash volume was reduced by half each time. After the washes, the cell pellets were resuspended in 40-60 µl of 10% glycerol, aliquoted and stored at -80°C for future use. Electroporation was conducted in 0.2 cm electrode gap Gene Pulser cuvettes (BioRad, UK) using 20 µl of competent cells and 20 pg of DNA. A pulse of 2.5 kV (200 %) was delivered using the BioRad Gene Pulsar connected to a BioRad pulse controller (BioRad, UK). Cells were resuspended in 1 ml of LB broth, incubated at 37°C for 1 h, plated onto LB agar plates containing appropriate antibiotics and grown overnight at 137°C.

#### 2.4.2.3. Generation of plasmid pME3087mpqsA (designated as pYCL1)

To construct the plasmid pYCL1, a pqsA deletion fragment that joined a 410-bp fragment upstream of the pqsA gene and a 423-bp downstream fragment were generated and amplified by overlap extension PCR using *P. aeruginosa* PAO1-L chromosomal DNA as template. In the first PCR, the upstream 410-bp fragment was amplified using the forward primer pqsAf1 (Table 2.2) which carries a XbaI restriction site, and the reverse primer pqsAr1 with an overhanging end containing the last 12 nucleotides of the pqsA gene (underlined) and 3 extra artificial nucleotides at the 3' end to enable the primer to anneal to the DNA template (bold); the 423-bp fragment was amplified by the forward primer pqsAf2 containing 3 nucleotides upstream of pqsA and the first 12 nucleotides of pqsA; reverse primer pqsAr2 which carries a *Hind*III restriction site. To perform the overlap extension PCR, a second PCR reaction was performed using the 410-bp and 423-bp fragments as templates and the primers pqsAr1 and pqsAf2 (Table 2.3). The final PCR product (mpqsA) was

cloned into pBluscript II KS(+) vector using the *Xba*I and *Hind*III restriction sites. The correct construction was confirmed by nucleotide sequencing. Subsequently the deletion fragment was cloned into the suicide vector, pME3087, resulting the new recombinant plasmid pYCL1 for further mutant generation.

#### 2.4.2.4. Mutation of the *P. aeruginosa* pqsA gene

The PAO1-Lausanne pqsA in-frame deletion was constructed by allelic exchange using the suicide vector pYCL1. The cloning strategy is illustrated in Fig. 2.5. Briefly, the first homologous recombination of mpqsA fragment with sequences on PAO1-L genome took place by conjugation of PAO1-L as recipient and *E. coli* S17-1 $\lambda$ pir/pME3087mpqsA as the donor cells on a LB agar plate containing tetracycline at 125  $\mu$ g/ml and nalidixic acid at 15  $\mu$ g/ml (Heurlier et al., 2004). Next day, colonies on the selective plate were picked for purification on LB agar plate with the same antibiotic concentration, cultured at 37°C overnight. The pqsA deletion mutants were firstly screened by colony PCR using primer pqsAf1 and pqsAr2. The desired PCR amplicon should be 833 bp, but the amplicon could also be 2,367 bp if recombination didn't occur. Mutant candidates selected from colony PCR were subjected to enrichment with carbenicillin to excise plasmid pYCL1 from PAO1-L. The enrichment was carried out by culturing colonies in 5 ml of LB without antibiotics overnight at 37°C, 200 rpm. Next day, a new culture was prepared using the overnight culture as inoculum and an initial OD<sub>600</sub> of 0.05-0.1. Tetracycline was added to the culture to a final concentration of 20  $\mu$ g/ml and the culture was incubated for 1 h at 37°C with shaking. Carbenicillin to a concentration of

2,000 µg/ml was added afterwards to kill dividing cells, leaving only cells that are tetracycline sensitive. This culture was thereafter cultured for another 6 hours, centrifuged at 4,000 xg for 10 min, and the pellets were resuspended in 1 ml of fresh LB to start a new overnight culture. The same procedure was performed again next day. At day 3, the overnight culture from day 2 was centrifuged, pellets resuspended in 1 ml LB and 100 µl from serial dilutions in LB were plated on LB agar plates and incubated at 37°C overnight. Colonies were re-streaked both on LB agar with and without tetracycline at 100 µg/ml to confirm loss of tetracycline resistance and screened by colony PCR. The pqsA deletion in the recombinant strain was then verified by nucleotide sequencing.

**Table 2.2 Primer sequences for *ΔpqsA<sub>L</sub>* mutant generation**

Primer	Oligonucleotide Sequence (5' → 3')	Description	T <sub>m</sub> (°C)
pqsAf1	ATAT <u>CTAGAC</u> CGCCTCGAACTGTGAGATTT	With an underlined XbaI restriction site	60
pqsAr1	TCAACATGCCCGTTC <u>CAATGTGGACATGAC</u> AGAACG	Underlined and bordered sequences are complementary therefore they join two DNA fragments during overlap extension PCR. Nucleotides ATG (CAT antisense) in bold indicate the start codon of pqsA	66.5
pqsAf2	<b>GTCATG</b> TCCACATTGGAACGGGCATGTTGATTCAGG		65.7
pqsAr2	TATA <u>AAGCTT</u> ACTCGCTGTCCACTTCCAAT	With an underlined HindIII restriction site	59.7

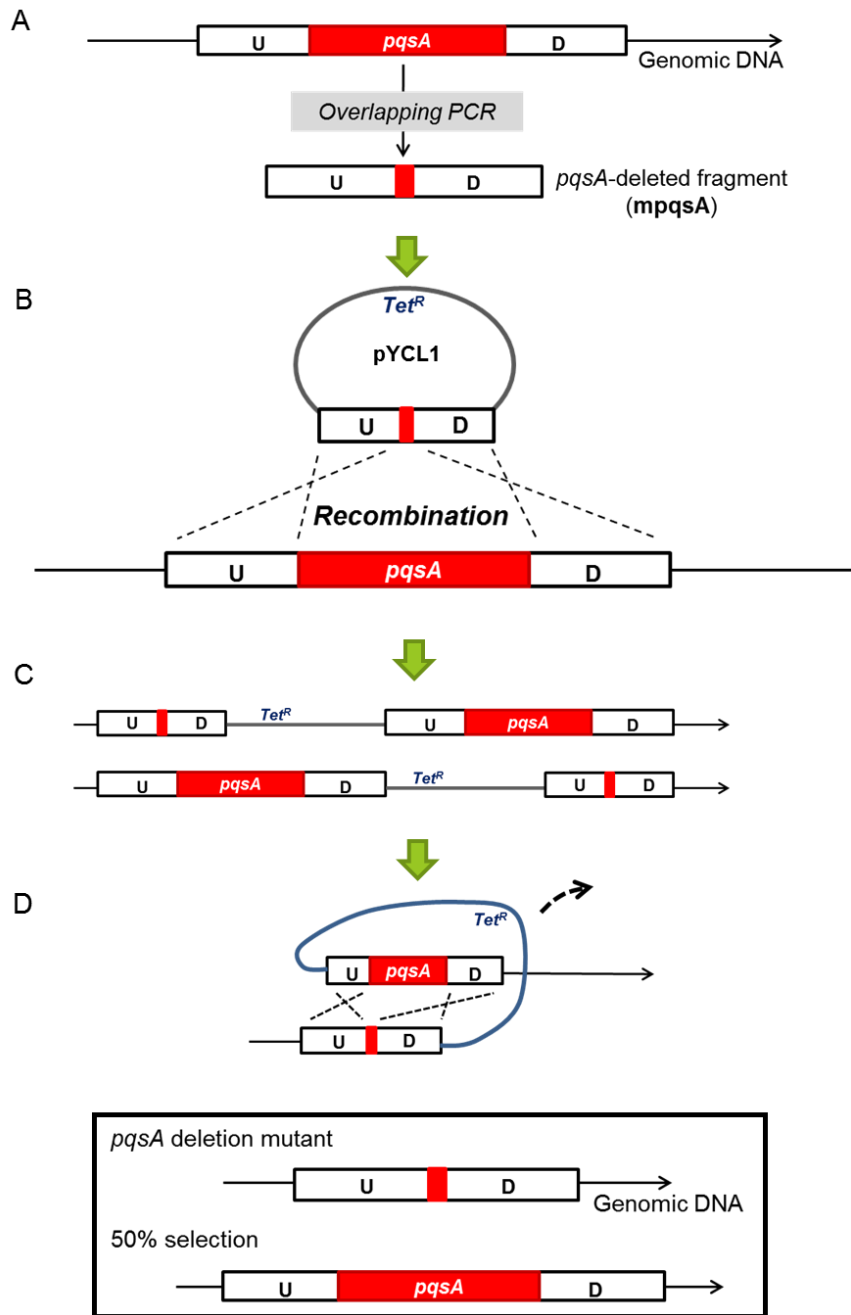
**Table 2.3 pqsA gene nucleotide sequence along with its 800 bp upstream and downstream sequence**

pqsA gene nucleotides are in blue colour; the pqsA upstream region (410 bp) and downstream fragment (423 bp) used to generate mpqsA fragment are shaded. Primer pqsAf1 and primer pqsAr2 were designed to contain a restriction site for XbaI and HindIII respectively.

```

>upstream 800 bp + pqsA 1,554 bp + downstream 800 bp
AAATTCGGTACCTTGAAGTCGAGCGGGAGTTCGAACCGGGAACGTTTGCCGGAAAAATATT
CCCAGCACTGGCGTTTCGGTTTCCGCCAGGAGGGAGCTGTCTCGGAGAGCCGCATCTCGTCC
AGCGGTACTCGGTTGGGACGCTCATGTGCCAAAGAATCGCGACCAGAAAGGCATCGTCCCT
GGCTACCAGGGTCAGTGTCCCGACCGGCGATTCCATTTTCTGTAGCTATGGGGCATGTAGG
TGTCCTCTTCGGCAGGCTCGCCAGTGTACTACGCAATGGGATTTCAACAGGGAAGCCTGCA
AATGGCAGGCGAGGCGGGGCGGAGCGCTATCGGCCCGATG
                                     primer pqsAf1 ATA TCTAGA
GATGGCCGCCTGCTTCCAGGCATGCCGTGCCCCCTTGGAGCCCAGGCCGAGCGCCTCGAAC
TGTGAGATTGGGAGGCGATTTGCCGAGCAAAGTGGGTTGTCAATTGGTTTGCCATCTCATGG
GTTTCGGACGAGGCCCTCGAGCAAGGTTGTAACGGTTTTTGTCTGGCCAATGGGCTCTTGGCT
AAAAAGGCTGCCGCCCTTCTTGGCTTGGTTGCCGTTCTCGGATCCCGCGACGCCCGTGGGTG
TGCCAAATTTCTCGCGGTTTGGATCGCGCCGATTGCCCGCGCCTACGAAAGCCCGTGGTTCTT
CTCCCCGAACTTTTTCGTTCCGACTCCGAATATCGCGCTTCGCCACAGCCGCTAGTTTCC
CGTTCCTGACAAAGCAAGCGCTCTGGCTCAGGTATCTCCTGATCCGGATGCATATCGCTGAA
GAGGGAACGTTCGTGCATGTCCACATTGGCCAACCTGACCGAGGTTCTGTTCCGCCTCGATT
TCGATCCCGATACCGCCGTTTATCACTATCGGGGCCAGACTCTCAGCCGGCTGCAATGCCGG
ACCTACATTTCTCCCAGGCCAGCCAACTGGCCCGCTGCTCAAGCCCGCGCATCGCGTGGT
GCTGGCGTTGAACGACTCGCCTTCGCTGGCCTGCCTGTTCTTGGCCTACGATCGCGTCCGCG
CCATTTCCCGCGTGATCAATCCCAAGTCCCGCGAGCAGGCCCTGGCCGATATCGCTGCCGAC
TGCCAGGCCAGCCTGGTGGTGCCTGAAGCCGATGCACCGTCCGCTGAGCGGTCTTTGGCGCC
GTTGACCCTGCGTGCGGCCGCCGACGCCCTTTGCTCGACGATTTCTCGCTGGACGCGCTGG
TCGGCCCTGCGGACCTCGATTGGAGTGCCTTCCATCGCCAGGACCCGGCGGCAGCCTGTTTC
CTGCAATACACCTCGGGTTCCACCGGGGCGCCCAAGGGGGTGATGCACAGCCTGCGCAACAC
GCTCGGTTTCTGCCGGGCGTTCGCTACGGAGTTGCTGGCATTGCAGGCGGGAGACCCGGCTGT
ATTTCGATTTCCCAAGATGTTTCTTCGCTATGGCATGGGCAACAGCCTGTTCTTTCCCTGGTTC
AGCGGAGCCTCGGCGCTGCTCGACGATACCTGGCCGAGCCCGAGCGGGTCTGGAGAACCT
GGTCGCCTTCCGCCCCCGGTCTGTTTGGGGTCCCGCCATCTATGCCTCGCTGCGTCCGC
AGGCCAGGGAGCTGTTGAGCAGCGTGCGCCTGGCGTTTTCCGCCGCGCTCGCCGCTGCCGCGC
GGCGAGTTTCAATTCTGGGCCGCGCACGGGCTGGAGATCTGCGACGGCATCGGGGCTACCGA
GGTCGGCCATGTGTTCTCGCCAACCGCCCGGGCCAGGCGCGTGGCAGACAGCACCAGGCTGC
CGTTGCTGGCTATGAGTGGCCGGTGGTGGACCGGAAGGACACACTATCGAGGAAGCGGGC
CGCAAGGCGTGCTGTTGGTGCCTGGCCAGGGCTGAGTCCGGGTTACTGGCGGGCCAGCGA
AGAGCAGCAGGCGCGCTTCGCAGGTGGCTGGTACCGCACCGGCGACCTGTTTCGAGCGCGACG
AGTCGGGTGCCTACCGTCACTGTGGGCGGAAGACGATCTGTTCAAGGTGAATGGCCGCTGG
GTGGTGGCAGCCAGGTGAGCAGCGCATCTGCCGTCATCTGCCGGAAGTGAAGCAGCGCGT
TCTGGTTCTTACCTGCCGGCTGCACGACGGCTTGCCTCCGACCTGTTTCGTACCCCTGGCCA
CTCCGCTGGACGACAACAGATCCTGCTGGCGCAGCGCATCGACCAGCATCTCGCCGAACAG
ATTCCCTCGCACATGCTGCCAGCCAATTGCATGTGCTGCCGGCCTTGGCCGCAACGACAAA
CGGCAAGTTGGCGCGCGGAGCTGCGCCACCTGGCCGACACCCTTTATCACGACAACCTTC
CGGAGGAACGGGCATGTTGATTCAAGCTGTGGGGGTGAACCTGCCCCATCCTATGTGTGTC
TGGAGGGGCCGCTGGGAGGCGAACGCCCTCGCGCCAGGGCGACGAGATGCTGATGCAGCGC
TTGCTGCCGGCGGTTTCGCAAGCCCTGGACGAGGCGGCGGTCAAGCCGAGGAGATCGACCT
GATCGTCCGCCCTCGCCCTGTCTCCGACCATCTGATCGAGAACCAGCGACATCATGGCGCGA
AGATCGGCCATCCGTTGCAGAAGGTCTCGGCGGAATCGCGCGCATGCTTTCGACCTCACC
GACTCGAGCCTGGCCCGCGCCCTTACGTGGTGCATACCTCGCCAGGACCCAGGGCTATCG
CAACGTCCTGGTGTGCGCGGCGAATCCAGCCAGGGATTGGAAGTGGACAGCGAGTCCGGCT
TCGCCCTTCCGACGGCGCCCTGGCGCTGCTC
                                     AAGCTT ATA primer pqsAr2
TGCCGGCCGACCGCAAGGCCGCGTTCGTCGCGGTGCGCTGGGCGGTGATCCGGCGCAGGA
ATGGCTGCCGCTGAGCATTCCGCTGAATACCGATATTCGCCAGGTAGGCGACGTCAGGGGAC
ACCTCAACCTGCCGGCCCAACCTGGATTGCCCGAAGCGGTACGCGCCGGATTACCCCGTTCG
CCGGGGACTTCCCGCAACTGAATGGGTGCGCGAGGAATGGTTCCGGCAGGGACGCCCTCGA
TGGTGCCTTCCCTGGGGCCGTTTCAACTGGCGTCCGCAACTCGCGCGGCACAGCGCGCCGTC
TGGATGAAGTGTGCTGATCAGCTTCGATCCGTTCCGCATGGT

```



**Figure 2.5 Strategy to generate a *pqsA* in-frame deletion in PAO1-L.**

To generate an in-frame deletion mutant, a suicide plasmid carrying a deleted fragment of *pqsA* gene was constructed. A. The deleted gene fragment was generated by overlapping PCR which joined the upstream and downstream sequence of *pqsA* gene (fragment mpqsA). B. The 833 bp mpqsA fragment was cloned in the suicide vector pME3087 to become pYCL1 and was subsequently conjugated to PAO1-L. C. Homologous recombination between pYCL1 and PAO1-L chromosomal DNA was expected to occur as a result of pME3087 insertion into the chromosomal DNA. Conjugants were subjected to tetracycline and nalidixic acid selective medium plates. D. The second homologous recombination carried on and by tetracycline and carbenicillin enrichment, tetracycline resistant plasmids were eliminated out of the *P. aeruginosa* genomic DNA. The chromosomal DNA resulted in two genotypes; the desired mutation was expected to comprise 50% of total population.

### 2.4.3. Phenotypic characterisation of *ΔpqsA<sub>L</sub>*

#### 2.4.3.1. Determination of bacterial growth

Bacterial growth was measured under aerated and static conditions. For aerated conditions *P. aeruginosa* was grown in 25 ml of LB or X-vivo in a 250 ml flask, 200 rpm 37°C and OD<sub>600</sub> was measured using a spectrophotometer (BioMate 3s, Thermo Scientific, UK) every hour for 12 h and at 24 h. For static condition, cultures were growth in 96-well plates and OD<sub>600</sub> was read every 30 min for 24 hours using a microplate reader (Infinite® M1000 PRO, TECAN, UK).

#### 2.4.3.2. Detection of alkyl-quinolone using a biosensor assay

*P. aeruginosa* PAO1-L, *ΔpqsA<sub>L</sub>*, PAO1-N, *ΔpqsA<sub>N</sub>* and the AQ biosensor strain PAO1 *ΔpqsA CTX::PpqsA-lux* (Fletcher et al., 2007) were cultured overnight at 37°C, 200 rpm in LB or X-vivo 15 (Lonza, UK). Five ml of each *P. aeruginosa* culture were harvested and spun at 10,000g at 4°C for 5 min to collect the supernatant. The AQ biosensor culture was adjusted with LB medium to OD<sub>600</sub> 1.0 and diluted 1 in 50 and 1 in 100 for the assay. Test bacterial supernatants were mixed with the same volume of the 1:50 diluted biosensor culture; 1:100 dilution of the AQ biosensor alone was added to negative control wells, positive control wells contained a 1:100 dilution of the biosensor with 4 serial dilutions of pure synthetic PQS or HHQ ranging from 100 μM to 0.8 μM. Bioluminescence production (OD<sub>495</sub>) and bacterial growth (OD<sub>600</sub>) were monitored at 37°C for 24 h using a microplate spectrophotometer



(Infinite® M1000 PRO, TECAN, UK). Luminescence was recorded as relative light units (RLU) per unit of OD<sub>600</sub>.

#### 2.4.3.3. Pyocyanin production assay

The pyocyanin quantification is based on a colorimetric method by measuring the absorbance of pyocyanin in acidic solution. A 5 ml of fraction of overnight culture in LB was centrifuged in a 15 ml falcon tube at 10,000 rpm (Allegra X-64R with C0650 fixed angle rotor, Beckman Coulter, UK) for 10 min at room temperature. The supernatant was transferred into a fresh tube and mixed with 3 ml of chloroform. After thorough mixing the mixture was centrifuged and the chloroform organic layer was transferred to a fresh tube and mixed with 1 ml 0.2 M HCl (Sigma-Aldrich, UK). After centrifugation at 10,000 rpm (Allegra X-64R with C0650 fixed angle rotor, Beckman Coulter, UK) at 4°C for 5 min, the top layer was collected to measure its absorbance at 520 nm. Concentrations of pyocyanin, presented as µg per ml, were determined by multiplying the value of OD<sub>520</sub> after adjusting to growth using OD<sub>600</sub> by 17.072 (Essar et al., 1990).

#### 2.4.3.4. Swarming assay

Overnight PA cultures in LB were adjusted to OD<sub>600</sub> 1.0 and 5 µl of the diluted cultures were drop dotted on the centre of a swarm agar plate. Swarm agar is composed of 0.5% of Bacto agar (Difco BD, USA), nutrient broth No.2 (Oxoid, USA) and 0.5% of D-Glucose (Sigma-Aldrich, UK). Swarm agar plates were then incubated at 38.7°C for 18 hours. Swarming images were obtained by placing plates on a black background with indirect illumination from below.

#### 2.4.3.5. Quantification of rhamnolipids production by the orcinol method

Quantification of rhamnolipids by the orcinol method was performed as described by Christova et al. (Christova et al., 2004) with the following modifications. Briefly, *P. aeruginosa* strains were cultured in 5 ml of CAA medium (1 g of casamino acid (Difco BD, USA), 4 g of glycerol (Sigma-Aldrich, UK), 0.115 g of  $K_2HPO_4$  (Sigma-Aldrich, UK) and 3 mM  $MgSO_4$  (Sigma-Aldrich, UK) to a final volume of 200 ml in distilled water) at 37°C, 200 rpm. After 18 h incubation, rhamnolipids were extracted twice from cell-free culture supernatants with equal volume of diethyl ether (Sigma-Aldrich, UK). The organic fractions were vacuum dried using a centrifugal evaporator (Jouan RC10 series, Thermo Scientific, UK) for 40 min and resuspended in 1 ml of orcinol solution (100  $\mu$ l of ddH<sub>2</sub>O, 100  $\mu$ l of 1.6% orcinol (MP Biomedicals, France) and 800  $\mu$ l of 60% H<sub>2</sub>SO<sub>4</sub>). Sample solutions and serially diluted rhamnose standards were then incubated at 80°C for 7 min, cooled down to room temperature and OD<sub>421</sub> was measured using a spectrophotometer. The amounts of rhamnolipids were calculated as mg per ml. Each sample was evaluated in triplicate.

#### 2.4.3.6. Biofilm formation, visualisation and analysis

UV-sterilised glass slides were placed in petri-dishes inoculated *P. aeruginosa* cultures in RMPI-1640 (Sigma-Aldrich, UK) and started with an overnight culture in RPMI-1640 diluted to OD<sub>600</sub> 0.05 in RPMI-1640. Cultures were incubated at 37°C with shaking at 60 rpm for 72 hours. Glass slides were washed with PBS 3 times, rinsed with distilled water once and stained with SYTO9 and propidium iodine (FilmTracer Live/Dead Biofilm Viability Kit;

Life Technologies, USA). Images were acquired by confocal laser scanning microscope (Zeiss LSM 700). Green-channel images were acquired using 488 nm excitation and 515 nm emission; red-channel images were collected using 594 nm excitation and emission at 625 nm. Biofilm surface coverage percentage was analysed by software ImageJ and the means of surface coverage were taken from 7 images from different fields on a glass slide.

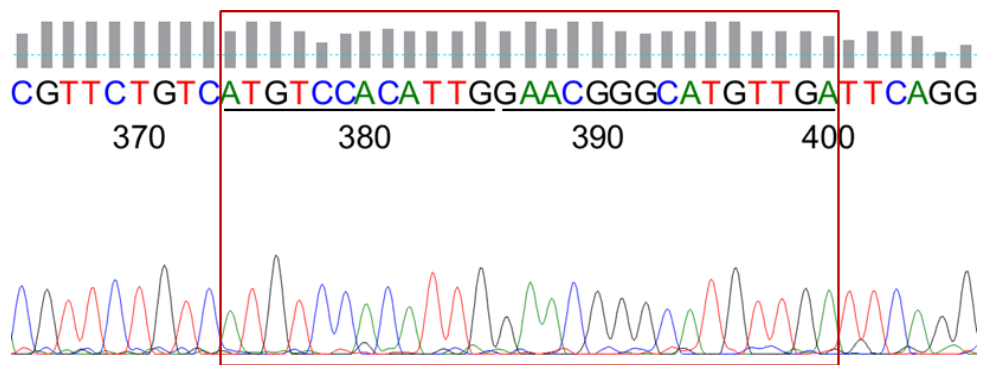
## 2.5. RESULTS

### 2.5.1. Generation of the *ΔpqsA<sub>L</sub>* mutant

The *pqsABCDE* operon is essential for PQS production. The *pqsA* gene for being the first gene from this operon in the AQ in *P. aeruginosa*, we decided to generate a *pqsA* knock-out mutant to block the biosynthesis of AQS.

The *P. aeruginosa* laboratory strain PAO1-L was chosen as the background strain to generate this mutant for the reasons specified in Section 2.1.5. The mutant was constructed under the concept of allelic gene exchange. To knock-out the target gene, we designed four primers *pqsAf1*, *pqsAr1*, *pqsAf2* and *pqsAr2* (Table 2.2). By using the primer pair *pqsAf1/r1*, *pqsAf2/r2* and the PAO1-L genomic DNA as the template, a 410-bp long amplicon containing a *Xba*I restriction site at its 5' end and the other 423-bp amplicon with a *Hind*III restriction site at the 3' end were generated (sequences displaying in grey shades are shown in Table 2.3). For the second PCR the overlapping PCR was performed, where the above two PCR products were both used as templates and PCR was conducted with primers *pqsAf1* and *pqsAr2*, resulting in an 833-bp fragment made from joining two template fragments by the over-hanging nucleotides designed on the primers. The 833-bp fragment contains only 27-nucleotide of the *pqsA* gene (the first 12 nucleotides and the last 15 nucleotides of *pqsA*) and was denoted as the *mpqsA* fragment (Fig. 2.5). The *mpqsA* fragment was digested with *Xba*I and *Hind*III and ligated into the cloning vector, pBluescript KS II (+) digested with the same enzymes. Subsequently, the *mpqsA* fragment was sub-cloned into the suicide vector, pME3087, resulting in pYCL1. Conjugation of *E. coli* s17-1  $\lambda$ pir which carries pYCL1

into *P. aeruginosa* PAO1-L, allowed homologous recombination to occur between the suicide vector and the PAO1-L genome (Fig. 2.5). After recombination, we screened the tetracycline sensitive mutant candidates using a three-day continuous enrichment method. The  $\Delta pqsA$  mutant sequence was verified by nucleotide sequencing showing that the first 12 nucleotides of *pqsA* were successfully linked to the last 15 nucleotides of *pqsA* (Fig. 2.6); the rest of nucleotides of the *mpqsA* fragment were aligned correctly with the gene PA0996 of *P. aeruginosa* PAO1-UW sequence obtained from Pseudomonas Genome Database (Winsor et al., 2011) (data not shown).



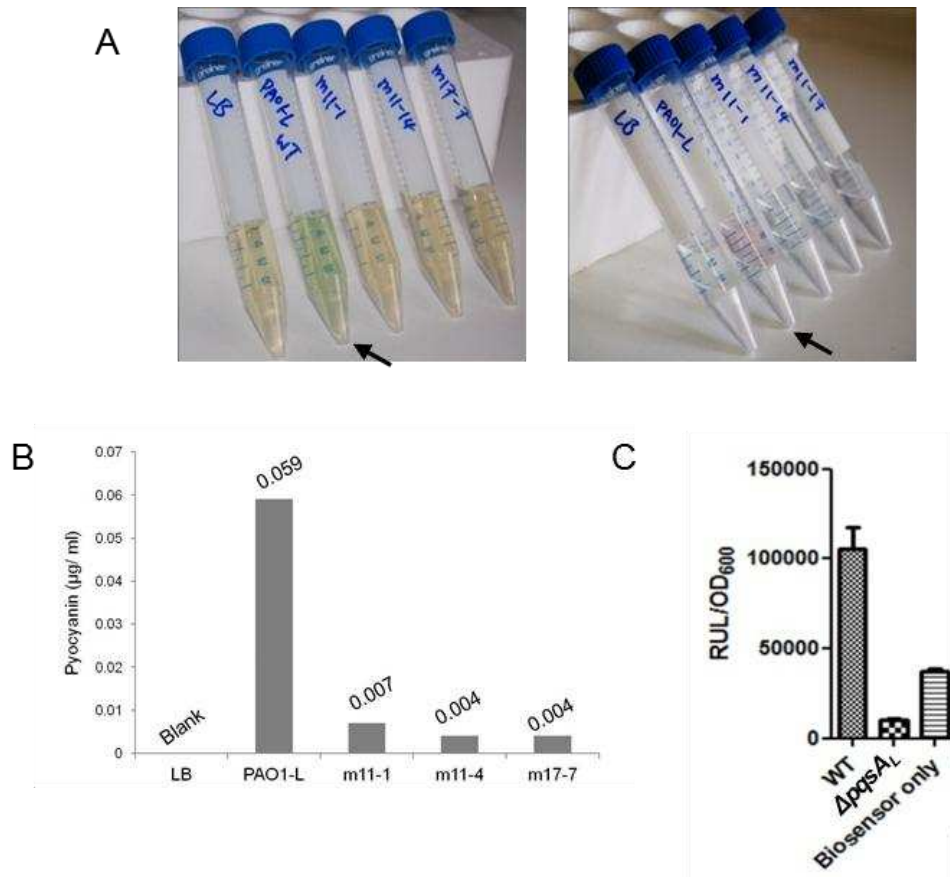
**Figure 2.6 Nucleotide sequencing confirmed that an in-frame deletion was generated by joining first 12 nucleotides and the last 15 nucleotides of the *pqsA* gene.**

The first 12 nucleotides ATGTCCACATTG (underlined) and the last 15 nucleotides GAACGGGCATGTTGA (underlined) were linked, making a *pqsA* in-frame deletion by knocking out 1,527 nucleotides out of 1,554 nucleotides.

To determine if AQ production has been lost in the  $\Delta pqsA_L$  mutant, mutant no. m11-1 was selected to examine this function using an AQ biosensor assay. Fig. 2.7 C shows a substantial reduction in PQS in  $\Delta pqsA_L$  mutant compared to PAO1-L. Collectively, these results indicate that a *pqsA* mutation that depleted 1,527 bp out of 1,554 bp of the *pqsA* gene has obtained and that this mutation

presented phenotypes of depleted pyocyanin biosynthesis and reduced secretion of alkyl-quinolones.

Several mutants were selected and pyocyanin production was used as a surrogate marker to screen these potential PQS deficient mutants because its biosynthesis is controlled directly by the *pqs* operon. The green pigment appeared in the organic layer from the WT PAO1-L culture supernatant after chloroform extraction and it turned pink after acidification (Fig. 2.7 A). To determine the concentrations of pyocyanin, the values of OD<sub>520</sub> after normalising to growth based on the OD<sub>600</sub> were multiplied by 17.072 (Essar et al., 1990). The amount of pyocyanin in PAO1-L WT was 0.059 µg/ml. However, pyocyanin was barely detectable in the selected mutants no. m11-1, m11-4 and m17-7 with concentration of 0.007 µg/ml, 0.004 µg/ml and 0.004 µg/ml respectively, indicating that there is a correlation between lack of *pqsA* function and pyocyanin biosynthesis (Fig. 2.7 B).



**Figure 2.7**  $\Delta pqsA_L$  mutants were deficient in the production of pyocyanin and alkyl-quinolones.

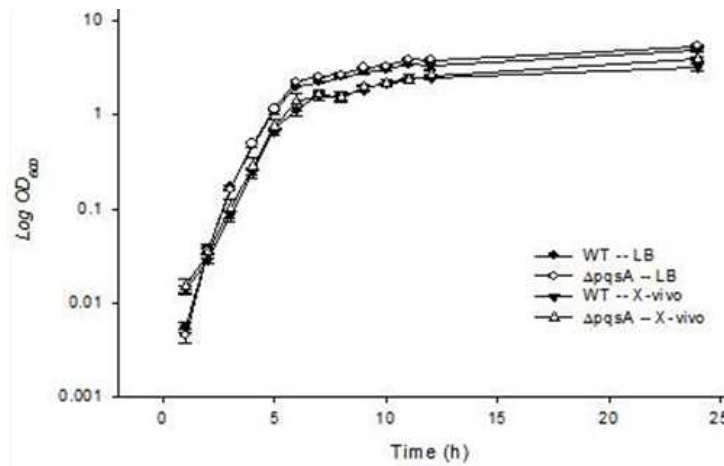
Two phenotypes, pyocyanin and Aqs production which are directly associated with PQS expression were used to screen for the potential  $\Delta pqsA_L$  mutants. A. Green pigment appeared in the chloroform layer of *P. aeruginosa* PAO1-L wild type (arrow) but this layer remained yellow in the case of  $\Delta pqsA_L$  mutants (left). The colour of the chloroform layer after 0.2 N HCl acidification became pink in WT (arrow), but not in  $\Delta pqsA_L$  mutants (right). B. Quantification of pyocyanin showed that  $\Delta pqsA_L$  mutants no. m11-1, m11-4 and m17-7 produced low amounts of pyocyanin compared with WT PAO1-L. C. The presence of Aqs in the supernatants of PAO1-L wild type and a selected  $\Delta pqsA_L$  mutant were examined using a Aqs biosensor assay. Aqs synthesis in  $\Delta pqsA_L$  mutant was highly decreased compared to the WT. Averages in (B) were from two independent experiments; Averages and standard deviations in (C) were from 3 independent experiments.

## 2.5.2. Phenotypic characterisation of $\Delta pqsA_L$ in comparison with $\Delta pqsA_N$

### 2.5.2.1. Bacterial growth

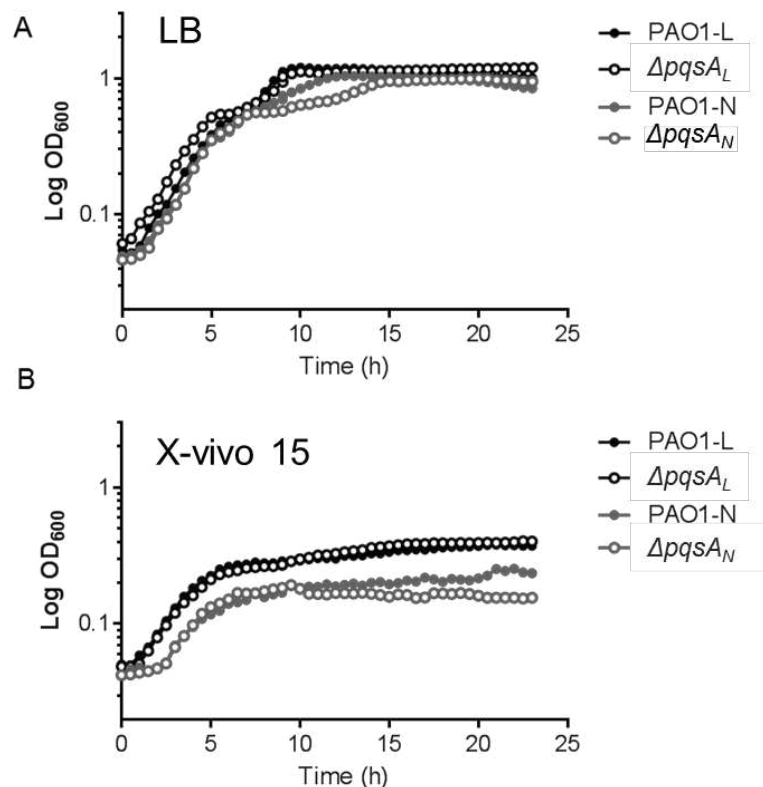
To examine whether the deletion of *pqsA* would alter fundamental metabolic processes, the growth of  $\Delta pqsA_L$  was compared to the growth of its isogenic WT strain PAO1-L. The two strains were cultured in LB and X-vivo 15 with aeration and OD<sub>600</sub> readings were taken every hour for 12 h and at 24 h. X-vivo 15 is a chemically defined, serum-free hematopoietic cell media that provides nutrient balanced environment for the growth of peripheral blood lymphocytes (PBL), tumour infiltrating lymphocytes (TIL) myeloid cells, human monocytes, macrophage cells and natural killer (NK) cells, etc. (Lonza, cell culture media reference (Wu et al., 2001, Jonuleit et al., 1997)). In our lab, X-vivo 15 has been used to growth human macrophages in the assay upon *P. aeruginosa* infection (Singh, 2012). As the original plan was to generate a multicellular epithelium system that includes human macrophages, it is essential to evaluate whether the growth of *P. aeruginosa* strain would differ in X-vivo 15 culture media. The growth rates of WT and  $\Delta pqsA_L$ , in LB and X-vivo 15 media were comparable as shown in Fig. 2.8. Additionally, the growth of the PAO1-L WT and  $\Delta pqsA_L$  were compared to that of PAO1-N and  $\Delta pqsA_N$  under static conditions. No distinguishable growth differences were observed among these 4 strains when cultured in LB at static condition (Fig. 2.9). When the four strains were incubated in X-vivo 15 under static conditions, the cell densities were generally lower particularly in the case of PAO1-N and  $\Delta pqsA_N$  compared to PAO1-L and  $\Delta pqsA_L$ . These results suggest that the deletion of the *pqsA* gene does not affect *P. aeruginosa* growth.





**Figure 2.8 Similar growth of *P. aeruginosa* PAO1-L (WT) and  $\Delta pqsA_L$  in LB and X-vivo 15 media under aerated conditions.**

Growth of *P. aeruginosa* WT and  $\Delta pqsA_L$  cultures grown in LB and X-vivo 15 was investigated by measuring OD<sub>600</sub> every hour for 12 h and at 24 h. PA cultures were grown in 25 ml LB in 250 ml flasks at 37°C, 200 rpm. N=1; averages and error bars were from two preparations of each bacterial strain.

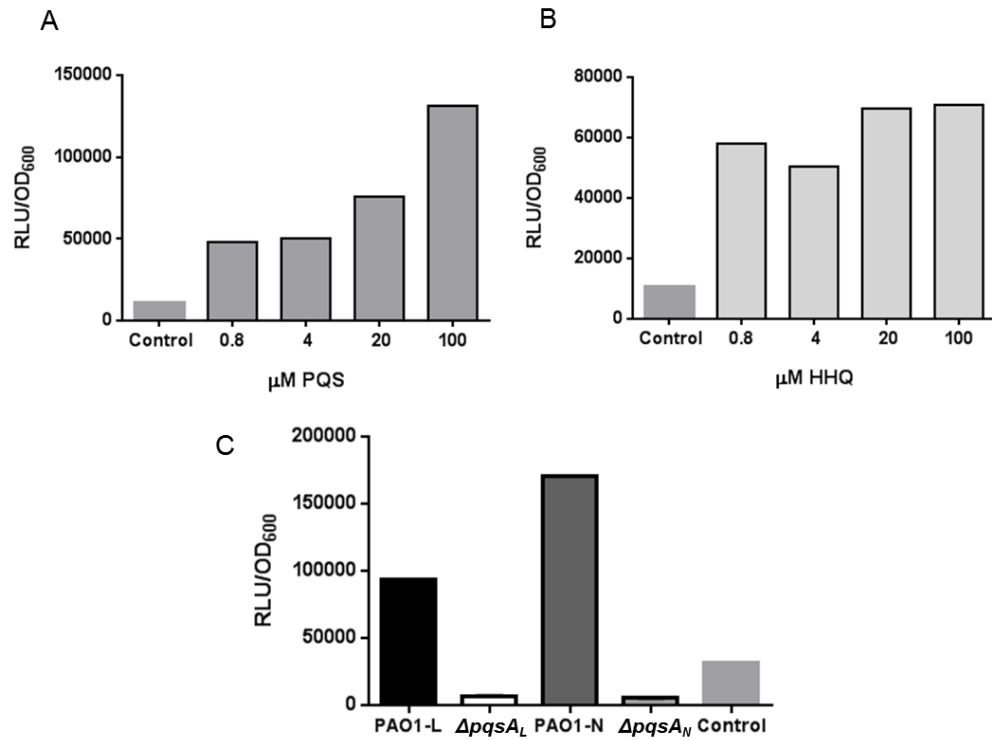


**Figure 2.9 Similar growth of *P. aeruginosa* PAO1-L, PAO1-N and their isogenic *pqsA* mutants in LB and X-vivo 15 under static conditions.**

Growth of *P. aeruginosa* WT and  $\Delta pqsA_L$  cultures grown in LB (A) and X-vivo 15 (B) was investigated by measuring OD<sub>600</sub> every 30 min for 24h. PA cultures were grown in 96 well plates. The cell density of PAO1-N and  $\Delta pqsA_N$  was slightly lower than that of PAO1-L and  $\Delta pqsA_L$  in X-vivo 15. Overall, PA grew slower and reached lower density in X-vivo 15 under static conditions. N=1; each condition was conducted in triplicate.

#### 2.5.2.2. Reduced alkyl-quinolones production in $\Delta pqsA_L$

To determine the PQS production capacity of PAO1-L and its isogenic  $\Delta pqsA_L$  mutant, the secretion of alkyl quinolones to the extracellular milieu was measured. PAO1-N and  $\Delta pqsA_N$  were also compared. AQs production from PAO1-L was detected by the luminescence (RLU/OD<sub>600</sub>) emitted by the AQ biosensor strain PAO1  $\Delta pqsA$  *CTX::PpqsA-lux* (Fletcher et al., 2007) as described in materials and methods. The bioluminescence levels detected from the PAO1-L supernatant was comparable to that obtained using 20 µg/ml of pure PQS compound as positive control (Fig. 2.10 C). The  $\Delta pqsA_L$  mutant secreted substantially lower amount of AQ compared to PAO1-L. Meanwhile, AQ production in PAO1-N was 85% higher to that of PAO1-L. AQ biosynthesis in the  $\Delta pqsA_N$  mutant was also highly reduced and comparable to that of  $\Delta pqsA_L$  (Fig. 2.10). In line with these results, the lack of *pqsA* gene function in PAO1-L causes a deficiency in PQS production that was also verified by liquid chromatography-mass spectrometry (LC-MS) (refer Fig. 4.18).

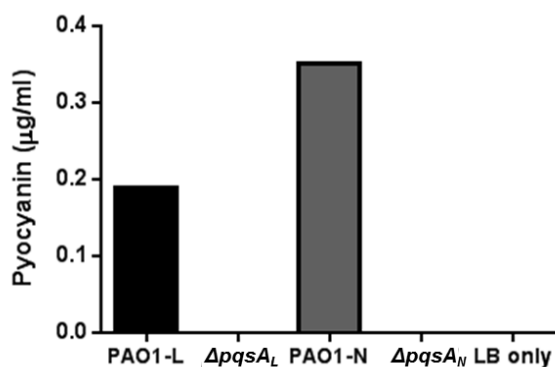


**Figure 2.10 Mutation in *pqsA* rendered PAO1-L AQ-negative.**

The two major AQs components, PQS and HHQ compounds were used as positive controls in the AQ biosensor (PAO1  $\Delta pqsA$  CTX::PpqsA-lux) assay. The mean maximal light output from the AQ biosensor in response to serial dilutions of PQS (A) and HHQ (B) is shown. For the doses tested (0.8 to 100  $\mu$ M) the AQ biosensor strain responded to PQS in a dose depended fashion, but this was not observed in the case of HHQ. (C) The maximal light output from the AQ biosensor in the presence of overnight cell-free culture supernatants from PAO1-L,  $\Delta pqsA_L$ , PAO1-N and  $\Delta pqsA_N$  respectively grown in LB. The biosensor strain emitted light in response to both WT PAO1 supernatants but not in response to the *pqsA* culture supernatant. Control represents the light emitted from biosensor in the presence of LB medium. The results were averaged from two independent experiments and each sample was done in triplicate. Averages and error bars were shown in the figures.

### 2.5.2.3. Reduced pyocyanin production in $\Delta pqsA_L$

Pyocyanin is a redox-active exotoxin compound considered as a virulence factor of *P. aeruginosa* essential for full pathogenesis in animal models and its expression has been shown to be QS-dependent (Das et al., 2013, Lu et al., 2012, Ran et al., 2003). In the absence of PQS there is no pyocyanin production. Therefore, the levels of pyocyanin are an indication of the presence of PQS. To determine whether pyocyanin production was affected by the lack of *pqsA* gene function, we examined the levels of pyocyanin extracted from culture supernatants of PAO1-L,  $\Delta pqsA_L$ , PAO1-N and  $\Delta pqsA_N$ . Pyocyanin production was reduced in  $\Delta pqsA_L$  to a barely detectable level as shown in Fig. 2.11. Pyocyanin secretion by PAO1-N was 85% higher than in PAO1-L. This was in accordance with the differences in PQS production between PAO1-L and PAO1-N. Impaired pyocyanin production was also observed in  $\Delta pqsA_N$  (Fig. 2.11) which is consistent with the result conducted by Rampioni et al. (Rampioni et al., 2010).

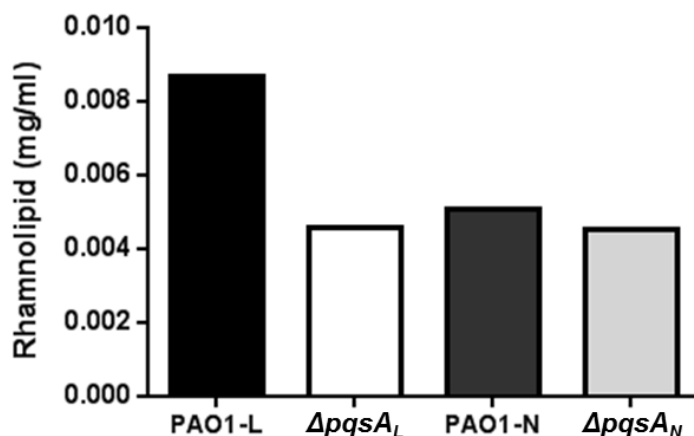


**Figure 2.11 Lack of pyocyanin synthesis upon mutation of *pqsA* in PAO1-L and PAO1-N.**

Pyocyanin production could not be detected in the supernatants from the  $\Delta pqsA_L$  and  $\Delta pqsA_N$  mutants. PAO1-L produced 85% less pyocyanin than PAO1-N. The mean of the results were taken from two independent experiments and samples were prepared in duplicates

#### 2.5.2.4. Production of surfactant rhamnolipids was significantly reduced in *ΔpqsA<sub>L</sub>*

Rhamnolipids are considered as virulence factors in *P. aeruginosa*. It was suggested that rhamnolipids modulate the innate immune response by suppressing pathogen-induced human  $\beta$ -defensin-2 expression in keratinocytes (Dossel et al., 2012). Mutations in *pqsR* and *pqsE* result in the inability to produce PQS but also decrease rhamnolipids biosynthesis (Reis et al., 2011, Deziel et al., 2005). To determine whether the production of rhamnolipids was inhibited as a result of a PQS deficiency in the *ΔpqsA<sub>L</sub>* mutant, the semi-quantitative orcinol method was used to compare rhamnolipid production in PAO1-L, *ΔpqsA<sub>L</sub>*, PAO-N and *ΔpqsA<sub>L</sub>* strains. By measuring the concentration of rhamnose, the amount of rhamnolipids could be calculated as two masses of rhamnolipids is equivalent of one mass of rhamnose (Christova et al., 2004). The concentrations of rhamnolipids produced by *ΔpqsA<sub>L</sub>* were about three times lower than those secreted by PAO1-L (Fig. 2.12), indicating that rhamnolipids biosynthesis was affected by the deletion of *pqsA* in PAO1-L. However, PAO1-N and the *ΔpqsA<sub>N</sub>* mutant produced equivalent amounts of rhamnolipids at the levels produced by *ΔpqsA<sub>L</sub>*, suggesting the existence of a genetic element missing in PAO1-N which may be present in PAO1-L and responsible for these differences. As mentioned above, a study comparing the genome difference between PAO1-N and PAO1-L revealed that a 58,000 base pairs DNA deletion fragment has occurred in PAO1-N. We postulate that the genes located in this region could be associated with rhamnolipids synthesis.

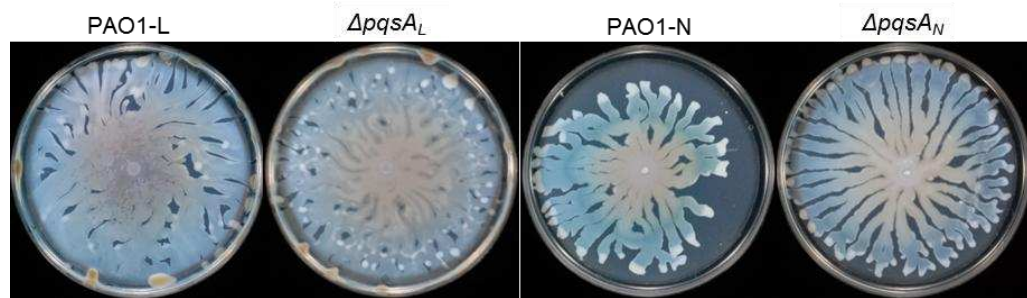


**Figure 2.12** The *pqsA* mutation decreased rhamnolipids production in  $\Delta pqsA_L$  but not in PAO1-N.

Rhamnolipid production in  $\Delta pqsA_L$  was substantially reduced compared with that of PAO1-L. However, there were no differences in rhamnolipids production between PAO1-N and  $\Delta pqsA_N$ . Data were analysed by un-paired t-test. PAO1-L produced more rhamnolipids than PAO1-N. The graph shows the average of the results from two independent experiments and samples in each experiment were conducted in triplicate.

#### 2.5.2.5. Effect of the *pqsA* mutation on *P. aeruginosa* motility

*P. aeruginosa* can colonise environmental niches by using three types of motility, swimming, twitching, and swarming (Heurlier et al., 2004). Swarming combines swimming and twitching motility and requires rhamnolipids production. The flagella and type IV pili are the two major components responsible for motility. To examine whether the *pqsA* mutation would affect bacterial motility, a swarming assay was performed in PAO1-L,  $\Delta pqsA_L$ , PAO1-N and  $\Delta pqsA_N$ . Both  $\Delta pqsA_L$  and  $\Delta pqsA_N$  swarmed slightly faster than their isogenic wild-type strain. PAO1-N strains (PAO1-N and  $\Delta pqsA_N$ ) generally swarmed slower than the PAO1-L strains (PAO1-L and  $\Delta pqsA_L$ ) (Fig. 2.13).

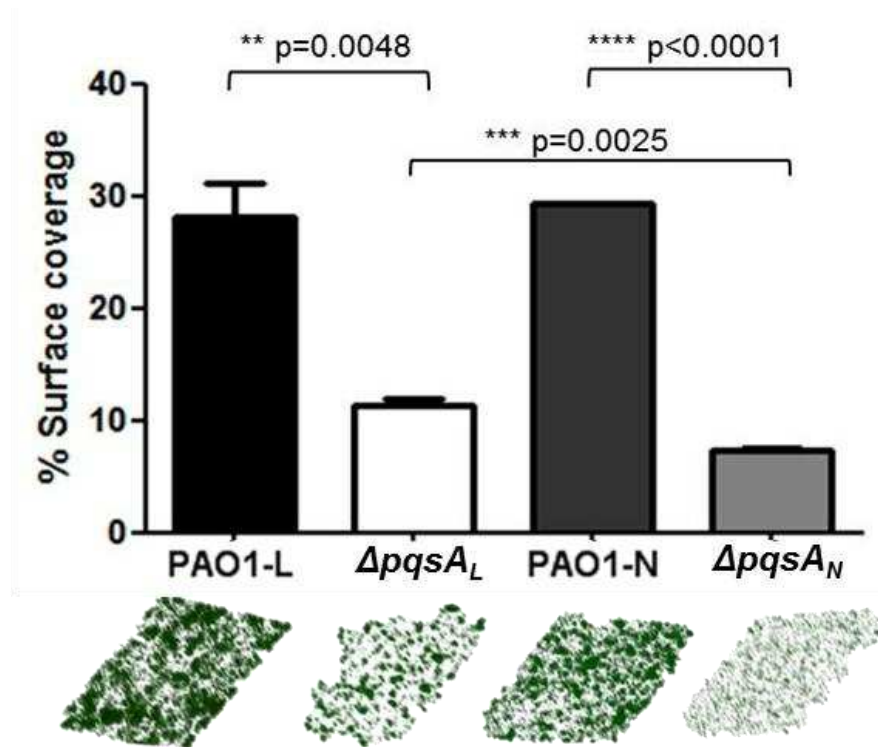


**Figure 2.13 Motility was increased in  $\Delta pqsA_L$  and  $\Delta pqsA_N$  mutants compared with their WT parental strains.**

Motility of PAO1-L,  $\Delta pqsA_L$ , PAO1-N and  $\Delta pqsA_N$  was examined on 0.5% swarming agar plates at 37°C for 18 hours. Both pqsA mutants displayed increased motility compared with the WT strains. Higher swarming motility was seen in PAO1-L WT compared to PAO1-N. These images are representative from three independent experiments showing similar trends in motility.

#### 2.5.2.6. $\Delta pqsA_L$ and $\Delta pqsA_N$ form fragile immature biofilms

Biofilm formation is another characteristic controlled by QS signalling. Once *P. aeruginosa* starts to develop as a population during the course of infection, antibiotics fail to penetrate the biofilm because of the thick alginate surrounding the cells. This phenomena could even drive *P. aeruginosa* resistant to antibiotics (Hoiby et al., 2010). To test whether biofilm formation was influenced by the deletion of pqsA in PAO1-L as it has been shown for PAO1-N, biofilms developed on glass slides for 72 h at 37°C with low speed shaking were visualised by confocal laser scanning microscopy and the surface coverage from each strain compared. Biofilm surface coverage of  $\Delta pqsA_L$  was 3-fold lower than that of PAO1-L and this reduction was significant.  $\Delta pqsA_L$  formed microcolonies on the glass slide while PAO1-L developed evident and mature biofilms. The biofilm surface coverage of PAO1-N and  $\Delta pqsA_N$  were similar to those shown in PAO1-L and  $\Delta pqsA_L$  (Fig. 2.14). Collectively, the loss of pqsA function influences biofilm formation.



**Figure 2.14**  $\Delta pqsA_L$  and  $\Delta pqsA_N$  formed fragile and immature biofilms compared with PAO1-L and PAO1-N.

The percentages of biofilm surface coverage from each strain were plotted. Below the graph shows representative 3D confocal laser scanning microscope images of biofilms.  $\Delta pqsA_L$  formed less biofilm than PAO1-L and bacterial cells were sparsely distributed;  $\Delta pqsA_N$ , however, was the most deficient in biofilm formation amongst these 4 strains. The experiment was conducted twice and showed the same trend in biofilm formation. The means and the standards deviation presented in the graph were calculated from 7 different fields acquired from confocal laser scanning microscope in an experiment.



## 2.6. DISCUSSION

### 2.6.1. *ΔpqsA<sub>L</sub>* mutant was compromised in the production of several virulence factors

In this chapter, a *pqsA* in-frame deletion mutant, *ΔpqsA<sub>L</sub>*, was successfully generated in the PAO1-L background and verified by nucleotide sequencing. In comparison to the wild-type, *ΔpqsA<sub>L</sub>* exhibited a substantial reduction in PQS, pyocyanin and rhamnolipids production and formed fragile biofilms of reduced surface coverage. Pyocyanin, rhamnolipids are virulence factors and their presence positively correlate with deteriorated lung function in CF patients. Based on this we concluded that *ΔpqsA<sub>L</sub>*, might present an attenuated phenotype upon infection of host cells. To understand the influence of PQS on the pathogenesis of *P. aeruginosa* during pulmonary infections, an in vitro human bronchial epithelium infection model has been established (see Chapter 3). Using this model we have investigated how the lack of *pqsA* affects the behaviour of *P. aeruginosa* upon infection of differentiated human bronchial epithelial cells (see Chapters 3 and 4).

Swarming motility is a dynamic process that requires a functional flagellum and the production of rhamnolipid biosurfactants and is also influenced by the environment (Davey et al., 2003, Caiazza et al., 2005). Both PAO1-L and *ΔpqsA<sub>L</sub>* were motile in swarming, but *pqsA* mutants swarmed slightly faster in swarming agar than its correspondent wild-types PAO1-L and PAO1-N. Despite the fact that rhamnolipids are considered to facilitate *P. aeruginosa* swarming by lowering surface tension and thus supporting the flagella based propulsion of the bacteria (Kohler et al., 2000), swarming was not impaired in

spite of the reduced production of rhamnolipids in *pqsA* mutants compared to its AQS competent wild-type strains in our study. Rhamnolipids are synthesized by a rhamnosyltransferase, encoded by the *rhlAB* operon (Deziel et al., 2003). It has been shown that *rhlB* mutant (deficient in mono- and dirhamnolipid production) and *rhlC* mutant (deficient in dirhamnolipid production) altered swarming patterns, whereas *rhlA* gene was indicated to be required for swarming (Deziel et al., 2003, Caiazza et al., 2005). AQS might indirectly regulate the production of rhamnolipids via transcriptional regulation on *rhl* operon that influences the swarming ability, where the mechanism circuit is still unclear. A study indicated that HHQ suppressed swarming (Ha et al., 2011) partially explained a mild inhibition of motility in wild-type strains that are competent in AQS production. In addition, both PAO1-L WT and  $\Delta pqsA_L$  were observed under SEM to carry a single flagellum (refer to Fig. 4.1 in Chapter 4) that is also one of the factors required for swarming. The above evidence suggests that the decreased production of rhamnolipids might reduce the motility or alter swarming patterns but cannot fully influence the swarming due to the counter effect of the lack of HHQ in *pqsA* mutants that increased the motility.

According to our in vitro study,  $\Delta pqsA_L$  appeared attenuated based on the phenotypic assays. However, a study investigating the profile of virulence factors expressed in *P. aeruginosa* strains from infants with cystic fibrosis published recently demonstrated that persistent strains refractory to antibiotic intervention expressed lower pyoverdine, rhamnolipids, haemolysin, total protease, swimming and twitching motility than strains that could be readily cleared by antibiotics (Manos et al., 2013). This study suggested that the

persistent strains in the lung might not directly correlate with the expression of virulence determinants that are commonly defined to cause acute infections. Thus, to gain a greater understanding of the impact of PQS on *P. aeruginosa* pathogenesis, the use of a physiologically-relevant experimental model that allows *P. aeruginosa* to fully-adopt the phenotype required to establish infection in the human lung is required. Towards this aim we have established an infection model using differentiated human bronchial epithelial cells which will be described in chapters 3 and 4.

### 2.6.2. Phenotype differences between PAO1-L and PAO1-N might due to the 58 kb deletion in PAO1-N and SNPs in PAO1-N subline

**Table 2.4 Phenotype summary of PAO1-L, PAO1-N and their correspondent *pqsA* mutants.**

Phenotype	PAO1-L	$\Delta pqsA_L$	PAO1-N	$\Delta pqsA_N$
AQs production	+	-	++	-
Pyocyanin production	+	-	++	-
Swarming	++	+++	+	++
Rhamnolipids production	+++	+	+	+
Biofilm formation	+++	+	+++	-

+, positive response; -, negative response; PQS, Pseudomonas quinolone signal

Due to its ubiquitous and metabolically versatile characteristics being an opportunistic pathogen, *P. aeruginosa* PAO1 is one of the most commonly used strains for research. The QS circuits reciprocally coordinate the regulation of virulence determinants. Strain PAO1 is a derivative from the original Australian PAO isolate that has been distributed worldwide to laboratories and strain collections. Discordant phenotypes of PAO1 sublines have emerged since the sequence was firstly published in 2000 (Stover et al., 2000). It has been shown that the PAO1 sublines differed in their ability to cope with nutrient limitation and their virulence varied in an acute murine airway infection model (Klockgether et al., 2010). An ongoing microevolution of strain PAO1 thus was suggested. In this regard, high-throughput genome re-sequencing will resolve more cases and could become a quality control for strain collections since the differences between genotype and phenotype may produce inconsistent findings between laboratory to laboratory (Klockgether et al., 2010). To understand the contribution of the genome difference between the PAO1 sublines PAO1-N and PAO1-L to different phenotypes, the phenotypic characterisation of PAO1-N and  $\Delta pqsA_N$  was also performed along with that of the main focus strain of the present project,  $\Delta pqsA_L$  and PAO1-L. We identified phenotypic differences between PAO1-L and PAO1-N. PQS and pyocyanin production in PAO1-N were 85% higher than those in PAO1-L. PAO1-N displayed slightly reduced swarming motility compared with PAO1-L. The production of rhamnolipids in PAO1-N was equivalent to those in  $\Delta pqsAL$  that was 3-fold lower than PAO1-L. No rhamnolipid production difference between PAO1-N and  $\Delta pqsAN$ . Surface coverage of biofilms was comparable between PAO1-L and PAO1-N.  $\Delta pqsA_L$  and  $\Delta pqsA_N$  both displayed highly

reduced PQS production, no detectable pyocyanin production and reduced rhamnolipids production compared with the phenotypes of their correspondent wild-type. The only phenotype difference between  $\Delta pqsA_L$  and  $\Delta pqsA_N$  was the biofilm surface coverage in  $\Delta pqsA_L$  was around 2-fold higher than  $\Delta pqsA_N$ , in both instances the biofilms were less-established compared with their respective isogenic WT strains (summarised in Table 2.4).

As mentioned earlier in the introduction section 2.1.3, swarming motility appeared to be different in the RsmA deletion mutants constructed in PAO1-N and PAO1-L backgrounds. Results from our laboratory showed that ToxR might enhance rhamnolipids production and swarming motility by positively regulating RsmA and activating the rhl QS system (Mai-Prochnow, et al., manuscript in preparation). Rhamnolipids production was suggested to be regulated via the rhl QS system (Rahim et al., 2001). In addition, whole genome high-throughput re-sequencing of PAO1-N and PAO1-L was conducted and SNPs were identified by comparison of the genetic difference between PAO1-L and PAO1-N that were aligned with the reference genome PAO1-UW (named after the University of Washington) (Klockgether et al., 2010) (Hardeep Naphra, on-going PhD thesis). Preliminary data revealed that SNPs such as *bifA* (PA4367) and *mexF* (PA2494) were identified in PAO1-N other than the 5.8 kb missing fragment and genome of PAO1-L is closer to the reference PAO1-UW (personal communication with Hardeep Naphra, on-going PhD thesis). *BifA* is a cyclic-di-GMP phosphodiesterase that localise at inner membrane of *P. aeruginosa*. It was demonstrated that a decreased swarming motility but an enhanced biofilm and polysaccharide production were presented in the *bifA* mutant in *P. aeruginosa* PA14 background (Kuchma et al.,

2007). The *bifA* SNP in the genome of PAO1-N might partially explain the slightly reduced swarming motility found in PAO1-N compared with PAO1-L. MexF is a resistance-nodulation-cell division (RND) multidrug efflux transporter that acts as an efflux pump protein (Winsor et al., 2011). At least four broad-spectrum efflux pumps (Mex) were found involved in elevated intrinsic antibiotic resistance as well as in acquired multidrug resistance in *P. aeruginosa* (Aires et al., 2002, Kohler et al., 1999). Additionally, the absence of ETA was also found in the culture supernatants of PAO1-N suggesting the deletion of *ToxR* in the genome of PAO1-N might influence the expression of ETA (Farah Hussain, on-going PhD thesis). Studies are in progress to characterise the genes and their functions that differentially expressed in PAO1-L and PAO1-N (Hardeep Naphra and Farah Hussain, on-going PhD theses). The above evidence suggested the intrinsic genetic differences between PAO1-N and PAO1-L and the genome of PAO1-L is closer to the reference PAO1-UW. The *pqsA* mutant generated in PAO1-L background is presumably to be more reflective to a phenotype attributed solely to the lack of the *pqsA* gene function but not from other defects derived from the depletion of the genome.

## 2.7. SUMMARY

An AQ deficient strain on PAO1-L background has been successfully generated using an in-frame deletion strategy that does not require antibiotic selection. Phenotypic characterisations of  $\Delta pqsA_L$  in comparison with PAO1-L, demonstrated barely detectable levels of AQs and pyocyanin, reduced rhamnolipid production, fragile biofilms and slightly increased motility, in spite of equivalent growth. Collectively, these data suggest that  $\Delta pqsA_L$  has an attenuated phenotype.

### **3. ESTABLISHMENT AND CHARACTERIZATION OF AN *IN VITRO* INFECTION MODEL TO STUDY THE INTERACTION OF *PSEUDOMONAS AERUGINOSA* WITH DIFFERENTIATED HUMAN BRONCHIAL EPITHELIAL CELLS**

---

#### **3.1. INTRODUCTION**

Mammalian airway epithelium represents the first line of defence encountered by microbial pathogens including bacteria, viruses, fungi and parasites. Not only providing a physical barrier against foreign bodies, the role of airway epithelial cells as immune modulators is also increasingly appreciated. Disturbance of this efficient defence system as in the case of ventilator-acquired respiratory injury or malfunction of the cystic fibrosis transmembrane conductance regulator (CFTR) in cystic fibrosis is a leading cause of mortality worldwide (El Solh et al., 2008, Campodonico et al., 2008, Eisele and Anderson, 2011). A comprehensive understanding of how AOs might impact on the initial encounter of *P. aeruginosa* with lung epithelium and the downstream immune response is still lacking. In addition, because in CF patients with ‘stable infections’ the majority of pseudomonal load is in the conducting airways but not in the alveolar spaces (Jelsbak et al., 2007), bronchial epithelium was considered as a suitable experimental model to study the initial recognition of *P. aeruginosa* in the human lung.



Thus, the aim of this project was to establish an airway epithelium infection model as a research platform applicable to the study of *P. aeruginosa* pathogenesis and particularly the impact of alkyl-quinolones. This work represents the first use of human airway epithelial cell cultures in our lab, thus it is important to demonstrate that the culture system consistently generates differentiated epithelial cells with physiological relevant features.

Three categories of pulmonary infection models are currently used (i) animal models; (ii) ex vivo organo-typic cultures and (iii) in vitro cell culture. Mouse animal models were excluded initially due to concerns regarding intrinsic species differences between murine and human respiratory systems. Anatomically, the human lung diverges up to 54,000 branches whilst in the mouse lung, it only extends to 5,000. The distribution of different epithelial cell types also differs between human and mouse (Rackley and Stripp, 2012). Mouse epithelium has an extra transmembrane TLR11 that has not been identified in human epithelium (Greene and McElvaney, 2005). In addition, comparison of the human and mouse CFTR in a Chinese hamster ovary (CHO) cell overexpression system showed that murine CFTR has a reduced channel open probability and gating, as well as shorter duration of bursts of channel activity compared to human CFTR (Lansdell et al., 1998, Cai et al., 2004). CFTR is a chloride anion channel pumping  $\text{Cl}^-$  ions out of the cell and it locates on the apical membrane of secretory epithelial cells. It is comprised of two six  $\alpha$ -helices spanning the plasma membrane region each connected to a nuclear binding domain which binds ATP called nuclear binding domain (NBD). The R-domain is located between the two NBDs and is involved in the regulation of CFTR by cAMP-dependent phosphorylation driven by protein

kinase A. (Denning et al., 1992a, Denning et al., 1992b, Linsdell, 2013, Randak et al., 2013). Patients with cystic fibrosis carry mutations in the CFTR gene with 70% of the patients bearing the mutation  $\Delta F508$  (List of CFTR mutations, 2013 version by US Cystic Fibrosis Foundation, National Institute of Health, US). The degradation of CFTR or CFTR protein misfolding at the apical membrane results in hyper-absorption of  $H_2O$  and  $Na^+$  at the epithelium. As a consequence, thick and viscous mucus accumulates on the epithelium and it becomes a niche for the colonisation of opportunistic pathogens such as *P. aeruginosa*. Biofilm development facilitates *P. aeruginosa* long-term persistence because biofilms are difficult to eradicate by antibiotics (Campodonico et al., 2008, Quinton, 2010). Studies have shown that not only the murine epithelial biology cannot fully recapitulate the properties of healthy human native epithelium, but the rising awareness of using in vitro tissue engineering as an alternative to animal experiments is also a current trend in research following the 3R 'Reduction, Refinement and Replacement' principle (Berube et al., 2010). To elucidate the signalling mechanisms involved in the pulmonary infection at the cellular level, cell culture models have been shown to be rather useful in predicting in vivo conditions. Indeed, primary human bronchial epithelial cell (NHBE) cultures have shown to recapitulate the physiological properties observed in the human lung (Berube et al., 2010). However, previous work on primary NHBE culture in our lab had been frustrating. Experimental difficulties including NHBE passage limitation (no more than p4), generation of un-differentiated squamous multi-layers instead of a desired pseudostratified layer, non-reproducible and inconsistent

differentiation (Sonali Singh, PhD thesis) deterred us from using primary NHBE to establish an infection model system.

With the support by our collaborator Dr. Cynthia Bosquillon (School of Pharmacy, University of Nottingham) and Dr. Victoria Hutter (School of Pharmacy, University of Nottingham), Calu-3 cell cultures were firstly introduced to our lab. The airway bronchial epithelial cell line Calu-3 was derived from a 25-year-old bronchial adenocarcinoma male and is commercially available (Fogh et al., 1977). The cells exhibited tight junctions, presented transepithelial resistance and increased short-circuit current (Isc) which are properties found in native serous airway epithelial cells (Shen et al., 1994, Florea et al., 2003). Further, the contribution of the Isc to cAMP-dependent Cl<sup>-</sup> secretion was in agreement with the expression of CFTR that was conducted by immunoprecipitation assays (Shen et al., 1994). Cultures of Calu-3 cells at air-liquid interface (ALI) were also compared with those in liquid covered culture (LCC) to evaluate the degree of differentiation in these two culture conditions. Calu-3 cells differentiated at ALI culture method displayed a thicker pseudostratified layer than Calu-3 cells in LCC. Tight junctions, microvilli and secretory granules were also more apparent in ALI culture than in LCC (Harcourt et al., 2011).

Nevertheless, several other bronchial epithelial cell models are also available. BEAS-2B, derived from human normal bronchial epithelium, is a transformed immortalised bronchial epithelium transfected with an adenovirus 12-SV40 virus hybrid (Lechner and LaVeck, 1985). However, no apparent differentiation capacities, mucin secretion or lack of tight junctions have been

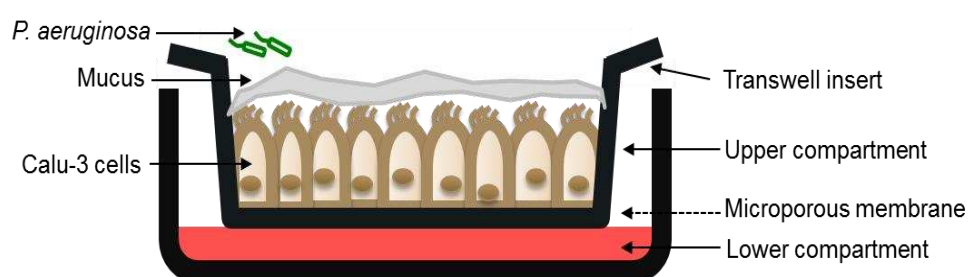
reported in previous papers. (Berube et al., 2010); 16HBE14o- is also a transformed bronchial epithelial cell line that develops cilia, microvilli, and forms tight junctions but are defective in mucin secretion (Papi and Johnston, 1999, Cozens et al., 1994, Wan et al., 2000). A comparison between the characteristics of commonly used bronchial epithelial cells was summarised in Table 3.1.

Compared to in vivo studies, in vitro models have the advantage of flexibility and control of experimental conditions. They also allow the study of airway epithelial functions in the absence and in the presence of other cells such as macrophages, neutrophils, and fibroblasts, etc. (Stewart et al., 2012, Zhu et al., 2010, Berube et al., 2010). We adapted the air-liquid interface culture system that has recently been recognised as one of the most physiologically relevant in vitro models for respiratory research (Berube et al., 2010). The schematic figure of our in vitro airway epithelial infection model shown in Fig. 3.1 illustrated that Calu-3 cells seeding at the top of transwell is designated 'upper compartment' and the basal chamber containing culture medium that supply the cells with nutrients is 'lower compartment.' The configuration that the apical surface of the cells exposed to air mimics the conditions found in the human airway and drives differentiation towards a mucociliary phenotype. *P. aeruginosa* infection from the apical surface was conducted once the in vitro airway epithelium achieved polarity and integrity. A cost-effective, robust, reproducible, physiologically relevant human in vitro bronchial epithelium model for *P. aeruginosa* infection was established in this chapter.

**Table 3.1 Summary of morphological characteristics and barrier function of commonly used in vitro human bronchial epithelial cell models.**

Cell Type	NHBE	Calu-3	BEAS-2B	16HBE14o-
Origin	Healthy tissue	Lung adenocarcinoma	Transformed healthy tissue	Transformed healthy tissue
Morphology and properties	Mixed airway cell population	Pseudostratified cilia-producing secretory cells	Secrete cytokines and antioxidants	Non-ciliated cuboidal cells
Mucus producing	YES	YES	NO	NO
Tight junction formation	YES	YES	NO	YES
Maximum TEER at ALI ( $\Omega \text{ cm}^2$ )	750	600	150	200

Adapted from (Stewart et al., 2012, Berube et al., 2010, Sporty et al., 2008)



**Figure 3.1 Schematic of the in vitro respiratory epithelium model for *P. aeruginosa* infection.**

Calu-3 cells grown on 0.4  $\mu\text{m}$  pore size membrane inserts at air-liquid interface drives differentiation of bronchial epithelial cells to a pseudostratified mucociliary epithelium. *P. aeruginosa* infection on the apical surface of the airway epithelium is to mimic bacterial infections occur in the human bronchial epithelium.

## **3.2. HYPOTHESIS**

Human lung epithelium represents the first barrier encountered by respiratory pathogens. Establishment of an in vitro infection model using differentiated human bronchial-epithelial cell line Calu-3 cells would provide a cost-effective and robust platform to investigate the initial interaction between pathogen and the host in the context of the lung.

## **3.3. AIM**

The purpose of this study was to establish an airway epithelium platform to examine the impact of AQs on the pathogenicity of *P. aeruginosa* in the human lung. To achieve this, an in vitro infection assay using differentiated Calu-3 cells and *P. aeruginosa* PAO1-subline Lausanne has been developed.

Conditions optimised for this infection model included:

- (1) Establishment and characterisation of differentiated Calu-3 cells cultures
- (2) Establishment of condition to generate consistent *P. aeruginosa* inoculum for the infection on differentiated Calu-3 cells
- (3) The efficacy of the in vitro bronchial epithelial infection model

## **3.4. MATERIALS AND METHODS**

### **3.4.1. Calu-3 cell culture and differentiation**

Calu-3 cell culture handling and differentiation were described previously (Grainger et al., 2006). Calu-3 human bronchial epithelial cells (ATCC no. HTB-55) were purchased from the American Type Culture Collection (Rockville, USA) and used between passage 19 and 35. Newly thawed cell stocks were cultured initially in 75 cm<sup>2</sup> flasks (Corning Life Sciences, the Netherlands) in 15 ml medium and maintained at 5% CO<sub>2</sub>, 37°C. Two culture media were evaluated in this study for their suitability for Calu-3 cell differentiation: (1) Dulbecco's modified Eagle's medium (DMEM)/ Nutrient Mixture F-12 Hams (1:1) (Sigma-Aldrich, UK) containing 10% fetal calf serum (FCS) (Sigma-Aldrich, UK), 1x non-essential amino acid solution (Sigma-Aldrich, UK) and 1x L-glutamine (Sigma-Aldrich, UK) (thereafter designated 'DMEM'); (2) minimum essential medium  $\alpha$  containing GlutaMAX™ I (Life Technologies, USA) containing 10% FCS (designated MEM onwards).

For differentiation, cells cultured in T-75 were washed with PBS (Sigma-Aldrich, UK) and trypsinised with 0.05% trypsin and 0.02% EDTA in phosphate buffered saline (PBS) solution (Sigma-Aldrich, UK) at 37°C for 15 min and seeded on 0.4  $\mu$ m pore size, 12-well transwell polyester inserts (Corning Life Sciences, the Netherlands). In some instances the polyester inserts were coated with rat tail type I collagen (BD Bioscience) or Matrigel (BD, Bioscience). Briefly, 100  $\mu$ l of collagen solution at a concentration of 3  $\mu$ g/ml in PBS was added to each transwell insert and inserts were transferred to

the CO<sub>2</sub> incubator, 37°C for 45 min. Collagen solution was aspirated, each insert washed once with 150 µl of PBS. To prepare Matrigel-coated inserts, 100 µl of Matrigel diluted 1:4 in serum-free DMEM and MEM were added to each insert and incubated at 5% CO<sub>2</sub>, 37°C for 4 h to allow for self-assembly as a thin film. Calu-3 cells were seeded in the transwell polyester inserts at a density of 100,000 cells per well in 500 µl of complete culture medium with 1 ml of medium in the basal chamber. After overnight culture at 37°C, 5% CO<sub>2</sub>, the medium in the insert was aspirated for the cells to differentiate at air-liquid interface (ALI). The medium in the bottom chamber was changed every other day up to 21 days.

### **3.4.2. Assessment of Calu-3 cell differentiation**

#### 3.4.2.1. Immunofluorescence staining and confocal fluorescence microscopy

##### Antibodies

The antibodies used for confocal imaging were of mouse origin and targeted the human cilia-associated tubulin IV (Life Technologies, USA), mucin MUC5AC (Life Technologies, USA), and zonula occludin-1 (ZO-1) protein (Life Technologies, USA). These primary antibodies were used at a dilution of 1:1,000 for anti-tubulin IV and anti-MUC5AC antibodies and 5 µg/ml for anti-ZO-1 antibody. A donkey anti-mouse antibody conjugated to Alexa Fluor 488 (Life Technologies, USA) diluted 1:250 was used as secondary antibody. Phalloidin conjugated to Alexa Fluor 488 (Life Technologies, USA) was used to detect F-actin. Cell nuclei were visualised with 4', 6-diamidino-2-



phenylindole hydrochloride (DAPI) (Sigma-Aldrich, UK) or Hoechst 33342 (Cell Signalling Technology, UK).

#### Fixation and staining

Calu-3 cells cultured in transwell inserts were fixed with 4% paraformaldehyde (16% paraformaldehyde, EM grade, Electron Microscopy Sciences, USA) in PBS overnight at 4°C. The following day, the filters were removed from the inserts and placed in a 24-well plate (Corning Life Sciences, the Netherlands) for processing. Cells were washed with PBS for 5 min three times, permeabilized with 0.15% Triton X-100 (Sigma-Aldrich, UK) in PBS for 20 min at room temperature. After 3 washes in PBS, non-specific binding sites were blocked with blocking solution (5% donkey serum, Sigma-Aldrich, in PBS) for 30 min. Cells were then incubated with the primary antibody diluted in blocking solution for 1 hr at room temperature. After rinsing three times with PBS, cells were incubated with the secondary antibody diluted in blocking solution for 30 min protected from light. Control samples were stained with the secondary antibody alone. For staining of the cytoskeleton, cells were incubated for 30 min with phalloidin-Alexa Fluor 488 at 1: 250 dilution. Cells were counter stained with DAPI or Hoechst 33342 at 1 µg/ml in PBS for 10 min at room temperature and then washed three times with PBS. After staining, samples were mounted with Vectashield HardSet Mounting Medium (Vector Laboratories, UK).

## Imaging

Optical sections of the cells were obtained using a Zeiss LSM 700 laser scanning microscope equipped with detectors and filter sets for monitoring emissions of the selected fluorophores and oil-immersion plan-apochromat 63x/1.4NA objective lens. Images were analysed using Zen 2009 (Zeiss, Germany)

### 3.4.2.2. Histological staining

Calu-3 cells cultured on transwell inserts uncoated or coated with collagen, type I solution (BD Biosciences, UK) from rat tail or Matrigel (BD Biosciences, UK) at ALI for 21 days in MEM or DMEM were fixed overnight with 4% paraformaldehyde (16% paraformaldehyde, EM grade, Electron Microscopy Sciences, USA) in PBS (Sigma-Aldrich, UK) at 4°C. After fixation, the filters were cut out, halved, and each half embedded in paraffin wax using a Leica TP1020 automated tissue processor. 5 µm thin cross-sections of wax-embedded inserts were obtained using a Leica RM2145 microtome. The air-dried cross-sections were rehydrated using decreasing concentrations of ethanol and stained with haematoxylin and eosin (Raymond A Lamb Laboratory Supplies, UK), alcian blue/Mayer's acid (Sigma-Aldrich, UK), or alcian blue/fast acid stain (Sigma-Aldrich, UK). Following staining, sections were dehydrated by passing through increasing concentrations of ethanol, dried, and mounted using DPX mounting medium (Raymond A Lamb Laboratory Supplies, UK). Mounted sections were viewed using a Zeiss Axioplan light microscope and images were captured with a Q Imaging MicroPublisher 5.0 RTV camera along with Openlab software.

#### 3.4.2.3. Scanning electron microscopy

Calu-3 cells cultured on transwell inserts at ALI in MEM for 21 days were fixed with 3% glutaraldehyde (Agar Scientific, UK) in 0.1 M sodium cacodylate buffer (Agar Scientific, UK) at 4°C. Samples were then post-fixed in situ with 1% osmium tetroxide (Agar Scientific, UK), dehydrated in serial concentrations of ethanol, and air-dried in a fume hood overnight. Once dry, inserts were cut out, mounted on inert supports and gold-sputter coated. Samples were visualised by using a Jeol JSM840 scanning electron microscope with an ISS Iscan digital frame grabber.

#### 3.4.2.4. Transepithelial electrical resistance

The barrier function of Calu-3 cell cultures in ALI was determined by measuring transepithelial electrical resistance (TEER) using an epithelial voltohmmeter-EVOM (World Precision Instruments, UK). Prior to the measurement, the apical surface of Calu-3 cell culture was balanced by adding 500 µl of culture medium for 30 min at 37°C, 5% CO<sub>2</sub>. Effective TEER ( $\Omega\text{-cm}^2$ ) was calibrated by subtracting the resistance of a cell-free transwell insert.

### **3.4.3. Pseudomonas aeruginosa culture**

#### 3.4.3.1. Comparison of *P. aeruginosa* growth in LB, DMEM and MEM

PAO1-L was streaked on a LB agar plate from a -80°C glycerol stock and cultured at 37°C overnight. The next day, a single colony was used to inoculate 5 ml of LB, DMEM or MEM in a 50 ml falcon tube. Cultures were incubated at 37°C, 200 rpm overnight. The next day the overnight liquid culture was diluted (1:100) in 25 ml of the corresponding media in 250 ml flasks and incubated at 37°C, 200 rpm OD<sub>600</sub> was measured every hour from 0 h to 12 h and at 24 h.

### **3.4.4. PAO1-L infection of differentiated Calu-3 cells**

#### 3.4.4.1. Preparation of PAO1-L inoculum for infection assay

PAO1-L was streaked on a LB agar plate from a -80°C stock and cultured at 37°C overnight. The next day, a single colony was used to establish a 5 ml overnight culture in LB (37°C, 200 rpm). The following day the OD 600 nm of the culture was measured using a spectrophotometer and the inoculum was adjusted to 1% to prepare a 25 ml culture in LB using a 250 ml conical flask. The new culture was incubated at 37°C, 200 rpm, for 4 hours. The culture was then transferred to a sterile 50 ml centrifuge tube and centrifuged at 10,000 rpm (Allegra X-64R with C0650 fixed angle rotor, Beckman Coulter, UK) at 4°C for 5 min. Bacterial pellets were washed twice with sterile tissue culture-grade PBS with CaCl<sub>2</sub> and MgCl<sub>2</sub> (Life Technologies, USA) using the same centrifugation conditions. After the second wash, bacterial cell pellets were resuspended in 5 ml PBS with CaCl<sub>2</sub> and MgCl<sub>2</sub>. An aliquot was diluted 1:10

in PBS and mixed 1:1 with 4% paraformaldehyde (16% paraformaldehyde, EM grade, Electron Microscopy Sciences, USA) in PBS. 2 µl of diluted, fixed PAO1-L were pipetted onto a Thoma counting chamber slide (Hawksley, UK). PAO1-L culture density was calculated using the following formula:

$$\text{Bacteria/ml} = \frac{\text{Total number of bacteria counted} \times (2 \times 10^7) \times \text{dilution factor}}{\text{Total number of smallest squares counted}}$$

Bacterial multiplicity of infection was adjusted accordingly using PBS with CaCl<sub>2</sub> and MgCl<sub>2</sub> based on the bacterial density determined by counting.

#### 3.4.4.2. Infection of differentiated bronchoepithelium with PAO1-L

The number of Calu-3 cells present in a confluent monolayer on Day 21 in ALI was counted after trypsinisation and estimated as 700,000 cells per transwell insert. 21-day old differentiated Calu-3 cells on the inserts were thereafter infected with PAO1-L (see Section 3.4.4.1.) at MOI 50 (3.5x10<sup>8</sup> CFU/ml, 100 µl per well) in 5% CO<sub>2</sub>, 37°C incubator for 3 h and 6 h.

#### 3.4.4.3. Quantification of bacterial colonisation of the bottom chamber

To assess whether *P. aeruginosa* breaches the epithelial barrier, bacterial CFU in the basal chamber were quantified at 3 h and 6 h post infection. Culture media in the basal chamber were collected, diluted in a 10-fold fashion in PBS. 100 µl of neat and diluted media were plated on LB agar plates. The agar plates were subsequently incubated at 37°C for 18 h. Bacterial colonies were counted

and the actual number of bacteria across the barrier was calculated according to the dilution factor.

#### **3.4.5. Statistical analysis**

All statistical analyses were carried out using GraphPad Prism v. 6.0. When two sets of data were compared, significance was calculated by unpaired Student's t test (data obtained in this study were considered normally distributed). p-value  $\leq 0.05$  was regarded significant.

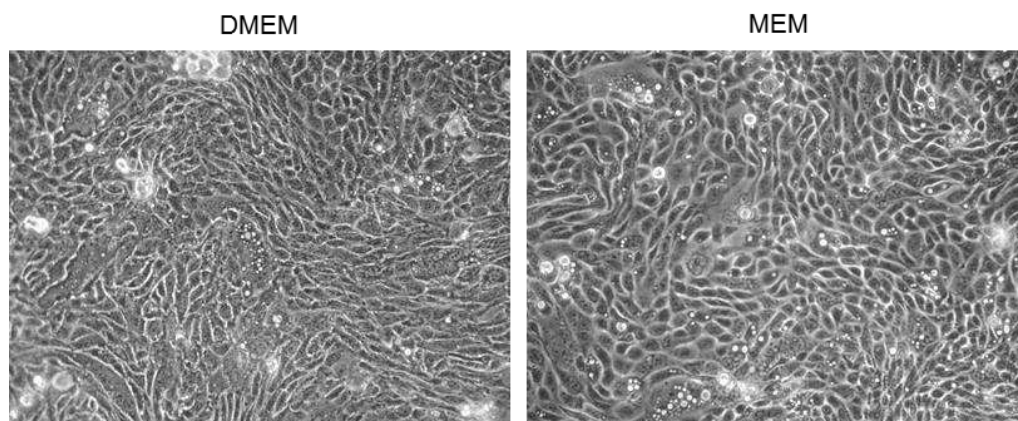
## **3.5. RESULTS**

### **3.5.1. Characterisation of Calu-3 cells differentiation at air-liquid interface**

#### 3.5.1.1. Human bronchial epithelial cells displayed polarity on non-coated polyester transwell inserts in minimal essential culture medium (MEM)

In the majority of published literature, DMEM was commonly used to grow and differentiate bronchial epithelial cells. Also, this culture medium was suggested by our collaborator Dr. Cynthia Bosquillon (Department of Pharmacy, University of Nottingham, U.K.) based on her experience in culturing Calu-3 cells (Stewart et al., 2012). However, as MEM is the medium recommended by ATCC for culturing Calu-3 cells (HTB-55), we decided to evaluate the effect of media on the differentiation of Calu-3 cells. Firstly, the morphology of undifferentiated Calu-3 cells in T-75 flask was compared using phase-contrast microscopy (Fig. 3.2). Calu-3 cells grew and displayed a spindle shape in both DMEM and MEM. Calu-3 cells grew slightly faster in DMEM than in MEM and appeared more vacuolated (Fig. 3.2).

A previous study demonstrated that Calu-3 cells grown in ALI produced a columnar epithelium with a more heterogeneous apical topography and greater mucin proteins secretion than when grown in liquid-covered culture (Grainger et al., 2006). Thus, we decided to establish ALI cultures for this study in an attempt to recapitulate the physical properties of native human airway epithelium.



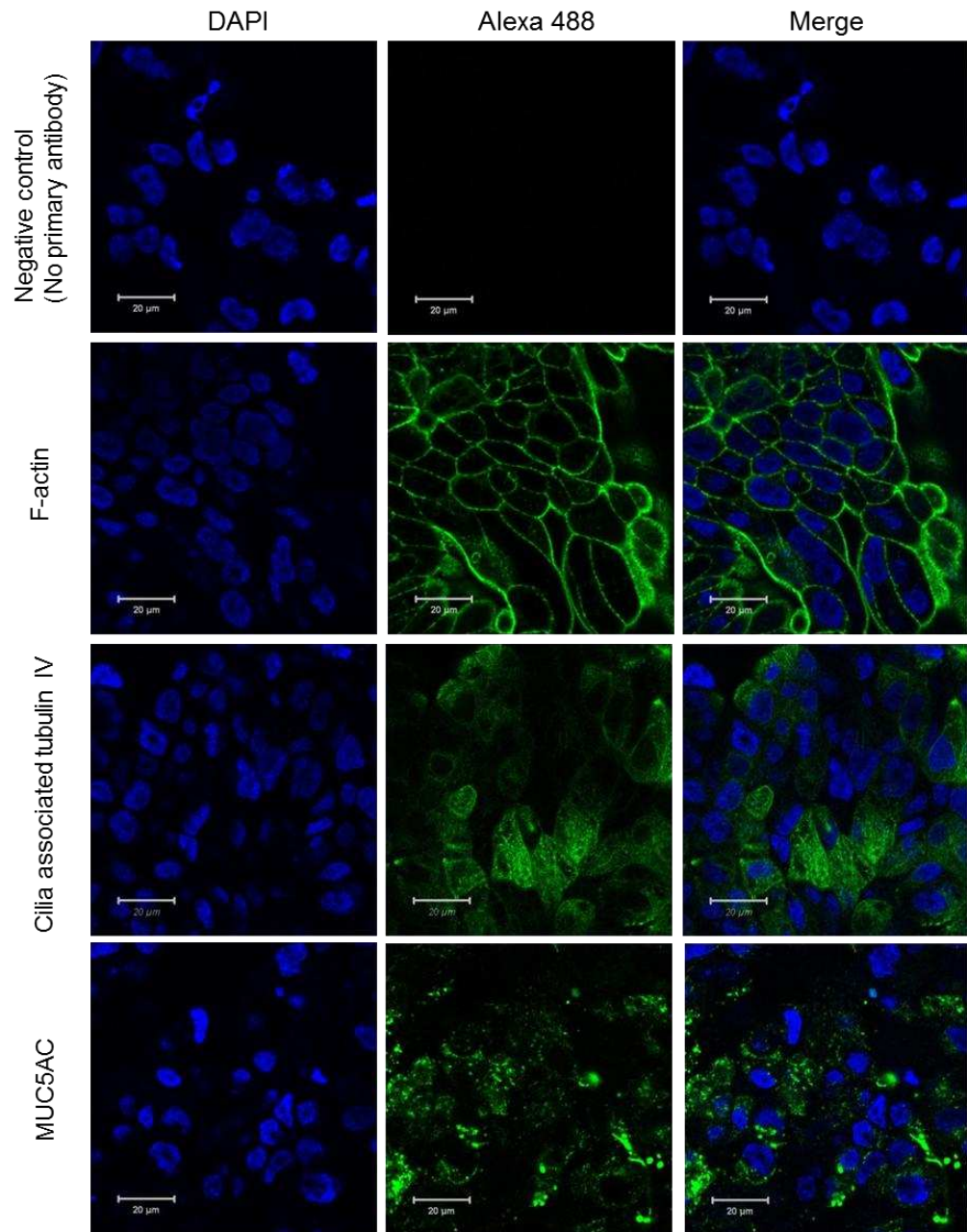
**Figure 3.2 Morphology of undifferentiated Calu-3 cells at confluency in a T-75 flask.** Spindle shaped Calu-3 cells were viewed under light microscopy in DMEM and MEM cultures. Magnification= 200x.

Calu-3 cells differentiation was firstly assessed using two cell markers: cilia associated type IV tubulin and the mucin protein, MUC5AC, the major component of airway mucus secreted exclusively by goblet cells (Ehre et al., 2012, Hovenberg et al., 1996) using cells cultured in DMEM. At day 7, cilia-like structure and secretion of mucin proteins were visualised in immunofluorescence images using anti-type IV tubulin and anti-MUC5AC antibody, respectively (Fig. 3.2). Individual cells were visualised with F-actin staining (Fig. 3.3). The specialised topology and mucin production showed that a considerable population of Calu-3 cells on the ALI inserts had differentiated into a heterogeneous epithelium containing ciliated cells and mucin-producing cells (goblet cells) only within 7 days.

Native pulmonary epithelium is layered on extracellular collagen matrix comprised of lamina, collagen and fibronectin that not only provide epithelial cells with structural support, but influence cell differentiation, adhesion, migration, as well as survival (Tam et al., 2011). Some studies suggested that

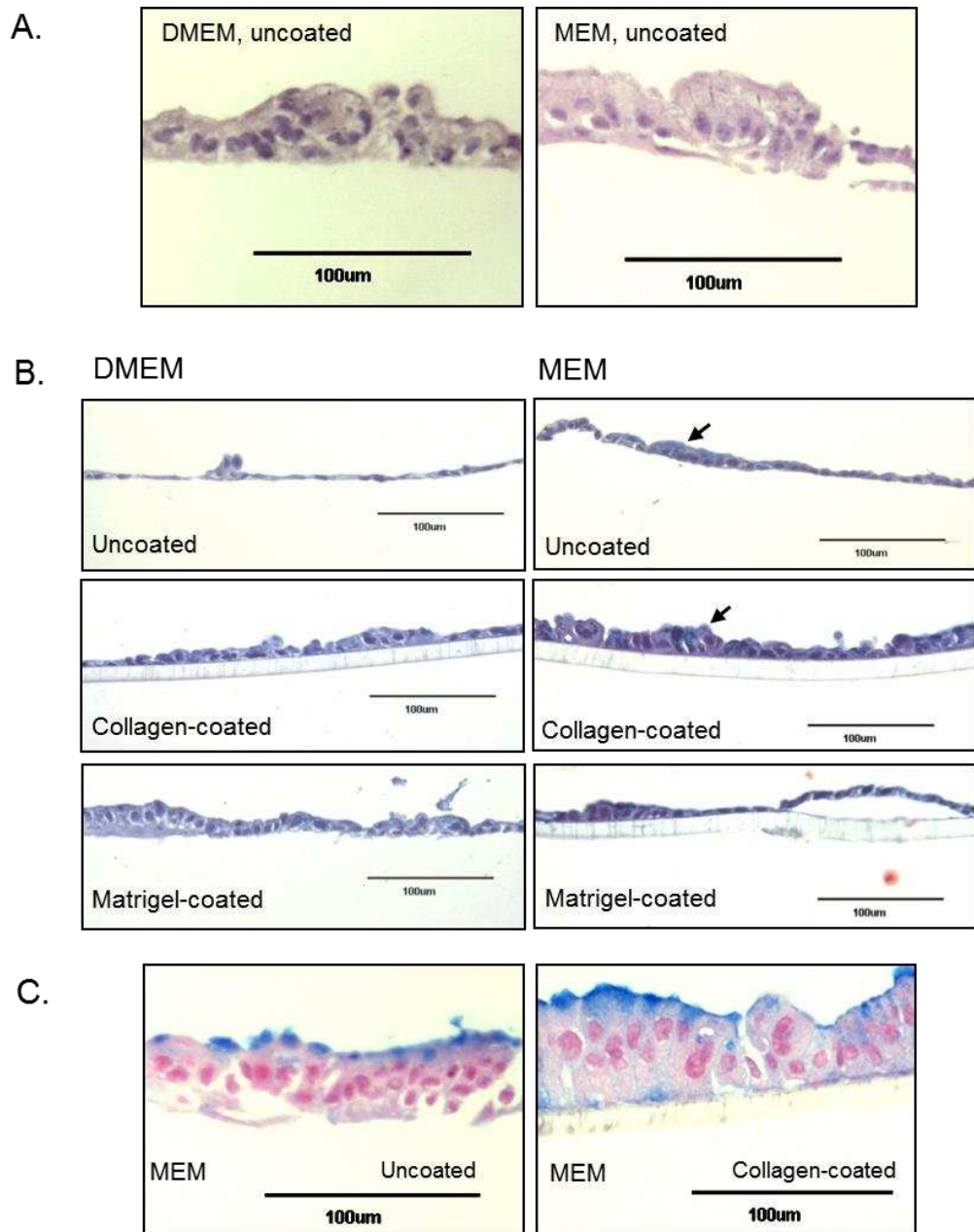


ciliated and secretory phenotypes in tracheal epithelial cells can only be achieved by culturing cells on collagen substratum (Kim, 1985, Wu et al., 1997). We therefore examined the impact of two culture substrata, collagen and Matrigel, on the efficacy of Calu-3 cell differentiation. Rat tail type I collagen is a coating material used as a cell culture substratum to support adherent cells growth and differentiation. Matrigel is a gelatinous heterogeneous protein mixture secreted by mouse sarcoma cells. The protein mixture resembles the complex extracellular environment and thus has been commonly used as a basal membrane layer for metastasis studies. Cells were seeded on transwell inserts with or without coating and cultured in DMEM or MEM for 21 days. Cultures were subjected to histological analysis to determine the degree of differentiation. Calu-3 cells formed more regular pseudostratified columnar shapes in MEM culture compared with DMEM culture based on H and E staining (Fig. 3.4A).



**Figure 3.3 Detection of cilia and mucin expression in one week-old Calu-3 cells cultured in DMEM at ALI.**

Immunofluorescence images of cilia-associated tubulin IV and mucin MUC5AC on one-week old Calu-3 cultures. Cells were stained with anti-tubulin IV and anti-MUC5AC antibody, respectively. F-actin was detected by phalloidin-conjugated with Alexa 488. Cell nuclei were stained with DAPI (blue).

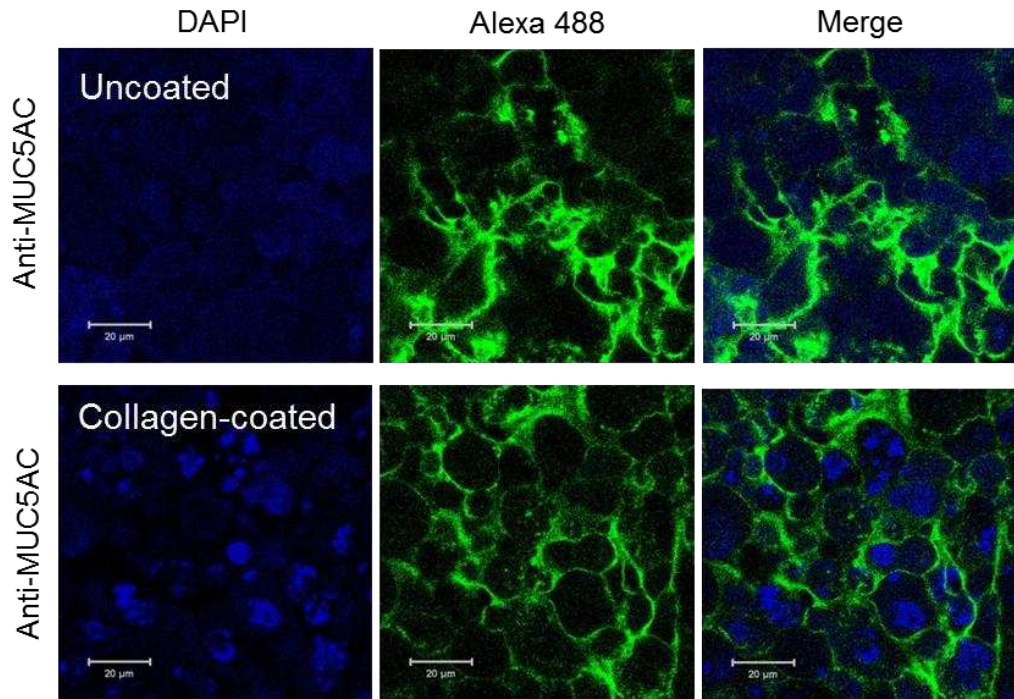


**Figure 3.4 Calu-3 cells grown on polyester inserts for up to 21 days differentiated into a pseudostratified monolayer and expressed mucins at the apical surface.**

Paraffin cross-sections of 3-week old Calu-3 cells cultures grown on 0.4  $\mu\text{m}$  pore size, polyester transwell inserts at ALI were visualised by histological staining. **A.** Hematoxylin and eosin (H and E) staining demonstrated the presence of columnar like cells in DMEM and MEM cultures. **B.** Alcian blue/Mayer's acid staining indicated mucus production at the apical side (blue colour pointed by arrows) regardless of the presence of collagen. Mucin accumulation was more apparent in cells cultured in MEM. **C.** Alcian blue and fast acid staining indicated mucin accumulation (blue) at the apical surface when Calu-3 cells were cultured on uncoated inserts in MEM; Calu-3 cells seemed to display poor polarity on collagen-coated inserts as mucins were seen on both the apical and basolateral sides. Dark pink represents cell nuclei and light pink area is cytoplasm. Each condition was assessed as biological duplicates. Image shown are representative from 3 images taken from each sample.

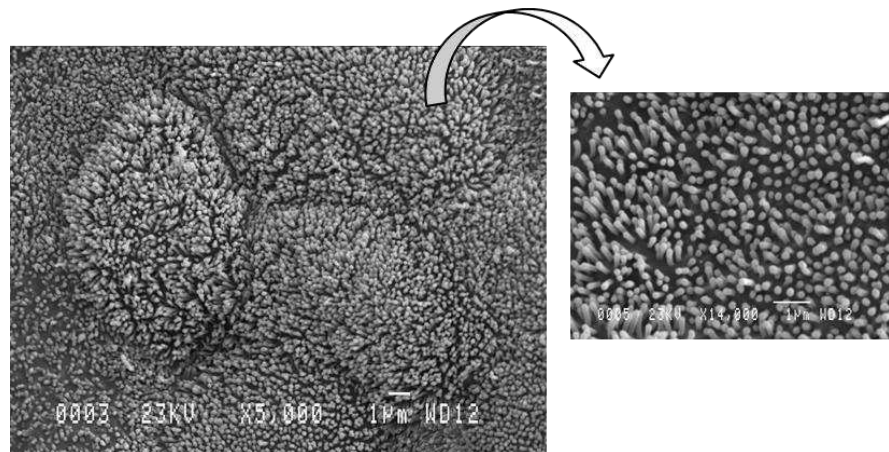
Cell polarity refers to the asymmetric positioning of cell surface, intracellular organelles and the cytoskeleton. Polarity is extremely important in the correct functioning of cells, intracellular protein trafficking, and actin cytoskeleton arrangement (Bryant and Mostov, 2008). Epithelial cells classically exhibit apical specialised protruding structures and their nucleus locates near the basolateral region. By using alcian blue staining to identify mucin production, we observed that Calu-3 cells in MEM produced mucin at their apical side in the presence and absence of collagen coating. Calu-3 cells differentiated into an organised pseudostratified cellular layer on inserts coated with Matrigel both in DMEM or MEM, but no mucins appeared to be secreted by the cells on the Matrigel coated inserts (Fig. 3.4B). To further identify the optimal differentiation condition, alcian blue/ fast acid staining was introduced to distinguish mucins (blue), cytoplasm (pale pink) and nuclear localisation (dark pink). Tall columnar shaped Calu-3 cells that produce mucin were clearly seen in Fig. 3.4C. However, the polarity of Calu-3 cells grown in collagen coated inserts seemed affected by the coating as mucins were detected in the basolateral region (Fig. 3.4C). Additionally, immunofluorescence images also showed extensive mucin accumulation in cells cultured in uncoated inserts (Fig. 3.5). Thus, ALI cultures of differentiated Calu-3 cells were supported by MEM in uncoated wells. Cilia-like apical protrusions were observed on the surface of Calu-3 cells at day 21 in ALI under scanning electronic microscopy (this part of work was supported by Dr. Lee Wheldon); again demonstrating cellular differentiation (Fig. 3.6).





**Figure 3.6 Extensive mucin accumulation in Calu-3 cells when seeded on transwell inserts without coating.**

Immunofluorescence staining of mucins, MUC5AC (green), on 3-week old ALI cultures of Calu-3 cells. Cell nuclei were stained with DAPI (blue). N=1.



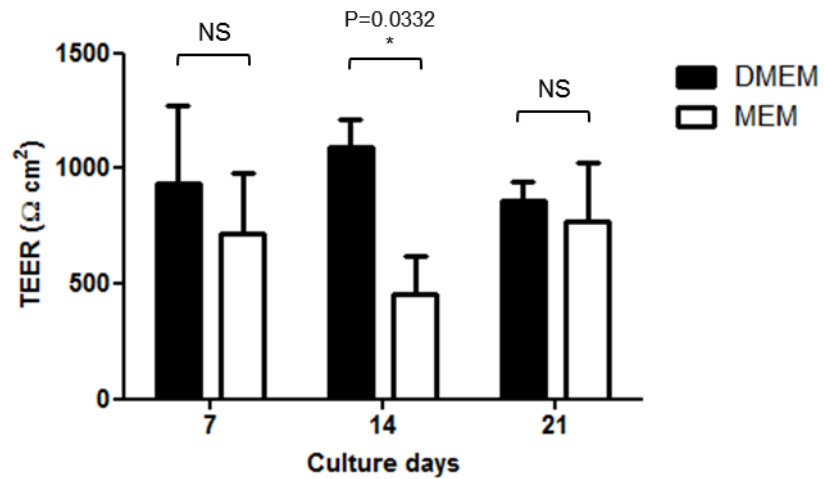
**Figure 3.5 Calu-3 cells at ALI for 21 days exhibited microvilli at their apical surface.**

Scanning electron microscopy images of Calu-3 cells grown at ALI. Calu-3 cells displayed short and thick microvilli at their surface. Image shown on the left is at 5,000x magnifications and individual microvilli were clearly observed when image was zoomed in to 14,000x magnifications (right). N=1.

### 3.5.1.2. Barrier function of differentiated ALI cultures of Calu-3 cells

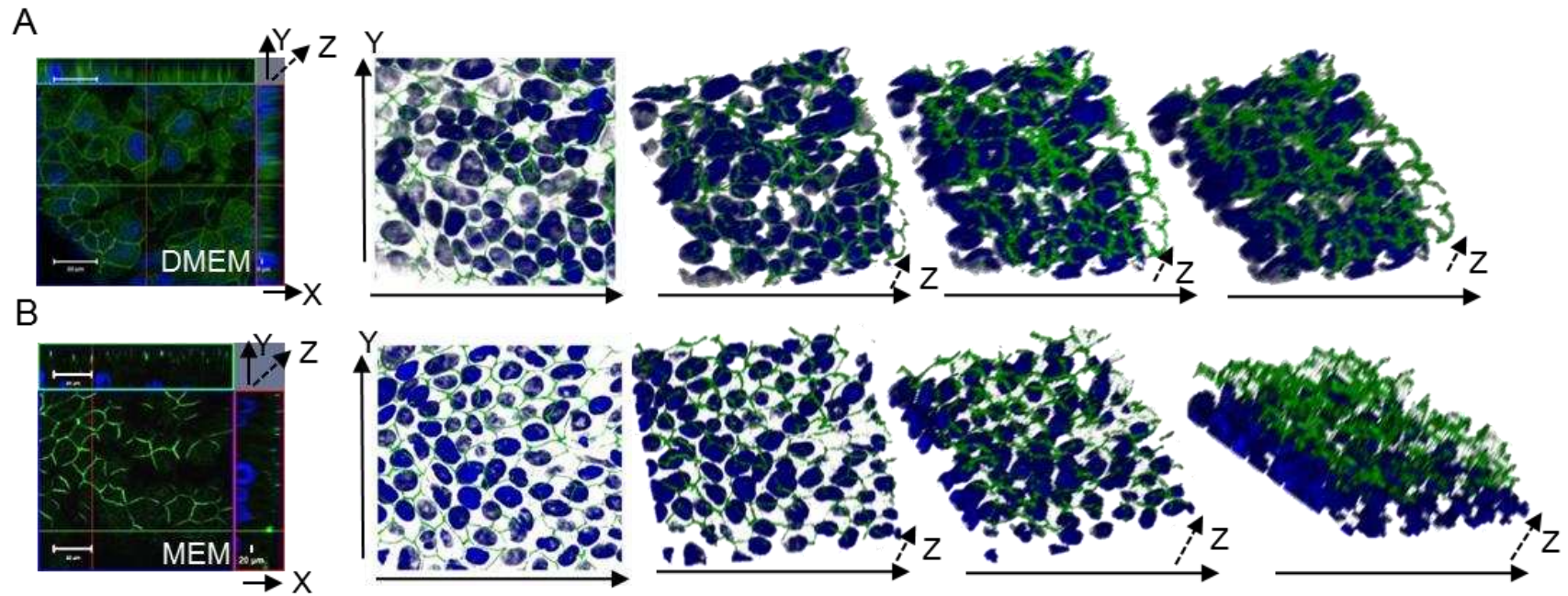
The maintenance of cellular integrity is essential for epithelium to provide a functional physical barrier against constant foreign intruders (Eisele and Anderson, 2011). Tight junction (TJ) proteins block passage of molecules in extracellular fluid diffusion and prevent the movement of molecules between the cells. Zonula occludin 1 (ZO-1) is prominently expressed in intestinal and airway epithelial cells near the apical compartment to form an effective barrier. The movement of ions and fluid can be evaluated by measuring the resistance to flow provided by the cell monolayer, therefore denoted transepithelial electrical resistance (TEER). To determine whether differentiated Calu-3 cells at ALI culture acted as a barrier, TEER and the expression of ZO-1 were examined. TEER in Calu-3 cell cultures at ALI in DMEM and MEM were compared and tracked every 7 days for 3 weeks. TEER in the DMEM culture reached  $939 \pm 578 \Omega\text{-cm}^2$  at day 7 and was maintained above  $850 \Omega\text{-cm}^2$  throughout the 3 weeks. In MEM, TEER reached  $721 \pm 450 \Omega\text{-cm}^2$  at day 7 but dropped at week two ( $457 \pm 277 \Omega\text{-cm}^2$ ) then increased to  $767 \pm 454 \Omega\text{-cm}^2$  at day 21 (Fig. 3.7). High TEER readings in both DMEM and MEM culture without significant difference at Day 21 indicated that ALI cultures of Calu-3 cells attained barrier integrity in both media.

Although both DMEM and MEM supported the expression of ZO-1 by Calu-3 cells ZO-1 was predominantly enriched at the apical side in Calu-3 cells incubated in MEM (Fig. 3.8), which is the location expected in epithelial cells (Gonzalez-Mariscal et al., 2003). Thus, Calu-3 cells cultured in MEM appeared to resemble native epithelium closer than those cultured in DMEM.



**Figure 3.7** Transepithelial electrical resistance of Calu-3 cells ALI cultures in both in DMEM and MEM.

The TEER measurements were taken every 7 days for 3 weeks. TEER measurements between 500 and 1,000  $\Omega \text{ cm}^2$  indicated that both DMEM and MEM supported Calu-3 cells ALI culture. TEER from DMEM cultures reached 1000  $\Omega \text{ cm}^2$  at day 7 and was maintained for 3 weeks. In MEM cultures, TEER dropped at week two and increased to 800  $\Omega \text{ cm}^2$  at day 21. TEER of 3 week old Calu-3 cells cultured in DMEM and MEM were comparable (NS). Measurements were from 3 independent experiments and each experiment was done in duplicate. TEER of Calu-3 cells in DMEM and MEM were compared by unpaired t-test. NS, no significant difference.



**Figure 3.8 Localisation of the tight junction protein ZO-1 in Calu-3 cells cultured in ALI for 21 days.**

Calu-3 cells cultured in DMEM (A) and MEM (B) expressed ZO-1. ZO-1 was enriched at the apical region of MEM cultures. ZO-1 protein was detected using mouse anti-ZO-1 antibody as described in materials and methods. The image is the representative from three independent experiments.

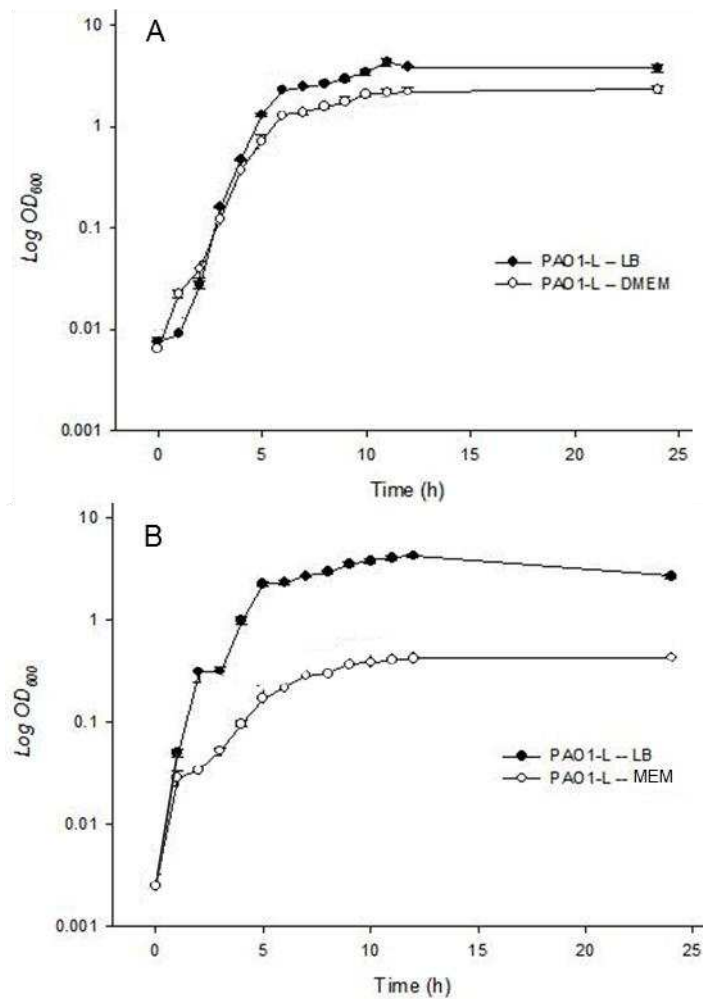


### **3.5.2. Optimisation of *P. aeruginosa* inoculum**

#### 3.5.2.1. Determination of PAO1-L culture condition for the infection of bronchial epithelium

Pathogen associated molecular patterns (PAMPs) such as lipopolysaccharide (LPS), lipopeptides, RNA and DNA trigger innate immune responses via recognition by pathogen associated molecular receptors (PRRs) on host cells, including toll-like receptors (TLRs), retinoid acid-inducible gene I (RIG-I)-like receptors (RLRs) and other cytosolic nucleic acid sensors, and nucleotide-binding and oligomerisation domain (NOD)-like receptors (NLRs) (Baccala et al., 2009). The non-defined medium Luria-Bertani (LB) medium, commonly used to culture *P. aeruginosa*, consists of yeast extract and tryptone which can be a reservoir of nucleic acids and endotoxins. To eliminate potential PAMPs and damage-associated molecular patterns (DAMPs) in the LB medium that could elicit an immune response even without the presence of the target of interest (*P. aeruginosa* in this study) on differentiated Calu-3 cells, two defined media, DMEM and MEM were tested for their ability to support growth of PAO1-L. In all instances the stationary phase was reached at 8 h (Fig. 3.9). Compared to LB, PAO1-L displayed an equivalent growth rate and reached the same cell density when cultured in DMEM (Fig. 3.9A). In contrast, lower cell density was seen when PAO1-L was cultured in MEM compared to LB medium (Fig. 3.9B). This might be due to the fact that the glucose content in MEM is 3-fold lower than in DMEM. Because MEM was found most suitable for the generation of differentiated Calu-3 cultures in ALI, using MEM to grow *P. aeruginosa* to infect Calu-3 cells seemed to be the sensible choice. However,

it remained a concern whether the phenotype of *P. aeruginosa* would change in this nutrient-deprived medium. Furthermore, the phenotypic characterisation of *P. aeruginosa* has been mostly performed in LB medium, including this study (Chapter 2). Thus, to minimise the phenotypic changes that might occur when *P. aeruginosa* is cultured in nutrient deficient medium, LB medium was chosen to grow *P. aeruginosa* to ensure optimal viability prior the infection assay but extensive washes in PBS were performed to minimise carryover of LB-derived products. For this *P. aeruginosa* cultures were centrifuged, culture supernatants were discarded, cell pellets were thoroughly washed twice with PBS. *P. aeruginosa* inocula were finally resuspended in PBS with  $\text{CaCl}_2$  and  $\text{MgCl}_2$ .



**Figure 3.9** *P. aeruginosa* PAO1-L growth rate was comparable in LB, DMEM and MEM but the final cell density was lower in MEM.

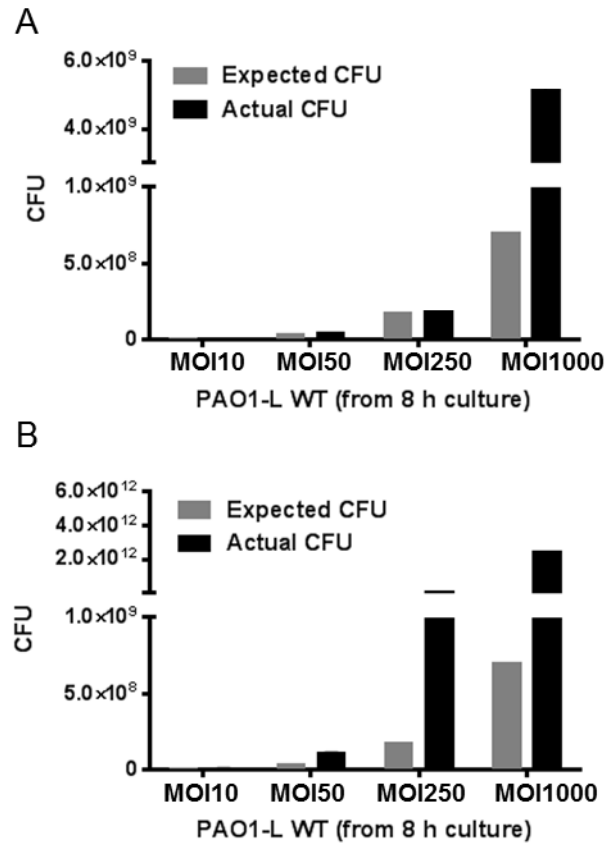
OD<sub>600</sub> of *P. aeruginosa* PAO1-L culture was measured every hour for 12 h and at 24 h. Bacteria were cultured in LB, DMEM or MEM at 37°C, 200 rpm. No lag phase was observed in any conditions and stationary phase was reached after 8 h incubation. PAO1-L growth pattern was similar in both DMEM and MEM. However, the cell density was lower in MEM (B) compared with DMEM (A). N=2.

### 3.5.2.2. Optimisation of bacterial inoculum

Initially, the inoculum used for the infection was prepared from 8h cultures in LB as PQS is largely expressed during stationary phase. To determine which multiplicity of infection was most suitable for studying the interaction of *P. aeruginosa* with differentiated Calu-3 cells, we examined bacterial dissemination using multiplicity of infection (MOI) 1 (means one cell is infected with one bacterium) and 10. In contrast to macrophages that are highly susceptible to PAO1-L infection with 50% killed even at MOI 1 at 4 hour post infection (hpi) (Singh, 2012), Calu-3 cells were more refractory to PAO1-L at MOI 1 and MOI 10 as only a few bacteria were observed on the epithelium in confocal images even at 6 hpi (data not shown). In an attempt to track the *P. aeruginosa* dissemination on the epithelium, we evaluated different MOI including MOI 1,000.

An important aspect of the optimisation of the infection assay was to ensure that the inoculum was accurate. We firstly evaluated whether the actual inoculum was equivalent to the expected CFU from inocula prepared to obtain a MOI of 1,000, 250, 50 and 10 upon infection. High variation was found among experiments and the actual CFU at high MOI failed to correspond the expected CFU (Fig. 3.10). Differences between expected and actual CFU might due to the loss of bacterial viability at 8 h culture when there might be bacterial lysis. Thus, a 6 h cultures were tested for their suitability as a reliable source of bacteria for infection. Using 6 h cultures we observed good correlation between expected and actual CFU for Wt PAO1-L. In this assay we

also included  $\Delta pqsA_L$  and we observed higher CFU than expected at MOI of 250 but lower CFU at MOI of 50 and 10 (Fig. 3.11A).

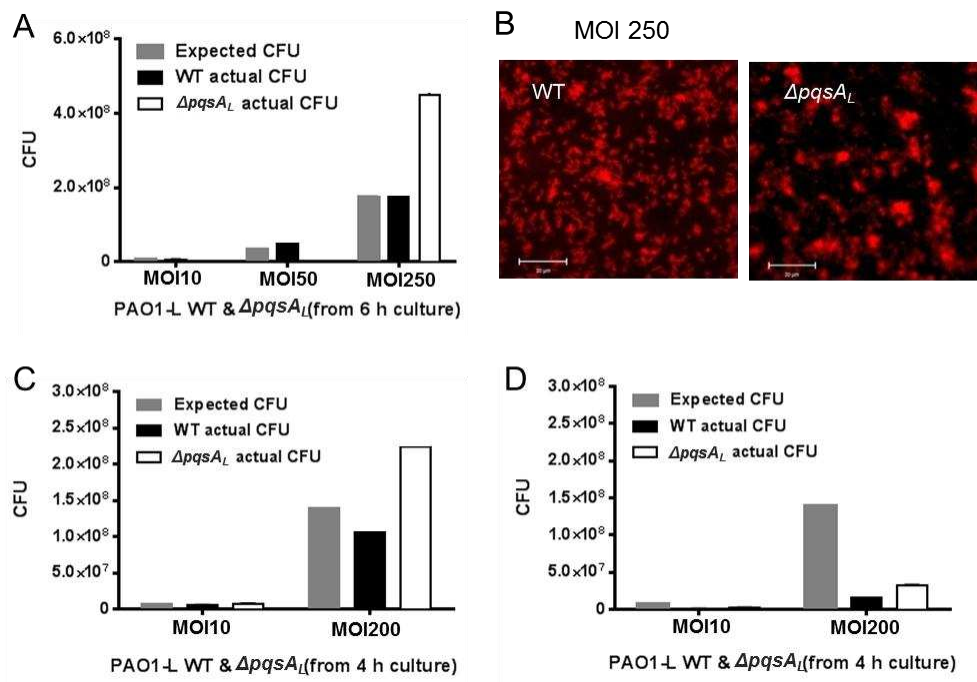


**Figure 3.10 Lack of correlation between experimental and expected CFU in high density inocula.**

High density inocula (MOI 250 and 1000) were prepared from 8 hour Wt PAO1-L cultures based on cell counting in the Thoma chamber (expected CFU) and serial dilutions were prepared and plated in LB to obtain the actual CFU. A and B correspond to two independent experiments.

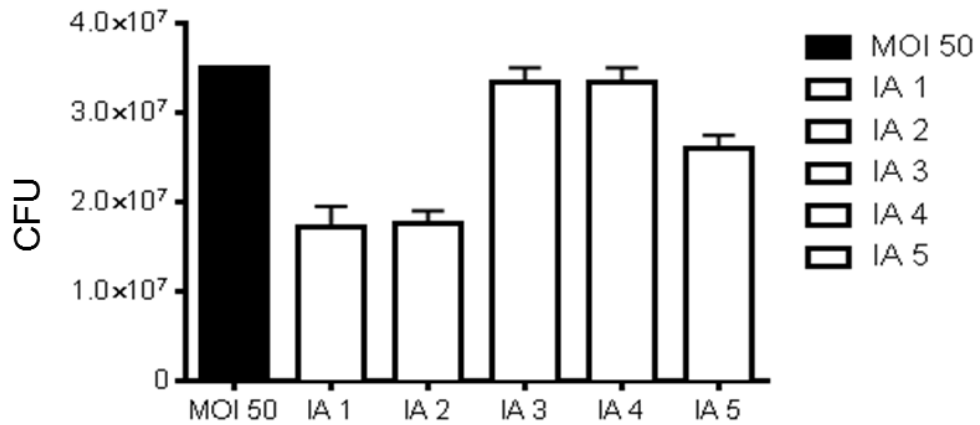
We found that  $\Delta pqsA_L$  formed clumps at MOI 200 ( $1.4 \times 10^{10}$  CFU/ml) compared to Wt PAO1-L (Fig. 3.11B). Therefore, the high variability might be caused by bacteria aggregation at high MOI. To overcome this problem, inocula were prepared from 4 h cultures in an attempt to avoid potential cell aggregates. CFU counting was again assessed in comparison with the expected CFU. However, the variation appeared again at the high density of MOI 200

both in WT and  $\Delta pqsA_L$  culture (Fig. 3.11C). Because the bacterial counting could be highly variable at high density, a MOI 50 was therefore chosen. Consistent and reproducible counting was achieved in 5 independent experiments when Wt PAO1-L was cultured in LB for 4 h and the inoculum was prepared to achieve MOI 50 (range from 27 to MOI 50) (Fig. 3.12). When  $\Delta pqsA_L$  cultures were prepared alongside WT cultures, the inocula from WT and  $\Delta pqsA_L$  were comparable and reproducible and ranged between MOI 27 and MOI 50 (Fig. 3.13). Thus, *P. aeruginosa* incubated in LB for 4 h and adjusted an inoculum to obtain a MOI of 50 were the conditions selected for the infection assays on differentiated Calu-3 cells.



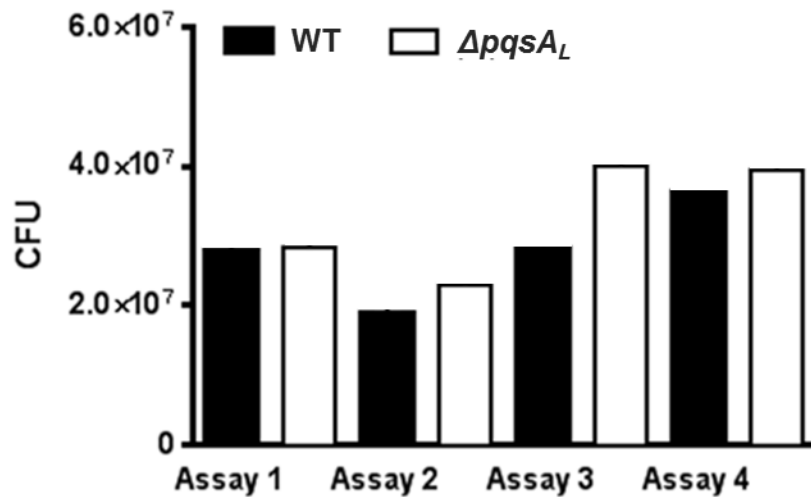
**Figure 3.11 Lack of correlation between actual and expected CFU in high density inocula for WT PAO1-L and  $\Delta pqsA_L$ .**

CFU variation occurred in  $\Delta pqsA_L$  inoculum prepared from 6 h culture (A) which might due to the formation of cell aggregates in the culture broth (B). *P. aeruginosa* PAO1-L and  $\Delta pqsA_L$  were detected with rabbit polyclonal anti-*Pseudomonas* antibody and images were obtained by confocal laser scanning microscope. CFU counting variations between experiments still occurred at a MOI of 200 for both Wt PAO1-L and  $\Delta pqsA_L$ . (A), N=1; (B), representative images from three independent experiments; (C) and (D), results from two independent experiments.



**Figure 3.12 Reliable bacterial counting was achieved when inocula for MOI 50 were prepared.**

Consistent PAO1-L inocula were achieved in 5 assays (MOI varied from 27 to 50; IA 1 to IA 5). The black bar represents the number of expected CFU at MOI of 50 ( $3.5 \times 10^8/\text{ml}$ ) and the white bars are actual CFU obtained from 5 independent assays. Standard errors were shown from each experiment when bacterial cultures were prepared in two individual flasks.



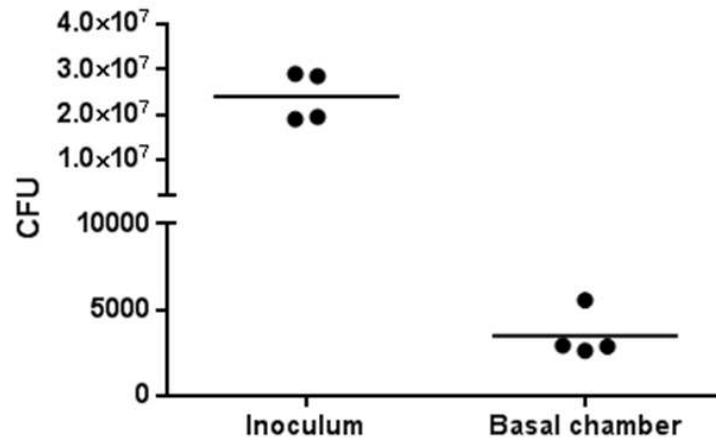
**Figure 3.13 WT and  $\Delta pqsA_L$  inocula were comparable and achieved consistency at MOI 50.**

Reliable counting was achieved at MOI of 50 from 4 hour bacterial cultures. The actual inocula were determined by CFU counting after plating the bacterial inoculum on LB agar plate.

### **3.5.3. Assessment of the suitability of differentiated Calu-3 monolayers to model PAO1-L infection**

*P. aeruginosa* infection on epithelium can be divided into three major events bacterial adherence, penetration/invasion, and barrier disruption/tissue dissemination (Heiniger et al., 2010). To assess the suitability of differentiated Calu-3 cell monolayer for modelling this series of events upon *P. aeruginosa* infection, the appropriate time windows that would provide information regarding (1) early recognition events with sustained epithelial barrier and (2) bacterial invasion and compromised epithelium need to be established. Following apical inoculation on the differentiated Calu-3 culture, barrier function was assessed by determining the number of bacteria in the basal chamber. By 2 and 3 hpi, no bacteria were found in the basal chamber (data not shown) suggesting the barrier function was maintained at this time point. At 6 hpi, bacteria were detectable in the basal chamber. The number of bacteria across the differentiated Calu-3 culture barrier consistently ranged between 3,000 and 6,000 from 4 independent experiments and duplicates in each experiment (Fig. 3.14). Thus, the differentiated Calu-3 cell monolayer can be used to study early and late events during the interaction with *P. aeruginosa* (Chapter 4 and 5).





**Figure 3.14 Detection of PAO1-L at the bottom chamber of differentiated Calu-3 cultures at 6 hpi.**

Calu-3 cell barrier integrity was compromised at 6 hpi during PAO1-L infection when bacteria appeared in the basal chamber. The bacterial numbers found in the basal chamber were consistent (CFU between 3,000 and 6,000). Four independent infection assays were conducted and each had biological duplicates.

## **3.6. DISCUSSION**

### **3.6.1. Successful generation of differentiated human bronchial epithelium cultures at air-liquid interface**

The lower airway epithelium is a pseudostratified layer lined up with columnar shaped ciliated cells, basal cells interspersed with goblet cells and club (Clara) cells (Berube et al., 2010). Culture of Calu-3 cells at ALI has been shown morphologically and functionally more relevant to in vivo airway epithelium compared to liquid submerged culture (Grainger et al., 2006). In particular, cells at ALI have been shown to possess a more columnar morphology and form a 20-45  $\mu\text{M}$  pseudostratified layer thicker than submerged cultures (Grainger et al., 2006). The present study was the first in our group to establish a differentiated human bronchial epithelial culture in an attempt to generate an in vitro model for *P. aeruginosa* respiratory infection. The first stage of the study involved the establishment of a robust culture condition for the in vitro differentiation of human bronchial epithelial cells, Calu-3. The 21-day old differentiated Calu-3 cells in this study consistently featured (1) cilia-expression and mucus production at the apical surface visualised by histological staining, confocal and scanning electronic microscopic images; (2) tight junctions and transepithelial resistance verified by the expression of ZO-1 tight junction protein and relatively high TEER.

Calu-3 cells grew faster in DMEM than in MEM and this might be caused by the fact that the glucose content in DMEM is 3.15-fold higher than in MEM. The fast growth of Calu-3 cells in DMEM might contribute to the high numbers of vesicle-like organelles observed in phase-contrast images. It is

likely the vesicle-like organelles were secretory vesicles that are produced by secretory club ('Clara cells' were renamed as 'club cells' in 2013 (Irwin et al., 2013)) cells. Club (Clara) cells are cuboidal non-ciliated cells involved in multiple functions including barrier maintenance, secretion and metabolism in the bronchioles (Stripp and Reynolds, 2008). Evidence showed that club (Clara) cells are progenitor cells capable of differentiate to other cell type in normal bronchial epithelium and also act as cancer stem cells (Reynolds and Malkinson, 2010). An over-differentiation of club (Clara) cells in Calu-3 cells might partially explain the fast-growing morphology phenotype in DMEM culture.

Despite the fact that Kim and Wu, et al. (Kim, 1985, Wu et al., 1997) suggested that collagen substratum is required for the differentiation of tracheal epithelial cultures, Calu-3 cells in this study were able to differentiate into cilia and mucin producing cells on the permeable polyester inserts without substratum. This result was in agreement with the study conducted by Stewart, et al. showing that Calu-3 cells possess a ciliated phenotype and produce mucins in the absence of collagen substratum (Stewart et al., 2012). Calu-3 cells on Matrigel coated inserts differentiated into columnar shaped cells and apical protrusions and mucin producing were also detected. Matrigel is an un-defined mixture of extracellular matrix proteins, predominantly comprised of laminin, collagen IV, and enactin extracted from Englebreth-Holm-Swarm tumours in mice (Hughes et al., 2010). The composition might be different from batch-to-batch which could cause undesired experimental variations. Regarding the cells cultured on collagen coating inserts, although mucin production was observed both by histological and immunofluorescence

staining, some mucin labelling appeared at the basolateral compartment indicating that Calu-3 cells might lack polarity under these culture conditions.

Contrary to the study by Stewart et al. (Stewart et al., 2012) showing that Calu-3 cells expressed low levels of ZO-1 junction proteins at the mRNA and protein levels, our results showed that ZO-1 proteins were present near the apical side of polarised Calu-3 cells, particularly those in the MEM culture. It could be possible that the immunofluorescence images in this publication (Stewart et al., 2012) were misleading as the images might have been acquired at the interphase (cross-section) where ZO-1 proteins are not supposed to be present.

Collectively, the morphology, polarity and barrier characteristics of the differentiated Calu-3 cell culture in our lab corresponded to the phenotype reported in the literature. Importantly, Calu-3 cells not only expressed CFTR channels but also were efficient in mediating  $\text{Cl}^-$  anion conductance and secretion of bicarbonate ( $\text{HCO}_3^-$ ) in response to cyclic adenosine monophosphate (cAMP)-stimulating agents (Shan et al., 2011, Devor et al., 1999, Haws et al., 1994). Thus, Calu-3 cells represent a relatively healthy airway that exhibits functional CFTR that would provide a baseline to study the molecular changes that occur in human epithelium in response to *P. aeruginosa* infection. In our lab, the CFTR mRNA transcripts were detectable in both undifferentiated and differentiated Calu-3 cells and the presence of CFTR protein at the molecular weight of 168 kDa was also validated by immunoblotting (Faraidon Qader, MSc dissertation).

Although differentiated Calu-3 cell cultures at ALI featured the properties of cultures derived from primary NHBE (Berube et al., 2010), we have to acknowledge that this lung adenocarcinoma cell line is hypotriploid. Therefore, some properties in Calu-3 cells may not fully reflect those in healthy native epithelium. For instance, Calu-3 monolayers secrete mostly bicarbonate flux that carry the short-circuit current when stimulated with forskolin in alkaline condition, whereas chloride ion is the main anion transported by primary epithelial cells under this condition (Shan et al., 2011).

### **3.6.2. Variation of *P. aeruginosa* inoculum occurred at high cell density**

The aim of this project was to investigate the impact of PQS on the interaction of *P. aeruginosa* with human bronchial epithelium. Therefore, for the infection assays it would be desirable to use bacterial cultures where maximum PQS production occurs. Because PQS production reached maximum at the late logarithmic phase (Diggle et al., 2003), cultures incubated for 8 h in LB were used to prepare the inocula in the first instance. In addition, as the immune-competent airway epithelium is usually not susceptible to *P. aeruginosa* infection, a considerable amount of *P. aeruginosa* inoculum would be required in this acute respiratory infection model. Difficulties in obtaining consistent bacterial counting with high bacterial density cultures (MOI 1,000 is  $7 \times 10^9$ /ml in our study) and the large variation in actual CFU obliged us to modify the experimental approach. *P. aeruginosa* genome harbours a prophage Pf4 that influence biofilm formation and virulence by inducing cell death (Rice et al., 2009). The filamentous phage played a role in shaping the biofilm structure from the formation of microcolonies to biofilm dispersal as it causes cell lysis

and release of DNA (Whitchurch et al., 2002, Rice et al., 2009). We postulate that prophage-mediated 'P. aeruginosa autolysis' might occur at high cell density after 8 h incubation. Since nutrients become limited in cultures, surviving bacterial cells would benefit from the molecules released from lysed cells, such as DNA. Extracellular DNA is a source of carbon, phosphate and nitrogen that can be used by P. aeruginosa through the action of an extracellular deoxyribonuclease (PA3909) (Mulcahy et al., 2010, D'Argenio et al., 2002). At stationary phase, bacterial cultures are a complex mixture composed of viable cells and cells undergoing autolysis which might cause counting of viable bacterial inconsistent. The P. aeruginosa culture time was thereby adjusted from 8 h to 6 h, and then to 4 h when the majority of the cells are viable. In addition, inconsistent bacterial counting and variations between experiments still occurred with wild-type PAO1-L and  $\Delta pqsA_L$  at MOI of 250 and 200. Based on the immunofluorescence images, both wild-type PAO1-L and  $\Delta pqsA_L$  formed clumps and aggregates which could be the cause for high CFU variability. Aggregates appeared to be larger in the case of  $\Delta pqsA_L$ . A study conducted by D'Argenio et al. demonstrated that PQS overproduction could promote cellular autolysis in P. aeruginosa strain PAO1 (D'Argenio et al., 2002). In a transposon mutant library screening, a pqsL mutation displayed autolysis phenotype that secreted pronounced PQS 4 times higher than the wild-type (D'Argenio et al., 2002). The gene pqsL is predicted to encode an enzyme involved in PQS degradation (McKnight et al., 2000). The pqsL mutation (PQS overproduction) resulted in substantial cell lysis in bacterial colonies; in contrast to pqsA and pqsR mutants (no PQS production) that presented no lysis (D'Argenio et al., 2002). It was suggested that extracellular

PQS could have a role in regulating cell survival as a means to adapt to the environmental change. In order to keep both PAO1-L WT and  $\Delta pqsA_L$  viable during inoculum preparation and avoid the potential problems with autolysis, 4 h (mid-logarithmic phase) *P. aeruginosa* cultures diluted to a MOI of 50 ( $3.5 \times 10^8$ /ml) were selected for the study.

### **3.7. SUMMARY**

A robust method to generate an in vitro human differentiated bronchial-epithelial infection model using Calu-3 cells was established. This pseudostratified bronchial epithelium displayed cilia-like microvilli, mucus production, tight junction integrity as well as cellular polarity that resembled the in vivo phenotype. The preparation of *P. aeruginosa* inocula suitable for the infection on differentiated epithelium was also optimised.



# 4. THE IMPACT OF ALKYL-QUINOLONE QUORUM SENSING ON THE INTERACTION OF *PSEUDOMONAS AERUGINOSA* WITH BRONCHIAL EPITHELIUM AND PHAGOCYTES

---

## 4.1. INTRODUCTION

*P. aeruginosa* alkyl-quinolone signal (PQS) molecules have been implicated in the immuno-modulation on host cells. PQS has been shown to modulate cell proliferation, the production of interleukin-2 (IL-2) and tumour necrosis factor (TNF- $\alpha$ ) in mitogen-stimulated human peripheral blood mononuclear cells (PBMCs) (Hooi et al., 2004). Aqs inhibited the production of IL-12 by LPS-stimulated bone marrow-derived dendritic cells which led to reduced T-cell proliferation (Skindersoe et al., 2009). In addition, AQ extracts derived from *P. aeruginosa* strain PA14 supernatant down-regulated host innate immune response via inhibition of the NF- $\kappa$ B and HIP-1 $\alpha$  pathways in murine cells from bronchoalveolar lavage fluid and macrophages (Kim et al., 2010a, Kim et al., 2010b, Legendre et al., 2012). However, the role of PQS on *P. aeruginosa* pathogenesis during the initial interaction of *P. aeruginosa* with human bronchial epithelium remains unknown. The aim of this chapter was to investigate the contribution of PQS to the pathogenesis of *P. aeruginosa* upon infection of human bronchial epithelium by comparing the infectivity of viable PAO1-L WT to that of its isogenic PQS deficient mutant. The

immunomodulatory properties of PQS in the context of *P. aeruginosa* infection of diffCalu-3 cells were also evaluated.

Numerous *P. aeruginosa* virulence factors interfere with the properties of epithelial cells including barrier function, cell viability and modulation of innate immune signalling. The presence of flagella was shown required for transmigration across polarized airway epithelial cells. Flagella elicited Toll-like receptor 5 (TLR5) dependent signalling that led to the induction of proinflammatory cytokines as well as neutrophil (CXCL1, CXCL2, CCL3) and macrophage (CCL20) attracting chemokines in 16HBE epithelial cells (Parker and Prince, 2013). Elastase B degraded two tight junction proteins, ZO-1 and ZO-2 in type II alveolar epithelial cells and Madin-Darby canine kidney (MDCK) cell monolayers (Azghani, 1996). *P. aeruginosa* exotoxin A (ETA) induced 16HBE14o- cell death via an early mitochondrial dysfunction and superoxide anion production (Plotkowski et al., 2002, Kipnis et al., 2006). Purified *P. aeruginosa* rhamnolipids disrupted intercellular tight junctions, inhibited ciliary beating, released mucus glyco-conjugates from trachea/bronchial epithelial cells (Read et al., 1985, Graham et al., 1993). In addition, rhamnolipids in *P. aeruginosa* supernatants inhibited the expression of human  $\beta$ -defensin-2 and interleukin 1 $\beta$  (IL-1 $\beta$ ) in keratinocytes via calcium-regulated pathways and protein kinase C activation (Dossel et al., 2012). Pyocyanin inhibits ciliary beat frequency that impedes the subsequent clearance of *P. aeruginosa* in the airway epithelium. Inhibition of vacuolar ATPase and catalase activity in airway epithelial cells by pyocyanin alters the localization and function of CFTR (O'Malley et al., 2003, Lau et al., 2004, Rada and Leto, 2013). Quorum-sensing circuits including the alkyl-quinolone dependent

system, positively regulates the expression of the majority of factors described above, we were intrigued to investigate whether the deficiency in PQS would affect the interaction of *P. aeruginosa* with human airway epithelium.

On the aspect of how host cells respond to infection, the following signalling pathways have also been investigated in the context of *P. aeruginosa* infection on airway epithelial cells. Both Toll-like receptor 4 (TLR4) which recognises lipopolysaccharide (LPS) and TLR5 that, as mentioned above, binds to flagellin are sufficient to induce the expression of interleukin 6 (IL-6) and tumour necrosis factor- $\alpha$  (TNF- $\alpha$ ), and the chemokines keratinocyte-derived chemokine (KC, also known as CXCL1) in murine alveolar macrophages and epithelial cells (Raoust et al., 2009). In view of the hyper-inflammatory state caused by recurrent infection in the CF lung, TLR5 could be a potential anti-inflammatory target. Indeed, a reduced response flagellin caused by a polymorphism in the TLR5 gene correlated with improved lung function ((Blohmke et al., 2010) et al., 2008, Blohmke et al., 2010). Epithelial cells also secrete anti-microbial mediators to promote an innate immune response. A significant decrease in *P. aeruginosa* strain PAK clearance in mice deficient in surfactant protein (SP)-A and SP-D were observed at 6 hpi (Giannoni et al., 2006). Epilysin, a matrix metalloprotease secreted by Club (Clara) cells (Irwin et al., 2013), acts as a negative regulator that restrains a rapid macrophage recruitment to the lung in a *P. aeruginosa* pneumonia infection model indicating that bronchial epithelial cells and macrophages collaborate to reduce the bacterial burden at early time points (Manicone et al., 2009). In cultured airway epithelial cells and in a mouse model of *P. aeruginosa* infection, TLR2 was shown not only to induce chemokine expression to recruit PMNs, but also

to initiate cleavage of junction proteins occludin and E-cadherin to accommodate transmigration of the recruited PMNs without breaching the epithelial integrity (Martin and Prince, 2008, Chun and Prince, 2009a, Chun and Prince, 2009b). The studies above illustrate numerous strategies employed by airway epithelial cells to protect against *P. aeruginosa* infection. Airway epithelium is also an important mediator for downstream activation of effector cells, such as macrophages and neutrophils.

In this chapter, we aimed to determine the contribution of PQS to the interaction of *P. aeruginosa* with human bronchial epithelial cells by using a PQS deficient mutant  $\Delta pqsA_L$  in comparison with its isogenic wild-type strain. Apart from the original plan of evaluating the impact of PQS on the initial recognition of *P. aeruginosa* by diffCalu-3 cells in an acute infection setting, an infection model attempting to recapitulate *P. aeruginosa* airway chronic infection was also assessed. We investigated whether PQS affects the barrier function of airway epithelia, the ability of *P. aeruginosa* to exert cytotoxicity, expression of proinflammatory cytokines and chemokines as well as the signaling pathways associated with TLR recognition and inflammation.

## 4.2. HYPOTHESIS

Pqs QS regulates a host of virulence factors in *P. aeruginosa* by orchestrating the quorum sensing circuits. AQS were detectable in the sputum and bronchoalveolar lavage fluids of CF patients throughout all stages of infection, from undetectable bacterial infection to late stage in spite of the fact that lasR mutants appeared in 70% of CF isolates. These results suggest that PQS plays an important role during *P. aeruginosa* infection in the lung.

We hypothesised that PQS might contribute to *P. aeruginosa* pathogenesis by affecting bacterial innate immune recognition by human airway epithelium.

## 4.3. AIM

Due to the lack of a comprehensive understanding of how PQS operates during the course of infection, an in vitro human bronchial epithelial infection model was used (see Chapter 3) to investigate the barrier competence, cytotoxicity, innate immune activation and the induction of signalling pathways in response to viable wild-type PQS competent *P. aeruginosa* PAO1-L and a  $\Delta pqsA_L$  mutant deficient in PQS production.

A preliminary investigation of the impact of PQS on phagocytes including neutrophils and M-CSF primed macrophages was also performed.

## 4.4. MATERIALS AND METHODS

### 4.4.1. Bacterial strains and culture conditions

Bacterial strains and culture conditions were described previously in Chapters 2 and 3.

### 4.4.2. Infection of differentiated Calu-3 cells with *P. aeruginosa*

#### 4.4.2.1. Infection assay with PAO1-L wild-type and $\Delta pqsA_L$

Calu-3 cells were plated on permeable Transwell insert (Corning, the Netherlands) and grown at an air-liquid interface for 21 days to form differentiated, polarised pseudostratified epithelium as previously described (Chapter 3, Section 3.4.1.). In the case of differentiated Calu-3 cells (diffCalu-3 cultures), two types of infections were performed during the course of this study.

1) *P. aeruginosa* PAO1-L wild-type (henceforth designated 'WT') and  $\Delta pqsA_L$  were grown to early-exponential growth phase for 4 h in LB broth, washed twice with sterile PBS containing  $\text{CaCl}_2$  and  $\text{MgCl}_2$  (Sigma-Aldrich, UK) and suspended in PBS at a concentration of  $3.5 \times 10^8$  CFU/ml. For each strain, 100  $\mu\text{l}$  of bacterial suspension (equivalent to MOI 50) was added to the apical surface of the diffCalu-3 cultures. Infected cultures were incubated at  $37^\circ\text{C}$ , 5%  $\text{CO}_2$  for 2, 3 and 6 h.

2) *P. aeruginosa* PAO1-L WT and  $\Delta pqsA_L$  were grown overnight for 16 h in LB broth, washed twice with sterile PBS containing  $\text{CaCl}_2$  and  $\text{MgCl}_2$  (Sigma-

Aldrich, UK) and suspended in PBS at a concentration of  $3.5 \times 10^6$  CFU/ml. For each strain, 100  $\mu$ l of bacterial suspension (equivalent to MOI of 0.5) was added to the apical surface of the diffCalu-3 cultures. Infected cultures were incubated at 37°C, 5% CO<sub>2</sub> for 6, 9, 12 and 24 h.

#### 4.4.2.2. Quantification of bacterial growth post infection of diffCalu-3 cultures

*P. aeruginosa* growth on diffCalu-3 cultures was quantified by determining bacterial CFU. In the case of bacteria grown on and within the epithelium (thereby designated as cell-associated bacteria), diffCalu-3 cells were lysed with 250  $\mu$ l of 0.1% Triton X-100 (Sigma-Aldrich, UK), homogenised with a 1 ml syringe plunger. Lysates were collected, subjected to serial dilutions in sterile PBS containing CaCl<sub>2</sub> and MgCl<sub>2</sub> (Sigma-Aldrich, UK) and plated on LB agar plates. After incubation at 37°C for 16 to 18 h CFU was calculated by multiplying the number of colonies on the plate by their dilution factors and adjusting the counts to the volume of the original lysate. For the bacteria that gained access to the basal chamber (designated transmigrated bacteria), the basal culture media were collected and CFU were calculated as described above. The number of bacteria grown in MEM alone during the infection assay was used as control (designated PA only).

#### **4.4.3. Assessment of the expression of proinflammatory cytokines and chemokines by diffCalu-3 cells in response to *P. aeruginosa* infection**

##### 4.4.3.1. Relative quantification of gene expression

RNA isolation

RNAs were extracted from diffCalu-3 using the Absolutely RNA Miniprep Kit (Stratagene, UK) according to manufacturer's instruction. In brief, cells were lysed in reconstituted Lysis Buffer containing  $\beta$ -mercaptoethanol and homogenised by pipetting. Homogenates were then transferred to a Prefilter Spin and centrifuged. Filtrates were mixed with an equal volume of 70% ethanol and vortexed. The mixtures were transferred to the RNA Binding Spin Cup and centrifuged as before. Following a salt-gradient extraction from low salt to high salt washes, RNA was eluted and resuspended in DNase/RNase-free water (Life Technologies, UK). The quantity and quality of RNA were determined using a Nanodrop 2000 spectrophotometer (Thermo Scientific, UK). The purity of RNA measured by the A260/A280 ratio ranging between 1.9 and 2.1 is acceptable.

#### Reverse transcription to cDNA

The quantity of RNA from multiple samples was adjusted to 3  $\mu$ g before reverse transcription. First strand cDNA strand was synthesized using random hexamers and Moloney Murine Leukemia Virus (M-MLV) reverse transcriptase (Life Technologies, UK) according to manufacturer's instruction with minor modifications. Generally, RNAs were mixed with random hexamers (Life Technologies, UK) and placed at 70°C for 5 minutes to eliminate any secondary structures that may have formed. The mixtures were then transferred to ice for 5 min to prevent reformation of secondary structures. Bulk mix composed of 5x first strand buffer (250 mM Tris-HCl, [pH 8.3]. 375 mM KCl, 15 mM MgCl<sub>2</sub>) and 0.1 M of dithiothreitol was added to the template and primer mixture. Reverse transcriptase was added to the whole mixture right



before starting the reaction. Samples were incubated at 37°C for 1 hour. cDNA was then incubated at 95°C for 10 minutes to inactivate the reverse transcriptase. Reverse transcript negative controls were also performed. cDNA were stored at -20°C until quantitative real-time PCR analysis.

#### Quantitative real-time PCR

Quantitative real-time PCR (qPCR) amplification mixtures (25 µl) containing template cDNA (2 µg to 3 µg), 2x SYBR green I qPCR master mix with 2.5 mM MgCl<sub>2</sub> (Stratagene, UK) were used along with ROX as the reference dye to correct for pipetting error. Reactions were run on an Agilent Mx3005P qPCR system. The cycling conditions were 10 min at 95°C and 40 cycles as follows: 95°C for 30 sec, and 72°C for 60 sec. Each sample was performed in triplicate. Primer efficiencies were evaluated by a standard curve performed with templates in 4-log serial dilutions and efficiencies between 99-110% are considered appropriate. A validation experiment was conducted in the input cDNA concentration for 4-log serial dilutions to assess whether the efficiency of the target gene amplification and the efficiency of the reference gene amplification is approximately equal. The relative gene expression between *P. aeruginosa* infected diffCalu-3 cells and non-infected diffCalu-3 cells (comparative C<sub>q</sub> method that compares the C<sub>q</sub> value of the gene of target to the control ( $2^{-\Delta\Delta C_q}$ ); the C<sub>q</sub> of target and the control were normalised with reference gene ( $\Delta C_q$ ) ) was analysed by program MxPro PCR software Mx3005P (provided by Stratagene, UK).

**Table 4.1 Primers used for qPCR**

Primer (Accession number)	Primer Sequences	Position	Amplicon length (nucleotides)
<b>NM_000194.2</b>			
HPRT_f	GTAATGATCAGTCAACGGGGGAC	484-660	177
HPRT_r	CCAGCAAGCTTGCAACCTTAACCA		
<b>NM_006098.4</b>			
GNB2L1S	TCTGCGGGGTCACCTCCACT	280-300	118
GNC2L1AS	TGGCCACAAATCGCCTCGT	398-417	
<b>NM_002180</b>			
IGHMBP2S	CCCACCACAGTCTCTCACAA	1318-1338	111
IGHMBP2AS	GTACTGCACCGTCAGTGTCC	1409-1428	
<b>NM_000758.3</b>			
GM-CSF_f	TCTVAGAAATGTTTGACCTCC	211-231	98
GM-CSF_r	GCCCTTGAGCTTGGTGAG	291-308	
<b>NM_000600.3</b>			
IL-6_f	GATGAGTACAAAAGTCCTGATCCA	548 - 571	130
IL-6_r	CTGCAGCCACTGGTTCTGT	659 - 677	
<b>NC_018922.2</b>			
IL-18_f	CAGAGTCAAGGACTGCCAACT	10311 - 10331	60
IL-18_r	TAGGCCCTGGGTTCCTGT	10353 - 10370	
<b>NM_000594.3</b>			
TNFAH_f	GACAAGCCTGTAGCCCATGT	28 - 47	105
TNFAH_r	TCTCAGCTCCACGCCATT	115 - 132	
<b>NM_000576.2</b>			
IL-1 $\beta$ _f	TACCTGTCCTGCGTGTGAA	637 - 656	76
IL-1 $\beta$ _r	TCTTTGGGTAATTTTGGGATCT	690 - 712	
<b>NM_000584.3</b>			
IL-8_h_f	AGACAGCAGAGCACACAAGC	76-95	62
IL-8_h_r	ATGGTTCCTTCCGGTGGT	120-137	
<b>NM_002982.3</b>			
MCP-1_f	AGTCTCTGCCGCCCTTCT	79-96	93
MCP-1_r	GTGACTGGGGCATTGATTG	153-171	
<b>NM_013278.3</b>			
IL-17c_f	CCCTCAGCTACGACCCAGT	293 - 311	126
IL-17c_r	CTTCTGTGGATAGCGGTCCT	399 - 418	
<b>NM_022789.3</b>			
IL-17e_f	GTGAAGATGGACCCCTCAAC	488 - 507	73
IL-17e_r	AGCCGGTTCAGTCTCTGTC	541 - 560	

#### 4.4.3.2. Cytokine protein quantification

##### Enzyme-linked immunosorbent assay (ELISA)

The levels of GM-CSF in the supernatants of diffCalu-3 cultures were quantified following manufacture's instruction (R&D, UK). Culture supernatants were centrifuged to remove cell debris and bacteria. Between each step, solutions were aspirated and the wells were washed three times with wash buffer (0.05% Tween-20 (Sigma-Aldrich, UK) in PBS, pH 7.2-7.4). Wells of

96-well MaxiSorp surface microplates (Thermo Scientific, UK) were coated with 100  $\mu$ l of mouse anti-human GM-CSF capture antibody at the concentration of 20  $\mu$ g/ml in PBS (Sigma-Aldrich, UK) and incubated at room temperature overnight. The solution was aspirated and wells were washed three times with 300  $\mu$ l of wash buffer. Each well was blocked with 300  $\mu$ l of Reagent Diluent (1% bovine serum albumin of protease free/ fraction V grade (Millipore, US) in PBS, pH 7.2-7.4, 0.2  $\mu$ l filtered) for 1 h at room temperature. 100  $\mu$ l of samples and recombinant human GM-CSF standards (2-fold serial dilutions diluted from 1,000 pg/ml to 15.625 pg/ml) and then incubated for 2 h at room temperature. Wells were aspirated, washed and 100  $\mu$ l of the Detection Antibody (biotinylated anti-rhGM-CSF) at a concentration of 0.5  $\mu$ l/ml was added and incubated for 2 h. After washes, 100  $\mu$ l of horseradish peroxidase conjugated (HRP)-streptavidin at working concentration (1:200) was added to each well and incubated for 20 min. 100  $\mu$ l of substrate solution containing 1:1 mixture of tetramethylbenzidine (TMB) and H<sub>2</sub>O<sub>2</sub> was then added and the plate was incubated in dark for 20 min. 50  $\mu$ l of 2N H<sub>2</sub>SO<sub>4</sub> was added to each well to stop the reaction and optical density (OD) incubation at room temperature for 20 min and read at 450 nm. The concentrations of GM-CSF in samples were calculated according to the equation obtained from the standard curve readings.

#### Bead-based immunoassay

Simultaneous quantification of the levels of interleukin-6, interleukine-8, tumour necrosis factor- $\alpha$ , interleukin-1 $\beta$ , and monocyte chemoattractant protein- 1 in diffCalu-3 culture supernatants was done using the bead-based immunoassay FlowCytomix Simplex kit in combination with FlowCytomix

human Basic kit (eBioscience, UK) according to the manual. Samples were analysed by flow cytometry using the software FlowCytomix Pro provided by eBioscience.

#### Polyacrylamide gel electrophoresis (SDS-PAGE) and immunoblotting

Protein separation based on their electrophoretic mobility was derived from Laemmli method and described previously by (Towbin et al., 1979). Briefly, difCalu-3 cultures were lysed with RIPA buffer (Thermo Scientific Pierce, UK) supplemented with protease and phosphatase inhibitors (Thermo Scientific, UK). Total lysate proteins were suspended in 1x SDS loading buffer (50 mM Tris-HCl pH 6.8, 1% SDS, 7.5% glycerol, and .002 % bromophenol blue) containing 1%  $\beta$ -mercaptoethanol and heated at 95°C for 5 min. Equal volume of each sample was loaded on a 12% polyacrylamide gel, electrophoresis ran at 30 mV for 90 min in Tris-glycine electrophoresis buffer (25 mM Tris base, 192 mM glycine, 0.1% SDS, pH 8.3) (BioRad, UK). After electrophoresis, proteins were transferred to an Immobilon-P PVDF membrane (Millipore, US) in a wet transfer system (transfer buffer: 25 mM Tris base, 192 mM glycine, 20% methanol, pH 8.3) overnight, and the membrane was then incubated overnight again in blocking solution comprised of PBS containing 0.1% Tween-20 (Sigma-Aldrich, UK) and 5% skimmed milk. Incubation with mouse anti-hGM-CSF (1  $\mu$ g/ml, R&D, UK) and mouse monoclonal anti- $\beta$ -actin (1  $\mu$ g/ml, Sigma-Aldrich, UK) as loading control was followed by secondary antibody HRP-conjugated goat anti-mouse antibody (1:10,000 dilution, Sigma-Aldrich, UK). Antibody binding was detected using Enhanced Chemiluminescence (ECL) Detection Reagent (GE Healthcare, UK).

#### **4.4.4. Immunofluorescence staining and confocal laser scanning microscopy**

To visualise the distribution of *P. aeruginosa* on Calu-3 cells, immunofluorescence labelling was performed using similar steps as described in Chapter 3. In short, after fixation, permeabilization and blocking, primary antibody rabbit polyclonal anti-*Pseudomonas* antibody (Abcam) at 4.5 µg/ml in blocking buffer was added for 1 hour, followed by three times washes. Donkey anti-rabbit antibody conjugated to Alexa Fluor 674 was used as secondary antibody (diluted 1:250 in blocking solution) together with Phalloidin Alexa 488 that labels F-actin (diluted 1:40 in blocking solution) after 30 min and 3 washes, glass slides were stored at -20°C before visualisation using a Zeiss LSM 700 laser scanning microscope. Images were processed using Zen 2009 (Zeiss, Germany).

#### **4.4.5. Microarray analysis of signalling pathways activation**

This part of the study was performed by Dr. Ola Negm at the Post-Genomic Technologies Facility, Queen's Medical Centre, University of Nottingham. Briefly, difCalu-3 cultures infected with PAO1-L and  $\Delta pqsA_L$  at 3 and 6 hpi were lysed with 70 µl of RPPA (Reverse Phase Protein Microarray) buffer (Thermo Scientific Pierce, UK) supplemented with protease and phosphatase inhibitors (Thermo Scientific Pierce, UK). Reverse phase protein microarray was carried out on the protein lysates in order to determine expression of the following signaling molecules and transcription factors (the prefix 'p' represents phosphorylated forms of these molecules): pp38, pNF-κB (p65), pERK1/2, pIRF7, pAKT-Serine and pAKT-Threonine. Data were analysed

using RPPAnalyzer software that is written in R. Expression of all proteins was normalised against  $\beta$ -actin. The expression of tight junction proteins ZO-1 and E-cadherin, mucin MUC5AC, cilia-associated  $\beta$ -type IV tubulin, heat-shock protein 90 (HSP90) and nuclear pore complex protein 98-kDa (NUP98) was also examined.

#### **4.4.6. Cytotoxicity**

4.4.6.1. Assessment of cytotoxicity based on the loss of fluorescence signal from  $\beta$ -actin using microarray.

During the course of the microarray signalling study a decrease in the fluorescence signal corresponding to the endogenous control protein  $\beta$ -actin was observed in the infected diffCalu-3 samples at 3 and 6 hpi. Based on confocal images suggesting substantial cellular damage during infection, it was considered that the reduction in  $\beta$ -actin could be used as a surrogate marker of cytotoxicity. For this the degree of actin degradation was quantified based on the decrease in arbitrary fluorescence units (AFU) from infected cells compared with the AFU obtained from untreated cells.

4.4.6.2. LDH cytotoxicity detection assay

Cytotoxicity was assessed using the lactate dehydrogenase (LDH) colorimetric assay according to the protocol provided by the manufacturers (Roche Applied Sciences, UK). Briefly, undifferentiated Calu-3 cells were seeded in a 24-well tissue culture plate (Corning Life Sciences, the Netherlands) at a cell density of 100,000 cells per well and cultured for three days to reach confluency. On the day of infection, culture medium was replaced with MEM without fetal bovine

serum. Cells were infected with PAO1-L WT or  $\Delta pqsA_L$  in PBS at MOI 50 for 3 and 6 h. Cells incubated with PBS were used as negative controls. Cell supernatants were collected and centrifuged to remove cell debris and bacteria. 50  $\mu$ l of supernatant was mixed with equal volume of reaction solution (diaphorase /  $NAD^+$  mixture, iodotetrazolium chloride, and sodium lactate) in a 96-well microtitre plate (Corning Life Sciences, the Netherlands) and incubated at room temperature for 20 min protected from light. Supernatants from uninfected cells were used as negative controls and those collected from Calu-3 cells lysed with 2% of Triton X-100 represented the 100% cell death positive control. The absorbance of sample and control wells was measured at 492 nm and 650 nm (reference wavelength used to correct for differences in absorbance between wells due to imperfections in the material of the microtitre plate) using a Labsystems Multiskan EX plate reader. The OD readings of the samples were firstly subtracted from the OD readings of negative controls, and the percentage of cell death was calculated by comparison with the OD readings from 100% cell death.

#### **4.4.7. Measurement of reactive oxygen species (ROS) production by neutrophils in response to PAO1-L**

##### Neutrophils isolation

Neutrophil isolation procedure and characterisation was previously optimised in our lab (Sonali Singh, PhD thesis). Healthy donors were recruited from amongst students and staff at the Queen's Medical Centre and Centre for Biomolecular Sciences, Nottingham. Ethical approval and informed consent was obtained for all individuals prior to sample collection. 12 ml of venous

blood was collected from each healthy donor in EDTA vacutainers (BD Diagnostics-Preanalytical Systems, UK) and neutrophil isolation begun no later than 1 h post-collection. To isolate neutrophils from fresh whole blood, 12 ml of Histopaque-1077 (Sigma-Aldrich, UK) was added to a 50 ml falcon tube (BD Biosciences, UK). 12 ml of Histopaque-1119 (Sigma-Aldrich, UK) was then carefully laid beneath the Histopaque-1077 layer such that both types of Histopaque formed two sharply separated layers. 12 ml fresh whole blood diluted with 12 ml RPMI-1640 (Sigma-Aldrich, UK) was layered over the Histopaque-1077 layer and the tube centrifuged at 700 x g, acceleration slow, brake off for 30 min at room temperature. The neutrophil layer was harvested using a Pasteur pipette after removal of the upper layers. Isolated neutrophils were washed once with RPMI-1640 to remove any Histopaque. 0.2% saline (Sigma-Aldrich, UK) was then added to the washed neutrophils and incubated at room temperature for 1 min in order to lyse contaminating red blood cells (RBCs). An equal volume of 1.6% saline was added to the cells to equilibrate the solution, and cells were washed once with RPMI-1640. Two more washes were carried out in buffer A in preparation for the subsequent ROS measurement assay (see below). Neutrophils were used immediately after purification to avoid loss of cell viability / function over time.

#### ROS production of neutrophils in response to *P. aeruginosa*

Production of ROS by neutrophils was assessed by the luminol chemiluminescence assay as described previously (Pleass et al., 2007). Briefly, 100  $\mu$ l of luminol solution (67  $\mu$ g/ml luminol (Sigma-Aldrich, UK) in buffer A; buffer A comprises 20 mM HEPES (Invitrogen, UK) and 0.1% BSA (Sigma-



Aldrich, UK) in Hank's buffered saline solution containing  $\text{Ca}^{2+}$  and  $\text{Mg}^{2+}$  without phenol red (Invitrogen, UK)) was added to the wells of a 96-well chemiluminescence microtitre plate (BD Biosciences, UK). The stimuli Zymosan A (Life Technologies, UK) or live PAO1-L diluted in buffer A were then added to the wells. Viable PAO1-L was prepared from 3 h cultures in X-Vivo 15 (Lonza, UK) as described previously in Chapter 3 (Section 3.4.4.1.) and resuspended in buffer A to achieve an MOI of 20. Unstimulated controls contained only Buffer A. All conditions were carried out in triplicate. In some instances PQS pure compound was added at a concentration of 1,000 nM to 1 nM. Diluent (HPLC-grade ethanol, Sigma-Aldrich, UK) was used as negative control. Finally neutrophils resuspended in buffer A were added to the microtitre plate at a density of 50,000 cells per well immediately prior to measurement. Chemiluminescence was measured at 2 min intervals for 2 h at 37°C using a Fluorostar Optima plate reader.

#### **4.4.8. Extraction of quorum-sensing signaling molecules and LC-MS analysis**

500  $\mu\text{l}$  culture supernatants collected from diffCalu-3 cultures infected with PAO1-L and  $\Delta pqsA_L$  as well as 500  $\mu\text{l}$  of MEM cultured with WT and  $\Delta pqsA_L$  were centrifuged and cell-free supernatants were retained for subsequent extraction. Equal volume of acidified ethyl acetate (100  $\mu\text{l}$  of glacial acetic acid (Sigma-Aldrich, UK) in 1 L of ethyl acetate (Sigma-Aldrich, UK)) was added to the cell-free supernatant and vortexed for 20 sec. A volume of 5  $\mu\text{l}$  of 10  $\mu\text{M}$   $\text{d}_9$  C5-HSL was added to the culture supernatant as internal standard. The organic phase was taken up to a 2 ml microcentrifuge tube and the extraction

was repeated twice more. The total extracted solutions were subjected to speed vacuum (Jouan RC10 series, Thermo Scientific, UK) to dry the solvents at 45°C for 20 min. The dried crude extracts were recovered by adding 50 µl of methanol (Sigma-Aldrich, UK), transferred to LC-MS glass vial and subjected to LC-MS analysis.

#### **4.4.9. In vitro infection of macrophages with PAO1-L WT and *ΔpqsA<sub>L</sub>***

##### 4.4.9.1. Preparation of M-CSF primed macrophages from peripheral blood mononuclear cells

Peripheral blood mononuclear cells (PBMCs) were isolated from leukocyte cones (Blood Transfusion Service, Sheffield, UK) by Histopaque-1077 (Sigma-Aldrich, UK) density gradient centrifugation. Briefly, the leukocyte cone was diluted with 35 ml of RPMI-1640 (Sigma-Aldrich, UK) to make the final volume around 50 ml. 25 ml of diluted blood was then layered over 12 ml of Histopaque-1077 in each of two 50 ml falcon tubes (BD Biosciences, UK) and centrifuged at 800 x g, acceleration slow, brake off at room temperature for 30 min. The buffy layer consisting of PBMCs was collected and washed three times with Hanks' balanced salt solution (modified with NaHCO<sub>3</sub>, without CaCl<sub>2</sub> and MgSO<sub>4</sub>) (Sigma-Aldrich, UK) to remove contaminating platelets. CD14<sup>+</sup> cells were then purified from the PBMC fraction by positive selection using human CD14 MicroBeads (human) and LS MACS columns (Miltenyi Biotec, UK) according to manufacturer's instructions. Purified monocytes were resuspended at a density of 2 x 10<sup>6</sup> monocytes/ml in RPMI-1640 (Sigma-Aldrich, UK) containing 15% human AB serum (PAA Laboratories Ltd, UK), 2 mM L-glutamine (Sigma-Aldrich, UK), 100 U/ml penicillin and 100 µg/ml

streptomycin (Sigma-Aldrich, UK), and 10 mM HEPES (Invitrogen, UK) – referred to in this study as ‘RPMI complete medium’. 50 ng/ml recombinant human monocyte-colony stimulating factor (rhM-CSF) (R&D Systems, UK) was added to the monocyte cultures.  $10^7$  monocytes in 5 ml RPMI complete medium were seeded per Teflon bottle (Nalgene, UK) (total capacity of each Teflon bottle = 125 ml) and incubated at 37°C, 5% CO<sub>2</sub> for 6 days. Culture cells were fed with 1.5 ml per bottle of fresh RPMI complete medium containing M-CSF on day 3. (Method derived and modified from Sonali Singh’s PhD thesis ‘Innate immune recognition of *Pseudomonas aeruginosa*)

#### 4.4.9.2. Quantification of *P. aeruginosa* growth during infection

M-CSF monocyte macrophages were harvested on day 7 and plated in 24-well tissue culture plates at a density of 250,000 cells per well in X-Vivo 15 and incubated overnight. The next day, cells were washed three times with cold PBS (Sigma-Aldrich, UK) to remove dead or non-adherent cells. PAO1-L mid-log phase (4 h) inoculum (350 µl at a density of  $7.14 \times 10^5$  cfu/ml in X-Vivo 15 containing M-CSF) was added to the wells and cultures were incubated at 37°C, 5% CO<sub>2</sub> for 2, 4 and 6 h. Controls were Mock-infected macrophages and bacteria only controls. To assess whether M-CSF primed macrophages were able to restrict the growth of PAO1-L and  $\Delta pqsA_L$  during infection, the amount of extracellular and macrophage-associated *P. aeruginosa* were quantified at 2, 4, and 6 hpi. The amount of extracellular and macrophage-associated *P. aeruginosa* was compared to bacteria only controls. CFU were determined as described above but to measure macrophage-associated bacteria in the samples, 250 µl of cold, sterile, ultra-pure distilled water (Invitrogen, UK) was added to

each well containing infected macrophages, the plates were placed on ice, and the bottom of the wells scraped with the plunger of a 1 ml syringe in order to lyse all the macrophages and release any associated bacteria.

#### **4.4.10. Statistical analysis**

All statistical analyses were carried out using GraphPad Prism v. 6.0. In this chapter, three data sets including untreated, WT-infected and  $\Delta pqsA_L$  infected conditions were compared at the same time; one-way analysis of variance with non-parametric Kruskal-Wallis test was executed to calculate significance. P-value  $\leq 0.05$  is regarded significant.

## 4.5. RESULTS

### 4.5.1. Effect of PQS on *P. aeruginosa* colonisation, invasion and growth on differentiated Calu-3 cells

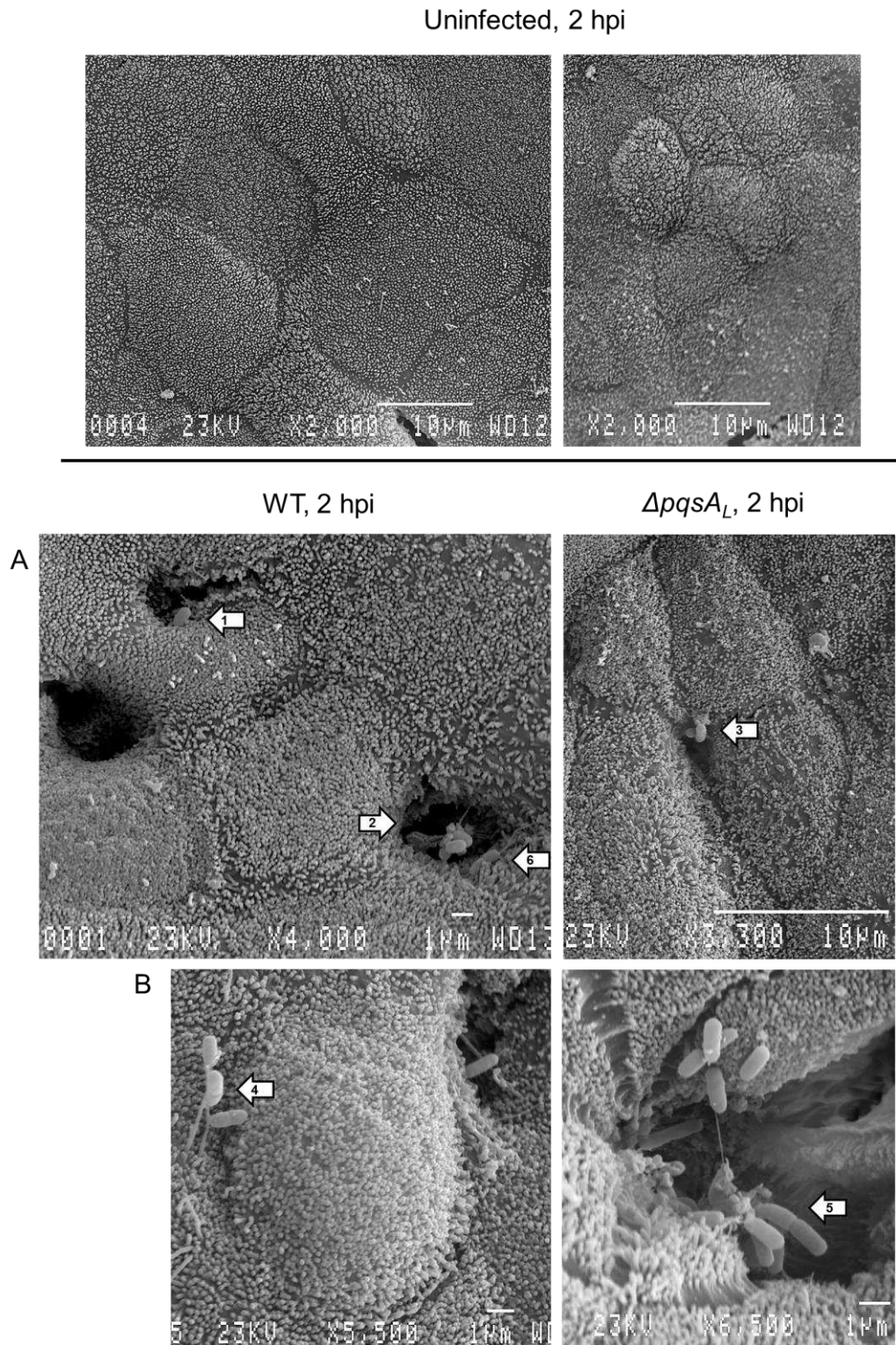
#### 4.5.1.1. *P. aeruginosa* invades differentiated Calu-3 cells at 2 hpi and 3 hpi with the epithelial integrity largely maintained

To investigate whether PQS affects the colonisation, invasion and growth of *P. aeruginosa* on differentiated bronchial epithelial Calu-3 cells, Calu-3 cells were infected with *P. aeruginosa* PAO1-L WT and  $\Delta pqsA_L$  at an MOI 50 for 2 h, 3 h and 6 h. In the first instance infected and uninfected Calu-3 cells were fixed with 3% glutaraldehyde at 2 hpi and subjected to scanning electronic microscopy to visualise the initial stages of the infection process. Surprisingly, given the MOI used, few bacteria were seen at the cell surface implying a low frequency of *P. aeruginosa* binding to the epithelial apical surface. The majority of the attached bacteria were found close to cell junctions that could correspond to areas where the tight junctions were being degraded (Fig. 4.1). These results are in agreement with previous observations by Lee et al. using FITC-labelled *P. aeruginosa*. According to these, approximately less than one per cent of the bacteria bound at the apical membrane of airway epithelial cells (Lee et al., 1999). Polarised Calu-3 cells displayed apical protrusions like prolonged microvilli that attached to WT and  $\Delta pqsA_L$  (Fig. 4.1C), although the real function of apical protrusion requires further characterisation.

Motility and attachment are major functions attributed to *P. aeruginosa* flagella (Parker and Prince, 2013). In our study, both WT and  $\Delta pqsA_L$  carried a single

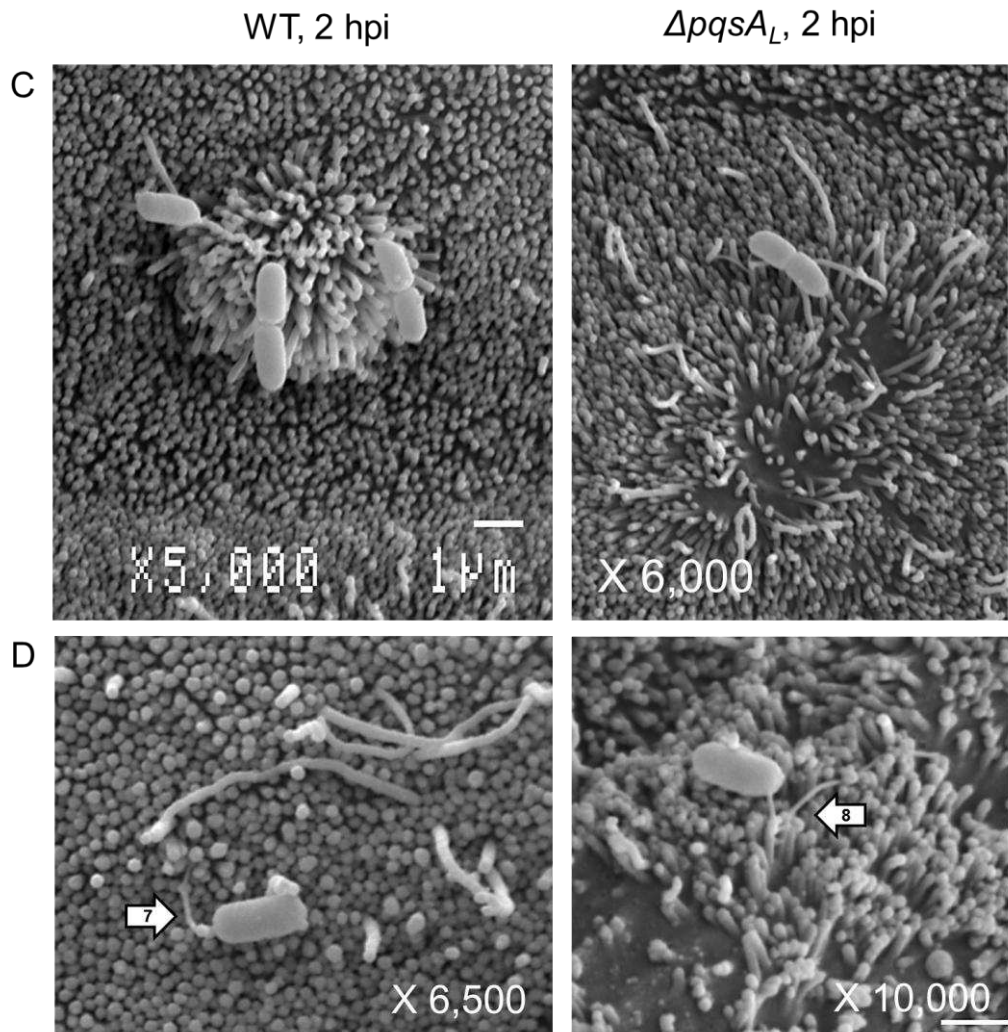
flagellum based on the images obtained by scanning electron microscopy (Fig. 4.1D). This observation is consistent with the fact that both WT and  $\Delta pqsA_L$  displayed swarming motility (Chapter 2, Section 2.5.2.5.). The capability of transmigration across epithelial cells by WT and  $\Delta pqsA_L$  was compared by enumerating the bacteria in the basal chamber at different time post- infection. At 2 hpi, neither WT nor  $\Delta pqsA_L$  was found in the basal compartment indicating the barrier integrity was maintained for up to 2 hpi (data not shown). Few to none bacteria were recovered randomly in the basal chamber at 3 hpi suggesting some of the cells on the diffCalu-3 monolayer started to compromise (data not shown).

To further examine the impact of PQS on the interaction of *P. aeruginosa* with bronchial epithelium, infected cells were labelled using an anti-Pseudomonas antibody and analysed by confocal laser scanning microscope. Although WT and  $\Delta pqsA_L$  were randomly detected across polarised Calu-3 cells at 3 hpi, bacterial invasion was observed (Fig. 4.2). Z-stacks of infected differentiated Calu-3 cells were obtained. The WT mainly accumulated at the apical surface forming small patches (Fig 4.2). White arrows indicated the bacteria inside Calu-3 cells while the integrity of the monolayer was maintained.



**Figure 4.1 Visualisation of differentiated Calu-3 cells infected with PAO1-L WT and  $\Delta pqsA_L$  by scanning electron microscopy.**

Uninfected Calu-3 cells presented short microvilli and formed cilia-like structures. Relatively long surface protrusions scarcely appeared on few cells. A and B. Both WT (arrows 1, 2 and 3) and  $\Delta pqsA_L$  (arrows 4 and 5) were seen at cellular boundaries and appear to induce disruption of the junctions. (Next page)



C. Protruding microvilli at the surface of Calu-3 cells appear responsive to WT and  $\Delta pqsA_L$ .  
D. Arrow 6, 7 and 8 indicate that both WT and  $\Delta pqsA_L$  carried a flagellum as their motile organelle.

It was clearly seen in the confocal image in Fig. 4.2 that the cell membrane remained mostly intact and surrounded by F-actin staining, suggesting that the plasma membrane was still linked to the actin filaments.  $\Delta pqsA_L$  also formed cell aggregates and could be detected inside the cells. However,  $\Delta pqsA_L$  seemed to cause cell misplacement in polarised Calu-3 cell as some cells were found climbing on each other (Fig. 4.2  $\Delta pqsA_L$  infection on Calu-3 cells at 3



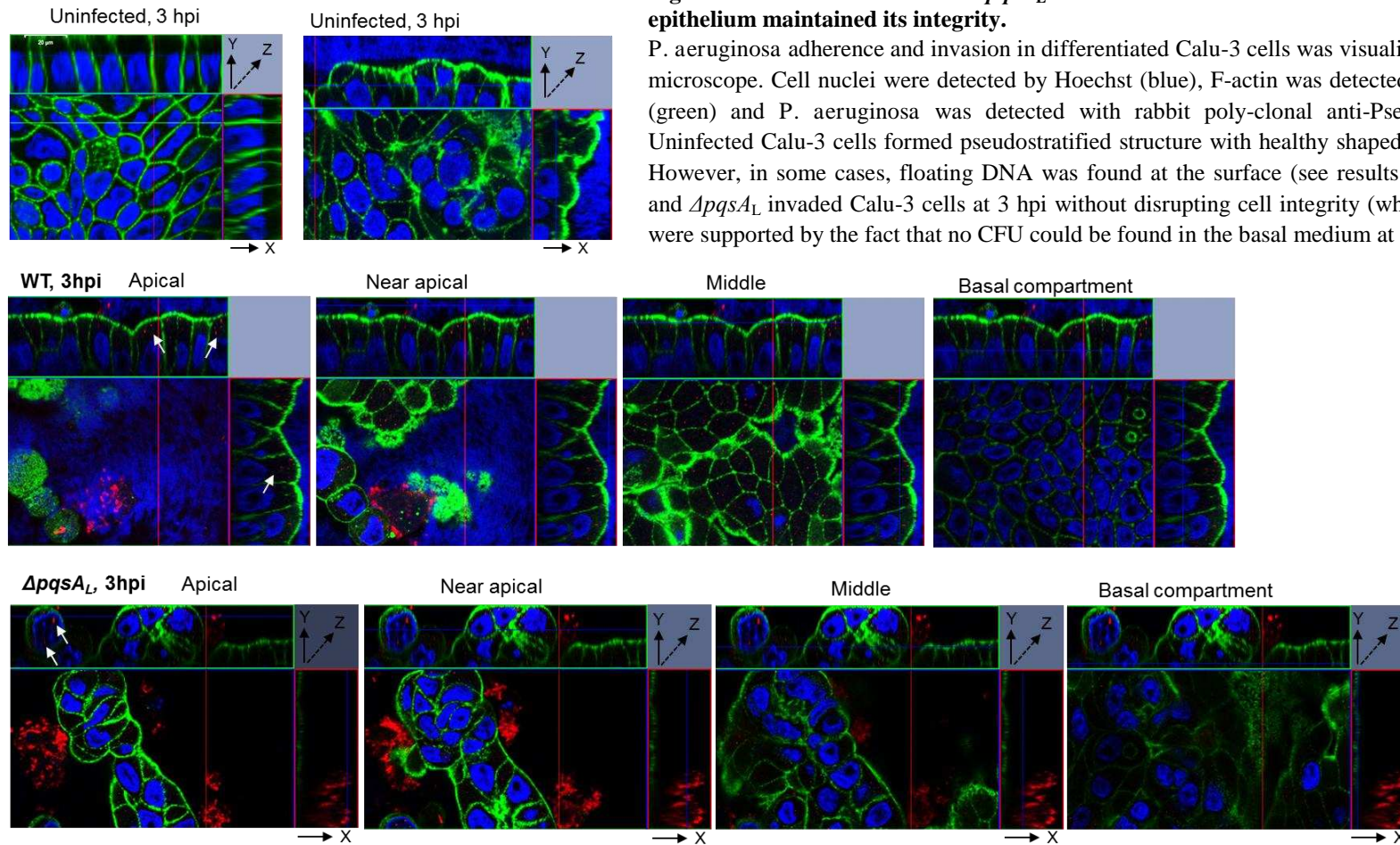
hpi shown in Y-axis). Previous studies indicated the type III secreted effectors ExoS, ExoT and ExoY enabled *P. aeruginosa* to invade and disrupt the actin cytoskeleton without compromising cell viability at early stage of infection (Cowell et al., 2005, Angus et al., 2010). This observation is compatible with our findings regarding the disturbance of the epithelial monolayer induced by  $\Delta pqsA_L$ .

#### 4.5.1.2. *P. aeruginosa* growth and colonisation of the epithelial layer at 6 hpi

At 6 hpi the epithelial layer was damaged and there was accumulation of bacteria forming a biofilm-like structure. In some instances bacteria were found tightly associated to extracellular DNA if this was present. In comparison with the cells infected with WT where the epithelial monolayer was largely maintained, Calu-3 cells infected with  $\Delta pqsA_L$  seemed to round up (Fig. 4.3).

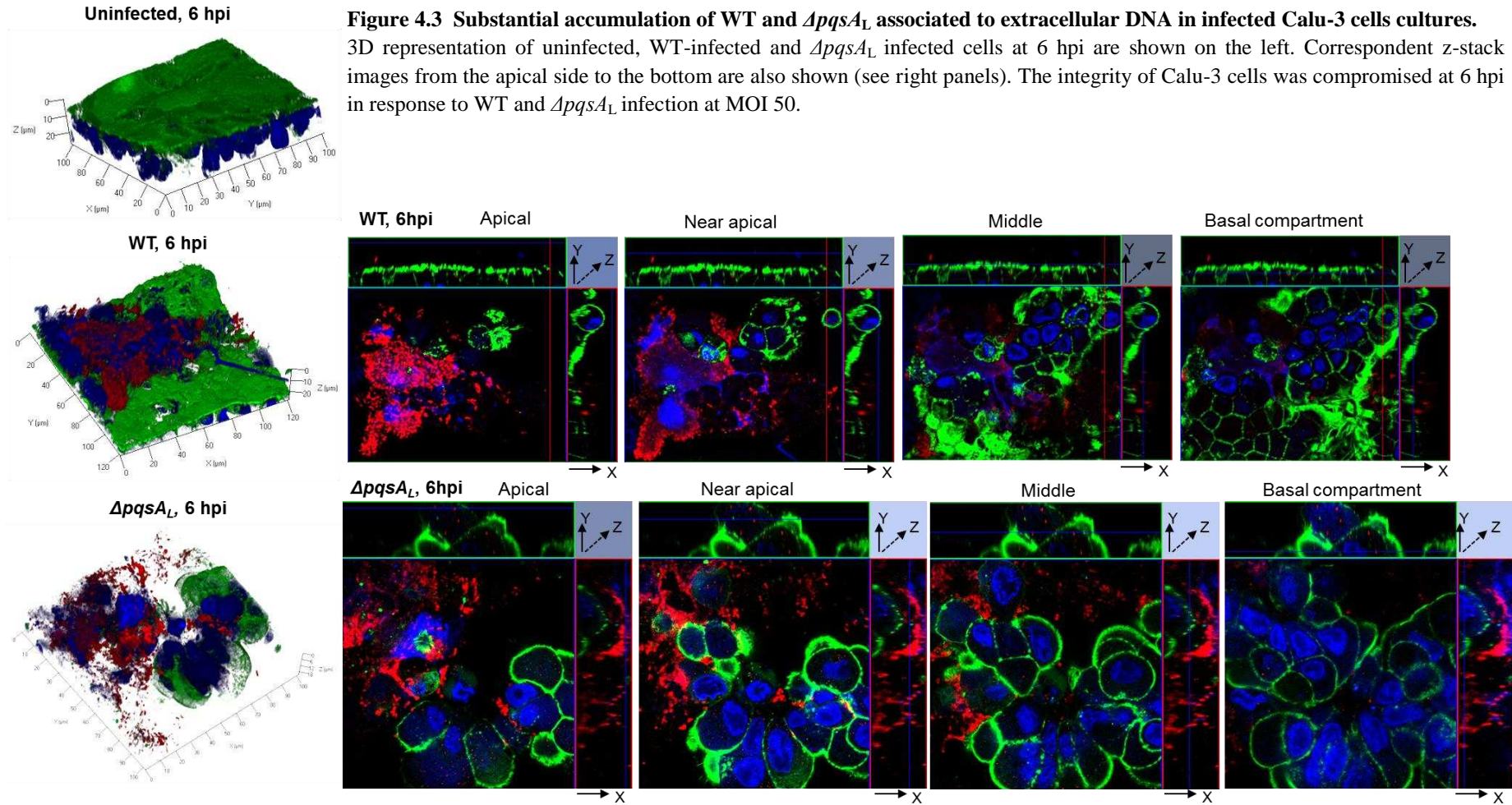
The capability of growth on the respiratory epithelium is the first step in the establishment of infection (Heiniger et al., 2010). We assessed the virulence of *P. aeruginosa* PAO1-L WT and  $\Delta pqsA_L$  by quantifying bacterial growth on the epithelium and bacteria transmigrated to the basal chamber at 6 hpi. Bacteria cultured in complete MEM were used as controls, and the bacterial inocula were validated for each infection assay (see Chapter 3 Section 3.5.2.2). The results showed that the inocula from both WT and  $\Delta pqsA_L$  were within the optimal range and the bacterial counts for WT and  $\Delta pqsA_L$  from each experiment were also consistent. Bacterial numbers in the control wells were 21 times and 18 times higher at 6 hpi compared to the initial inocula for WT and  $\Delta pqsA_L$  respectively. This was consistent with previous observations

(Section 2.5.2.1.). A wide range of values, between 2-logs and 4-logs, were obtained for the bacteria present in the basal chamber and these differed among experiments (Table 4.2; Fig. 4.3). In fact, the majority of bacteria remained cell-associated with numbers up to 8-logs at 6 hpi. Given the fact that the numbers of randomly transmigrated bacteria were 4-logs to 6-logs lower than the numbers of cell-associated bacteria, the transmigration events were negligible compared to numbers of cell-associated bacteria. In addition, we found the ratio 'cell associated-bacteria' to 'MEM only bacteria' was 0.36 and 0.32 for WT and  $\Delta pqsA_L$ , respectively. This suggested that the growth of *P. aeruginosa* was reduced by approximately 64-68% in differentiated Calu-3 cell monolayers compared to MEM-only controls.



**Figure 4.2 Invasion of WT and  $\Delta pqsA_L$  in differentiated Calu-3 cells occurred at 3 hpi whilst epithelium maintained its integrity.**

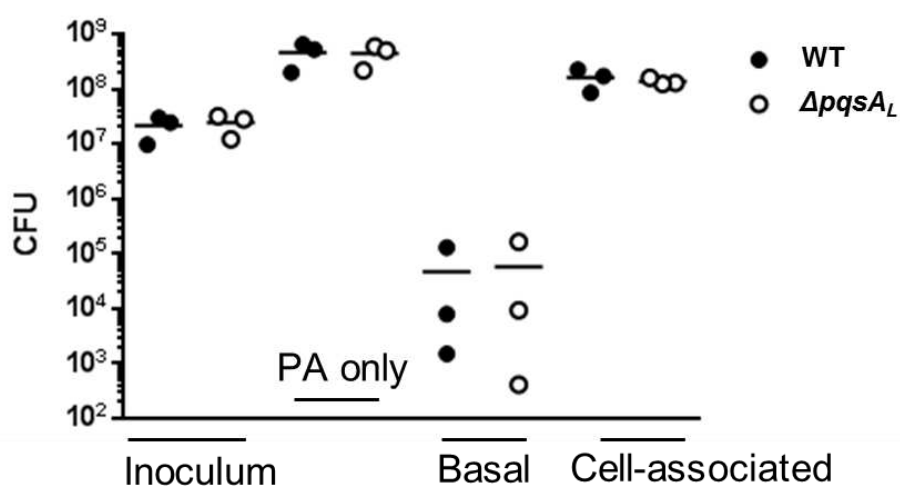
*P. aeruginosa* adherence and invasion in differentiated Calu-3 cells was visualised by confocal fluorescent microscope. Cell nuclei were detected by Hoechst (blue), F-actin was detected with Phalloidin-Alexa488 (green) and *P. aeruginosa* was detected with rabbit poly-clonal anti-*Pseudomonas* antibody (red). Uninfected Calu-3 cells formed pseudostratified structure with healthy shaped nuclei seen on the picture. However, in some cases, floating DNA was found at the surface (see results and discussion). Both WT and  $\Delta pqsA_L$  invaded Calu-3 cells at 3 hpi without disrupting cell integrity (white arrows). These findings were supported by the fact that no CFU could be found in the basal medium at 3 hpi.



**Table 4.2 Summary of the averages of bacterial colony forming units of inocula, PA only controls, transmigrated and cell-associated bacteria at 6 hpi.**

Total CFU (Average, n=3)	WT $\pm$ SD	$\Delta pqsA_L \pm$ SD
Inoculum ( $10^7$ )	$2.1 \pm 1.1$	$2.4 \pm 1.1$
PA* only in MEM ( $10^8$ )	$4.5 \pm 2.3$	$4.4 \pm 2.0$
Transmigrated bacteria ( $10^4$ )	$4.7 \pm 7.2$	$5.8 \pm 9.2$
Cell-associated bacteria ( $10^8$ )	$1.6 \pm 0.7$	$1.4 \pm 0.2$
Cell-associated bacteria/ PA only in MEM	0.36	0.32

\*PA, *P. aeruginosa*



**Figure 4.4 The majority of PAO1-L WT and  $\Delta pqsA_L$  remained cell-associated at 6 hpi during infection of diffCalu-3.**

Bacterial growth after infection of diffCalu-3 cells was assessed by counting bacterial CFU in the cell-associated fraction and in the basal chamber. CFU values for the inocula and MEM only-controls are also shown. The experiment was conducted for three times (n=3). Each dot shown in the figure represents the mean from one single experiment.

## **4.5.2. Induction of pro-inflammatory cytokines in diffCalu-3 cells in response to PAO1-L WT and $\Delta pqsA_L$**

### 4.5.2.1. Validation of endogenous control genes for gene expression studies on Calu-3 cells

In this part of the study, quantitative real-time PCR was introduced to evaluate the relative levels of mRNA in diffCalu-3 cells upon WT and  $\Delta pqsA_L$  infection. When performing relative quantification of the expression of a target gene, the choice of a suitable gene for use as an endogenous control is important. An endogenous control gene is a gene whose expression level should not differ between samples, such as a housekeeping gene that is constitutively expressed. Comparison of the  $C_q$  value of a target gene with that of the endogenous control gene allows the expression level of the target gene to be normalized to the amount of input cDNA. The use of an endogenous control gene corrects for variation in RNA content, reverse-transcription efficiency, nucleic acid recovery, possible RNA degradation or presence of inhibitors in the RNA sample and differences in sample handling (Huggett et al., 2005). The stability of the endogenous gene is another critical issue when performing real-time quantitative PCR. The expression of a good internal control should not change upon treatment among samples (He et al., 2008, Kulkarni et al., 2011). To perform an endogenous gene validation test that is suitable for our study, the expression of the gene should be maintained in Calu-3 cells after *P. aeruginosa* infection. Three reference genes commonly used in bronchial epithelial cells were compared for consistency and efficiency between samples: hypoxanthine phosphoribosyltransferase 1 (HPRT), guanine nucleotide-binding protein,  $\beta$ -

peptide 2-like-1 (GNB2L1) and immunoglobulin  $\mu$  binding protein 2 (IGHMBP2) (Table 4.3). The expression of HPRT, GNB2L1 and IGHMBP2 were firstly investigated in uninfected diffCalu-3 cells. Their  $C_q$  (quantification cycle) values were  $23.40 \pm 0.01$ ,  $19.35 \pm 0.25$  and  $27.28 \pm 0.27$  (Fig. 4.5) respectively. The averages and standard deviations were obtained from two independent experiments, with each experiment containing two samples analysed in triplicate. The suggested  $C_q$  value of HKG to use is around 25. The relatively higher  $C_q$  value for IGHMBP2 compared to the other two HKGs suggested a lower gene expression than the other two. Despite the fact that HPRT and GNB2L1 were both constitutively expressed at relatively high levels in diffCalu-3 cells HPRT appeared to perform more consistently based on the smaller standard deviations between experiments. Furthermore, to verify whether the HPRT is consistently expressed in polarised Calu-3 cells upon *P. aeruginosa* infection,  $C_q$  values of HPRT from Calu-3 cells infected with WT and  $\Delta pqsA_L$  were also examined. Based on the  $C_q$  values obtained, HPRT was shown to be consistently expressed in uninfected and infected diffCalu-3. HPRT was therefore selected as the endogenous control for normalisation of the expression levels of target genes in samples.

**Table 4.3 Brief description of references genes tested using qPCR**

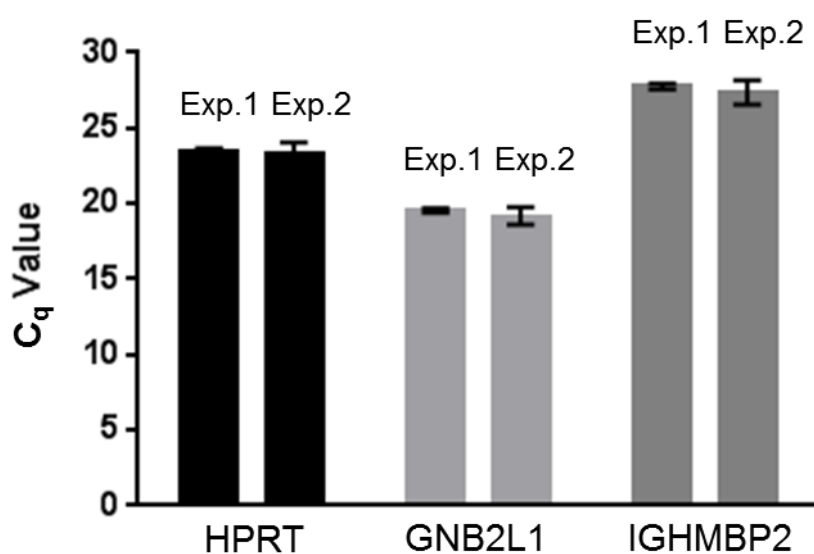
Abbreviation	Gene name	Gene function
HPRT*	Hypoxanthine phosphoribosyltransferase 1	A transferase in the generation of purine nucleotides through the purine salvage pathway
GNB2L1*	Guanine nucleotide-binding protein, $\beta$ -peptide 2-like-1	Binding and anchorage of protein kinase C
IGHMBP2*	Immunoglobulin $\mu$ binding protein 2	A 5' to 3' helicase that unwinds RNA and DNA duplices in an ATP-dependent reaction

\*(He et al., 2008)



**Table 4.4 HPRT C<sub>T</sub> values in diffCalu-3 cells collected after exposure to *P. aeruginosa* infection at MOI 50 for 2 hpi and uninfected control**

Treatment	HPRT C <sub>q</sub> value (triplicate)			Average ± SD
Uninfected	23.02	22.96	22.29	22.99 ± 0.031
Infected with WT	23.38	23.59	23.51	23.49 ± 0.106
Infected with $\Delta pqsA_L$	23.54	23.56	23.38	23.49 ± 0.099



**Figure 4.5 Consistent C<sub>q</sub> values of reference genes in uninfected diffCalu-3 cells in two independent experiments.**

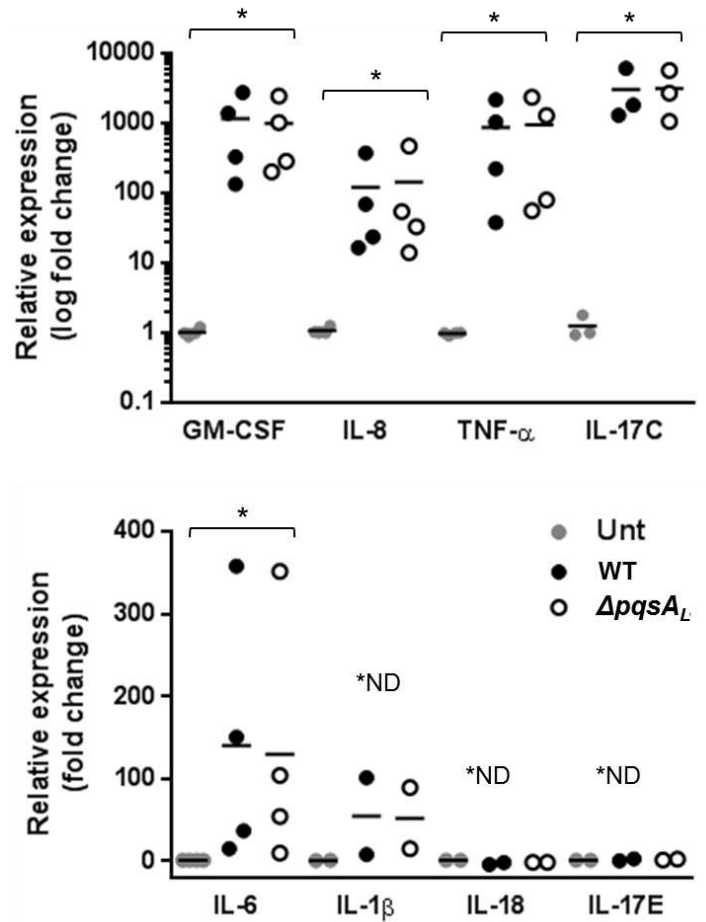
All three reference genes HPRT, GNB2L1 and IGHMBP2 showed consistent C<sub>q</sub> values between two independent experiments. However, HPRT was chosen as endogenous control in this study because its relatively lower variation compared with the other two.

#### 4.5.2.2 Similar induction of pro-inflammatory cytokines gene expression in response to WT and $\Delta pqsA_L$ infection of diffCalu-3 cells.

In addition to producing broad-spectrum antimicrobial agents in the mucus, such as defensins and surfactant proteins, airway epithelial cells secrete chemokines and cytokines in response to pathogens that lead to the recruitment



of inflammatory cells to the site of infection (Martin et al., 1997, Polito and Proud, 1998, Tam et al., 2011). To understand whether proinflammatory genes were differentially induced in diffCalu-3 upon WT and  $\Delta pqsA_L$  infection, levels of mRNA encoding for several proinflammatory cytokines and chemokines were examined by qPCR. The products investigated included GM-CSF, IL-8, TNF- $\alpha$ , IL-6, IL-1 $\beta$ , IL-18, IL-17C and IL-17E. Our results show that transcription of GM-CSF, IL-8, TNF- $\alpha$  and IL-6 was significantly induced in diffCalu-3 cells upon WT and  $\Delta pqsA_L$  infection (Fig. 4.6). The levels of IL-17C transcripts were also highly upregulated in diffCalu-3 cells after exposure to WT and  $\Delta pqsA_L$ , whereas the expression of IL-17E was not increased. No induction of the expression of IL-1 $\beta$  and IL-18 in Calu-3 cells upon PAO1-L WT and  $\Delta pqsA_L$  infection was observed in our study (Fig. 4.6).



**Figure 4.6 Induction of pro-inflammatory cytokines, GM-CSF, IL-8, TNF- $\alpha$ , IL-17c, and IL-6 in Calu-3 cells in response to WT and  $\Delta pqsA_L$ .**

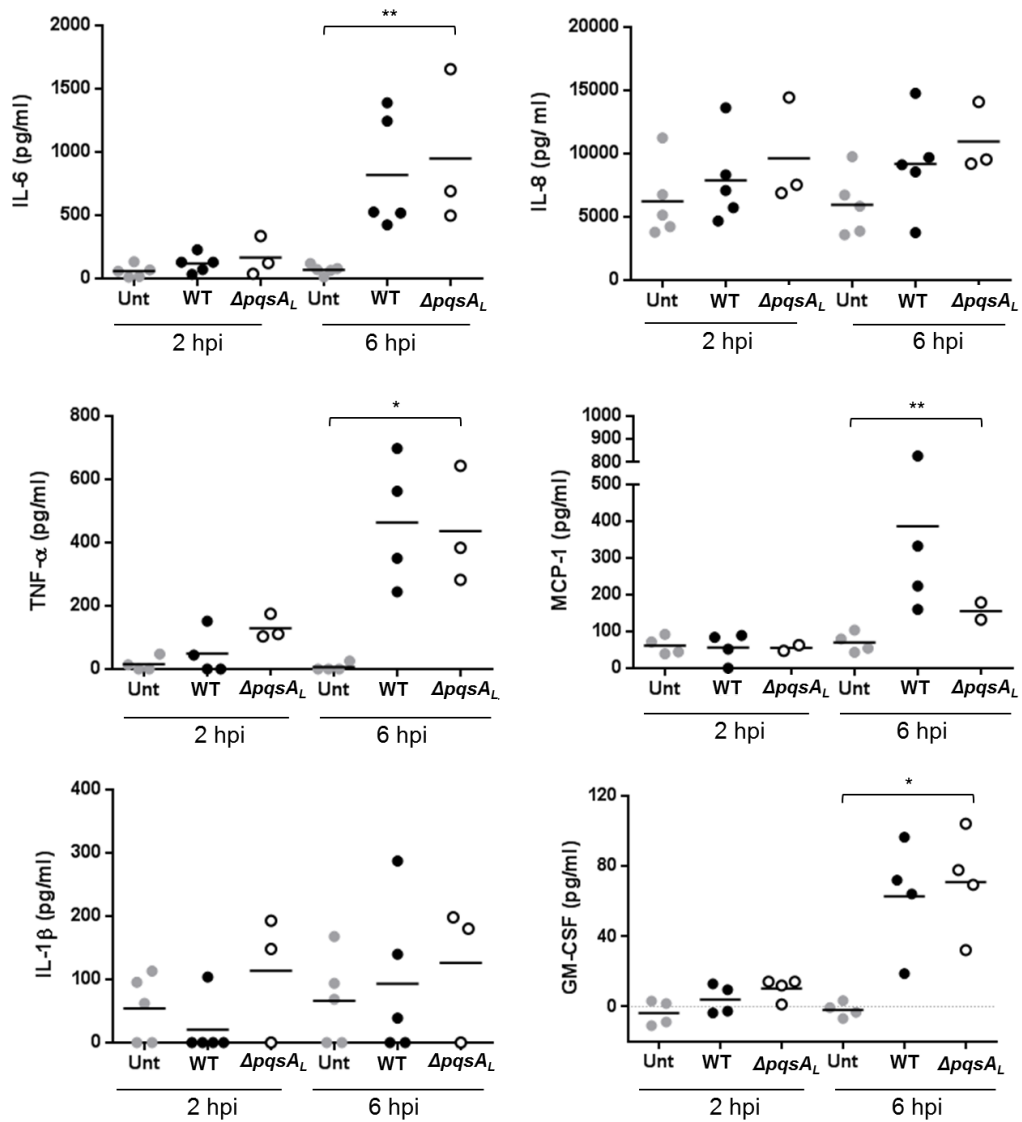
Expression of transcripts encoding for GM-CSF, IL-8, TNF- $\alpha$  and IL-17c was increased by the infection with WT (black dots) and  $\Delta pqsA_L$  (white dots) compared to uninfected controls (grey dots). IL-6 expression was also induced by *P. aeruginosa* infection but levels varied among experiments (n=2-4). Each dot represents the result from an independent experiment performed in duplicate. QPCR assay was done in triplicate. \*ND, not detectable in one single experiment. P-values were calculated by one-way ANOVA and non-parametric Kruskal-Wallis test. \*p < 0.05

#### 4.5.2.3. Similar induction of pro-inflammatory cytokines at protein level in response to WT and $\Delta pqsA_L$ infection of diffCalu-3 cells.

While qRT-PCR quantifies the relative expression of mRNA transcripts, levels of mRNA do not always correlate with protein expression. In addition, whether cytokines are transported to the extracellular milieu to play their roles as immune mediators also remains unknown. To address this question, we quantified the levels of the proinflammatory cytokines IL-6, TNF- $\alpha$ , GM-CSF, IL-1 $\beta$ , and chemokines IL-8 and monocyte chemotactic protein-1 (MCP-1, also known as CCL2) either by a high-throughput bead-based immunoassay or the enzyme-linked immunosorbent assay (ELISA). At 2 hpi, the levels of IL-6, IL-8, TNF- $\alpha$  and GM-CSF were slightly increased in response to WT and  $\Delta pqsA_L$  but this was not significantly different. The levels of MCP-1 in the supernatant at 2 hpi remained unchanged compared to untreated cells. The productions of IL-6 ( $819 \pm 458$  in WT infection;  $947 \pm 621$  in  $\Delta pqsA_L$  infection) and TNF- $\alpha$  ( $434 \pm 204$  in WT infection;  $436 \pm 186$  in  $\Delta pqsA_L$  infection) were dramatically increased at 6 hpi, whilst the secretion of MCP-1 ( $386 \pm 303$  in WT infection;  $155 \pm 33$  in  $\Delta pqsA_L$  infection) and GM-CSF ( $63 \pm 32$  in WT infection;  $71 \pm 30$  in  $\Delta pqsA_L$  infection) were also enhanced to levels significantly different from the uninfected cells. IL-8 seemed to be intrinsically secreted by both untreated and infected Calu-3 cells at relatively high levels. No consistent production of IL-1 $\beta$  was detected.

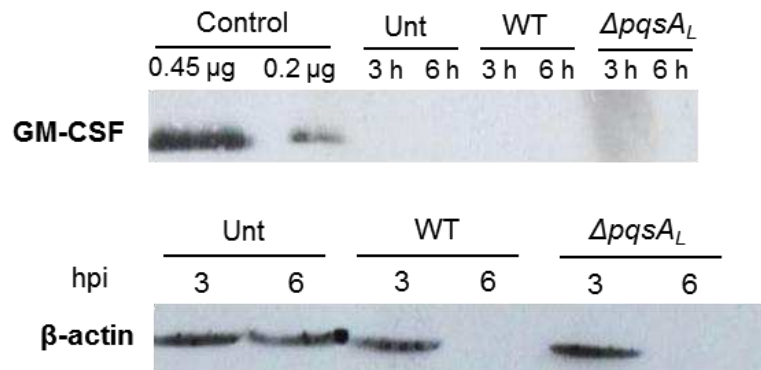
Providing the high induction of GM-CSF and TNF- $\alpha$  of mRNA in Calu-3 cells upon both WT and  $\Delta pqsA_L$  infection, the levels of GM-CSF production in the supernatant did not seem to correlate with its high mRNA expression. We

speculated that the production of GM-CSF might be retained in the cytoplasm of infected cells. To test this hypothesis, lysates of uninfected and infected Calu-3 cells were collected at 3 and 6 hpi and subjected to Western blotting against anti-rhGM-CSF antibody. The positive control was purified recombinant human GM-CSF at a concentration of 0.45  $\mu$ g and 0.2  $\mu$ g;  $\beta$ -actin was used as the endogenous control for each condition. The results showed that GM-CSF was not detectable in any of the lysates (Fig. 4.8). Thus, low levels of GM-CSF secretion were not attributed to cytosolic accumulation. However, we noticed that  $\beta$ -actin disappeared in cells infected with WT and  $\Delta pqsA_L$  at 6 hpi. GM-CSF production might be inhibited due to severe cell damage leading to a halt of metabolism and protein trafficking.



**Figure 4.7 Infection on Calu-3 cells with WT and  $\Delta pqSA_L$  induced the secretion of proinflammatory cytokines at 2 and 6 hpi.**

Differentiated Calu-3 cell basal media were collected after infection with WT,  $\Delta pqSA_L$  and PBS only as negative control. Media were centrifuged and were subjected to cytokine quantification. Production of pro-inflammatory cytokines IL-6, TNF- $\alpha$ , MCP-1 and GM-CSF was induced by *P. aeruginosa* infection but the levels did not differ between the WT and  $\Delta pqSA_L$ . Each dot represents the mean from one single experiment. (n=2-5). \*p < 0.05 \*\*p < 0.005. Unt, untreated. P-values were calculated by one-way ANOVA with non-parametric Kruskal-Wallis test.



**Figure 4.8 Low levels of GM-CSF secretion was not due to the accumulation in the cytoplasmic compartment.**

Differentiated Calu-3 cells were infected with WT and  $\Delta pqsA_L$  at a MOI of 50. Cells were lysed with RPPA cell lysis buffer at 3 and 6 hpi. Lysate proteins were resuspended in SDS-PAGE sample buffer, electrophoresed on 12% SDS-PAGE, transferred to a PDVF membrane and incubated with mouse anti-rhGM-CSF and mouse anti- $\beta$ -actin antibody as endogenous control. Goat anti-mouse IgG-horseradish peroxidase conjugate was used as a secondary antibody. Two concentrations of recombinant hGM-CSF, 0.45  $\mu$ g and 0.2  $\mu$ g, were used as positive control. GM-CSF was not detectable in the cytoplasm. Unt, untreated. Noted that actin was significantly degraded at 6 hpi in this experiment (Representative image from n=2).

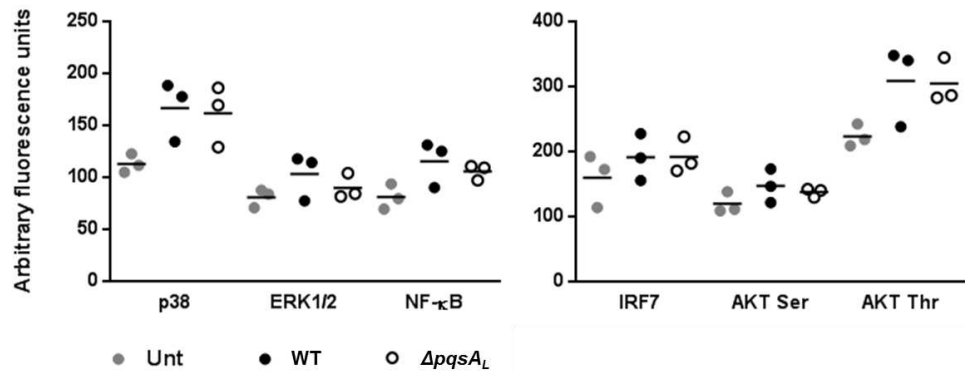
#### 4.5.3. Similar activation of innate signalling pathways in diffCalu-3 cells upon *P. aeruginosa* PAO1-L WT and $\Delta pqsA_L$ infection

In spite of the similar levels of cytokines and chemokines (mRNA and protein) in Calu-3 cells when exposed to WT and  $\Delta pqsA_L$  infection, how these downstream consequences were initiated has not been clarified. The binding of bacteria and shed bacterial components to pattern recognition receptors (PRRs) leads to the activation of signalling pathways that can result in the secretion of cytokine and chemokines. Changes in cytokines and chemokines gene expression are coordinated by latent transcription factors of the nuclear factor- $\kappa$ B (NF- $\kappa$ B) and interferon regulatory factor (IRF) families. Also, mitogen-activated protein kinase (MAPK) p38, c-Jun N-terminal kinase (JNK), and extracellular-signal-regulated kinases (ERK1/2), the serine–threonine kinase

Akt (AKT Ser and Thr) are often involved in the proinflammatory signalling. The signalling pathways need to be tightly regulated to ensure the induction of cytokines and chemokines is appropriate in magnitude and duration (Ryu et al., 2010, Takeuchi and Akira, 2010). To further establish the potential consequences of PQS on skewing the activation of Calu-3 cells upon *P. aeruginosa* infection, activation of a series of signalling kinases and transcriptional factors associated with proinflammatory activation were measured by reverse phase protein microarray and normalised against actin. As the ability to accurately discriminate between small changes in protein expression is limited in a Western-blot based technique such as this one, only changes greater than 2-fold were considered true results. (The microarray work was conducted by Dr. Ola Negm).

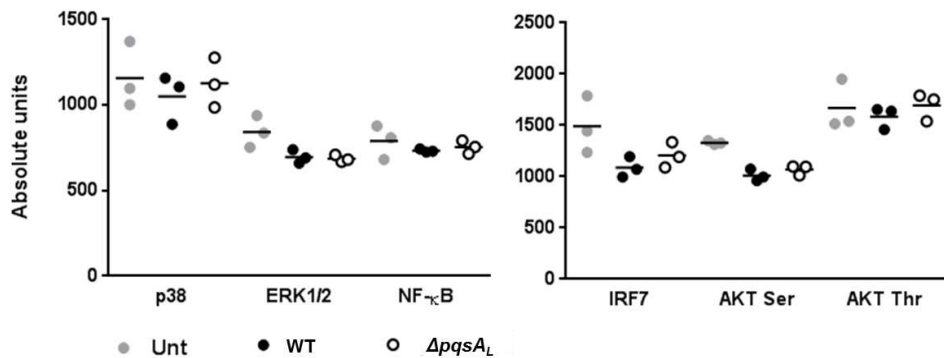
The results showed that infection of differentiated Calu-3 cells with WT and *ΔpqsA<sub>L</sub>* led to a mild activation of mitogen protein kinase (p38 and ERK1/2), transcriptional factor NF-κB (p65 subunit), IRF7, and AKT Threonine to comparable levels at 3 hpi (Fig. 4.9). An increase to 1.4 fold was seen on the activation of p38, NF-κB and AKT Threonine signaling pathways and to 1.2 fold in the case of ERK1/2 and AKT Serine compared to uninfected cells. These changes cannot be considered as a real induction. Dr. Ola Negm mentioned a concern about the loss of fluorescence signals due to actin in the cells infected with *P. aeruginosa* (refer section 4.5.4. Fig. 4.12A). Due to the concern that the arbitrary intensity of signal transduction proteins might be concealed by the normalisation with actin, we recalculated the activation level of signalling proteins based on absolute values without normalisation. However, the results showed none to even less signal induction in *P. aeruginosa* infected

cells compared to the signal from untreated cell control (Fig. 4.10). This suggested actin normalisation is essential to calibrate the levels of activation. The activation of signalling cascades detected in Calu-3 cells upon WT and  $\Delta pqsA_L$  infection was too weak to be regarded as a true induction.



**Figure 4.9** A small induction of mitogen activated protein kinase, NF- $\kappa$ B, serine/threonine AKT and IRF7 signaling pathways in Calu-3 cells in response to WT and  $\Delta pqsA_L$  infection.

Several canonical signaling pathways associated with proinflammatory response and respiratory inflammation were investigated including MAP kinase, NF- $\kappa$ B, serine/threonine AKT and IRF7 in differentiated Calu3 cells upon WT and  $\Delta pqsA_L$  infection at 3 hpi. WT and  $\Delta pqsA_L$  induced comparable activation of signaling in Calu-3 cells. However, the signaling induction by *P. aeruginosa* infection was not significant enough to discern from the untreated. Significance was assessed by one-way ANOVA and non-parametric Kruskal-Wallis test. (n=3)



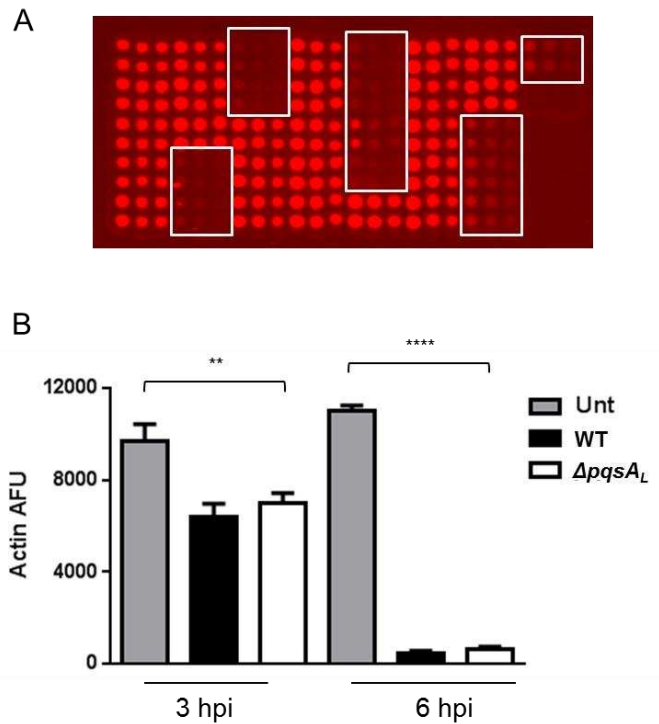
**Figure 4.10** Actin normalisation is essential for interpretation of signaling data. Absolute fluorescence signals for each phosphorylated signalling proteins were plotted (n=3)



#### **4.5.4. Assessment of *P. aeruginosa*-mediated cytotoxicity in response to WT and $\Delta pqsA_L$ infection.**

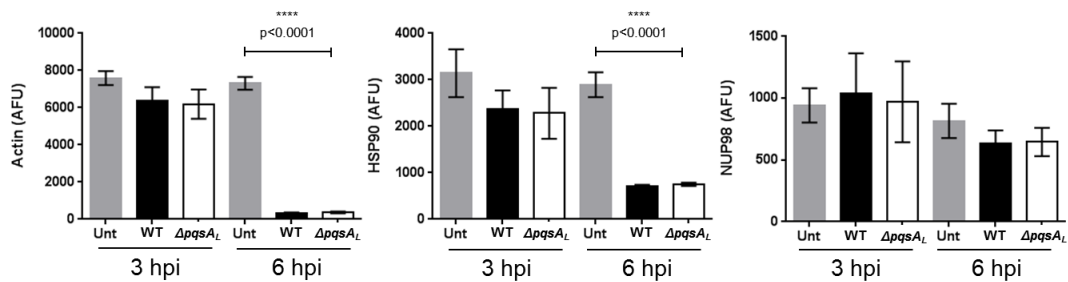
Actins are highly conserved proteins involved in the maintenance of cell structure and integrity.  $\beta$ -actin was used as an endogenous control to normalise the signals for signalling proteins in the microarray-based signalling study. Unexpectedly, we found that WT and  $\Delta pqsA_L$  infection induced the loss of actin fluorescence signal at 3 hpi and 6 hpi. It is well-established that actin depolymerisation takes place when cells are exposed to either drugs, chemicals or pathogen infection and cell survival is compromised. Thus, actin degradation can be used as an indication of cytotoxicity through apoptosis or necrosis (Geijtenbeek, 2012). The absolute intensity of actin fluorescent signals from lysates obtained at 3 hpi and 6 hpi were therefore taken as a means to evaluate cytotoxicity. Loss of actin signals on the microarray chip is showed in Fig. 4.11A. Signals due to actin from untreated Calu-3 cells were  $9667.8 \pm 1851$  arbitrary fluorescence unit (AFU) and they dropped to  $6403 \pm 1638$ ,  $6978 \pm 1118$  AFU at 3 hpi upon WT and  $\Delta pqsA_L$  infection, respectively. At 6 hpi, the actin signals from uninfected cells was  $10,984 \pm 612$  and those from cells infected with WT and  $\Delta pqsAL$  dropped dramatically to  $475 \pm 210$  and  $602 \pm 360$ , respectively (Fig. 4.11B). No significant differences were observed between Calu-3 cells infected with WT and  $\Delta pqsAL$ . The loss of actin during *P. aeruginosa* infection of diffCalu-3 is in an agreement with the lack of  $\beta$ -actin in cell lysates of diffCalu-3 infected with *P. aeruginosa* at 6 hpi observed by Western blotting (Fig. 4.8) and suggest that both WT and  $\Delta pqsA_L$  infection caused actin degradation in diffCalu-3 cells.

Furthermore, to understand whether  $\beta$ -actin was an exclusive target during WT and  $\Delta pqsA_L$  infection in bronchial epithelial cells, the expression of two other commonly used endogenous control proteins, heat-shock protein 90 (HSP90) and nucleoporin 98 kDa (NUP98), was also examined by reverse phase protein microarray (Fig. 4.12). HSP90 is an abundant ATP-dependent molecular chaperone essential for activating many signaling proteins in the eukaryotic cell (Retzlaff et al., 2009). Similarly, the 98 kDa NUP98 is constitutively generated from a cleavage of a 186 kDa precursor protein resulting in its localisation on the nucleoplasmic side of nuclear pore complex (NPC). NPC proteins are critical in regulating nucleocytoplasmic traffic of macromolecules across the nuclear envelope (Franks and Hetzer, 2013, Xu and Powers, 2013). Levels of NUP98 are constant under non-pathological situations. As shown for actin, levels of HSP90 were significantly reduced in both WT and  $\Delta pqsA_L$ -infected cells at 6 hpi. In contrast the levels of NUP98 on infected cells remained intact compared with the untreated cells. These results suggest that both WT and  $\Delta pqsA_L$  cause cytotoxicity in Calu-3 cells by inducing degradation of cytoskeleton components and chaperon proteins which might lead to the downregulation of downstream signalling proteins.



**Figure 4.11 WT and  $\Delta pqsA_L$  induced actin degradation on differentiated Calu-3 cells.**

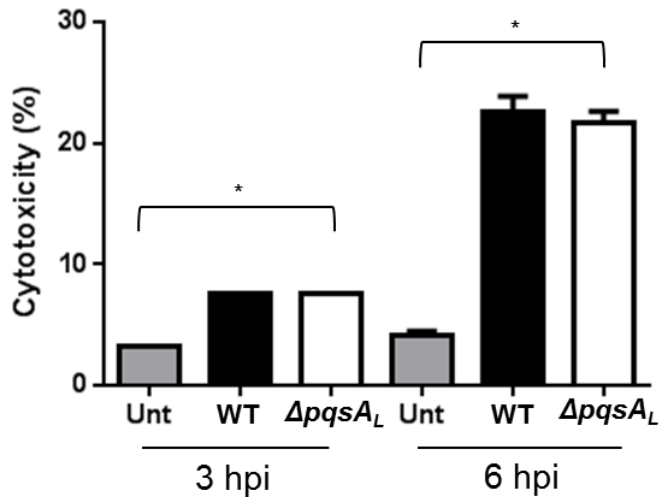
White rectangles indicated the dots where actin red fluorescent signals were missing on the array slide (A). Absolute fluorescence values from untreated cells and cells infected with WT and  $\Delta pqsA_L$  for 3h and 6 h were plotted in (B). Significant actin degradation in response to WT and  $\Delta pqsA_L$  infection compared with untreated cells started at early at 3 hpi; substantial actin degradation was observed at 6 hpi. The amount of actin in uninfected cells at 3 and 6 hpi remained constant. Data were obtained from three independent experiments each performed in duplicate. P-value was calculated by one-way ANOVA. \*\*  $p < 0.005$  and \*\*\*\*  $p < 0.0001$ .



**Figure 4.12 *P. aeruginosa* PAO1-L WT and  $\Delta pqsA_L$  induced actin and HSP90 degradation, but did not affect NUP98 levels.**

Degradation of actin (left panel) and HSP90 (middle panel) on Calu-3 cells was induced by WT and  $\Delta pqsA_L$  infection. Each bar is the mean from 3 independent experiments. At 6 hpi, the reduction was significant with p-value  $< 0.0001$  calculated by one-way ANOVA. Nucleoporin 98-kDa (NUP98) remained intact during the course of *P. aeruginosa* infection (right panel).

Cytotoxicity is a general term that encompasses cell death by apoptosis or necrosis. Lactate dehydrogenase (LDH) is a stable cytoplasmic enzyme presents in all cell types. It is readily released to the cell culture supernatant when the plasma membrane integrity is compromised upon damage. The LDH activity is determined in an enzymatic test; firstly, LDH reduces  $\text{NAD}^+$  to  $\text{NADH}^+$  and  $\text{H}^+$  by the conversion of lactate to pyruvate; secondly, 2H are transferred from  $\text{NADH}^+$   $\text{H}^+$  to the yellow tetrazolium salt by a catalyst turning pale yellow colour to a red colour formazan salt. Quantification of cell death is based on a reliable correlation of the amount of LDH in the supernatant with the amount of cell death. Initially, the LDH assay was performed using culture supernatants from the basal chamber of infected diffCalu-3 cultures. However, a significant background caused by the presence of 10% FBS which interfered with the colorimetric reaction was observed. To overcome this problem, WT and  $\Delta pqsA_L$  were used to infect on undifferentiated Calu-3 cells grown to confluency in a 24-well plate. In this setting, culture media were replaced with serum-free medium prior to infection assay. By comparing with cell supernatants obtained from cells lysed with 1% Triton-X100 that represented 100% cytotoxicity, it was estimated that WT and  $\Delta pqsA_L$  induced 7% cell death at 3 hpi and 22% at 6 hpi (Fig 4.13). Intrinsic cell death of uninfected cells was 3-4% at 3 and 6 hpi. Thus, WT and  $\Delta pqsA_L$  induced similar cytotoxicity at 3 and 6 hpi and this is in agreement with the degradation of actin and HSP90 previously described.



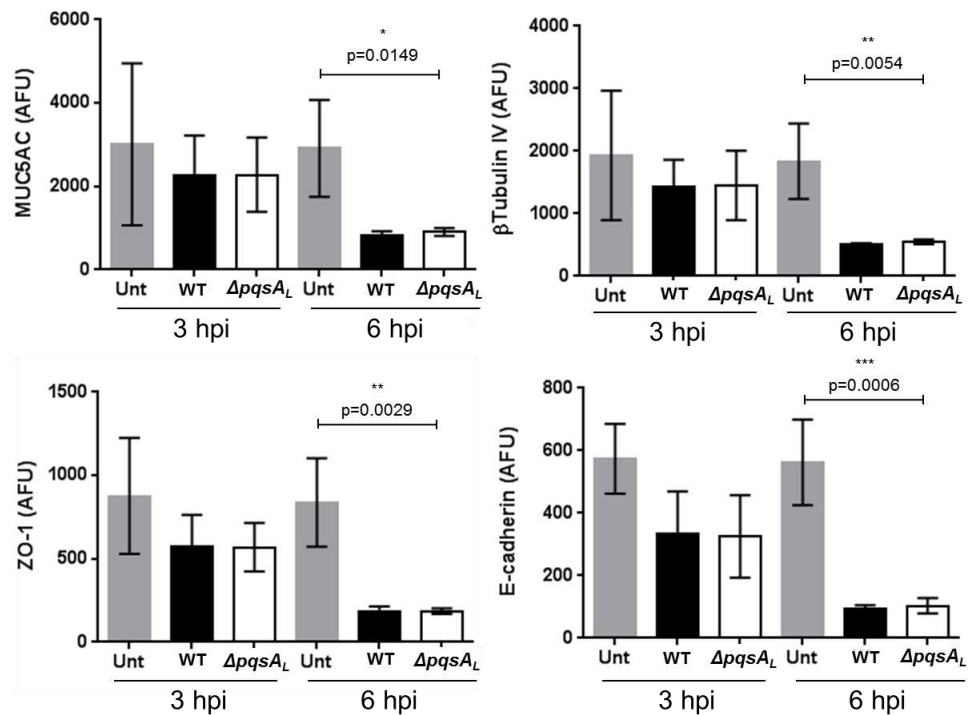
**Figure 4.13 Calu-3 cell death during the course of infection with WT and  $\Delta pqsA_L$ .**

Cell death caused by WT and  $\Delta pqsA_L$  infection increased from  $7.7 \pm 1.1\%$  and  $7.7 \pm 1.6\%$  at 3 hpi to  $22.6 \pm 2.6\%$  and  $21.7 \pm 1.9\%$  at 6 hpi, respectively. Cytotoxicity was assessed in comparison with LDH content released from 100% cell death prepared from cells lysed with 1% Triton X-100. Data presented were mean  $\pm$  SD from 3 independent experiments. Significance was calculated by one-way ANOVA and Kruskal-Wallis test. \* $p < 0.05$ .

#### **4.5.5. WT and $\Delta pqsA_L$ disrupted tight junctions and abrogated barrier function**

*P. aeruginosa* causes disruption of tight junctions, resulting in decreased epithelial barrier function and increased access to the basolateral surface (Rejman et al., 2007). It has been shown that *P. aeruginosa* is cytotoxic to human airway epithelia only when the bacteria have direct access to the basolateral membrane where the *P. aeruginosa* adhesins flagella and type IV pili mediate the initial adherence (Lee et al., 1999, Bucior et al., 2010, Bucior et al., 2012). Using protein microarray, in comparison to the readings from uninfected Calu-3 cells, AFU readings of tight junction proteins ZO-1 and E-cadherin, mucin protein MUC5AC and cilia-associated  $\beta$ -tubulin IV dropped slightly at 3 hpi, and were significantly reduced at 6 hpi on the cells infected

with WT and  $\Delta pq s A_L$ . Thus it appears that WT and  $\Delta pq s A_L$  induce the loss of junction proteins, mucin and cilia in Calu-3 cells at equivalent levels suggesting that PQS production during *P. aeruginosa* infection didn't affect the breaching of the epithelial cell barrier.



**Figure 4.14 PQS was not essential for PAO1-L on epithelial barrier destruction and tight junction disruption.**

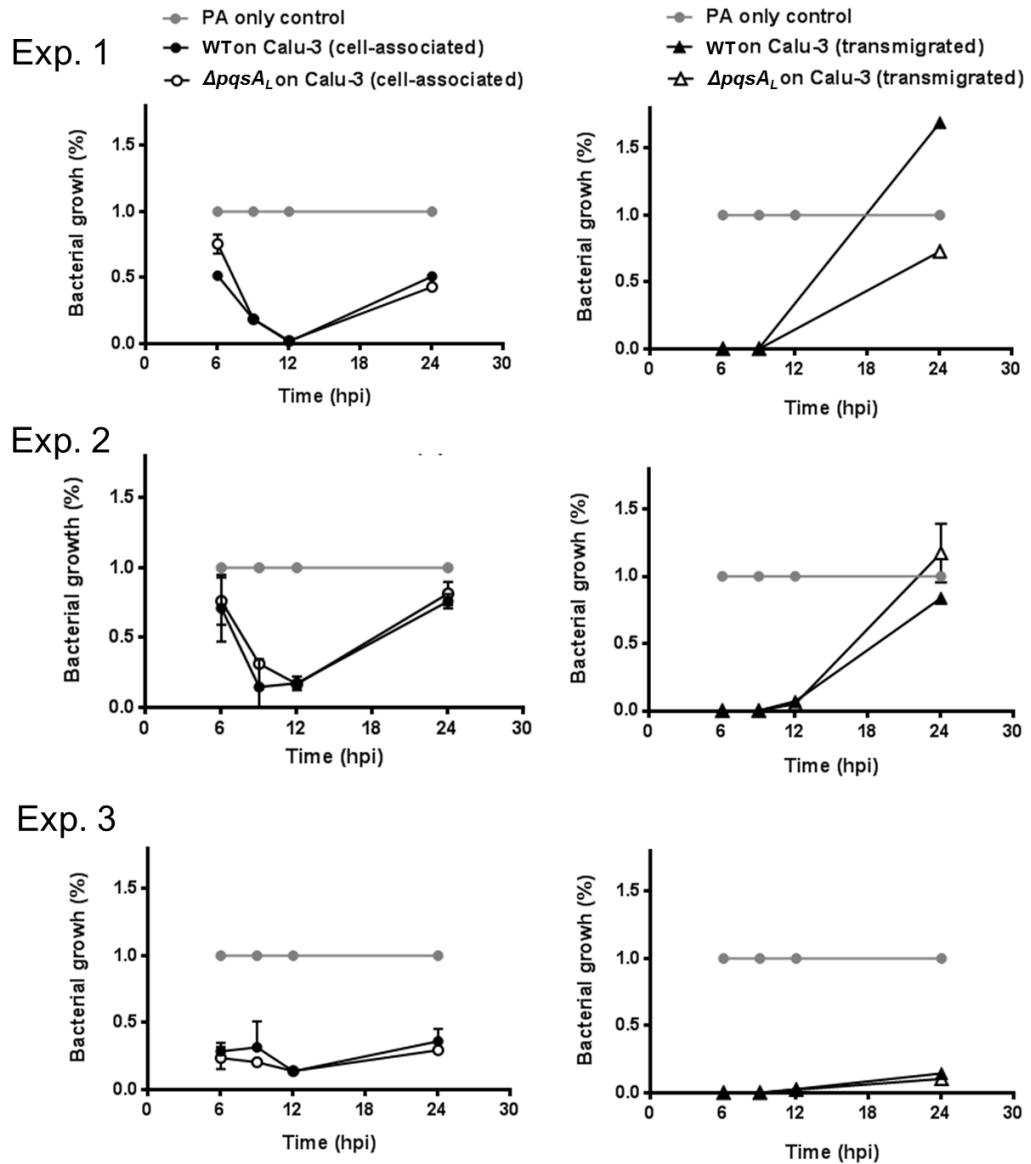
Calu-3 cells surface glycoprotein MUC5AC, cilia associated  $\alpha$ -tubulin IV and tight junction proteins ZO-1 and E-cadherin were compromised to WT and  $\Delta pq s A_L$  infection at comparable levels. Significant protein reductions happened at 6 hpi. Each bar is the mean from three independent experiments. P-values were evaluated by one-way ANOVA.

#### **4.5.6. Analysis of the interaction of WT and $\Delta pqsA_L$ with differentiated Calu-3 cells at low MOI**

Based on the above experiments, WT and  $\Delta pqsA_L$  displayed similar phenotypes during their interaction with bronchial epithelial cells regarding bacterial growth, cytotoxicity, induction of proinflammatory response and signalling. However, the capability of *P. aeruginosa* to exploit the amino acid tryptophan for PQS biosynthesis but not for AHLs QS molecules suggests a predominant role for PQS in coordinating *P. aeruginosa* metabolism during long-term host colonisation (Collier et al., 2002, Heeb et al., 2011). In addition, the fact that mutations in *lasR* are commonly found in chronic CF isolates imply PQS QS might override the effect from AHL-dependent QS in modulating *P. aeruginosa* pathogenesis during chronic infection (Winstanley and Fothergill, 2009). To test this hypothesis, we adapted the diffCalu-3 infection model in an attempt to better recapitulate the long-term persistence of *P. aeruginosa* in native lung. For this low inocula (MOI 0.5) were used to infect polarised Calu-3 cells. In this assay, the growth of cell-associated bacteria and the bacteria transmigrated to the basal chambers were assessed at 6, 9, 12 and 24 hpi. Bacteria cultured in MEM was again used as the PA only control. The ability of Calu-3 cells to restrict *P. aeruginosa* growth was presented as the ratio of the cell-associated bacteria to PA only control and the ratio of transmigrated bacteria to PA only control. Surprisingly, at low MOI the integrity of the polarised Calu-3 cells barrier was compromised at 6 hpi upon infection with both WT and  $\Delta pqsA_L$  as bacteria was detected in the basal chamber (Fig. 4.15) despite the fact that the MOI was 0.5 which is 100-fold less than the MOI used in the previous assays (see Section 4.5.1). Although the barrier function of

diffCalu-3 cells culture was compromised at 6 hpi, bacterial growth was restricted until 12 hpi. For instance at 12 hpi, the growth of WT and  $\Delta pqsA_L$  within the epithelial cells was reduced up to 70% compared with the number of bacteria in the PA only controls. However, the infectivity and bacterial growth of  $\Delta pqsA_L$  in bronchial epithelial cells were comparable to those observed for WT even in this long-term infection setting. Thus, PQS might not contribute to *P. aeruginosa* pathogenesis during the infection of human bronchial epithelial cells even by using low MOI.





**Figure 4.15 Both WT and  $\Delta pqsA_L$  breached the epithelial barrier at 6 hpi at MOI 0.5 but the epithelium restrained PA growth till 12 hpi.**

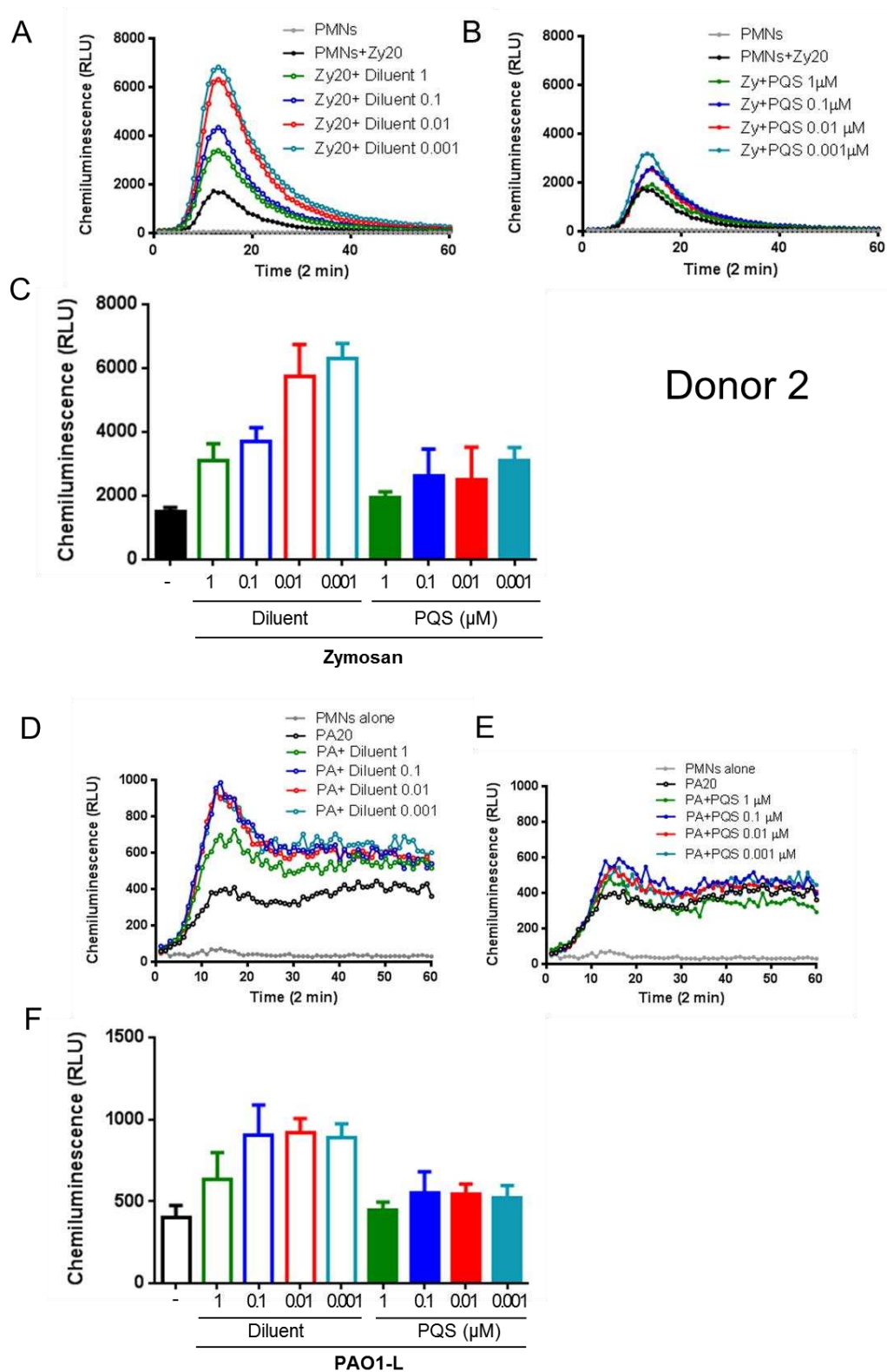
Infections on Calu-3 cells with PAO1-L WT and  $\Delta pqsA_L$  at MOI 0.5 were performed three times independently (Exp. 1, 2 and 3). Cell-associated bacterial growths (circle, on the left of the graph) and transmigrated bacteria (triangle, on the right of the graph) at 6, 9, 12 and 24 h were compared with growth in MEM only and presented as percentage. The epithelium consistently restrained PA growth until 12 hpi. *P. aeruginosa* grew mainly associated to Calu-3 cells therefore the bacteria transmigrated to the basal chamber were relatively low. Surprisingly, *P. aeruginosa* at MOI 0.5 breached the epithelial barrier starting at 6 hpi as at MOI 50. No significant differences between WT and  $\Delta pqsA_L$  could be discerned at this MOI.

#### **4.5.7. Analysis of the potential role of PQS in modulating ROS production by human neutrophils in response to PAO1-L**

So far, despite *in vitro* phenotypic characterisation demonstrated the  $\Delta pqsA_L$  mutant has lost the expression of numerous virulence factors, PQS deficiency in *P. aeruginosa* does not seem to affect the interaction with human bronchial epithelial cells. We wondered whether the lack of professional immune cells in this single cell model was intrinsically inert to *P. aeruginosa* infection and could not provide an appropriate model to discriminate the impact of PQS on *P. aeruginosa* virulence. Neutrophils are key players in the innate immune response to microbial infections. During infection, following the phagocytosis of pathogens and their delivery to phagolysosomes, a reaction called respiratory burst releases high concentrations of super oxide into the phagosome and a cascade of reactions occur resulting in the generation of additional reactive oxygen species (ROS) finalise the destruction of pathogens (Robinson, 2008). ROS production is used as an approach to assess the ability of neutrophils to respond to stimuli and can be quantified by a robust chemiluminescence assay. To determine whether PQS would alter the production of ROS by neutrophils in response of *P. aeruginosa*, PAO1-L at MOI 20 were administered to neutrophils in the presence or absence of exogenous Aqs using zymosan (20 particles per cell) as the positive control. Because Aqs (PQS (2-heptyl-3-hydroxy-4(1H)-quinolone) and Me-PQS) were initially reconstituted in methanol, methanol diluted to the same concentrations as those used for PQS compounds was used as control. Unexpectedly, methanol affected ROS production by neutrophils in response to zymosan and/or PAO1-L (Fig. 4.16A and 4.16D) and there was variability regarding the

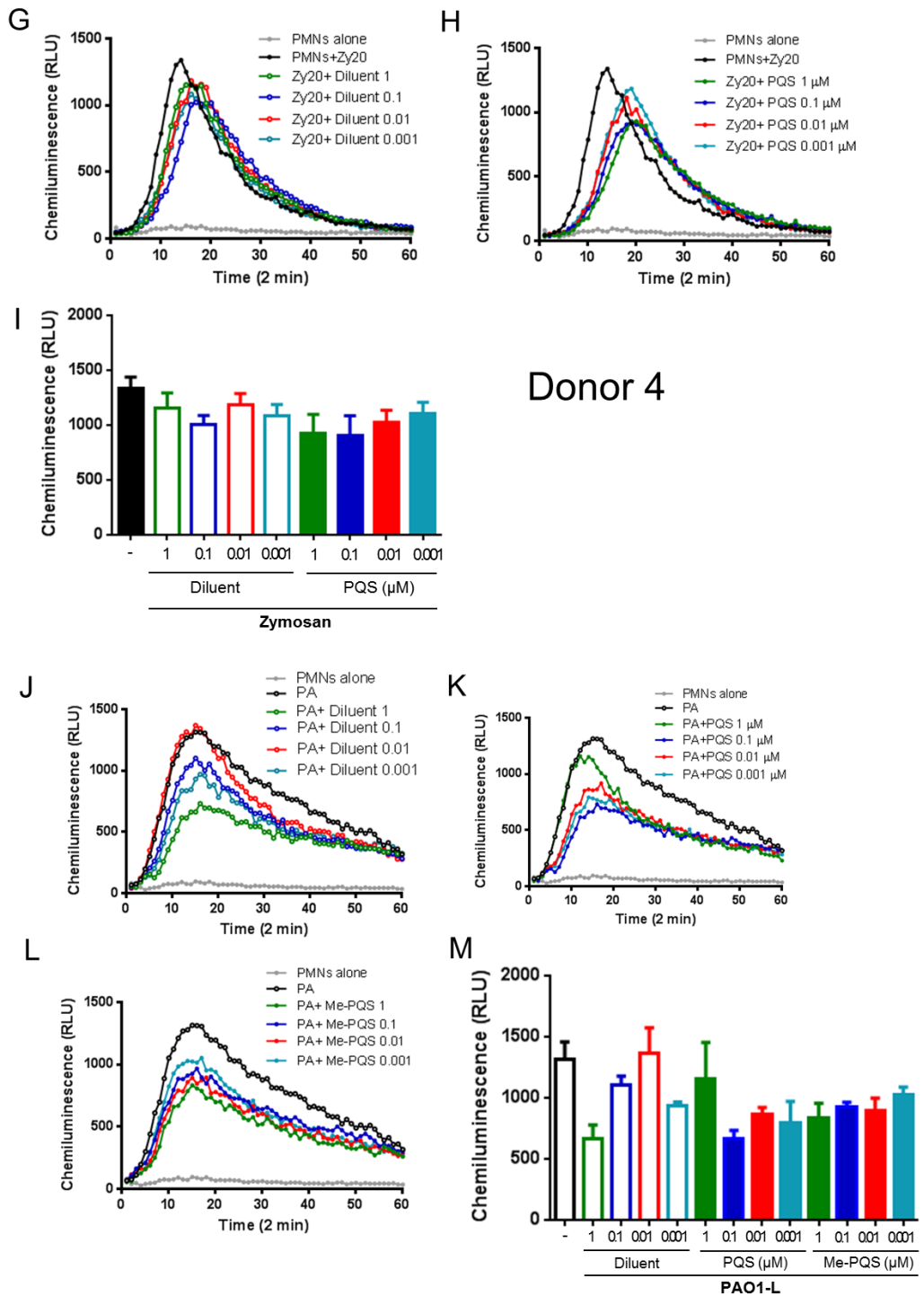
ability of *P. aeruginosa* to elicit ROS production in human neutrophils (see below). The preliminary data obtained from only two donors are inconclusive and the analysis of the ability of PQS to modulate ROS production by neutrophils requires further investigation.

In addition, donor dependent variability in ROS production by neutrophils in response to PAO1-L was observed. As shown in Fig. 4.17, ROS production elicited by PAO1-L exhibited two major patterns. A weak response to PAO1-L results in continuous low to intermediate production of ROS throughout the assay (Fig.4.17 A, B and C from donor 1, 2 and 5). The other pattern showed a rapid high production of ROS to levels equivalent to or higher than those elicited by zymosan followed by a sharp decrease (Fig.4.17 D and E from donor 3 and 4).

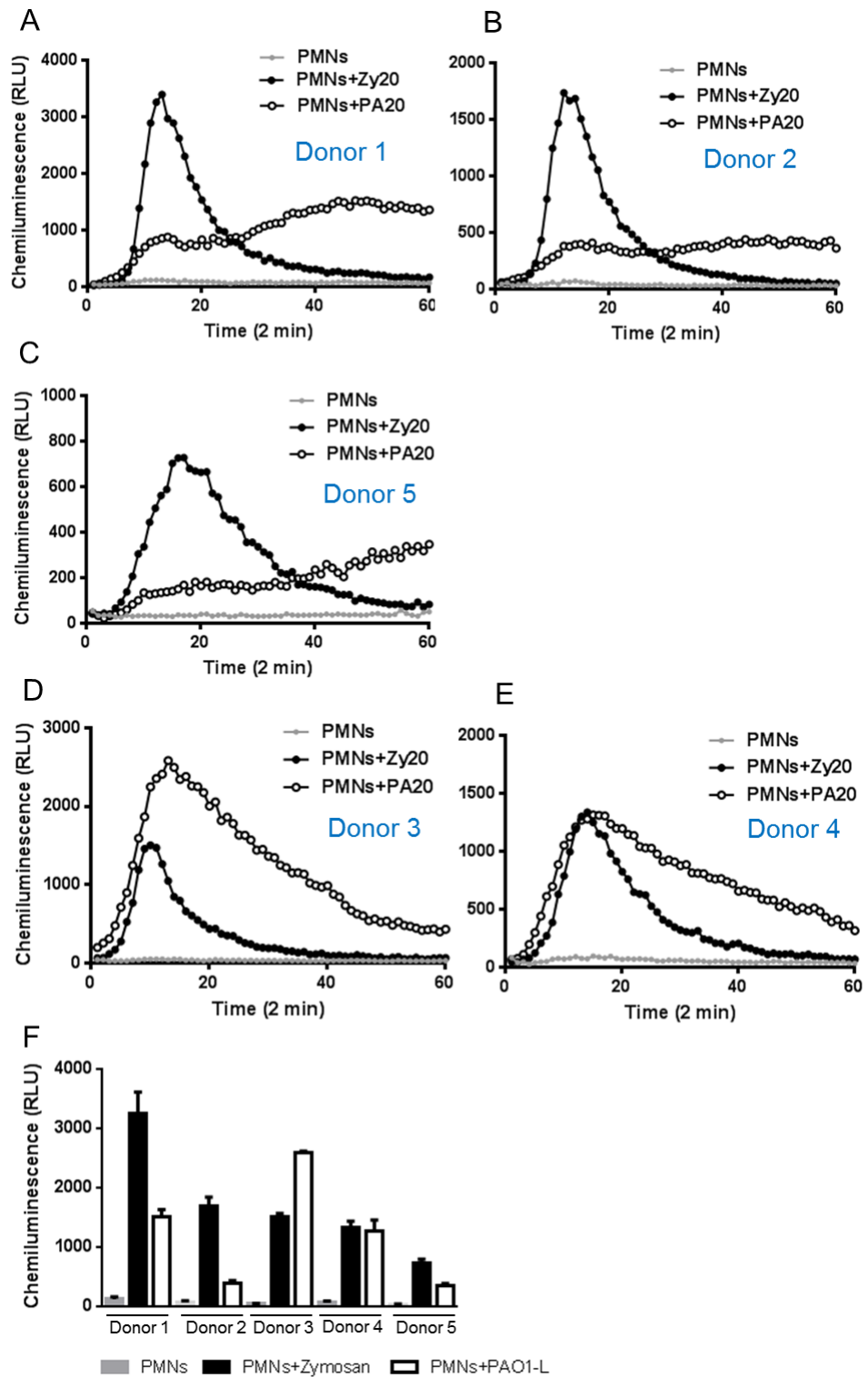


**Figure 4.16 Effect of PQS on ROS production by human neutrophils.**

ROS production by neutrophils (PMNs) in response to zymosan and PAO1-L were examined. In donor 2, in spite of a background induction of ROS production by the diluents, addition of PQS inhibited ROS production by PMNs in response to zymosan (A and B) and PAO1-L (D and E) in a dose-dependent manner. Maximum chemiluminescence peaks in response to zymosan (C) and PAO1-L (F) in the presence of diluents and different doses of PQS. Continued next page



(Continued from Fig. 4.16) In donor 4, the influence of the diluent in the generation of PQS was negligible but still no major effects of PQS were observed (G, H, J, K, L). Maximum chemiluminescence peaks in response to zymosan (I) in the presence of different doses of diluents and PQS; Maximum chemiluminescence peaks in response to PAO1-L (M) in the presence of different doses of diluent, PQS and methylated PQS (Me-PQS).



**Figure 4.17 Donor dependent variability in ROS production by human neutrophils.**

Viable PAO1-L elicited two patterns of ROS production by neutrophils (PMNs). A B and C represent pattern I in which low level ROS was persistently produced by PMNs in response to PAO1-L throughout the assay; D and E represent another pattern in which there was a high peak of ROS production that dropped gradually afterwards. F, maximum luminescence peaks in response to zymosan and PAO1-L in 5 donors. Black symbols denote PMNs treated with zymosan, white circles denote PMNs treated with PAO1-L and grey dots are PMNs alone.

## 4.6. DISCUSSION

The presence of PQS in CF lungs and the fact that CF sputum has been shown to induce high PQS biosynthesis in *P. aeruginosa* suggested that PQS might play a role in promoting *P. aeruginosa* persistence in the CF lung (Collier et al., 2002, Guina et al., 2003, Palmer et al., 2005). Regarding the role of PQS in immune modulation, PQS has been implicated in down-regulating the inflammatory response via inhibition of NF- $\kappa$ B and hypoxia-inducible factor 1 (HIF-1) signalling in human and mouse airway epithelial cells (Kim et al., 2010b, Legendre et al., 2012). *P. aeruginosa* pqsA knock-out mutant (PAO1 Nottingham background) was attenuated in a mouse burned wound model (Rampioni et al., 2010). The above studies suggested that PQS support *P. aeruginosa* persistence by inhibition of inflammatory signalling. We thus postulated that Pqs QS might be positioned at a higher hierarchy to coordinate the expression of a range of virulent factors in *P. aeruginosa*. Understanding the effect of PQS in the host response in human bronchial epithelial cells could provide us with a potential intervention target for immune modulation.

However, here we demonstrated that PQS does not play a role in the initial recognition of *P. aeruginosa* PAO1-L by differentiated human bronchial epithelial cells. This conclusion is based on the analysis of bacterial colonisation/growth, cellular cytotoxicity, barrier integrity, induction of pro-inflammatory cytokines and activation of inflammation and upstream kinase signalling pathways. Furthermore, a preliminary investigation of the influence of AQS on the respiratory burst by human neutrophils was also performed. The addition of exogenous PQS on PAO1-L WT-treated neutrophils seemed to

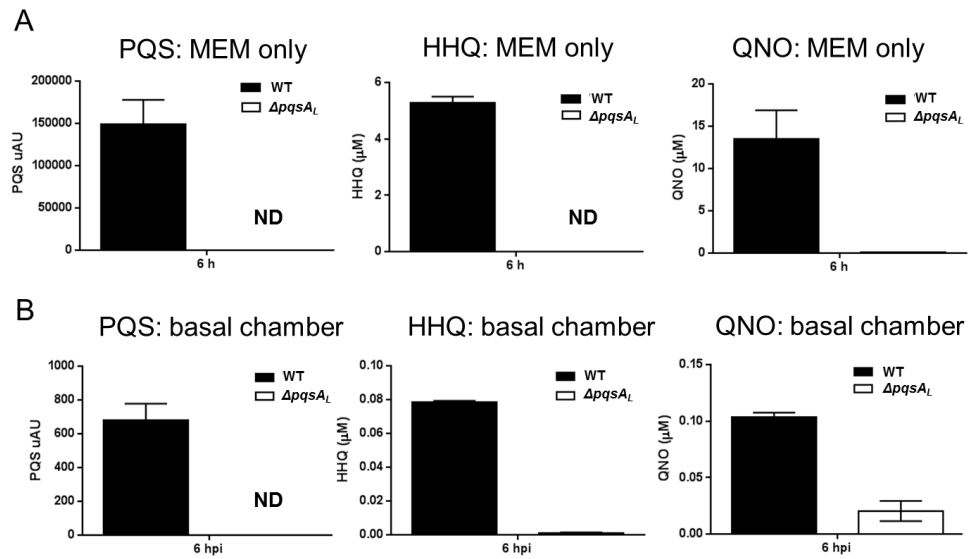
inhibit the generation of ROS by neutrophils, although the results were not conclusive and further repeats are required to address the donor variation effect. The diluent methanol itself might disturb host cell membrane permeability resulting in altered ROS production which makes data interpretation difficult (Hancock et al., 2001, Burch and Heintz, 2005).

Despite the in vitro phenotypic characterisation showing that  $\Delta pqsA_L$  mutant was deficient in the production of various virulence factors compared to PAO1-L WT (Chapter 2), the conditions during the infection of differentiated bronchial epithelial monolayer might profoundly impact the physiology of WT and  $\Delta pqsA_L$  as well as their capability to secrete AQS to the extracellular milieu. To address this concern we tested whether AQS were produced and secreted to the extracellular compartment by WT but not by  $\Delta pqsA_L$  in the context of differentiated human airway. Basal media from infected diffCalu-3 cells were collected, centrifuged to remove cell debris, and subjected to liquid chromatography-mass spectrometry (LC/MS) for the quantification and identification of QS molecules. Supernatants from WT and  $\Delta pqsA_L$  cultures in MEM were used as controls. (LC-MS analysis was supported by Dr. Catharine Ortori and data interpretation was assisted by Dr. Jean Dubern.) AQ molecules 2-heptyl-3-hydroxy-4(H)-quinolone (PQS), 2-heptyl-4H-quinolone (HHQ) and 2-heptyl-4(H)-quinolone N-oxide (QNO) were all detectable in the supernatants of WT MEM cultures at 6 hpi but only a minimal amount of AQ molecules was detected in the  $\Delta pqsA_L$  infected culture (Fig. 4.18A). PQS, HHQ and QNO were detected in the basal chamber from WT-infected diffCalu-3 cells but much less to none were identified in  $\Delta pqsA_L$  infected cultures (Fig. 4.18B). In addition, the AHL-QS molecules C4-HSL and 3-oxo-C12 were also



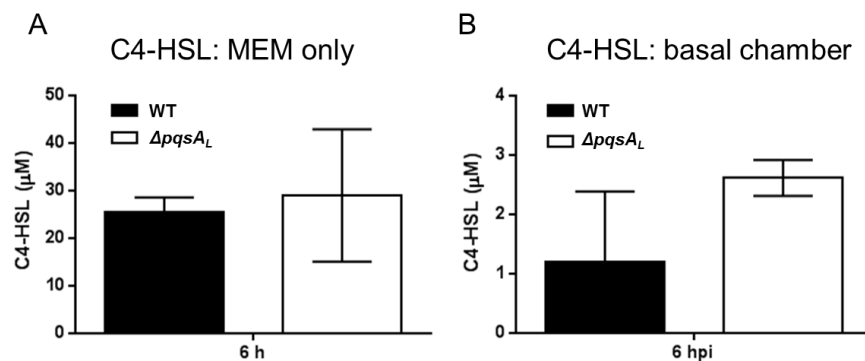
included in the LC/MS study. No major differences in the levels of C4-HSL and 3-oxo-C12-HSL secreted by WT and  $\Delta pqsA_L$  in MEM only (Fig. 4.19A) and in the Calu-3 cell basal chambers (Fig. 4.19B) were observed, although the large error bars due to lack of repeats rendered the results inconclusive.

The QS molecule identification supported our initial assumption that minimal to none PQS, HHQ and QNO were secreted by  $\Delta pqsA_L$  during the infection with diffCalu-3 cells. Thus, comparable cytotoxicity and infectivity of WT and  $\Delta pqsA_L$  were unlikely attributed to the lack of PQS production by WT or the complementation of PQS production in  $\Delta pqsA_L$ . However, since the initial plan of this project was to establish a robust co-culture model including epithelial cells and phagocytes to study the innate immune response upon microbial infections, infections of M-CSF primed macrophages (a model for resident tissue macrophages (Hamilton, 2008) derived from CD14<sup>+</sup> monocytes purified from PBMCs) with WT and  $\Delta pqsA_L$  was also performed. The results showed that the growth of WT and  $\Delta pqsA_L$  on macrophages was comparable at 2, 4 and 6 hpi. M-CSF primed human macrophages inhibited WT and  $\Delta pqsA_L$  growth to an equivalent level and no significant differences were identified (Fig. 4.20). The differences between experiments might be due to donor to donor variation. Thus, no infectivity difference was identified between the PQS-competent strain and PQS-deficient strain in macrophages.



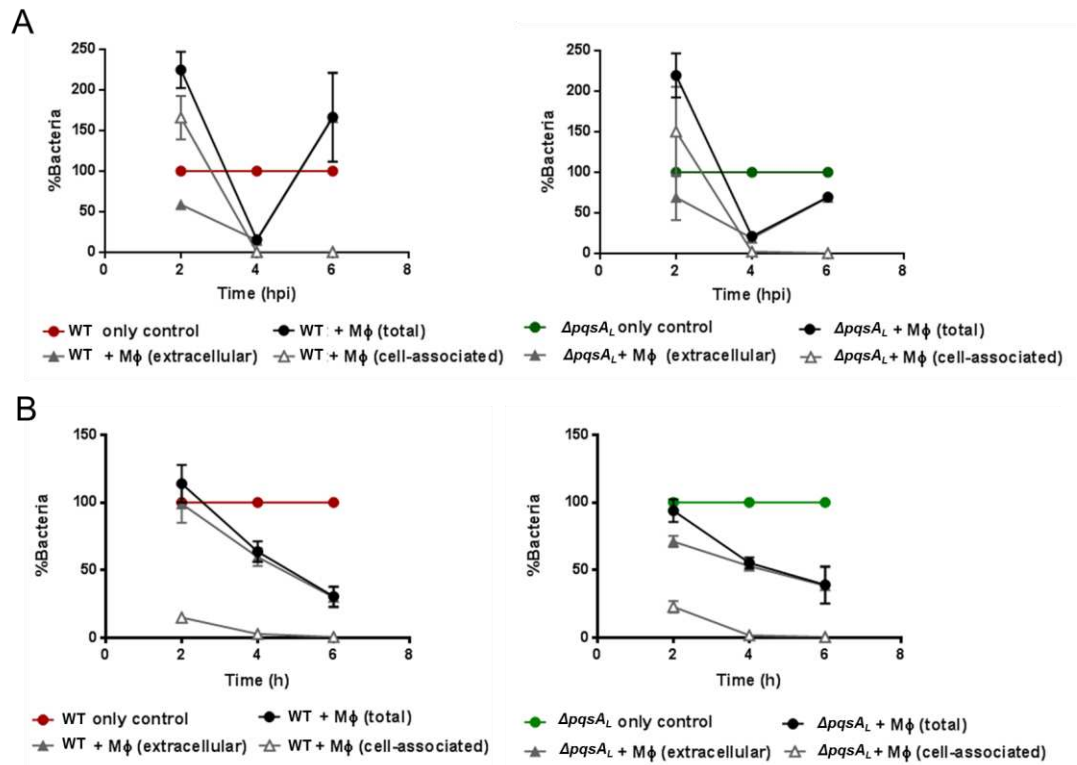
**Figure 4.18** PQS, HHQ and QNO were detectable in MEM only and the basal medium from Calu-3 cells infected with WT, but not  $\Delta pqsA_L$ .

Concentration of PQS (presented in micro absorbance unit, mAU), HHQ ( $\mu$ M) and QNO ( $\mu$ M) were determined by LC-mass spectrometry. PQS, HHQ and QNO were detectable in MEM culture supernatants of Wt (A) and the basal medium of differentiated Calu-3 cells infected with WT (B). None to small amounts of PQS, HHQ and QNO were detected in samples from  $\Delta pqsA_L$  infection either in MEM medium only or in the basal medium after infection of differentiated Calu-3 cells. No PQS, HHQ and QNO were detectable in MEM medium or basal medium from uninfected Calu-3 cells used as negative controls (data not shown). The results were obtained from one experiment with duplicates and the standard errors from the mean. ND, not detectable.



**Figure 4.19** WT and  $\Delta pqsA_L$  produced comparable amounts of C4-HSL and 3-oxo-C12-HSL in MEM and in the basal medium of diff Calu-3 cells after infection.

Concentrations of C4-HSL and 3-oxo-C12-HSL were determined by LC-mass spectrometry in the cell-free supernatants from WT and  $\Delta pqsA_L$  in MEM (A) or supernatants from WT and  $\Delta pqsA_L$  infected diffCalu-3 cells (B). Graphs present the mean of duplicates from one experiment and the standard error from the mean.



**Figure 4.20 Equivalent growth of WT and  $\Delta pqsA_L$  on M-CSF primed macrophages.**

The impact of PQS on the infection of *P. aeruginosa* at MOI 1 of M-CSF primed macrophages was analysed at 2, 4 and 6 h. In experiment A, macrophages restrained the WT and  $\Delta pqsA_L$  infection at 4 hpi (80% bacteria reduction); at 6 hpi, WT overgrew than the control but  $\Delta pqsA_L$  growth was still under control by macrophages to 30% inhibition. In experiment B, macrophages elicited approximately 50% of killing of both WT and  $\Delta pqsA_L$  and the killing effect continued till 6 hpi to 70%.

Thus, we wondered why WT and  $\Delta pqsA_L$  did not differ in pathogenicity when infecting on the diffCalu-3 cells despite the different phenotypes identified in vitro.

During early infection, apical protrusions of diffCalu-3 cells were observed in contact with WT and  $\Delta pqsA_L$  and both displayed a single flagellum based on SEM images at 2 hpi. WT and  $\Delta pqsA_L$  were also seen attached near cellular junctions. *P. aeruginosa* binding to adjacent host cell junctions has been shown to activate and recruit phosphatidylinositol 3-kinase (PI3K) to the apical

surface (Kierbel et al., 2005, Kierbel et al., 2007). PI3K, localised to the epithelial cell basolateral surface, is required for the synthesis of phosphatidylinositol 3,4,5-triphosphate (PIP<sub>3</sub>) leading to the activation of a downstream serine/threonine kinases Akt. The enrichment of PIP<sub>3</sub> and actin at the apical surface of bacteria binding site via the activation of PI3K/PIP<sub>3</sub>/AKT pathway was shown to be necessary and sufficient for *P. aeruginosa* internalisation in polarised epithelial cells (Kierbel et al., 2005). In addition, it has been shown that *P. aeruginosa* type IV pili bound to apical receptors N-glycans whereas flagella preferentially bound to heparan sulfate proteoglycans which are enriched at basolateral region in either injured or polarised MDCK and Calu-3 cells (Bucior et al., 2010, Bucior et al., 2012). These studies suggested *P. aeruginosa* is subverting host cell polarity to transform apical into basolateral membrane with the aid of pili and flagellum at early stages of infection thus generating a niche for colonisation of the local host cell environment. Subsequently, the formation of bacterial aggregates as microcolonies takes place (Engel and Eran, 2011). As both WT and  $\Delta pq s A_L$  had comparable swarming ability which is a phenotype dependent on type-IV pili (TFP) and flagella, their colonisation capacity on host cells was expected to be equivalent. Meanwhile, WT and  $\Delta pq s A_L$  induced comparable levels of mRNA of pro-inflammatory cytokines including GM-CSF, TNF- $\alpha$ , IL-8 and IL-17C in diffCalu-3 cells at 2 hpi. The results above suggest that PQS might not influence *P. aeruginosa* infectivity and immune modulation at early times post-infection.

*P. aeruginosa* has been shown to form aggregates rapidly upon the interaction with epithelial cells and the internalisation of bacterial microcolonies taking

place at PIP<sub>3</sub>-enriched protrusions in a Lyn-mediated manner (Lepanto et al., 2011). Lyn is a member of Src family tyrosine kinases. Consistent with this finding, internalisation of WT and *ΔpqsA<sub>L</sub>* by diffCalu-3 cells and small patches of microcolonies cells were observed in our confocal microscopy images at 3 hpi. Type III secretion system (T3SS) of *P. aeruginosa* is a syringe-like apparatus that translocates cytotoxic effector proteins from the bacteria, across the bacterial membranes and into the eukaryotic cytoplasm by forming a pore in the eukaryotic membrane. Previous studies demonstrated that T3SS effector proteins ExoS and ExoT, which possess GTPase activity at the N-terminal region and ADP-ribosylates activity at the C-terminal region, could disrupt tight junctions, actin cytoskeleton and result in caspase 1-dependent apoptosis (Engel and Balachandran, 2009). Angus et al. further provided evidence that the ADP-ribosylation domain of ExoS is required for *P. aeruginosa* to reside in membrane blebs thereby promoting bacterial survival by inducing apoptosis rather than acute necrotic cell death (Angus et al., 2010). In agreement with these observations our data showed small amounts of actin degradation, tight junction protein disruption and cytotoxicity in WT and *ΔpqsA<sub>L</sub>* infected diffCalu-3 cells at 3 hpi.

At 6 h of WT and *ΔpqsA<sub>L</sub>* infection on diffCalu-3 cells, substantial actin degradation, loss of tight junction proteins and transmigrated bacteria were consequently identified. The release of elastase B (LasB) and exotoxin A (ETA) by *P. aeruginosa* might aid this effect. LasB has been shown to disrupt tight junction proteins ZO-1 and ZO-2 as well as release mucins from rabbit trachea epithelial cells, whereas ETA inhibits protein synthesis via blockade of elongation factor-2 and therefore abrogates the restoration of tight junction

proteins once cells are injured (Klinger et al., 1984, Kipnis et al., 2006). *P. aeruginosa* PAO1-L has been shown to secrete ETA to the supernatant whereas PAO1-N subline was found deficient in ETA production (Farah Hussain, on-going PhD thesis). The production of ETA by  $\Delta pqsA_L$  can also be tested if required. Collectively, our data suggest that type IV pili, flagellum, T3SS toxins and extracellular proteases could be the predominant virulence factors that cause the infectivity of *P. aeruginosa* in an acute epithelial infection model rather than the role of PQS in regulating the expression of virulence factors. To prove the hypothesis, T3SS and PQS double mutant ExoS/pqsA, ExoT/pqsA or triple mutant ExoS/ExoT/pqsA could be generated to investigate the pathogenicity of *P. aeruginosa* in a similar infection setting.

A recent study demonstrated an inverse association between the secreted levels of T3SS exotoxin ExoU and PQS, and their association with the disease progression of a patient with ventilator-acquired pneumonia (Singh et al., 2010). High levels of PQS reversely correlated with ExoU secretion, whereas the expression of elastase and pyoverdine are positively controlled by PQS. Decreased PQS shifted the virulence profile from a chronic infection state to an acute phenotype that promotes the secretion of T3SS exotoxins. The phenotypic change paralleled the transition of a ventilator-acquired pneumonia clinical isolate to an acute T3SS secreting phenotype within a short period of time. Based on the above results the PQS deficient mutant  $\Delta pqsA_L$  was expected to have a more cytotoxic phenotype as the secretion of T3SS toxins would not be inhibited by extracellular Aqs. However, due to the lack of ExoU in the genome of WT and  $\Delta pqsA_L$  (Winsor et al., 2011), the phenotype transition according to the axis of PQS and T3SS toxin cannot fully apply to

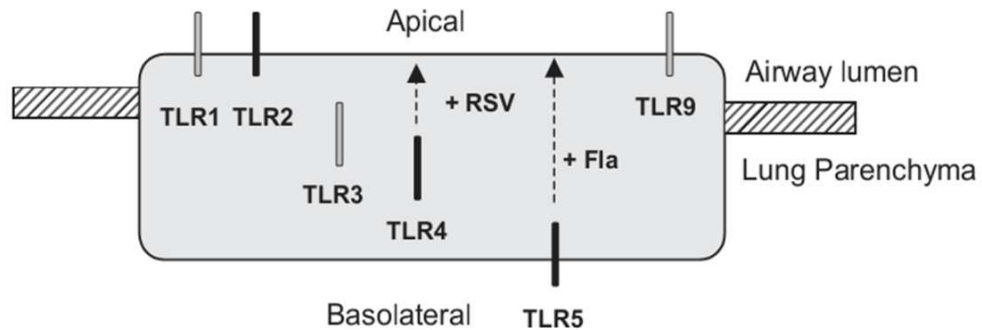
the strain PAO1-L, at least ExoS and ExoT do not seem to elicit a similar effect in the Aqs deficient strain.

Nasal airway epithelial cells and lung epithelial cells were shown to secrete the proinflammatory cytokines GM-CSF, IL-8, and IL-6 when exposed to *P. aeruginosa* rhamnolipids, autoinducer 3-oxo-C12 HSL and mucoid exopolysaccharides (Bédard et al., 1993, Smith et al., 2001). IL-8, also known as neutrophil chemotactic factor, readily recruits neutrophils and binding at the site of inflammation. GM-CSF not only stimulates myeloid cells survival, proliferation, and differentiation but is essential for normal pulmonary surfactant homeostasis and alveolar macrophage function (Trapnell and Whitsett, 2002). For instance, mice deficient in GM-CSF showed decreased survival to *P. aeruginosa* lung infection as a consequence of impaired killing and phagocytosis by alveolar macrophages (Ballinger et al., 2006). The cytokine TNF- $\alpha$  participates in multiple biological effects and has been implicated in chronic inflammatory diseases such as asthma and pulmonary fibrosis. TNF- $\alpha$  secreted by epithelial cells also stimulates IL-6, IL-8 and GM-CSF production as a positive feedback loop and alters tight junction integrity (Ye et al., 2006, Martin et al., 1997). The IL-17 family of cytokines consists of at least six members IL-17A to IL-17F. To date, IL-17A which secreted mostly by Th17 cell subset has been best studied and it is essential in maintaining the mucosal homeostasis and mice deficient in IL-17A are more susceptible to respiratory infections. Attention to IL-17C has been drawn in recent studies as it is exclusively expressed in epithelial cells. Human bronchial epithelial cells (HBECs) have been shown to express IL-17C in response to *P. aeruginosa*, *Haemophilus influenzae*, and TLR-3 as well as TLR-5 agonist stimulation. In

addition, IL-17C, acts as an autocrine cytokine; by binding to the receptors IL-17RA and IL-17RE expressed in epithelial cells, promotes the expression of proinflammatory cytokines, chemokines and antimicrobial peptides in a skin-inflammation model (Pappu et al., 2012, Pfeifer et al., 2012, Reynolds et al., 2012). In accordance with a previous study, IL-1 $\beta$  was not detectable in 16HBE cells upon *P. aeruginosa* PAK flagella stimulation following 2 h to 24 h given the presence of a *Nlrc4* transcript was readily detected (Parker and Prince, 2013). The results of the cytokine profiling demonstrated that in vitro differentiated human bronchial epithelial cells mount a robust proinflammatory response upon viable PAO1-L WT and  $\Delta pqsA_L$  infection. High levels of the transcripts encoding for the proinflammatory cytokines GM-CSF, TNF- $\alpha$ , IL-6 and IL-17C and the chemokine IL-8 were detected at 2 hpi. Secretion of cytokines and chemokines was also evaluated. Abundant TNF- $\alpha$  and IL-6 were detected at levels comparable with the high mRNA expression; however, the production of GM-CSF was relatively low given the high expression detected at mRNA level. Cytosolic GM-CSF accumulation was not detected. Whether the amount of GM-CSF protein is relatively low compared to TNF- $\alpha$  due to translational inhibition or protein degradation in the cytoplasm requires further study. Chemokine IL-8 seemed constitutively produced at high levels by diffCalu-3 cell even in the absence of *P. aeruginosa* infection. In fact, the low  $C_T$  values of IL-8 mRNA transcripts obtained from untreated Calu-3 cells might explain why the high levels of IL-8 secretion in uninfected cells were similar to those produced by *P. aeruginosa*-infected cells. It should be taken into consideration that IL-8 and IL-6 are more abundantly secreted apically than at the basal chamber shown in reproductive tract epithelial cells (Fahey et



al., 2005). Asymmetrical cytokine secretion could be a confounding factor as apical secretion has not been quantified in our study.



**Figure 4.21 TLR protein expression in bronchial airway epithelial cells.**

TLR2 is the predominant TLR expressed on the apical surface of airway epithelial cells. TLR3 and TLR4 reside intracellularly and TLR5 is located at the basolateral surface. Black TLR, confocal data; grey TLR, flow cytometry or slide-based fluorescent cell counting data. Figure was adopted from (Greene and McElvaney, 2005).

To date, TLRs 1-10 have been found in airway epithelial cells, both in CF and non-CF tracheal and bronchial epithelial cell lines (Muir et al., 2004). TLR2 and TLR5 are amongst the mostly studied and have been frequently associated with cellular activation in response to *P. aeruginosa*. The activation of intracellular signal pathways is initiated via the binding of flagellum and pili to asialoGM1 and TLR5. Further adherence is conferred by interactions between LPS and asialoGM1, CD14 and/or CFTR. Both flagellar interaction with TLR5 and LPS binding to TLR4/MD2 activates myeloid differentiation primary response 88 (MyD88) adaptor protein-dependent NF- $\kappa$ B pathways leading to increased IL-8 transcription. TLR signaling also leads to activation of AP1 and the MAP kinases JNK, p38 and ERK1/2. TLR3, TLR4 and TLR5 in epithelial cells were found to reside mainly intracellularly (Greene and McElvaney, 2005). TLR4 has also been shown expressed at low levels at the apical surface

in type II alveolar cell line A549 (Guillot et al., 2004). Additionally, studies in human bronchial epithelial cells including BEAS-2B, 16HBE, HAEo- and MM-39 showed that TLR4 resided intracellularly and that TLR in bronchial epithelial cells were hyporesponsive to Gram negative bacteria. Relatively low expression of TLR on the airway epithelium is suggested to avoid uncontrolled activation by inhaled bacteria. In our study, we found that the high levels of pro-inflammatory activation seen at 2 hpi do not correlate with a less than 2-fold induction of upstream signalling at 3 hpi. This can be partly explained by the protein degradation taking place at 3 hpi that could have underestimated the overall signalling events. This problem can be solved by moving the time-frame prior to 2 hpi or by monitoring an early time course. Moreover, the signalling pathways in this study including MAPK, NF- $\kappa$ B, IRF and AKT do not inclusively respond to bacterial infection but are also involved in the regulation of a variety of events, such as cell apoptosis, inflammation and metabolism. For instance, serine/threonine AKT pathway, in close cooperation with PI3K pathways, promotes cell growth through protein synthesis driven by mTOR signalling and inhibits apoptosis by blocking FoxO1 activity in cancer cells (Engelman, 2009, Weichhart and Saemann, 2008). Calu-3 cells used in this study were derived from lung adenocarcinoma that might inherently express high levels of PI3K/AKT signalling in which could mask the induction from *P. aeruginosa* infection.

Because no differences in pathogenicity could be identified between a PQS-competent and PQS deficient strain of *P. aeruginosa* using diffCalu-3 cells, the highly virulent CF clinical isolate Liverpool epidemic strain B58 (LESB58) was introduced in our study in order to verify the efficacy of this in vitro

human bronchial epithelial model. This investigation will be discussed in next chapter.

## 4.7. SUMMARY

PQS is not required for the pathogenesis of *P. aeruginosa* PAO1-L during the initial innate immune recognition by bronchial epithelial cells based on bacterial colonisation, cytotoxicity, barrier breakage, and activation of proinflammatory response. Also,  $\Delta pqsA_L$  was not attenuated in the infection of M-CSF primed macrophages suggesting a marginal effect of PQS on *P. aeruginosa* pathogenesis even in the interaction with phagocytes.

# 5. THE INTERACTION BETWEEN *PSEUDOMONAS AERUGINOSA* STRAIN LESB58 AND HUMAN BRONCHIAL EPITHELIUM

---

## 5.1. INTRODUCTION

In the previous chapter, a AQs deficient mutant  $\Delta pqsA_L$ , displayed similar cytotoxic properties and infectivity to its isogenic wild type strain upon infection of diffCalu-3 cells (Chapter 4) in spite of its attenuated phenotype in vitro (Chapter 2). These results suggest that AQs might not be required during the infection of human bronchial epithelial cells by *P. aeruginosa* PAO1-L. However, we also wondered whether this infection model was capable of discerning between virulent and non-virulent strains of *P. aeruginosa*. To further examine the efficacy of this in vitro differentiated human bronchial epithelial infection model in differentiating between virulent and non-virulent *P. aeruginosa* strains, the Liverpool epidemic strain subtype B58 (LESB58), a CF clinical isolate, was studied. The ability of LESB58 to growth, disrupt the cellular cytoskeleton and induce the expression of pro-inflammatory cytokines was compared with those of PAO1-L.

The Liverpool Epidemic Strain (LES) of *Pseudomonas aeruginosa* is a  $\beta$ -lactam-resistant isolate firstly identified at a children's CF centre in Liverpool, United Kingdom (Cheng et al., 1996). LES is transmissible and is the clone most frequently isolated from CF patients in England, Wales, Scotland and

Australia (Edenborough et al., 2004, Lewis et al., 2005, Armstrong et al.). In 2002, a case report described the transmission of a super virulent LES strain from a CF patient to both her non-CF parents leading to significant morbidity and recurrent infections (McCallum et al., 2002). LESB58 is one of the LES CF isolates; it exhibits an unusual upregulation of the quorum sensing regulon that results in the overexpression of virulence-related exo-products LasA, elastase and pyocyanin and hyper production of biofilms (Salunkhe et al., 2005, Fothergill et al., 2007, Kukavica-Ibrulj et al., 2008). In addition to its resistance to ceftazidime which is how this widespread strain was identified during an anti-microbial screening of multiple LES isolates, it is known that the LES strains can acquire resistance to several antibiotics such as meropenem, aztreonam, tobramycin, and ciprofloxacin (Fothergill et al., 2007). Hence, the LES isolates are considered aggressive strains capable of adapting to the CF lung, because of their ability to mutate and resistance to the antibiotics commonly used for therapy. The *P. aeruginosa* strains PAO1 and PA14 were previously compared with LESB58 to assess in vivo growth, bacterial persistence, and localization within tissues in a rat model of chronic lung infection (Kukavica-Ibrulj et al., 2008). The three *P. aeruginosa* strains demonstrated similar growth in vivo and lung colonisation but were differentially distributed in lung tissues. Different infectivity profiles based on the bacterial CFU in mouse lung tissues 7 days post-infection were identified when the results were presented as competitive index (CI) values: 0.02 for PAO1-PA14, 0.002 for PAO1-LES and 0.14 for LES-PA14. The results indicated a 1,000-fold reduction in PA14 CFU when compared with PAO1, LESB58 showed 10,000-fold attenuation when compared with PAO1, whereas

PA14 was 10-fold attenuated when compared with LESB58 (Kukavica-Ibrulj et al., 2008). The LESB58 strain remained in the agarose beads used to deliver bacteria to the lung lumen, whereas PAO1 and PA14 strains disseminated into the alveolar regions and grew as macrocolonies at 14 days post-infection. These observations were consistent with the fact that LESB58 was less motile than PAO1 and PA14 but produced more biofilm *in vitro*.

LESB58 is the earliest LES isolate archived and its whole genome has been sequenced (Winstanley et al., 2009). Compared to the genome of PAO1-L that harbours two tendon-defective prophages pyocin R2 and F2 (Stover et al., 2000), five prophage clusters, one defective (pyocin) prophage and five non-phage genomic islands were identified in the sequence of LESB58 (Winstanley et al., 2009). Because LESB58 appeared to be highly adapted to the human lung and behaved so differently to PAO1 and PA14 during chronic lung infection, we questioned whether AQS production could contribute to LESB58 virulence by promoting persistence in the lung lumen and if this could be modelled using diffCalu-3 cells. The use of the virulent clinical strain LESB58 would pave the road towards a better understanding of how virulent clinical isolates interact with bronchial human epithelium and the inflammatory response triggered upon infection with clinical strains.

## **5.2. HYPOTHESIS**

A clinical virulent CF strain LESB58 would differ from PAO1-L regarding its ability to cause cytotoxicity, grow and induce a pro-inflammatory response upon infection of diffCalu-3 cells.

## **5.3. AIM**

To evaluate the suitability of the differentiated human bronchial epithelial cells, diffCalu-3 cells, as an in vitro infection model for the examination of the pathogenesis of *P. aeruginosa*, a transmissible virulent CF clinical isolate LESB58 was used to infect diffCalu-3. The phenotypic characterisation of LESB58 infection was performed in comparison with the laboratory strain *P. aeruginosa* PAO1-L. The parameters analysed were: bacterial growth on the epithelium, expression of pro-inflammatory cytokines and chemokines, cellular cytotoxicity and alterations in barrier function.



## **5.4. MATERIALS AND METHODS**

### **5.4.1. Phenotypic characterisation of LESB58**

The methodology used for the phenotypic characterisation of LESB58 was described previously in the materials and methods section in Chapter 4.

### **5.4.2. Infection of diffCalu-3 cells with PAO1-L and LESB58**

Differentiated Calu-3 cell cultures were prepared as described in Chapter 3, section 3.4.1. For infection, *P. aeruginosa* PAO1-L and LESB58 were grown overnight for 16 h in LB broth at 37°C, 200 rpm, washed twice and suspended in sterile PBS containing CaCl<sub>2</sub> and MgCl<sub>2</sub> (Sigma-Aldrich, UK) at a concentration of 3.5x10<sup>8</sup> CFU/ml. For each strain, 100 µl of bacterial suspension (equivalent to moi of 50) was added to the apical surface of diffCalu-3 cell cultures. Infected cultures were incubated at 37°C, 5% CO<sub>2</sub> for 3 and 6 h.

### **5.4.3. Assessment of pathogenesis of LESB58 on diffCalu-3 cells in comparison with PAO1-L**

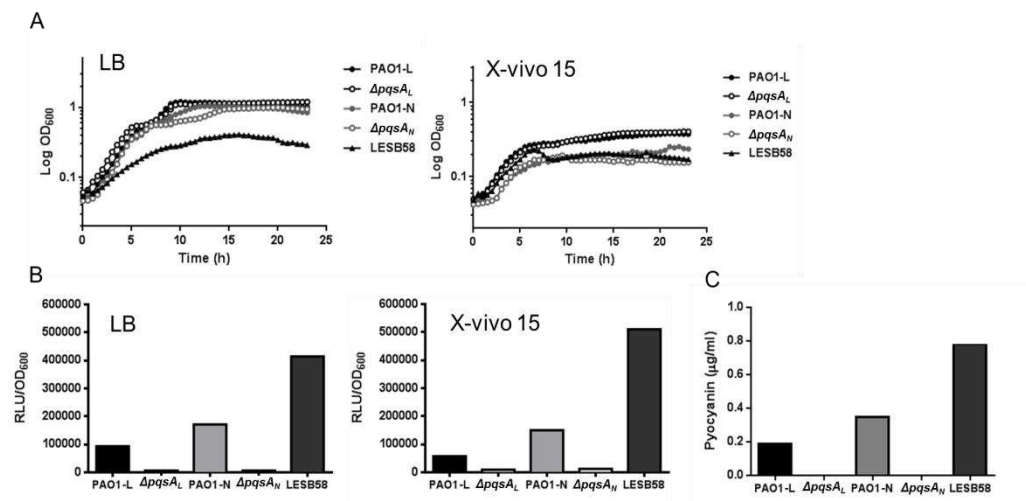
The methodology for the assessment of bacterial pathogenesis including bacterial growth, induction of pro-inflammatory response at mRNA and protein levels, and the cytotoxicity have been described previously in Chapter 4.

## 5.5. RESULTS

### 5.5.1. Phenotypic characterisation of LESB58 in comparison with PAO1 laboratory strains

#### 5.5.1.1. Growth characteristics, PQS and pyocyanin production by LESB58

Initially, the bacterial growth and features associated with PQS QS regulation including the secretion of PQS molecules and the production of pyocyanin were examined in LESB58. LESB58 grew following a kinetics similar to that of the laboratory strain PAO1 (PAO1-L, PAO1-N,  $\Delta pqsA_L$  and  $\Delta pqsA_N$ ) but reached a lower density at stationary phase when cultured in LB medium (Fig. 5.1A, LB). However, in X-vivo 15 medium all *P. aeruginosa* strains displayed similar growth kinetics and reached comparable cell density (Fig. 5.1A, X-vivo 15). Overnight cultures (16 h) of LESB58, PAO1-L and its isogenic  $\Delta pqsA_L$  mutant, PAO1-N and its isogenic mutant  $pqsA-N$  were collected, centrifuged and supernatants were retained for the analysis of PQS and pyocyanin production. The results showed that LESB58 produced 4-fold more PQS (Fig. 5.1B) and pyocyanin (Fig. 5.1C) than PAO1-L in LB cultures; a 9-fold increase in PQS production by LESB58 compared to PAO1-L in X-vivo 15 cultures. Thus, although LESB58 reached lower cell density than PAO1-L at stationary phase, the productions of PQS and pyocyanin by LESB58 were higher than in PAO1-L. The results were consistent with the finding that most of the *P. aeruginosa* Liverpool CF epidemic strains are characterized by over-production of quorum sensing-regulated virulence factors including pyocyanin and LasA protease (Fothergill et al., 2007, Salunkhe et al., 2005).

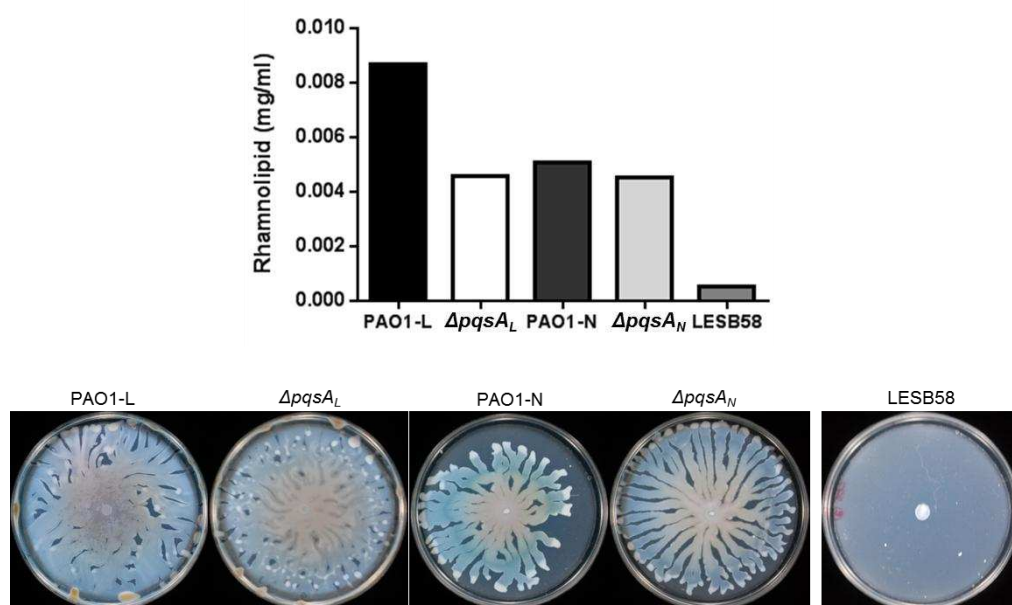


**Figure 5.1 LESB58 produced high amounts of PQS and pyocyanin compared to PAO1 strains, despite reaching lower cell density in culture.**

Bacterial growth of LESB58 and PAO1 lab strains were monitored for 24 h in a static system (Tecan) in LB and X-vivo 15 medium. LESB58 reached stationary phase at the same time as PAO1 strains in LB, whilst in X-vivo 15 medium the growth between all strains was comparable (A). LESB58 produced 5-fold PQS more than PAO1-L (B) in agreement with pyocyanin production (C). A, n=1; B and C, averages were from two independent experiments and each sample was done in triplicate. (Each experiment was conducted with LESB58 and 4 PAO1 strains simultaneously for comparison. The data for PAO1 strains have been shown previously in chapter 2.)

### 5.5.1.2. LESB58 is non-motile and produces less rhamnolipids than PAO1-L

As described in Chapter 2, the production of surfactant rhamnolipids and motility are two of the factors associated with virulence in *P. aeruginosa*. Analysis of the capability of LESB58 to swarm and to produce rhamnolipids in vitro demonstrated that LESB58 displayed reduced rhamnolipid production and motility (Fig. 5.2). The reduced motility of LESB58 observed in this study is in agreement with its persistence in the bronchial lumen in a rat model of chronic lung infection (Kukavica-Ibrulj et al., 2008). Additionally, neither flagella nor pili were detected on the surface of LESB58 (Winstanley et al., 2009).



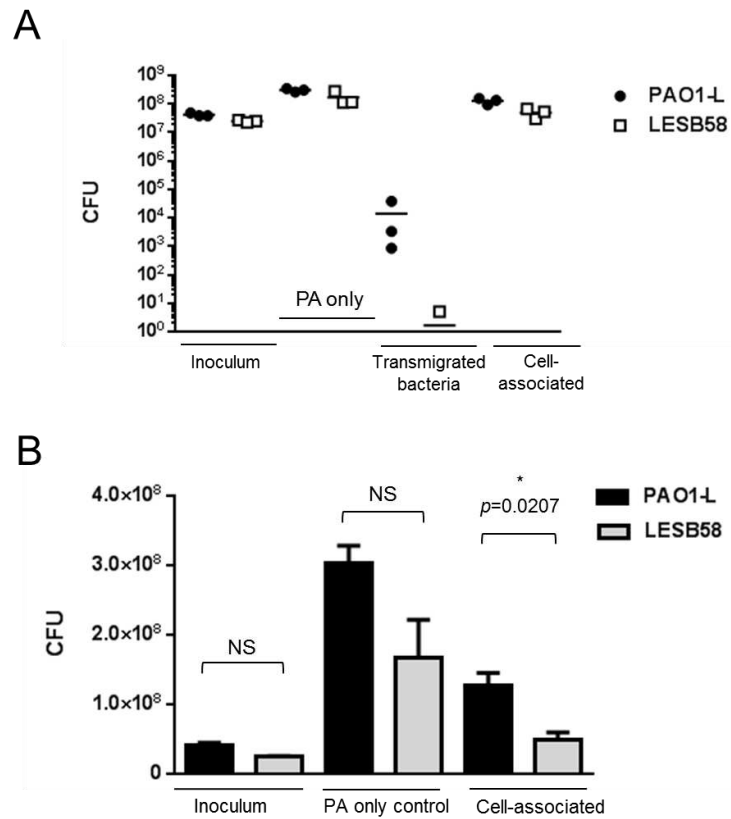
**Figure 5.2 LESB58 produces low levels of rhamnolipids and is non-motile.**

Rhamnolipids production and motility of LESB58 were compared with PAO laboratory strains. LESB58 produced no detectable rhamnolipids and appeared non-motile in a swarming plate. Two independent experiments were conducted for rhamnolipid production assay. Images for biofilm formation are representative from three independent experiments showing similar trends in motility. (Each experiment was conducted with LESB58 and 4 PAO1 strains simultaneously for comparison. The data for PAO1 strains have been shown previously in chapter 2.)

### **5.5.2. Reduced translocation of LESB58 upon infection of diffCalu-3 cells**

Among the strategies employed by live pathogens to infect their hosts, the most common is the ability to grow in their host upon infection (Vance et al., 2009). Thus, the growth of LESB58 on differentiated diffCalu-3 cells in comparison with Wt was evaluated in the first instance to assess its correlation with virulence. Due to LESB58 achieved low cell density at mid log-phase culture (4 h,  $3.5 \times 10^8$ /ml) overnight cultures (16 h) of PAO1-L and LESB58 were used for the infection of diffCalu-3 cells (MOI 50) instead. Using 21-day old differentiated Calu-3 cells, we quantified: 1) the bacteria growth in the cellular fraction (cell-associated bacteria), 2) bacteria able to cross the epithelial barrier to the basal chamber (transmigrated bacteria) and 3) bacteria grown in MEM only wells (PA only). The mean values for the Wt inocula were 1.7-fold higher than for the LESB58 inocula but these differences were not significant. The bacteria grown in MEM only reached  $10^8$  for both strains and the mean values for Wt were 1.8-fold higher than for LESB58 (Fig. 5.3). The majority of bacteria remained cell-associated and the mean for PAO1-L was 2.6-fold higher than for LESB58. Although this difference was statistically significant, its biological relevance is questionable because it represented less than 1 log change. The reduced growth of LESB58 on Calu-3 cells might be caused by the inherent low growth rate of LESB58 compared to PAO1-L based on the growth curve. Despite the fact that the number of cell associated bacteria and the bacteria in MEM cultures were non-significantly different between Wt and LESB58, the amount of transmigrated bacteria for LESB58 were 4-logs lower than for Wt infected cultures (summarised in Table 5.1). This indicated that LESB58 mainly accumulated within the epithelium and was less invasive than

PAO1-L.



**Figure 5.3 LESB58 remained mainly cell-associated upon infection of diffCalu-3 cells.**

The numbers of bacteria in the inocula and PA only controls were comparable between PAO1-L and LESB58. Although the numbers of cell-associated bacteria for WT were significantly higher than for LESB58, the 2.6-fold change represented less than one-log difference. Few to none LESB58 crossed the polarised diffCalu-3 cells barrier. Three independent experiments were conducted.

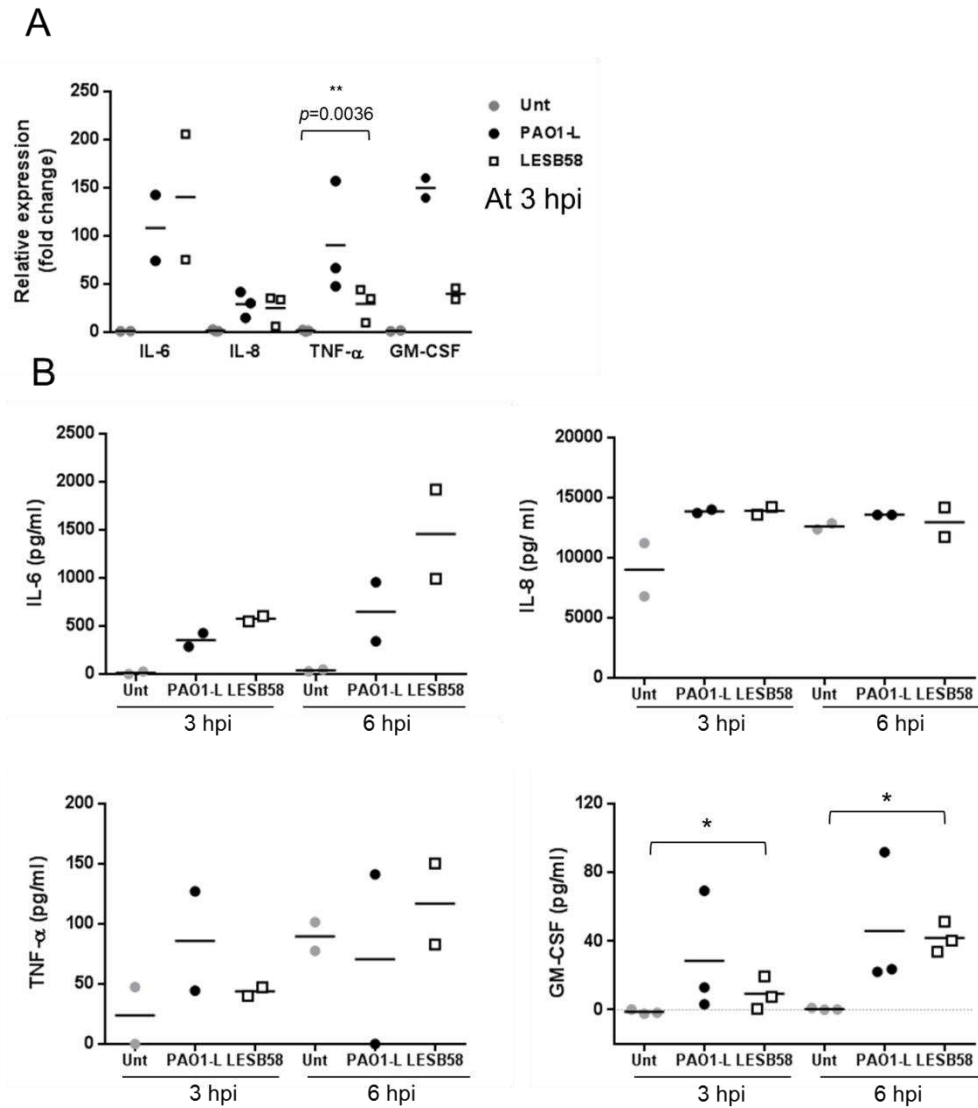
**Table 5.1 Summary of the average number of bacteria  $\pm$  standard deviation for Wt and LESB58 in each compartment at 6 hpi of diffCalu-3**

Total CFU (Average, n=3)	PAO1-L	LESB58
Inoculum ( $\times 10^7$ )	$4.2 \pm 0.6$	$2.5 \pm 0.2$
PA* only in MEM ( $\times 10^7$ )	$30.4 \pm 4.2$	$16.8 \pm 9.3$
Transmigrated bacteria	$14,228 \pm 20,566$	$1.7 \pm 2.9$
Cell-associated bacteria ( $\times 10^7$ )	$12.7 \pm 3.1$	$4.9 \pm 1.8$
PA* only in MEM/ inoculum	7.3	6.8
Ratio cell-associated bacteria/ PA only in MEM	0.42	0.29

\*PA, *P. aeruginosa*

### **5.5.3. LESB58 induced a lower pro-inflammatory response upon infection of diffCalu-3 cells compared to PAO1-L**

To understand whether Wt and LESB58 cause differential induction of pro-inflammatory cytokines by diffCalu-3 cells, levels of mRNA coding for selected pro-inflammatory cytokines and chemokines including IL-6, TNF- $\alpha$ , GM-CSF, and IL-8 were examined. Transcripts encoding for IL-6, IL-8, TNF- $\alpha$ , and GM-CSF were all induced in diffCalu-3 cells upon LESB58 infection and levels ranged from 25-fold to 150-fold compared to uninfected cells. However, the expression was differentially induced compared to the levels of expression when diffCalu-3 cells were infected with PAO1-L. LESB58 induced 1.3-fold higher IL-6 expression than PAO1-L but this difference was not significant. In contrast the levels of TNF- $\alpha$  and GM-CSF transcripts after LESB58 infection were 3-fold and 3.8-fold lower than after PAO1-L infection (Fig. 5.4A). Similarly, the levels of pro-inflammatory cytokine protein production displayed the same trend and were consistent with the mRNA analysis (Fig. 5.4B). This was a preliminary observation and more repeats (IL-6, IL-8, TNF- $\alpha$ , n=2; GM-CSF, n=3) need to be performed to achieve statistical significance. However, these results suggest LESB58 might exert a relatively lower activation of a pro-inflammatory response compared with PAO1-L upon infection of airway epithelial cells.



**Figure 5.4 Induction of pro-inflammatory cytokines and chemokines by diffCalu-3 cells upon Wt and LESB58 infection.**

A, Expression of IL-6, TNF- $\alpha$ , GM-CSF and IL-8 was investigated in diffCalu-3 cells infected with PAO1-L and LESB58 at a moi 50 for 3 h by qPCR. LESB58 induced 1.3-fold higher expression in IL-6 than PAO1-L but significance was not achieved. The levels of TNF- $\alpha$  and GM-CSF induced by PAO1-L infection was 3-fold and 3.8-fold respectively higher than the expression elicited by LESB58. B, Cytokines were quantified in the culture supernatants at 3 hpi and 6 hpi. The trend in cytokine production correlated with the mRNA quantification shown in A. Each symbol represents one experiment. Each sample in each experiment was prepared in duplicate. Significance was calculated by one-way ANOVA. \*  $p < 0.05$  is considered significantly different.

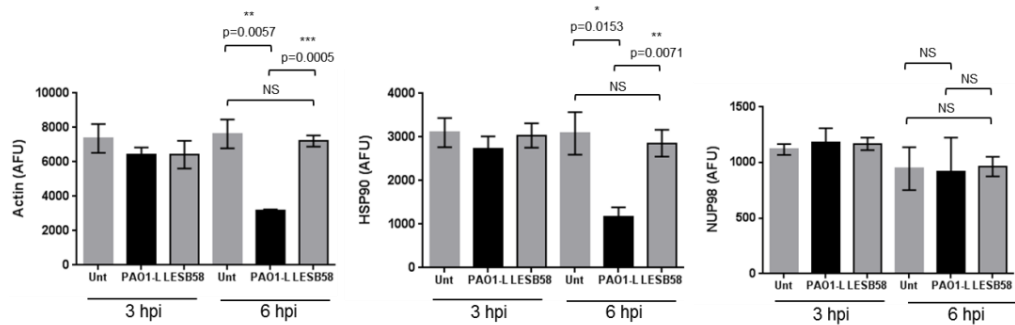


#### **5.5.4. LESB58 was less cytotoxic than PAO1-L upon infection of diffCalu-3 cells**

Hijacking and disrupting normal host cytoskeleton function is a pattern of pathogenesis employed by a variety of intracellular bacterial pathogens. This strategy facilitates intracellular pathogens to gain access to the cell for subsequent replication (Vance et al., 2009). In spite of the fact that *P. aeruginosa* is commonly considered as an extracellular pathogen, PAO1-L Wt and its isogenic mutant  $\Delta pqsA_L$  were seen previously to invade diffCalu-3 cells and disrupted the barrier functions via degradation of actin and tight junction proteins ZO-1 and E-cadherin. To investigate the pathogenicity of LESB58 on the diffCalu-3 infection model, the amount of actin and other two endogenous proteins HSP90 and NUP98 as well as proteins associated with barrier integrity were examined by reverse protein array. Actin and HSP90 remained intact in diffCalu-3 after LESB58 infection. However, substantial degradation of actin and HSP90 on diffCalu-3 cells infected with Wt was observed at 6 hpi. This result was consistent to previous findings described in Chapter 4.

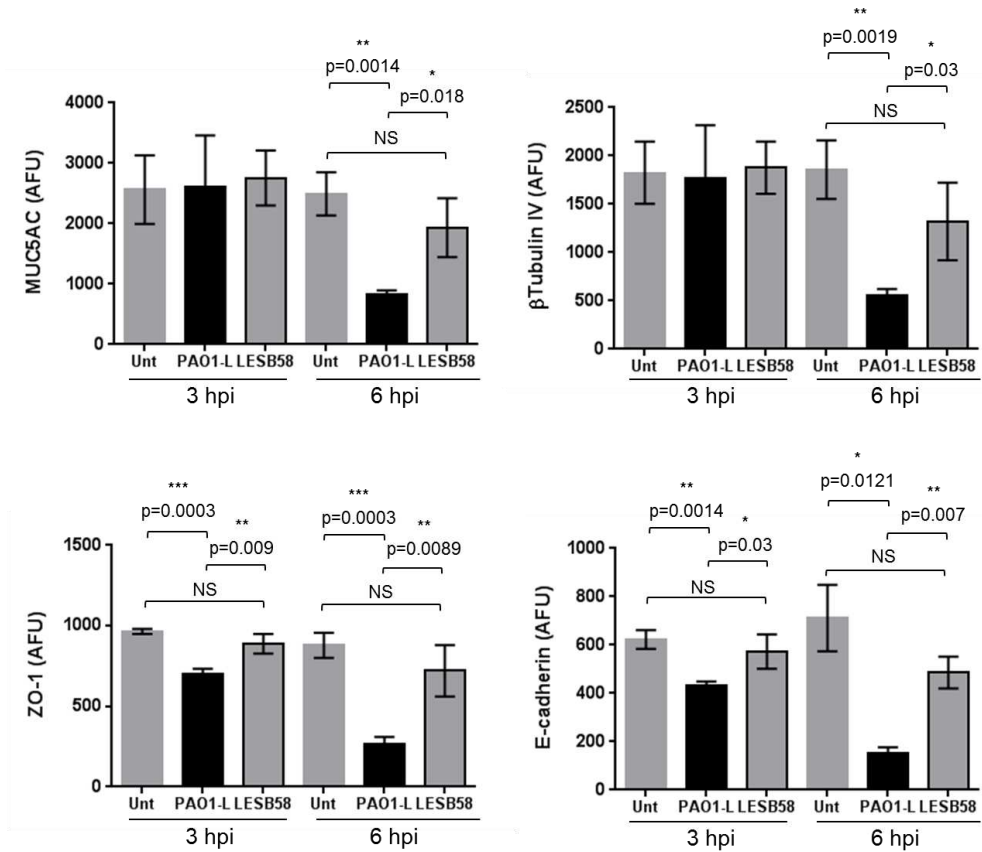
In Chapter 4, airway epithelial barrier function including the anti-microbial glycoprotein MUC5AC,  $\beta$ -tubulin-associated cilia that propel intruding pathogens away from the epithelium, and tight junction proteins that control the molecular passage to the basal compartment from the airway lumen were all readily disrupted by both PAO1-L Wt and its isogenic mutant  $\Delta pqsA_L$  as these effects could be detected at 3 hpi and a substantial degradation seen at 6 hpi (refer Fig. 4.14). These results suggested that Aqs might not directly

influence the loss of epithelial cell integrity. To understand whether LESB58, a strain that overproduces Aqs, could disturb the barrier function of diffCalu-3 cells, the levels of MUC5AC,  $\beta$ -tubulin, ZO-1 and E-cadherin were measured in LESB58 and PAO1-L infected cells. Surprisingly, compared to the substantial degradation of MUC5AC,  $\beta$ -tubulin, ZO-1 and E-cadherin in diffCalu-3 cells infected with PAO1-L, these proteins were largely maintained in diffCalu-3 cells upon LESB58 infection for 6 hpi (Fig. 5.6). In summary, LESB58 did not elicit actin degradation in diffCalu-3 cells until 6 hpi and only minimal degradation of mucin, tubulin and junctional proteins were observed.



**Figure 5.5 Calu-3 cells actin, HSP90 and NUP98 remained intact upon LESB58 infection at 6 hpi.**

Protein expression of endogenous proteins actin, HSP90 and NUP98 was analysed by protein microarray. At 6 hpi levels of actin and HSP90 were reduced in Wt-infected cells but not in LESB58-infected cells. NUP98 was maintained during the course of infection with Wt and LESB58. Each bar is the mean and SD from three independent experiments. Significance was assessed by un-paired t-test and \*p-value < 0.05 is considered significantly different. NS, not significant.



**Figure 5.6 The barrier function of Calu-3 cells was maintained after LESB58 infection compared to PAO1-L infection**

Whole cell lysates collected from Calu-3 cells infected with PAO1-L and LESB58 at 3 and 6 hpi were subjected to protein microarray analysis to examine the levels of tight junction proteins, mucins and cilia-associated tubulin. The above proteins remained intact after LESB58 infection. Each bar is the mean and SD from three independent experiments. Significance was assessed by un-paired t-test and \*p-value < 0.05 is considered significantly different. NS, not significant.

## 5.6. DISCUSSION

The establishment of an *in vitro* bronchial epithelial infection model aimed to generate a robust platform which can readily discern between virulent and non-virulent strains of *P. aeruginosa*. In this study, parameters including bacterial translocation, induction of inflammatory mediators, cytotoxicity and epithelial barrier integrity were used to evaluate the efficacy of the infection model, diffCalu-3 cell culture to determine differences in pathogenesis between a clinical CF isolate LESB58 and *P. aeruginosa* laboratory strain PAO1-L. We found that swarming motility and rhamnolipids production were reduced but PQS and pyocyanin were over-produced in LESB58 cultures *in vitro*. LESB58 was capable of growing on diffCalu-3 cells, barely crossed the epithelial barrier and caused relatively mild inflammation and no apparent cytotoxicity on diffCalu-3 cells compared to PAO1-L.

The cell density of LESB58 was lower in LB medium, although the growth kinetics was equivalent to that of *P. aeruginosa* strain PAO1-L and both strains reached stationary phase at the same time. However, the growth of PAO1-L and LESB58 was similar when cultured in X-vivo 15. This was in agreement with the finding that the growth of LESB58 *in vivo* was similar to that of PAO1 and PA14 in a rat chronic lung infection model (Kukavica-Ibrulj et al., 2008). This implies the growth of *P. aeruginosa* in X-vivo 15 medium might reflect more closely the growth in the host environment than LB medium. The growth of LESB58 on diffCalu-3 cells was always slightly less than the growth of PAO1-L although the change was within one-log difference. However, the capacity of LESB58 to attain less cell density compared with laboratory *P.*

aeruginosa strains correlated with a study demonstrated that the planktonic growth rates of *P. aeruginosa* CF isolates were significantly lower than non-CF strains (Salunkhe et al., 2005). LESB58 over-expressed PQS and pyocyanin compared to PAO1-L. The maximum amount of PQS and pyocyanin produced by LESB58 was 4 times higher than the amount produced by PAO1-L in LB cultures. We also noticed that the accumulation of PQS in the extracellular milieu in vitro was independent of the lower cell density in LESB58 strain. It has been demonstrated that AQS are substantially produced at late-logarithmic phase that overcomes the cell-dependent AHL-QS hierarchy (Diggle et al., 2003). In addition, AQS can also be produced in the absence of *lasR* and has been isolated in the bronchoalveolar lavage fluid and sputum in CF patients infected with *P. aeruginosa*. This supports the hypothesis that the continuous production of PQS might contribute to the persistence of *P. aeruginosa* in the CF lung (Collier et al., 2002, Guina et al., 2003). In addition, the prevalence of AQS in vivo also suggests that AQS promotes *P. aeruginosa* long-term colonisation in the CF lungs in a *LasR* QS-independent manner (Diggle et al., 2003). AQS controls the synthesis of phenazine, including pyocyanin and iodinin which perform diverse roles in *P. aeruginosa* physiology and act as virulence factors in CF. The genome of LESB58 contains two gene clusters encoding putative phenazine biosynthesis pathways orthologs of PAO1 *PhzA2-G2* and *phzB*, which probably have redundant roles (Winstanley et al., 2009). A recent study proposed that the redundancy in phenazine production can be considered an advantage for environmental adaptation. Production of phenazine mediated by *Phz1* or *Phz2* depended on the culture conditions (planktonic liquid culture vs biofilm aggregates) (Recinos et al., 2012). This

evidence again suggests that AQs may contribute to the environmental fitness and virulence of *P. aeruginosa*. The reduced motility on swarming agar plates of LESB58 was consistent with the observation that LESB58 remained tightly associated with the agar beads rather than invading the lung (Kukavica-Ibrulj et al., 2008). The lack of any form of motility can also be explained by the lack of flagella or pili at the surface of LESB58 based on electron microscopy analysis (Kukavica-Ibrulj et al., 2008, Winstanley et al., 2009). The redox-active exotoxin pyocyanin has been shown to induce mucin MUC2/MUC5AC secretion, lymphocytes infiltration, release of inflammatory cytokines and growth factors via the epidermal growth factor receptor (EGFR) pathway in mouse airways (Hao et al., 2012). CF clinical isolates display a pyocyanin over-production phenotype in vitro and the overproduction of pyocyanin correlated with pulmonary exacerbations (Fothergill et al., 2007, Caldwell et al., 2009). Therefore, we postulate that LESB58 could be more virulent than PAO1-L by producing 4 times higher levels of pyocyanin in vitro. Surprisingly, LESB58 exerted no significant cell damage and relatively lower activation of pro-inflammatory cytokines on diffCalu-3 cells compared to PAO1-L. Since pyocyanin is a secondary metabolite of *P. aeruginosa* produced at maximum amounts during late-logarithmic phase and has been recovered from chronic infected CF patients, it is possible that PAO1-L and LESB58 have not started producing pyocyanin within the 6 h infection time on diffCalu-3 cells. Moreover, the fact that AQs can be detected in culture supernatants (refer Chapter 4 Fig. 4.18) argues that the lack of AQs expression might not be responsible for these observations. The effect of pyocyanin on pathogenesis of strain PAO1-L and LESB58 in the acute infection model needs to be re-

evaluated. Previous studies to investigate the impact of pyocyanin on bronchial epithelial cells and animal models were conducted using purified pyocyanin rather than the whole viable bacteria; whether the effects identified reflect events that occur during infection with viable bacteria needs to be taken into consideration.

Infection of LESB58 on diffCalu-3 cells revealed an attenuated pattern of pathogenesis demonstrated by few to none bacterial transmigration, no actin and tight junction protein degradation up to 6 hpi, and relatively mild induction of inflammation compared to PAO1-L. Particularly, given the pleiotropic feature of IL-6, the preliminary data showed an enhanced IL-6 in the context of low TNF- $\alpha$  induced by LESB58 in bronchial epithelial cells might imply a different pattern of activation in human epithelium by CF isolates. These results were consistent with the data demonstrated by Carter et al. (Carter et al., 2010) in assessing the virulence of the CF LES subtypes in an acute murine infection model. Compared with the three other LES subtypes, LESB58 (QS-overproduction) was less virulent than subtype LES400 (QS-deficient) 96 h post respiratory acute infection in mice. However, LESB58 was shown rather to persist in the lung epithelium than cause drastic cell damage in a chronic rat infection model (Kukavica-Ibrulj et al., 2008). In the case report describing the infection of non-CF parents with an epidemic *P. aeruginosa* strain from their CF child, the mother who carries single allele  $\Delta$ F508 was referred to a microbiological screening of her sputum after 5-month of flu-like symptoms, chest pain, dramatic weight loss and production of 30 ml sputum per day. But no evident bronchiectasis was identified by computed tomography (CT) scan. A *P. aeruginosa* strain resistant to ceftazidime was identified in her sputum

later on. Although she was given intravenous antibiotics and discharged when her lung function was back to normal, the symptoms resumed in one month time and antibiotic resistant *P. aeruginosa* was continuously isolated from her sputum. The father with genotype G551D, however, was initially admitted to hospital because of pneumonia. He had a past history of right upper lobectomy and thoracoplasty because of bronchiectasis and no tuberculosis or *Pseudomonas* was isolated in the sputum in the past. This admission found lingula consolidation in the thoracoplasty part and two *Pseudomonas* strains resistant to ceftazidime were identified in the sputum. Despite receiving intravenous antibiotics and discharged when sputum was negative with microorganisms, resistant *Pseudomonas* was constantly isolated from his sputum afterwards and the patient seemed to develop chronic infections with mild bronchiectasis in his right lung (McCallum et al., 2002). Whilst the symptoms in the father could be explained by the lung susceptibility due to the disease in the past, more studies are required to understand how and why did the physically healthy mother also receive LES infection.

The LESB58 genome carries all the reported virulence genes of *P. aeruginosa* strain PAO1 located in the 'core genome' which comprised 90% of the genome such as type II and III secretion systems and iron transport as well as gene clusters involved in determining O-serotype, flagellin, type IV pili, siderophore production, genomic/ pathogenicity islands and prophages that compose the 'accessory genome' (Winstanley et al., 2009). The 'accessory clusters' that compose 10% of the genome may provide clinical isolates with the capability to adapt environmental changes that leads to strain diversity (Shen et al., 2006). Excluding the prophage shared between PAO1 and the other one commonly



appeared in *P. aeruginosa* epidemic strains, the rest of the four prophages have been studied for their potential to provide plasticity for environmental adaptation that makes LES the dominant transmissible CF strain. It has also been suggested that the horizontal transfer of prophages and the integrase/transposase-driven plasticity contribute to the bacterial genomic evolution.

The introduction of a clinical CF isolate to the diffCalu-3 epithelial culture provided us with a new understanding of the patterns of pathogenesis employed by *P. aeruginosa*. Loss of motility organelles flagellum and type IV pili restrict LESB58 colonisation of the airway epithelium but in turn, LESB58 might evade the recognition of flagellin by TLR5 in the epithelial cells leading to no subsequent NF- $\kappa$ B signalling and no production and release of proinflammatory cytokines that could recruit neutrophils to the infected area. LESB58 shows mild infectivity which in turn could represent its strength by favouring the establishment of biofilms for long-term persistence in the lung.

The results were based on the experiments conducted on a CFTR competent epithelial cell line Calu-3 cells. CFTR deficient epithelium has been shown to be hyper-inflammatory although the claim remains controversial (Machen, 2006). It needs to be clarified how the innate immune system responds to LESB58 infection in the absence of a functional CFTR. Tissue models such as CFTR knock-out cell lines, primary or immortalised CF bronchial epithelial cells or CF animal models are available (porcine CF lung (Stoltz et al., 2010, Pezzulo et al., 2012) for instance is the closest to a human CF model) and can be applied for studying the mechanism of LESB58 pathogenicity. In addition, the culture condition for LESB58 may also be adjusted to resemble the

environment in CF lung by using artificial sputum medium (Sriramulu et al., 2005, Kirchner et al., 2012). *P. aeruginosa* in the form of microcolonies or biofilm is an important element to consider in the infection of CF lung. Studies to target biofilms by inducing biofilm dispersal or blocking biofilm formation suggest that this is a plausible therapeutic target (Majik and Parvatkar, 2013, Sharma et al., 2013, Wei and Ma, 2013). Inoculation of biofilm matrix developed by embedding *P. aeruginosa* in homogeneous agarose beads (50-500  $\mu\text{m}$  diameter) or porous beads containing pores (260  $\mu\text{m}$  diameter) (Strathmann et al., 2000) can be an alternative to study the virulence in the form of bacterial aggregates shown in CF lung; meanwhile, this method may overcome the issue of low cell density of LESB58 in the planktonic liquid culture.

In the present study, diffCalu-3 cells stand as a robust bronchial epithelial model by demonstrating the expression of tight junction proteins, exhibition of polarity with apical cilia-like protrusions and the induction of an inflammatory response upon *P. aeruginosa* infection. DiffCalu-3 culture is a suitable model demonstrated for a reliable and consistent preliminary evaluation of *P. aeruginosa* pathogenicity. However, due to the plasticity and complex phenotype of *P. aeruginosa*, more complex models containing professional immune cells, animal models or 3-dimensional multiple cell culture systems (Barrila et al., 2010) can be developed to address this research question.

## **5.7. SUMMARY**

The clinical CF isolate *P. aeruginosa* LESB58 displayed reduced motility but over-produced AQS and pyocyanin compared with *P. aeruginosa* PAO1-L. LESB58 elicited minor cell damage and mild activation of pro-inflammatory response in diffCalu-3 cells in comparison with PAO1-L.

## **6. SYSTEMIC IMMUNE RESPONSES IN IDIOPATHIC PULMONARY FIBROSIS**

---

### **6.1. INTRODUCTION**

This chapter on the systemic immune responses in patients with idiopathic pulmonary fibrosis (IPF) was initiated as a side project to a study on the analysis of the association between thrombophilia and the tendency to develop IPF. This study identified a strong association between the presence of a prothrombotic state and clinical disease in IPF (Navaratnam et al., 2013). The pathogenesis of IPF is widely considered to be caused by the inability of type II alveolar epithelial cells to restore pulmonary tissue after continuous microinjuries rather than an inflammation-driven disease. However macrophage polarization has been also shown to be critical in disease progression (Homer et al., 2011, Wynn and Barron, 2010). We postulated that inherent differences in immune status between diseased and healthy donors might contribute to the progressive pulmonary fibrosis whereas the role of chronic inflammation in IPF remains elusive.

In this exploratory study, we aimed to determine the cytokine profiles of peripheral blood mononuclear cells (PBMCs) from healthy individuals and patients with IPF. PBMCs were isolated from the blood pellets once sera had been preserved for the thrombophilia study. PBMCs were stimulated with a panel of stimuli including a mitogen, a superantigen, canonical Th1 and Th2

primers and a crude extract of *P. aeruginosa* in an attempt to obtain an immune response profile in an unbiased but comprehensive manner. Additionally, access to a large population cohort was one of the strengths of this study as correlations with clinical outcomes could be established in an attempt to identify potential prognostic biomarkers.

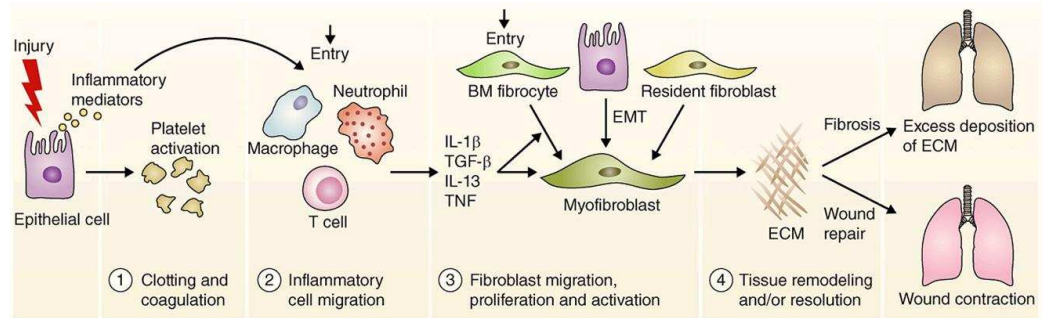
The following introduction addresses the conceptual molecular mechanisms in pathogenesis together with current hypotheses on the role of inflammation and potential biomarkers in IPF that constituted the basis for the rationale of our study.

#### **6.1.1. Pathogenesis and molecular mechanisms of IPF**

Interstitial lung diseases (ILDs), categorised as known and unknown causes, are initially triggered by an inflammatory response but followed by an impaired repair process of epithelial cells that result in fibroblast proliferation, collagen deposition and destruction of lung architecture and function (Jakubzick et al., 2004, Noble et al., 2012). Idiopathic pulmonary fibrosis (IPF) is the most common form of idiopathic interstitial pneumonia that characterised by heterogeneously thickened, stiff, and scarring tissue in the lung. IPF is a devastating fatal disease, median survival is merely 2 to 3 years following diagnosis in populations above 40 years and the mean age is 66 (Meltzer and Noble, 2008). People with IPF usually suffer from chronic dyspnoea and cough due to the limited lung capacity for gas-exchange. IPF prevalence estimated in Europe has risen to 23.4 cases per 100,000 populations according to reliable data from 2005 till 2011. The annual incidence in Europe ranged between 0.22 and 7.4 per 100,000 population and the incidence of IPF clinical symptom in

primary care is from 5.10 to 7.44 per 100,000 person-years in United Kingdoms (Navaratnam et al., 2011, Nalysnyk et al., 2012). The prevalence in men is 1.5 fold higher than women (Hoo and Whyte, 2012). Difficult to diagnose, aggressive progression with random exacerbations, and poor prognosis are the problems underlying the disease waiting to be solved. No effective treatment is available and the aetiology remains unclear (King et al., 2011).

Currently IPF pathogenesis is thought to be initiated by the aberrant activation of alveolar epithelial cells caused by recurrent environmental microinjuries in the ageing, susceptible lung. Upon activation resident epithelial cells and fibroblasts differentiate into mesenchymal cells. Exaggerated activation of epithelial-mesenchymal transition (EMT) thereby induces the migration of resident fibroblasts and bone marrow-derived progenitor cells fibrocytes and the production of extracellular matrix at the sites of microinjuries (King et al., 2011, Meltzer and Noble, 2008). IPF patients eventually succumb to respiratory failure due to the accumulation of extracellular matrix in the gas-exchanging region. The deregulated regeneration, proliferation and migration of epithelial cells exhaust the airway remodelling process and develop fibroblast foci heterogeneously distributed in the so-called honeycomb-like lung (Hoo and Whyte, 2012). Recent evidence indicates that environmental insults and genetic predisposition contribute to the pathogenesis of IPF. Cigarette smoking, viral infection or occupational exposure to microaspiration such as metal dust, wood dust, farming, hairdressing, and stone cutting are associated to the development of IPF (Odds ratio ranges from 1.7 to 4.4) (Steele and Schwartz, 2013).



**Figure 6.1 Dysregulation in wound healing contributes to pulmonary fibrosis.**

The four stages of wound healing: (1) clotting, (2) infiltration of inflammatory cells, (3) fibroblast migration, proliferation and activation to myofibroblast and (4) tissue remodelling (Wynn, 2011).

The continuous apoptosis of progenitor cells AECII (Barkauskas et al., 2013b) failing to regenerate type I alveolar epithelial cells upon injury may ultimately lead to persistent pulmonary fibrosis (Noble et al., 2012, Steele and Schwartz, 2013). Mutations in telomerase (gene TERT/hTR) have been identified in familial IPF and shorten telomeres have been identified in sporadic cases of IPF. Single nucleotide polymorphisms (SNPs) in mucin 5B (gene MUC5B) result in over-expression of mucin by bronchial epithelial cells has also been found common to both familial and sporadic IPF. However, the underlying mechanisms need to be determined of how the genetic variants and overproduction of mucin 5B lead to pulmonary fibrosis.

Mediators involved in the regulation of epithelial-mesenchymal crosstalk such as activin, bone morphogenetic protein 4 (BMP4) and BMP7, TGF- $\beta$ 1, Wnt/ $\beta$ -catenin and sonic hedgehog (Shh) belong to TGF- $\beta$  morphogenic cytokine family. Activation of TGF- $\beta$  by alveolar macrophages has been implicated a critical promoter for fibrogenesis; the up-regulation of integrin  $\alpha$ v $\beta$ 6 on the epithelium is required for the activation of latent TGF- $\beta$  (Bringardner et al., 2008, Noble et al., 2012).

### **6.1.2. The immunology of IPF**

Inflammation is considered the secondary feature in IPF. The fact that (a) no substantial infiltration of immune cells occurs in the IPF lung, (b) no histological differences have been found between early and late stage IPF lungs, and (c) failure of conventional immunosuppression treatments, suggest that inflammation may not be critical for disease progression (Bringardner et al., 2008, Homer et al., 2011). However, a novel hypothesis suggests that macrophage interference in the wound-healing process might account for the atypical inflammation in the IPF lung (Homer et al., 2011).

Difficulties in diagnosis due to the heterogeneity of the IPF lung prompted the study of biomarkers. An ideal biomarker should be able to distinguish IPF from other interstitial lung diseases to provide early diagnosis and predict disease prognosis (Bargagli et al., 2011, Richards et al., 2012, Vij and Noth, 2012). SP-A is a lipoprotein secreted by club (Clara) cells and type II alveolar epithelial cells. The levels of SP-A in the BAL fluid of IPF patients were significantly lower compared with healthy controls, whereas the effect was inverse when SP-A was identified in serum. Glycoprotein Krebs von den lungen-6 antigen (KL-6) expressed by type II alveolar epithelial and bronchial epithelial cells acts as a chemotactic factor that promotes migration and proliferation of lung fibroblast is at significantly higher levels in serum and BAL fluid of IPF patients compared to healthy populations. Levels of macrophage-derived chemoattractant proteins such as CCL18, IL-8, CCL2, S100A9; matrix metalloprotease 1 and 7, and the proinflammatory cytokine osteopontin, correlated with lung functions in IPF patients. These molecules were identified



in serum and/or BAL and are considered as potential biomarkers (van den Blink et al., 2010, Bargagli et al., 2011, Vij and Noth, 2012). However, all above biomarkers have their limitations; some of the biomarkers cannot differentiate IPF from other interstitial lung diseases; patients in some studies were immunosuppressed as a result of corticosteroid treatment which might bias the study. The present study was initiated with the aim to identify a potential cytokine profile that could distinguish between IPF patients and healthy controls.

### **6.1.3. Rationale of experimental design**

Agents such as bleomycin, silica asbestos, and irradiation using different administration methods have generated numerous animal models of pulmonary fibrosis with different inflammatory profiles. Despite the animal models provide a plethora of information to ‘known cause’ pulmonary fibrosis for humans including bleomycin induced lung fibrosis models, growth factor gene overexpression (TGF- $\beta$ , IL-1 $\beta$ , IL-13, etc.), irradiation and particle irritation models such as asbestos, silica, etc. (Gharaee-Kermani et al., 2005, Degryse and Lawson, 2011, B et al., 2013), none of them can fully recapitulate the phenotype of patients with IPF. Human PBMCs which contain 70% T lymphocyte, up to 25% monocyte/macrophage and dendritic cells are widely used to assess the individual immune condition in health and disease. The availability of a large clinical cohort to investigate the response of PBMCs to stimulation is one of the strengths of this study. The strategy we employed was to assess the systemic immune status in IPF patients compared with normal controls through the use of non-specific antigens such as mitogen and

superantigen, Th1, Th2 primers as well as *P. aeruginosa*-crude extract. Phytohaemagglutinin (PHA) is a plant lectin that induces polyclonal proliferation of T lymphocytes and monocytes (Mire-Sluis et al., 1987, Christmas et al., 2006). The preparation of PHA used in this study was a crude sodium chloride extract of the red kidney bean *Phaseolus vulgaris*. The efficacy of this crude extract was tested prior to our study and was found to induce proliferation of more than 90% of CD4<sup>+</sup> T cells in healthy control PBMCs (Singh, 2012). Both monocytes/macrophages and T cells in PBMCs upon PHA stimulation would contribute to cytokine production. Superantigens (SAGs) such as Streptococcal exotoxin B (SEB) are immuno-stimulatory molecules that cross-link host MHC class II and the T cell receptor that activate up to 25-40% of T cells in the body. The trimolecular complex triggers the protein kinase C pathway and the protein tyrosine kinase pathways resulting in profound non-specific T-cell proliferation and release of pro-inflammatory cytokines (Baker and Acharya, 2004, Sriskandan et al., 2007, Balaban and Rasooly, 2000). Mycobacterium tuberculosis purified protein derivative (PPD) induces the secretion of IFN- $\gamma$  by PBMCs (Dockrell et al., 1996) and house dust mite (HDM) induces allergen-specific CD4<sup>+</sup> Th2 cells that orchestrate the allergic response via induction of IgE (Wang, 2013). In addition to extend our general interest in the recognition of *P. aeruginosa* by immune cells, *P. aeruginosa* PAO1-L crude extract (PA extract) was also included as one of the stimuli. 12-O-phorbol-myristic-13-acetate (PMA), a mitogen that strongly activates protein kinase C, was added at day 6 to promote the overall cytokine production by PBMCs (Blumberg, 1988, Han et al., 1998, Chang et al., 2005). PBMC supernatants harvested on Day 7 were assayed for

the presence of a panel of cytokines which would reflect the action of activated T cells and monocytes/ macrophages.

## **6.2. HYPOTHESIS**

The fibrotic process in the lung of IPF patients is associated with a skewed immune response and presence of type 2 alternatively activated macrophages.

## **6.3. AIM**

The purpose of this study was to examine systematically the immunological status of IPF patients in attempt of discovering potential prognostic biomarkers. To achieve this, the levels of selected cytokines representing Th1 (IFN- $\gamma$ ), Th2 (IL-13), anti-inflammatory (IL-10) and Th17 (IL-17A) responses produced by PBMCs from IPF patients and healthy populations in response to mitogen, super antigen, Th1 and Th2 inducers and *P. aeruginosa* crude extract were quantified. We then conducted a case-control study using this cytokine profile to investigate the association between cytokine production and IPF disease, and whether the levels of cytokine production related to mortality in IPF patients.

## **6.4. MATERIALS AND METHODS**

### **6.4.1. Study design**

The study was initiated as a side study from a project of assessing the risk of the presence of thrombophilia in the development of IPF in the East-midlands region in UK (funded by Medical Research Council) to identify potential biomarkers. Blood sources and ethics were obtained before starting this study.

### **6.4.2. Study populations**

In the first cohort, blood pellets (plasma removed) were collected from 38 healthy donors (9 females and 29 males) and 34 diseased (9 females and 25 males) with clinical data available; the second cohort made it total populations of 66 healthy subjects (15 females and 51 males) and 66 cases (19 females and 47 males). The age of subjects in both populations were grouped in 6 categories: those less than 65 years old; 65-69 years old; 70-74 years old; 75-79 years old; 80-84 years old and those more than 85 years old (Table 6.2 and Table 6.7). Clinical data including lung functions and survival were available.

### **6.4.3. Determination the levels of IFN- $\gamma$ , IL-17A, IL-10, and IL-13 in peripheral blood mononuclear cells (PBMCs) supernatant by multiplex immunoassays**

#### **6.4.3.1. Isolation of PBMCs from IPF patients and healthy controls**

Whole blood samples were obtained from the cohort of IPF patients and healthy controls in the Trent Lung Fibrosis Study. Blood cell pellets from four

to seven anti-coagulant 10-ml EDTA vacutainers (BD Diagnostics-Preanalytical Systems, UK) collected either from IPF patients or healthy controls were pooled in a 50-ml falcon tube, diluted with Hanks' balanced salt solution (modified with NaHCO<sub>3</sub>, without CaCl<sub>2</sub> and MgSO<sub>4</sub>) (Sigma-Aldrich, UK) up to 35 ml. Diluted blood was layered on 12 ml of Histopaque-1077 (Sigma-Aldrich, UK) and centrifuged at 800xg for 30 min at room temperature with low acceleration and deceleration. The PBMCs layer appeared as a yellow interface after density gradient separation was collected and washed in Hanks' balanced salt solution and re-suspended in RPMI (Sigma-Aldrich, UK) containing 10% of human AB serum (Sigma-Aldrich, UK) and antibiotics 100 U/ml Penicillin/100 µg/ml Streptomycin (Sigma-Aldrich, UK).

#### 6.4.3.2. PBMCs stimulation

PBMCs were plated on 96 round bottom plates at a density of 200,000 cells per well in 100 µl RPMI-10% AB serum and stimulated in duplicate with 2 µl of phytohaemoagglutinin (PHA) (Invitrogen, UK), 10 ng/ml of Staphylococcus enterotoxin B (SEB) (Sigma-Aldrich, UK), 2 µg/ml of the Th1 primer, Mycobacterium tuberculosis purified protein derivative (PPD) (Statens Serum Institut, DK) and 10 µg/ml of the Th2 primer house dust mite extract (HDM) (Greer allergy immunotherapy, US). In order to compare the cytokine expression with those from cystic fibrosis patients, two independent preparation of *P. aeruginosa* PAO1-L (6,250 ng/ml) crude extract from 3-hour cultures (PA extract) were also included in this assay (PAO1-L lysates were provided by Sonali Singh). High concentrations of PA extracts 6,250 ng/ml and 1,562 ng/ml, and low concentrations 97.7 ng/ml and 24.4 ng/ml were initially

tested (Fig. 6.1, marked as PA11-PA14, representing PA extract preparation 1 at four concentrations from high to low; likewise, PA21-PA24 represented PA extract preparations 2 at four concentrations). At day 6, PBMCs cultures were re-stimulated with phorbol 12-myristic 13-acetate (PMA) (Sigma-Aldrich, UK) at a concentration of 15 ng/ml and incubated at 37°C, CO<sub>2</sub> for another 24 h. At day 7, PBMCs supernatants were collected and stored at -80°C until to cytokine analysis.

#### 6.4.3.3. Cytokine quantification

Simultaneous quantification of the level of cytokines in PBMCs supernatants was done using the bead-based immunoassay FlowCytomix Simplex kit in combination with FlowCytomix human Basic kit (eBioscience, UK) according to the manual. Samples were analysed by flow cytometry using the software FlowCytomix Pro provided by eBioscience.

#### 6.4.4. Statistical analysis

Before conducting logistic regression to generate odds ratio (ORs) for evaluating the association between IPF and a particular cytokine response, the levels of cytokine were grouped into composite binary variables low response and high response. Logistic regression was used to generate ORs for the association between the levels of cytokine and IPF adjusted for age and sex. The association between categorical data were assessed by  $\chi^2$  test. Cox regression modelling was used to investigate whether the levels of cytokines were associated with mortality in IPF patients. The date participants gave consent to enter the study was considered as the 'start date', and the date of

death or last data collection as the 'stop date'. Prism Version 6.0 (GraphPad Software) and Stata version 11.0 (Texas) were used for statistical analyses and hypothesis testing.



## 6.5. RESULTS

### 6.5.1. Optimisation of PBMCs stimulation

To understand the systemic immune status of IPF patients PBMCs isolated from IPF patients and healthy controls (age and sex matched) were treated with a panel of stimuli including PHA, SEB, Mycobacteria tuberculosis purified protein derivative (PPD), a Th1 response primer (Dockrell et al., 1996), house dust mite (HDM) that promotes a Th2-biased allergic response (Wang, 2013) and PA extract. Th1 Th2, Th17 responses were evaluated by quantifying the levels of IFN- $\gamma$  (Th1 response), IL-17 (Th17 response), IL-13 (Th2 response) and IL-10 (anti-inflammatory response). Meanwhile, to investigate if PBMCs from IPF patients and age-matched healthy control are responsive to *P. aeruginosa*, PBMCs treated with *P. aeruginosa* whole cell crude extracts (PA extracts) were also included in the cytokine profile study. To determine the concentration of PPD and HDM required for stimulating PBMCs, 5-fold serial dilutions from 10  $\mu\text{g/ml}$  to 0.08  $\mu\text{g/ml}$  were tested (Fig. 6.1). High concentrations of PA extracts 6,250 ng/ ml and 1,562 ng/ ml, and low concentrations 97.7 ng/ ml and 24.4 ng/ml were also included (marked as PA11-PA14, representing the first prep of PA extract at four concentrations from high to low; likewise, PA21-PA24 represented the second prep of PA extract at four concentrations). PBMCs isolated from two healthy subjects and two IPF patients and the cytokines IFN- $\gamma$ , IL-10, IL-13 and IL-17A were included in the quantification. The results indicated the levels of IFN- $\gamma$  in PBMCs upon PPD and HDM stimulation were dose-dependent (Fig. 6.1 IFN- $\gamma$ ). Considering that readings needed to be within the linear scale of the assay,

concentrations of 2 µg/ml for PPD and 10 µg/ml for HDM were chosen to stimulate PBMCs in the following assays. Likewise, in order to obtain readable values of cytokine production, the concentration of 6,250 ng/ml of PA extracts was used for stimulation.

### **6.5.2. Comparison of the cytokine profile between IPF patients and healthy donors**

To investigate the cytokine profile of patients with IPF, levels of IFN- $\gamma$ , IL-17A, IL-10 and IL-13 in the supernatants of PBMCs from 39 healthy donors (HD) and 38 IPF patients (IPF) stimulated with mitogen, superantigen, Th1 and Th2 primers and PA extract were quantified and plotted. Fig. 6.3 shows that the levels of IFN- $\gamma$  were significantly higher in PBMCs treated with PPD (Th1 primer) than in cultures treated with the Th2 primer HDM ( $p < 0.0001$ ); same effect was observed in the supernatant of PBMCs in IPF patients ( $p = 0.0053$ ). This indicated that PPD indeed induced the release of higher amounts of IFN- $\gamma$  than HDM which is a Th2 inducer. Levels of IL-10 in PBMCs upon HDM stimulation were significantly higher ( $p = 0.0209$  in HD samples) than in those treated with PPD (Fig. 6.3).

Secretion of IFN- $\gamma$  by both IPF patients and healthy controls PBMCs was substantially induced upon non-specific stimulation with PHA and SEB with half of the participants producing IFN- $\gamma$  levels above the detection limit of the assay (20,000 pg/ml). No significant differences in the levels of IFN- $\gamma$  between HD and IPF were identified. The levels of IL-17A in PBMCs treated with PHA were marginally significantly ( $p = 0.0461$ ) higher in IPF patients than in healthy individuals. On the contrary, the levels of IL-10 in PBMCs treated with PMA

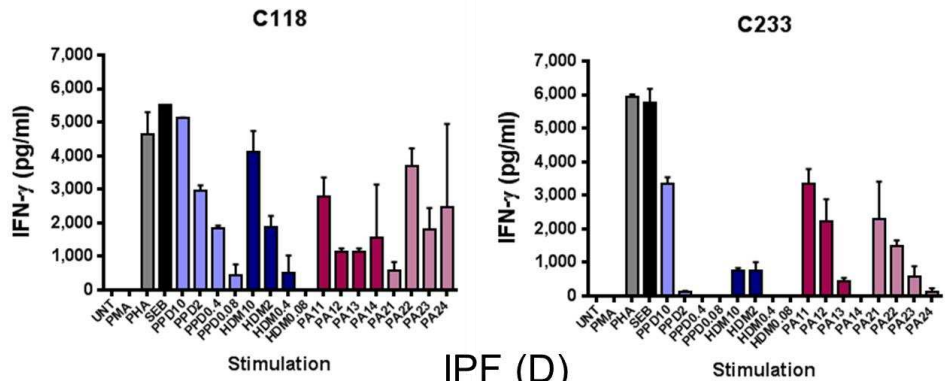
were significantly lower ( $p=0.0003$ ) in IPF patients than healthy controls (Fig. 6.3). Levels of IL-17A in PBMCs treated with PA extract were also significantly lower ( $p=0.0246$ ) in IPF patients than in healthy controls. However, the levels of IFN- $\gamma$ , IL-17A, IL-10 and IL-13 in PBMCs of IPF patients and healthy donors in response to the other stimuli were comparable. Thus, no pattern of immune response could be identified when differences in cytokine production between patients with IPF and healthy controls were assessed by comparing the mean of cytokine levels from all participants using an un-paired t-test.

**Table 6.1 Significant cytokine production difference between treatments or between the cases and healthy donors**

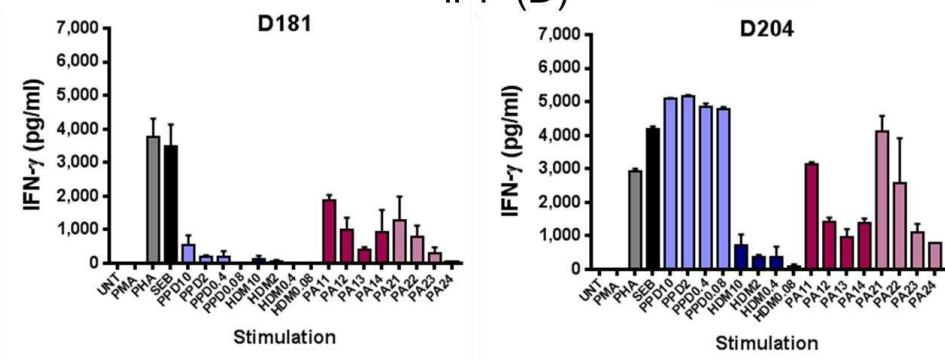
Cytokine	Stimulus	Comparison between the Th1 and Th2 stimulation	<i>P</i> -value
IFN- $\gamma$	PPD <i>versus</i> HDM	Production upon PPD > production upon HDM	0.0001 (HD) 0.0053 (IPF)
Cytokine	Stimulus	Comparison between IPF and HD	<i>P</i> -value
IL-17A	PHA	IPF > HD	0.0481
IL-17A	PA	IPF < HD	0.0246
Cytokine	Stimulus	Comparison between IPF and HD	<i>P</i> -value
IL-10	PHA	IPF < HD	0.0003
Cytokine	Stimulus	Comparison between the Th1 and Th2 stimulation	<i>P</i> -value
IL-10	PPD <i>versus</i> HDM	Production upon PPD < production upon HDM	0.0209 (HD)

IFN- $\gamma$

HD (C)

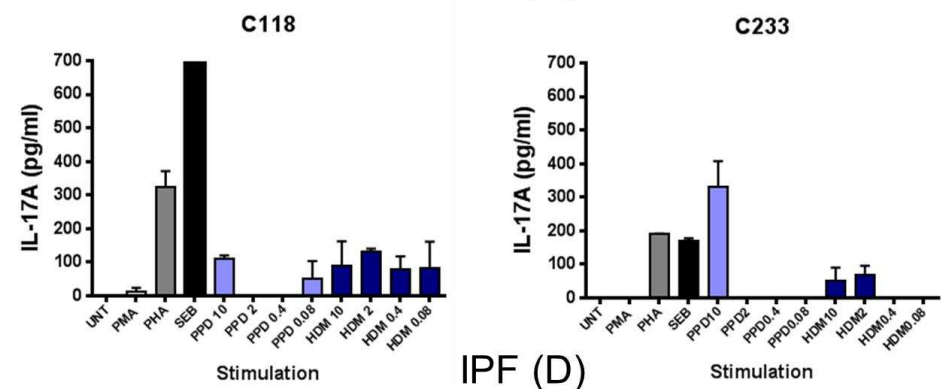


IPF (D)

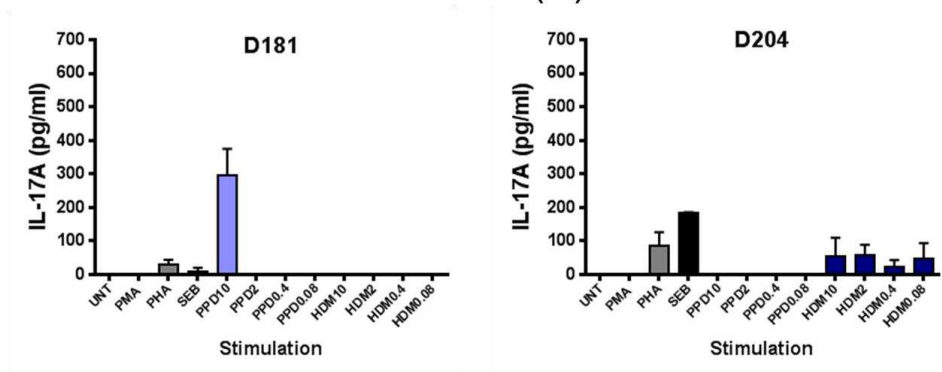


IL-17A

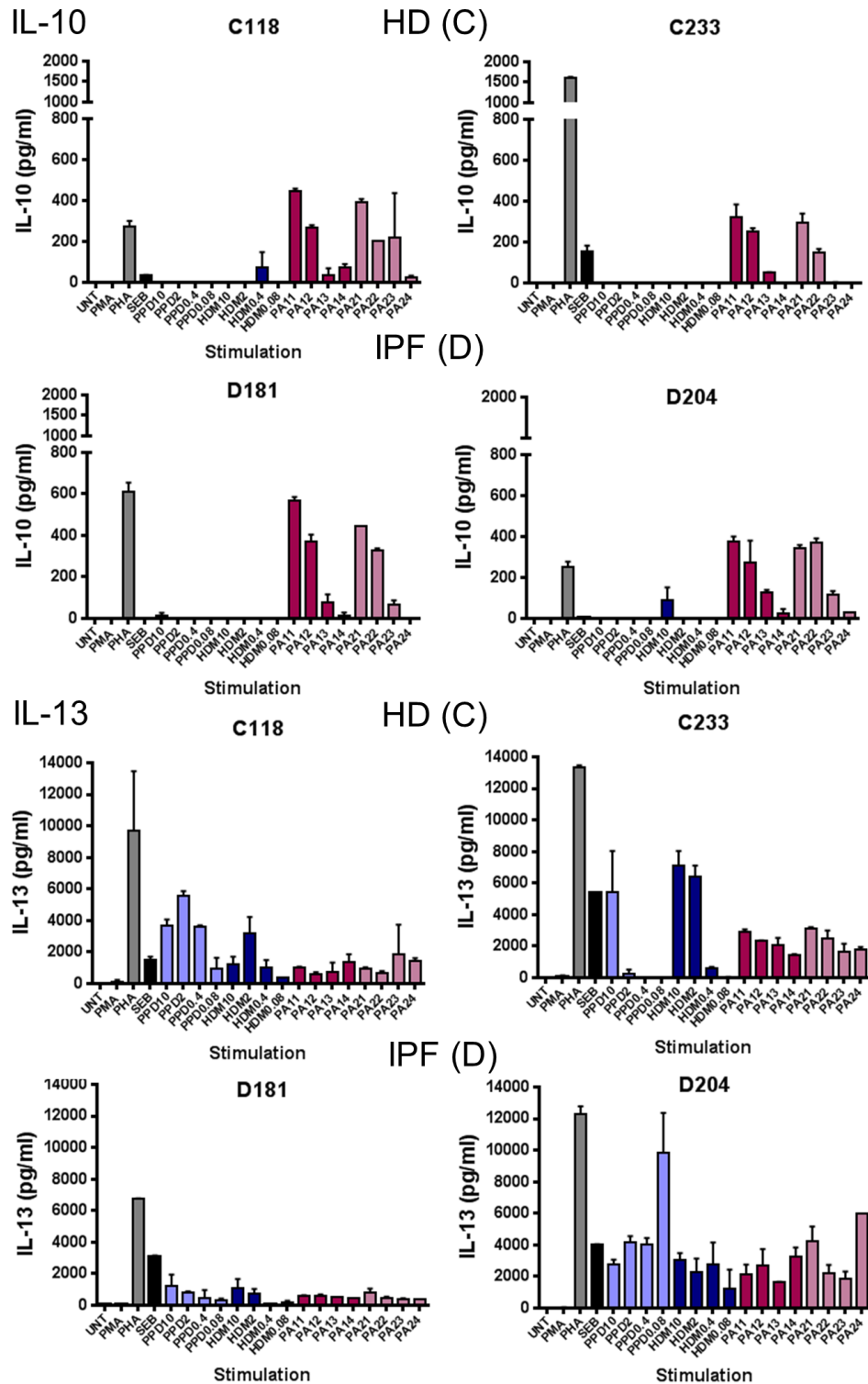
HD (C)



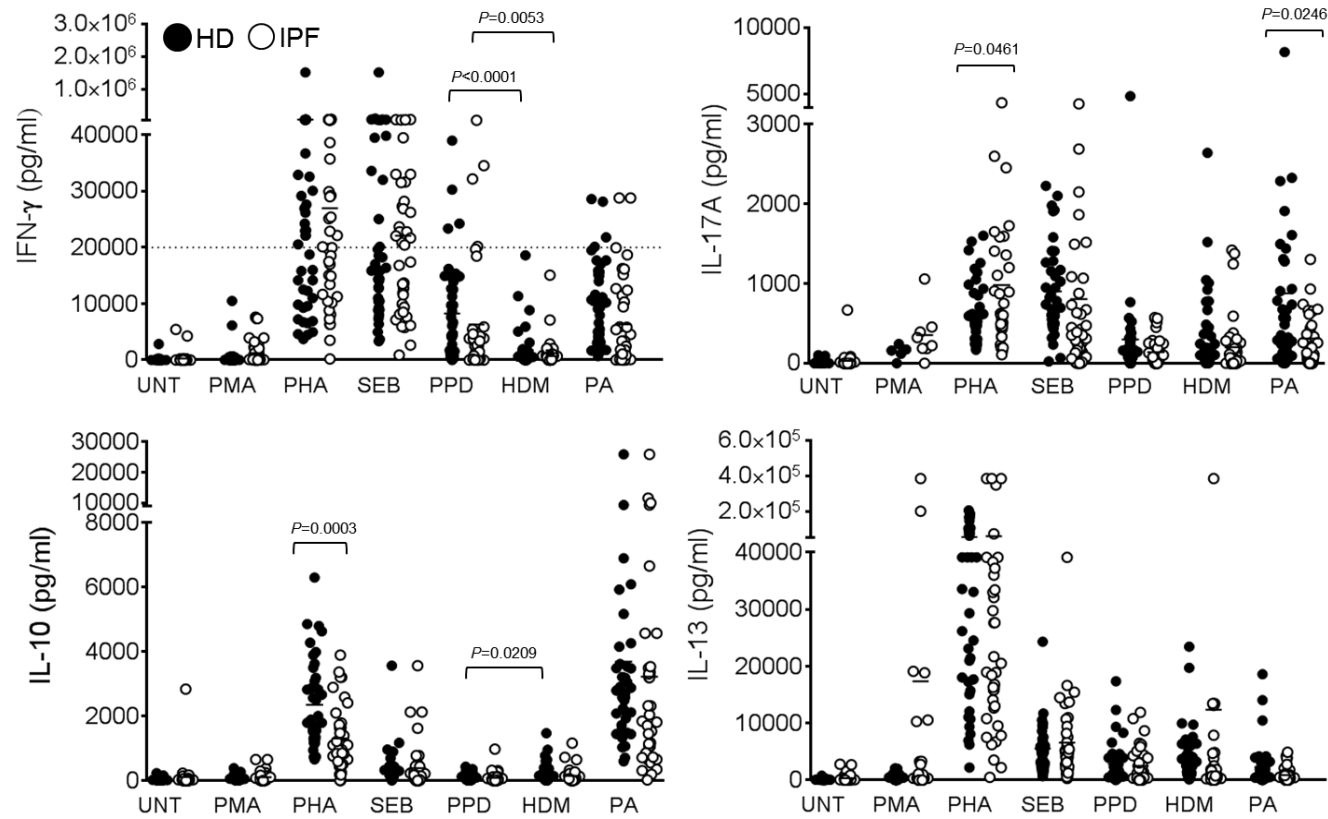
IPF (D)



(continued)



**Figure 6.2** The levels of cytokines, IFN- $\gamma$ , IL-17A, IL-10 and IL-13 secreted by PBMCs in response to PPD, HDM and PA01-L lysates were mostly dose dependent. PBMCs from two healthy controls (C118 and C233) and two IPF patients (D181 and D204) were stimulated with serial 5-fold dilutions of PPD, HDM from 10  $\mu\text{g/ml}$  to 0.08  $\mu\text{g/ml}$  and PA extracts at high concentrations 6250 ng/ml and 1562 ng/ml (PA11 and PA12; PA21 and PA22), and low concentrations 97.7 and 24.4 ng/ml (PA13 and PA14; PA23 and PA24). PBMCs supernatants from above treatments were subjected to cytokine quantification.



**Figure 6.3 Levels of IFN- $\gamma$ , IL-17A, IL-10 and IL-13 in PBMCs from healthy donors (HD) and IPF patients (IPF) in response to a panel of stimuli.**

The levels of cytokines IFN- $\gamma$ , IL-17A, IL-10 and IL-13 in PBMCs isolated from IPF patients (white circles) and healthy donors (black circles) in response to a panel of stimuli, including mitogen PMA, PHA, super antigen SEB, PPD and HDM as Th1 and Th2 inducers respectively and PA crude extract. PBMCs treated with PPD secreted significantly higher levels of IFN- $\gamma$  than when treated with HDM as expected. This occurred in healthy controls and IPF patients, implying that this assay was working as expected in both populations. PBMCs from IPF patients produced more IL-17A than HD in response to PHA stimulation, whilst PBMCs from IPF patients produced less IL-10 under the same stimulation. However, no significant differences were achieved between IPF patients and HD in PBMCs IL-13 production upon any stimulation. The dashed line at 20,000 pg/ml in IFN- $\gamma$  graph indicated that those readings above 20,000 pg/ml were beyond the linear detection range (20 - 20,000 pg/ml) when samples were not yet diluted.

### **6.5.3. Case-control study: the association between IPF and the cytokine production**

In this section, a case-control study method was introduced to investigate whether there is any association between cytokine profile and IPF. For this end, demographic features between the healthy donors and IPF patients should have been taken into consideration as matching factors before recruiting the study cohort. Demographic features from the first half participants (in Section 6.5.2.) including 38 controls (one clinical data set was missing) and 34 patients with IPF (5 missing clinical data) are listed in Table 6.2. Due to the collection of clinical data were attributed to the efforts made by research nurses and clinical scientists in the city hospital, University of Nottingham, the missing data could be the volunteers dropped out from the clinic for unforeseen reasons or the inevitable generic data handling error given this was a collaborative study. However, the majority of data were kept synchronised in both sides (clinical and laboratory). The mean age was  $70.7 \pm 10.3$  years for the cases,  $69.3 \pm 9.8$  years for the controls and the cases were predominantly male (9 females and 25 males). Men were therefore predominantly recruited in healthy donors (9 females and 29 males) to match with cases. The numbers in each smoking habit groupings between cases and controls also matched. The levels of highly sensitive C-reactive protein (hsCRP) were grouped as low (less than 1 mg/ml), intermediate (between 1-3 mg/ml) and high (more than 3 mg/ml). hsCRP is commonly used in clinic to assess the risk of developing cardiovascular disease. Numbers of cases with high levels of hsCRP were more than in healthy controls. The cases were 3 times (odds ratio (OR) 2.97, 95% CI 0.51-17.28)

more likely to have intermediate levels of hsCRP than the controls; 16 times (OR 16.04, 94% CI 2.75-93.57,  $p < 0.002$ ) more likely to have high levels hsCRP than the controls after adjusting for age category and sex.

In a case-control study, logistic regression is the method to generate odds ratio (OR). OR works as an indicator that describes the association between the response and the exposure. The response in this study was the disease outcome, IPF; the exposure was one of the cytokines measured in this assay. Cytokines including IFN- $\gamma$ , IL-17A, IL-10 and IL-13 produced by PBMCs in response to different stimuli were assessed individually. For OR above 1 means an increased tendency of disease associated with exposure (cytokine production) and OR less than 1 indicates a decreased tendency of disease associated with exposure. The levels of cytokine production were divided into two groups: high response and low response using 'binary quantize method' in Stata. Numbers of patients and healthy donors corresponded to high levels or low levels of cytokine were segregated in comparable numbers using the same method (refer to Table 6.3 – Table 6.6 for detail).

Table 6.3 showed that cases (IPF patients) were 1.5 times more likely to produce IFN- $\gamma$  in than the controls when PBMCs were treated with PMA (OR 1.55, 95% confidence interval (CI) 0.61-3.97) and SEB (OR 1.53, 95% CI 0.60-3.90). When PBMCs were treated with PPD and PA extract, IPF patients were 60% less likely to produce IFN- $\gamma$  than the controls (OR 0.42, 95% CI 0.15-1.16; OR 0.34, 95% CI 0.12-0.96), whereas secretions of IFN- $\gamma$  in IPF patients and controls were comparable when PBMCs were treated with PHA (OR 0.99, 95% CI 0.39-2.51) and HDM (OR 1.08, 95% CI 0.40-2.93)



stimulation. ORs were adjusted for sex and age category. Fig. 6.3 summarised the ORs and 95% CI. However, none of the associations between IFN- $\gamma$  production by PBMCs in response to any stimuli and IPF were significant.

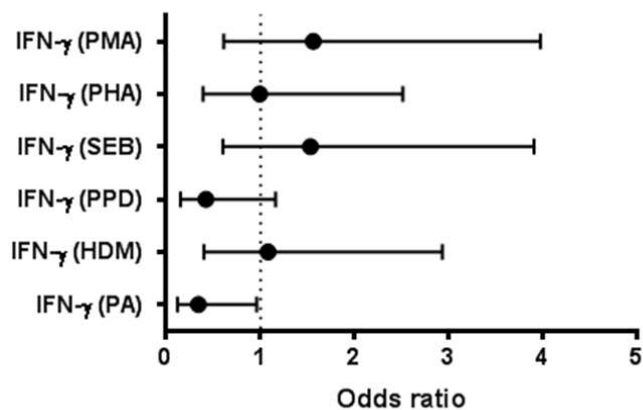
**Table 6.2 Demographic characteristics of controls and IPF patients from the first part of the population in this study**

Characteristic		Controls	Cases	Total	OR (95% CI) <sup>†</sup>
Number (% total)		38 (52.78%)	34 (47.22%)	72 (100%)	
Sex	Female	9	9	18 (25.97%)	
	Male	29	25	54 (74.03%)	
Age category (years)	<65	17	9	26	
	65-69	2	8	10	
	70-74	8	7	15	
	75-79	4	4	8	
	80-84	4	2	6	
	>85	3	4	7	
Mean age $\pm$ SD		69.3 $\pm$ 9.8	70.7 $\pm$ 10.3		
Smoking habit	Never smoked	17 (45%)	11 (32%)	28 (39%)	1.00
	Ex-smoker	19 (50%)	20 (59%)	39 (54%)	1.77 (0.63 to 4.94)
	Current smoker	2 (5%)	3 (9%)	5 (7%)	3.05 (0.40 to 23.34)
*hsCRP category (mg/ml)	<1	11	2	13 (18.06%)	1.00
	1-3	17	8	25 (34.72%)	2.97 (0.51-17.28)
	>3	10	23	33 (45.83%)	16.04 (2.75-93.57), $p=0.002$

\*hsCRP, highly-sensitive C-reactive protein. <sup>†</sup> ORs are adjusted for age category and sex.

**Table 6.3 The association between IFN- $\gamma$  secretion and IPF**

IFN- $\gamma$ production					
Stimuli	Binary	Controls (n=38)	Cases (n=34)	Unadjusted OR (95% CI)	OR adjusted for age_cat and sex (95% CI)
PMA				1.56 (0.62-3.97)	1.55 (0.61-3.97)
	Low	21	15		
	High	17	19		
PHA				1.00 (0.40-2.52)	0.99 (0.39-2.51)
	Low	19	17		
	High	19	17		
SEB				1.56 (0.62-3.97)	1.53 (0.60-3.90)
	Low	21	15		
	High	17	19		
PPD				0.51 (0.20-1.30)	0.42 (0.15-1.16)
	Low	16	20		
	High	22	14		
HDM				1.25 (0.49-3.16)	1.08 (0.40-2.93)
	Low	20	16		
	High	18	18		
PA				0.32 (0.12-0.83)	0.34 (0.12-0.96)
	Low	14	22		
	High	24	12		



**Figure 6.4 Summary of OR assessing the association between IPF and IFN- $\gamma$  production in PBMCs in response to a panel of stimuli.**

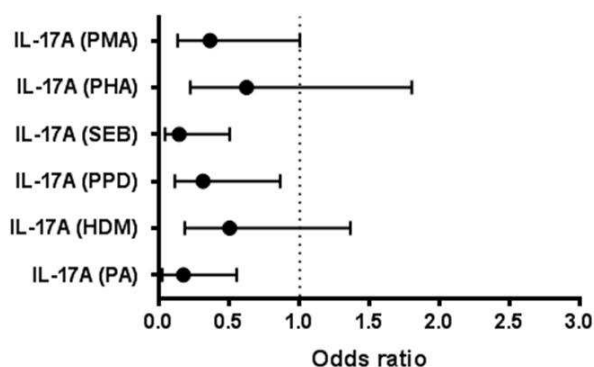
IPF patients had no evident tendency to have more IFN- $\gamma$  production than controls in PBMCs upon PMA, PHA, SEB and HDM stimulation. IPF patients PBMCs were 58% and 66% less likely to produce IFN- $\gamma$  in response to PPD and PA respectively.

PBMCs in cases were 86% (OR 0.14, 95% CI 0.04-0.50,  $p=0.003$ ), 70% (OR 0.31, 95% CI 0.11-0.86,  $p=0.025$ ) and 83% (OR 0.17, 95% CI 0.02-0.55,  $p=0.003$ ) less likely to produce IL-17A than the controls in response to SEB, PPD and PA extract respectively and the effects were significant (Table 6.3). PBMCs upon PMA, PHA and HDM stimulation in IPF patients were also less likely (64%, 38% and 50% respectively) to produce IL-17A than the healthy donors, although no significance was obtained (Table 6.3). ORs summarised in Fig. 6.4 indicated that PBMCs in IPF patients were generally less likely to produce IL-17A than the controls in response to all stimuli. This result suggests the production of IL-17A (Th17 differentiation) in PBMCs from patients with IPF might be down-regulated or dysfunctional compared to the healthy controls.

Regarding the association between the production of IL-10, the anti-inflammatory cytokine, and IPF, PBMCs of IPF patients upon PHA and PA were 80% (OR 0.20, 95% CI 0.06-0.61,  $p=0.005$ ) and 70% (OR 0.30, 95% CI 0.10-0.89,  $p=0.03$ ) less likely to produce IL-10 than healthy donors (Table 6.4). PBMCs in IPF patients treated with PMA, SEB, PPD and PDM were also less likely (60%, 40%, 26%, and 32% respectively) to produce IL-10 than the healthy individuals, although no significance was achieved (Table 6.4). Fig. 6.5 highlighted not only PBMCs in IPF patients stimulated with PHA had a tendency to produce less IL-10 than the healthy controls when the levels of IL-10 were grouped in binary, but the mean of IL-10 production in PBMCs in IPF patients was also significantly less (Un-paired t-test,  $p=0.0003$ ) than the mean in healthy donors.

**Table 6.4 The association between the production of IL-17A and IPF**

IL-17A production					
Stimuli	Binary	Controls (n=38)	Cases (n=34/32)	Unadjusted OR (95% CI)	OR adjusted for age_cat and sex (95% CI)
PMA				0.36 (0.14-0.93) <i>p</i> =0.034	0.36 (0.13-1.00)
	Low	15	22		
	High	23	12		
PHA				0.80 (0.32-2.02)	0.62 (0.22-1.80)
	Low	18	18		
	High	20	16		
SEB				0.25 (0.063-0.66) <i>p</i> =0.006	0.14 (0.04-0.50) <i>p</i> =0.003
	Low	13	23		
	High	25	11		
PPD				0.32 (0.12-0.83) <i>p</i> =0.02	0.31 (0.11-0.86) <i>p</i> =0.025
	Low	14	22		
	High	24	12		
HDM				0.51 (0.20-1.30)	0.50 (0.18-1.36)
	Low	16	20		
	High	22	14		
PA			32	0.24 (0.09-0.65) <i>p</i> =0.005	0.17 (0.02-0.55) <i>p</i> =0.003
	Low	13	22		
	High	25	10		

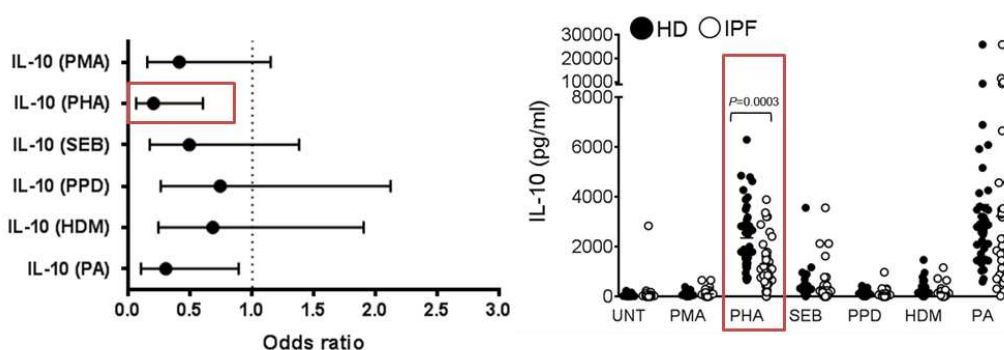


**Figure 6.5 Summary of OR assessing the association between IPF and IL-17A production in PBMCs in response to a panel of stimuli.**

IL-17A production in people with IPF was lower than healthy controls when PBMCs were treated with a variety of stimulants. Moreover, PBMCs from IPF patients were up to 86% and 83% significantly less likely to produce IL-17A in response to SEB and PA respectively than healthy subjects

**Table 6.5 The association between the production of IL-10 and IPF**

IL-10 production					
Stimuli	Binary	Controls (n=38)	Cases (n=33/32)	Unadjusted OR (95% CI)	OR adjusted for age_cat and sex (95% CI)
PMA				0.47 (0.18-1.22)	0.41 (0.15-1.15)
	Low	16	20		
	High	22	13		
PHA				0.23 (0.083-0.61) <i>p</i> =0.004	0.20 (0.06-0.61) <i>p</i> =0.005
	Low	13	23		
	High	25	10		
SEB				0.50 (0.19-1.29)	0.49 (0.17-1.38)
	Low	16	19		
	High	22	13		
PPD				0.63 (0.24-1.62)	0.74 (0.26-2.12)
	Low	17	18		
	High	21	14		
HDM				0.63 (0.24-1.62)	0.68 (0.24-1.90)
	Low	17	18		
	High	21	14		
PA				0.31 (0.11-0.82) <i>p</i> =0.018	0.30 (0.10-0.89) <i>p</i> =0.03
	Low	14	21		
	High	24	11		



**Figure 6.6 Summary of OR assessing the association between IPF and IL-10 production by PBMCs in response to a panel of stimuli.**

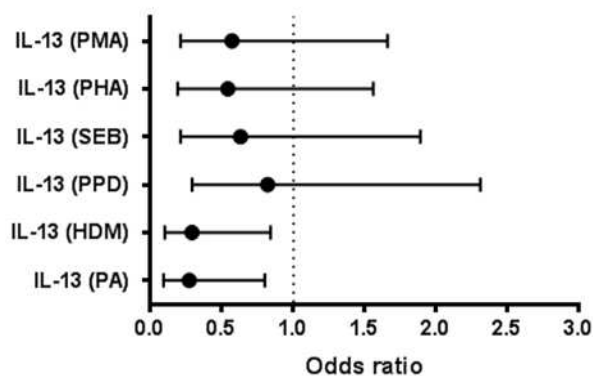
IPF patients PBMCs were less likely to produce IL-10 in response of a panel of stimuli. OR indicated that PBMCs stimulated with PHA from people with IPF were 80% less likely to produce IL-10 than the healthy donors (OR 0.20; 95% CI 0.06-0.61) (red box). The association identified by calculating OR corresponded to the result obtained when the levels of IL-10 were assumed to have a normal distribution.

Th2-associated cytokines IL-4, IL-5, and IL-13 have been linked to the development of fibrosis in a variety of chronic inflammatory diseases. IL-13 signalling pathway is considered as one of the dominant inducers of Th2-dependent fibrosis in several chronic lung diseases (Wynn, 2011). High expression of IL-13 receptors IL-4R $\alpha$  and IL-13R $\alpha$ 2 were identified in surgical lung biopsies and fibroblasts from patients with IIP compared with normal patients without pulmonary fibrosis (Jakubzick et al., 2004). In addition, levels of IL-13 and IL-13R $\alpha$ 1 in the BAL fluids in patients with IPF were inversely correlated with lung function (Park et al., 2009, Wynn, 2011). Extensive collagen deposition secreted by fibroblasts upon IL-13 and TGF- $\beta$ 1 stimulation also support the role of IL-13 as a profibrotic mediator (Murray et al., 2008).

In the present study, PBMCs from IPF patients upon HDM and PA stimulation were 71% (OR 0.29, 95% CI 0.10-0.384, p=0.022) and 73% (OR 0.27, 95% CI 0.09-0.80, p=0.018) less likely to produce IL-13 than healthy subjects (Table 6.5). PBMCs in IPF patients were also less likely to secrete IL-13 in response to PMA, PHA, SEB and PPD (from 46% to 18%) than healthy controls, although the effects were less potent and not significant (Table 6.5; Fig. 6.7). Contrary to the high expression of IL-13 in the local pulmonary environment, PBMCs in IPF patients seemed to produce less IL-13 than the matched controls upon the stimulation of HDM and PA extract.

**Table 6.6 The association between induced production of IL-13 and IPF**

IL-13 production					
Stimuli	Binary	Controls (n=37/38)	Cases (n=32)	Unadjusted OR (95% CI)	OR adjusted for age_cat and sex (95% CI)
PMA	Low	17	18	0.66 (0.26-1.71)	0.57 (0.20-1.66)
	High	20	14		
PHA	Low	16	21	0.52 (0.20-1.36)	0.54 (0.19-1.56)
	High	19	13		
SEB	Low	16	19	0.50 (0.19-1.29)	0.63 (0.21-1.89)
	High	22	13		
PPD	Low	19	16	1.00 (0.39-2.56)	0.82 (0.29-2.31)
	High	19	16		
HDM	Low	14	21	0.31 (0.11-0.82) <i>p</i> =0.018	0.29 (0.10-0.84) <i>p</i> =0.022
	High	24	11		
PA	Low	14	21	0.31 (0.11-0.82) <i>p</i> =0.018	0.27 (0.09-0.80) <i>p</i> =0.018
	High	24	11		



**Figure 6.7 Summary of OR assessing the association between IPF and IL-13 production in PBMCs in response to a panel of stimuli.**

IPF patients PBMCs were less likely to produce IL-13 in response of the panel of stimuli in this study.

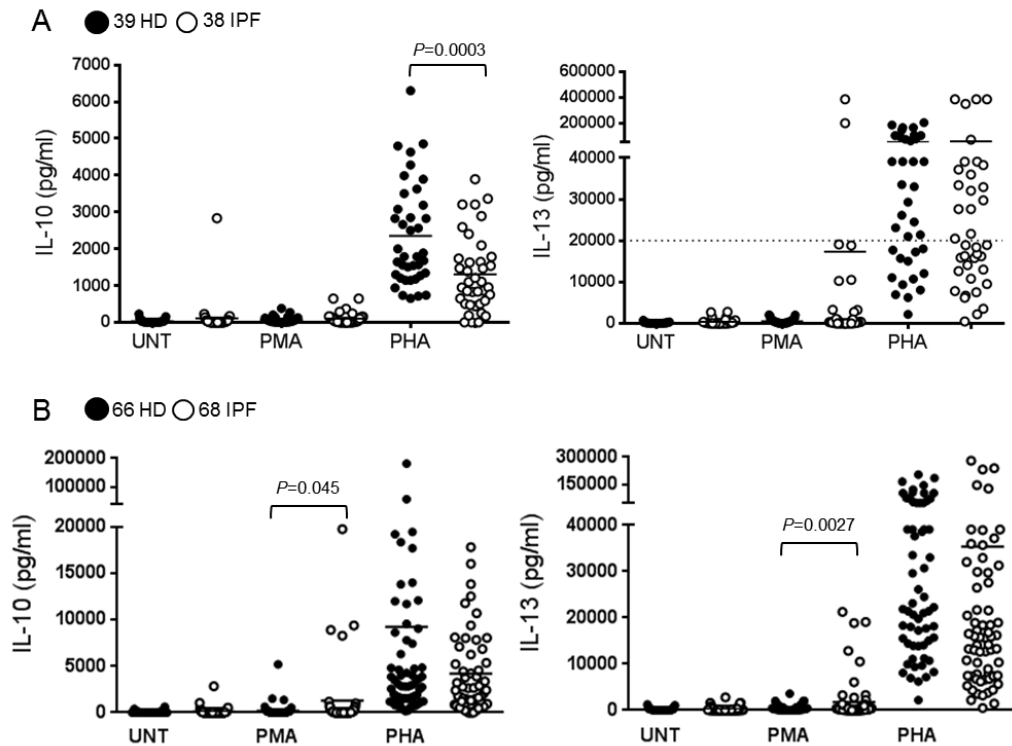
#### **6.5.4. Assessing the association between IPF and the production of IL-10 and IL-13 in PBMCs upon PMA and PHA stimulation in the total population (66 patients and 66 healthy controls)**

Next it was decided to focus on IL13 and IL10 for the following reasons: (1) the mean of IL-10 production in PBMCs of IPF patients upon PHA stimulation was significantly lower than the controls (refer Table 6.5), which suggested that patients with IPF seemed prone to a pro-inflammatory systemic immune status; (2) PBMCs from 7 random patients produced substantial amounts of IL-13 in response to PMA than the rest of the patients and the controls. We hypothesised that in a subgroup of patients with IPF their PBMCs were particularly hyper-responsive to PMA and produced higher levels of IL-13. To test the two hypotheses above, quantification of the levels of IL-10 and IL-13 in PBMCs upon PMA and PHA stimulation in the other half population was performed. In addition, supernatants of PBMCs in response to PMA were diluted in 1:5 to obtain readings retain in the linear range due to the levels of IL-13 production from PBMCs in the first half population (14 of 39 controls; 21 of 38 patients) were higher than the detection limit (above 20,000 pg/ml) by using immuno multiplex assay.

The results showed that the mean IL-10 production in PBMCs from 68 IPF patients in response to PMA was significantly higher than the mean from 66 healthy controls (Fig. 6.8B). The significance of the mean IL-10 production in PBMCs upon PHA stimulation between HD and IPF was lost when the whole population was considered but the trend towards reduced levels of IL-10 in IPF PBMCs remained (Fig. 6.8). The mean of IL-13 in PBMCs from 68 IPF in



response to PMA were also significantly higher than the mean from the healthy donors (Fig. 6.8B).



**Figure 6.8 Mean of the IL-10 and IL-13 production in PBMCs from 68 IPF patients (IPF) upon PMA stimulation was higher than that of 66 healthy donors (HD) and the trend of lower IL-10 production in PBMCs of IPF patients.**

A, levels of IL-10 and IL-13 in PBMCs in response to PMA and PHA from the first half population (39 HD and 38 IPF) were shown in dot plots. B, levels of IL-10 and IL-13 in PBMCs in response to PMA and PHA from the whole population (66 HD and 68 IPF) were shown in dot plots.

Demographic features of the whole population listed in Table 6.7 showed that the controls (66 HD) and cases (66 IPF available due to 2 missing clinical data) were matched in age and sex. Patients with IPF were 2 times (OR 2.16, 95% CI 1.08-4.31,  $p=0.05$ ) more likely to have been ex-smokers than the controls. IPF patients in general secrete higher hsCRP than the general population. The results summarised in Table 6.8 showed that PBMCs from patients with IPF

upon PMA stimulation were 57% (OR 0.43, 95% CI 0.21-0.89) less likely to produce IL-10 than the healthy controls when levels of IL-10 were binary grouped; PBMCs in IPF patients were 26% (OR 0.74, 95% CI 0.49-1.11) less likely to produce IL-10 than the general population when levels of IL-10 were categorised in 3 groups: low, medium and high response. Whilst PBMCs from patients with IPF upon PHA stimulation were 38% (OR 0.62, 95% CI 0.30-1.28) less likely to produce IL-10 than the healthy controls when levels of IL-10 were binary grouped; PBMCs in IPF patients were 28% (OR 0.72, 95% CI 0.46-1.11) less likely to produce IL-10 than the general population when levels of IL-10 were categorised in 3 groups: low, medium and high response. However, none of the above associations were significant (summarised in Fig. 6.9).

Results in Table 6.9 showed that no apparent association exists between IL-13 production in response to PMA and IPF (OR 1.01, 95% CI 0.53-2.23). PBMCs from patients with IPF upon PHA stimulation were 70% (OR 0.31, 95% CI 0.14-0.66,  $p=0.003$ ) less likely to produce IL-13 than the healthy controls when levels of IL-13 were grouped in binary categories; when levels of IL-13 were categorised in 3 groups, PBMCs in IPF patients also appeared 50% (OR 0.50, 95% CI 0.32-0.80,  $p=0.004$ ) less likely to produce IL-13 than the general population (summarised in Fig. 6.10).

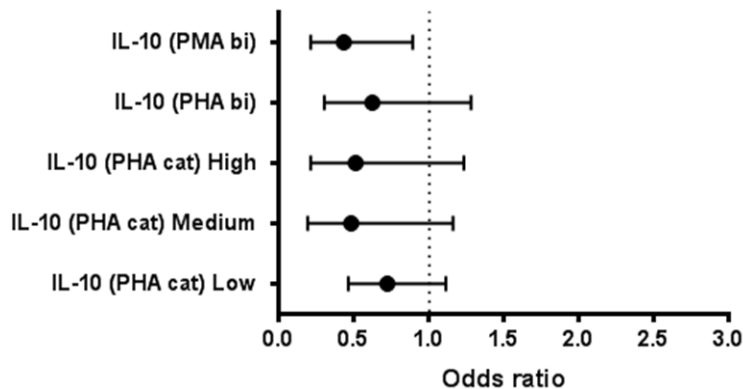
**Table 6.7 Demographics containing the whole population of incident cases of IPF and healthy controls in this study**

Characteristic		Controls	Cases	Total	OR (95% CI)*
Number (% total)		66 (50%)	66 (50%)	132 (100%)	
Sex	Female	15	19	34 (26%)	
	Male	51	47	98 (74%)	
Age category (years)	<65	26	17	43	
	65-69	4	12	16	
	70-74	14	16	30	
	75-79	9	10	19	
	80-84	6	4	10	
	>85	7	7	14	
Mean age		69.6 (9.9)	71.5 (9.8)		
Smoking habit	Never smoked	30	17	47 (35.6%)	1.00
	Ex-smoker	32	45	77 (58.3%)	2.16 (1.08 to 4.31), <i>p</i> <0.05
	Current smoker	4	5	9 (6.8%)	2.60 (0.60 to 11.22)
hsCRP category (mg/ml)	<1	23	6	29 (21.9%)	1.00
	1-3	29	18	47 (35.6%)	2.40 (0.87 to 6.57)
	>3	14	41	56 (42.4%)	7.77 (2.86 to 21.09), <i>p</i> <0.0001

\*OR adjusted for age category and sex.

**Table 6.8 The association between PMA and PHA induced production of IL-10 and IPF in the whole population in this study**

IL-10 production		Controls (n=66)	Cases (n=66)	Unadjusted OR (95% CI)	OR adjusted for age_cat and sex (95% CI)
PMA	Binary			0.48 (0.24-0.96)	0.43 (0.21-0.89)
	Low	27	39		
	High	39	27		
PMA	Category			0.78 (0.53-1.15)	0.74 (0.49-1.11)
	Low	36	39		
	Medium	18	5		
	High	22	22		
PHA	Binary			0.61 (0.31-1.22)	0.62 (0.30-1.28)
	Low	29	37		
	High	37	29		
PHA	Category			0.76 (0.48-1.10)	0.72 (0.46-1.11)
	Low	17	27	1.00	1.00
	Medium	25	19	0.48 (0.20-1.12)	0.48 (0.19-1.16)
	High	24	20	0.52 (0.22-1.22)	0.51 (0.21-1.23)



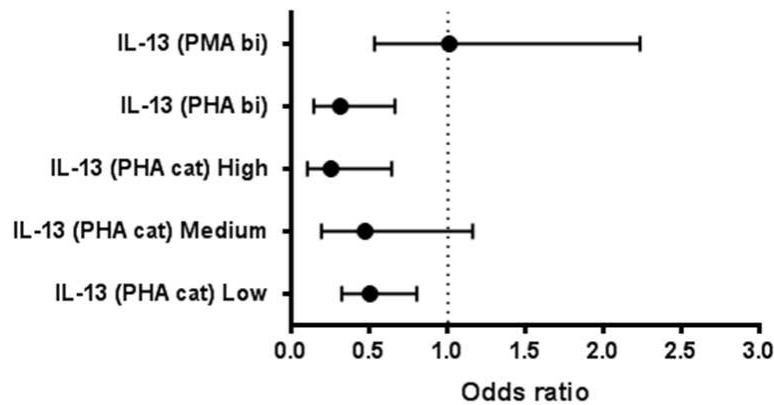
**Figure 6.9 A summary plot illustrates the association between IPF and the induced production of IL-10 in response to PMA and PHA from the whole population in this study.**

OR consistently less than 1 indicates that IPF patients were less likely to produce IL-10 when PBMCs were stimulated with PMA and PHA although no significance was achieved.

**Table 6.9 The association between PMA and PHA induced production of IL-13 and IPF in the whole population in this study**

IL-13 response		Controls (n=66)	Cases (n=66)	Unadjusted OR (95% CI)	OR adjusted for age_cat and sex (95% CI)
PMA	Binary			1.00 (0.56-1.97)	1.01 (0.53-2.23)
	Low	33	33		
	High	33	33		
PHA	Binary			0.36 (0.18-0.74) <i>p</i> =0.0006	0.31 (0.14-0.66) <i>p</i> =0.003
	Low	25	41		
	High	41	25		
PHA	Categorical			0.52 (0.33-0.80) <i>p</i> =0.003	0.50 (0.32-0.80) <i>p</i> =0.004
	Low (490.69-13963.21)	15	29	1.0	1.0
	Medium (14,063.49- 31,319)	22	22	0.52 (0.22-1.22)	0.47 (0.19-1.16)
	High (32,068-348,679.3)	29	15	0.27 (0.11-0.65) <i>p</i> =0.003	0.25 (0.10-0.64) <i>p</i> =0.004

The concentration of cytokine was measured in pg/ml.



**Figure 6.10 A summary of odds ratios quantifying the association between IPF and IL-13 production in response to a panel of stimulation.**

PBMCs from IPF patients were 69% less likely to produced IL-13 upon PHA stimulation than the healthy controls (OR 0.31; 95% CI 0.14-0.66). IPF patients were 75% less likely than healthy controls to produce IL-13 at high levels (PHA cat High).

### **6.5.5. Correlation between the levels of cytokine production and survival in the IPF cohort**

To determine whether the levels of cytokine production by PBMCs correlated with the clinical outcome in the IPF cohort, Cox regression modelling of individual cytokine production and survival performed. In Cox regression modelling, hazard is the slope of the survival curve indicating how rapidly subjects are dying. The hazard ratio (HR) is defined as the hazard in the exposed groups divided by the hazard in the unexposed groups (Hernan, 2010). For instance, HR 2.0 means a patient in group one who has not died has twice the probability of having died in group two. The groups used in this analysis, high levels and low levels of IFN- $\gamma$ , IL-17A, IL-10 and IL-13, were the same used in the logistic regression analysis. Group one in our analysis default setting was 'low levels of cytokine production' and group two was 'high levels of cytokine'.

The results showed that the survival of patients with lower levels of IL-17A production in PBMCs upon PMA, PHA, HDM and PA extract stimulation had increased risk of mortality than those with high levels of IL-17A (Fig. 6.9). Lower production of IL-17A increased mortality by 4 times in average (see Table 6.10 for detail). Similarly, lower levels of IL-13 in PBMCs upon HDM and PA stimulation increased mortality by 6 and 4 times respectively compared with those IPF patients with higher levels of IL-13 (See Table 6.10 for detail; Fig. 6.10). Lower levels of IFN- $\gamma$  in PBMCs upon HDM and PA stimulation also increased mortality by 4 times compared with those with higher levels of

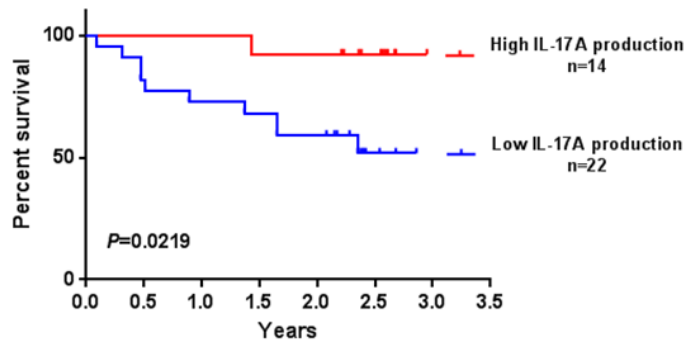
IFN- $\gamma$  (Table 6.10 for detail; Fig. 6.11). However, lower levels of IFN- $\gamma$  in PBMCs upon SEB stimulation correlated with decreased mortality (0.3 times) compared with higher levels of IFN- $\gamma$  (Table 6.10). Levels of IL-10 in PBMCs in response to any of the stimuli used in the study cohort did not correlate with mortality.

Overall, this preliminary analysis suggests that in general lower levels of cytokines in PBMCs of IPF patients correlate with higher risk of mortality.

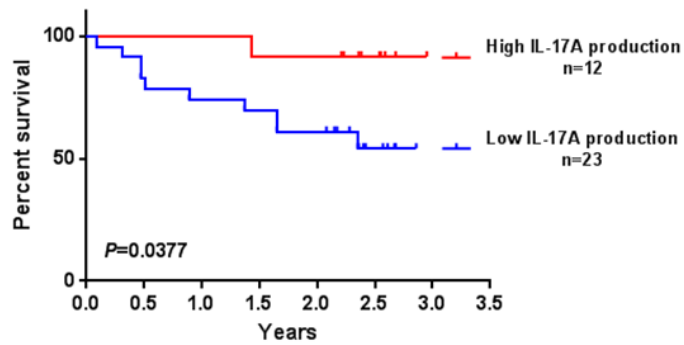
**Table 6.10 Significant Cox regression correlations between individual cytokine production and survival in the IPF cohort**

Variable	Hazard ratio	95% CI	<i>P</i> -value
<i>IFN-<math>\gamma</math></i> (SEB)	0.29	0.085 to 0.99	0.0487
IFN- $\gamma$ (HDM)	3.94	1.17 to 13.31	0.0271
IFN- $\gamma$ (PA)	4.31	1.29 to 14.41	0.0176
Variable	Hazard ratio	95% CI	<i>P</i> -value
IL-17A (PMA)	4.10	1.23 to 13.69	0.0219
IL-17A (SEB)	3.65	1.08 to 12.35	0.0377
IL-17A (HDM)	4.45	1.34 to 14.80	0.0148
IL-17A (PA)	4.60	1.37 to 15.50	0.0138
Variable	Hazard ratio	95% CI	<i>P</i> -value
IL-13 (HDM)	6.13	1.72 to 21.84	0.0052
IL-13 (PA)	4.02	1.13 to 14.34	0.0318

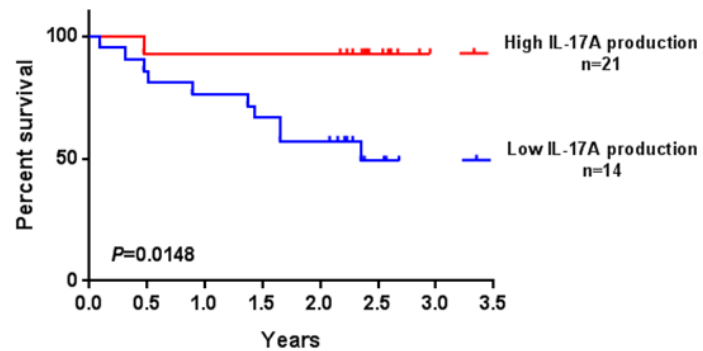
**Survival of IPF patients with high/low levels of IL-17A in PBMCs (PMA)**



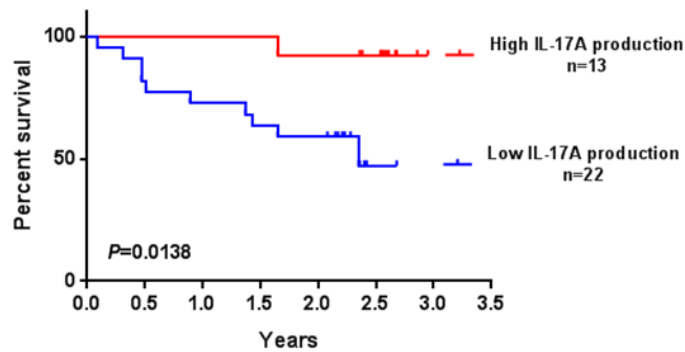
**Survival of IPF patients with high/low levels of IL-17A in PBMCs (SEB)**



**Survival of IPF patients with high/low levels of IL-17A in PBMCs (HDM)**



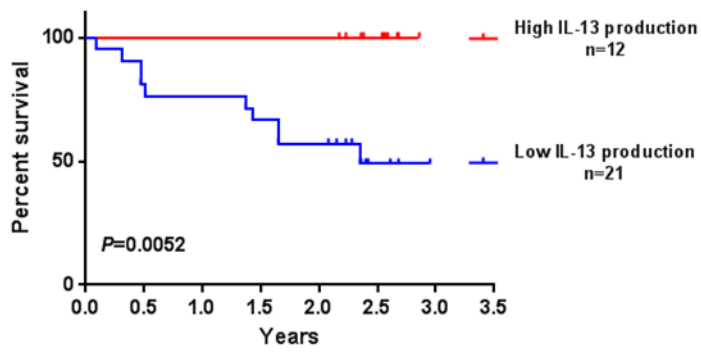
**Survival of IPF patients with high/low levels of IL-17A in PBMCs (PA)**



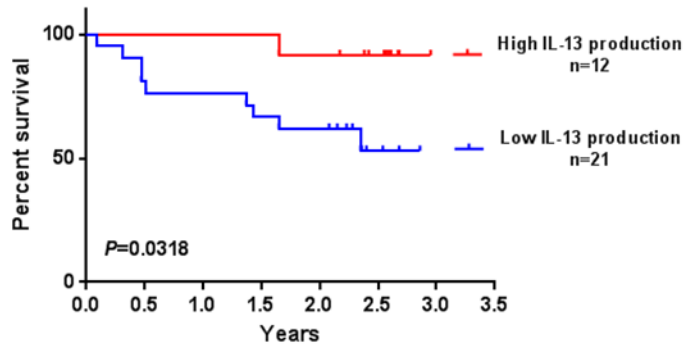
**Figure 6.11** Survival plot of IPF patients with high and low levels of IL-17A in PBMCs upon PMA, SEB, HDM and PA extract stimulation.



**Survival of IPF patients with high/low levels of IL-13 in PBMCs (HDM)**

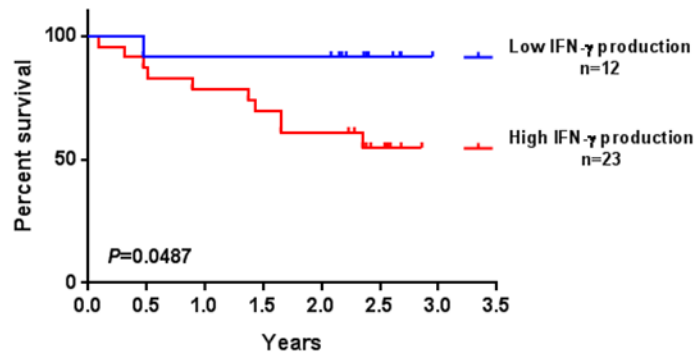


**Survival of IPF patients with high/low levels of IL-13 in PBMCs (PA)**

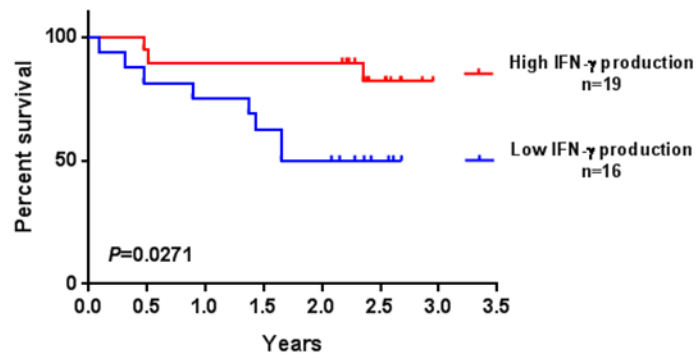


**Figure 6.12 Survival of IPF patients with high and low levels of IL-13 in PBMCs upon HDM and PA extract stimulation.**

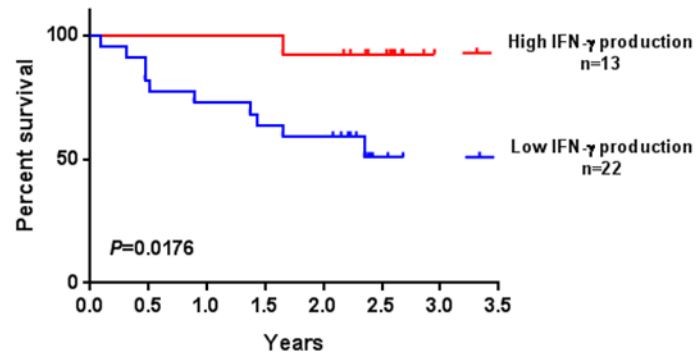
**Survival of IPF patients with high/low levels of IFN- $\gamma$  in PBMCs (SEB)**



**Survival of IPF patients with high/low levels of IFN- $\gamma$  in PBMCs (HDM)**



**Survival of IPF patients with high/low levels of IFN- $\gamma$  in PBMCs (PA)**



**Figure 6.13** Survival of IPF patients with high and low levels of IFN- $\gamma$  in PBMCs upon SEB, HDM and PA extract stimulation.

## 6.6. DISCUSSION

Repetitive apoptosis of alveolar epithelial cells leading to epithelial mesenchymal transition and massive accumulation of extracellular matrix is considered the primary factor that causes impaired tissue remodelling in patients with IPF. However, numerous cytokines derived from T cells, monocytes/macrophages and other myeloid cells are also important regulators of myofibroblast differentiation (Duffield et al., 2013). In this study, the systemic immune status in patients with IPF was investigated by analysing the cytokine profile in PBMCs upon unbiased stimulation in comparison with age- and sex-matched healthy individuals. We demonstrated that the production of IL-17A was 90%, IL-10 80% and IL-13 70% more likely at lower levels in PBMCs of patients with IPF than in the general population controls. Additionally, lower levels of IL-17A, IL-13 and IFN- $\gamma$  were associated with disease severity, with IPF patients in the low production group being 4 to 6 times more likely to die. Our study showed that circulating immune cells in patients with IPF were generally less responsive to both non-specific and specific antigens than healthy donor cells.

Numerous studies have suggested the involvement of the cytokine milieu in regulating disease progression caused by aberrant epithelial damage can lead to exaggerated deposition of extracellular matrix in the lung (Duffield et al., 2013, Hams et al., 2014). Th2 response cytokine IL-13 has been widely considered a profibrotic mediator in tissue remodelling, including chronic asthma, IPF and lung fibrosis models (Murray et al., 2008, Duffield et al., 2013). The bleomycin-induced mouse pulmonary fibrosis model demonstrated that

increased levels of IL-13 induced fibrosis via up-regulating the production of TGF- $\beta$  (Lee et al., 2001). Concentrations of IL-13 in the serum, the BAL, smooth muscle, bronchial epithelium and alveolar macrophages of patients with IPF were higher than healthy controls and the levels were inversely correlated with lung function (Xiao et al., 2003, Park et al., 2009). Increased production of IL-13 by innate lymphoid cells in pulmonary fibrosis has also been shown. In addition to T-cell -mediated antigen-specific immune responses, a recent study described elevated IL-25 production by type 2 innate lymphoid cells (ILC2) in which also express IL-13 in a *Schistosoma mansoni* egg-induced pulmonary granuloma model. This finding of increased IL-25, IL-13 and TGF- $\beta$  production correlated with a population of ILC2 in the BAL and lung biopsy in patients with IPF suggested an innate mechanism was also involved in the generation of pulmonary fibrosis (Hams et al., 2014).

IL-17A is a proinflammatory cytokine involved in autoimmune disease and chronic airway remodeling (Tan and Rosenthal, 2013, Nembrini et al., 2009). Recently, enhanced IL-17A production was identified in murine pulmonary fibrosis models and in the lungs of patients with IPF. The bleomycin-induced mouse fibrosis model indicated that IL-1 $\beta$  and IL-23 promote pulmonary fibrosis by inducing IL-17A which causes significant neutrophilia (Wilson et al., 2010, Gasse et al., 2011). Early IL-17A and IL-17F expression by ROR $\gamma$ t(+)  $\gamma\delta$  T cells was shown to be required for pulmonary fibrosis and this was enhanced by TGF- $\beta$ 1 production; inversely, blocking of IL-17A promoted the resolution of pulmonary inflammation via TGF- $\beta$ 1 dependent and independent pathways (Gasse et al., 2011, Mi et al., 2011). In addition, elevated IL-17 expressed by macrophages, CD3+ T cells and epithelial cells has also been

detected in the aggressively fibrotic region in the lungs of patients with IPF (Nuovo et al., 2012). The above studies suggest that fibrogenesis in IPF could be predominantly regulated by enhanced local production of IL-13 and IL-17 in the interstitial lung.

However, our data contradicts to previous studies by showing that peripheral blood from IPF patients are more likely to secrete lower levels of cytokines than healthy controls. This might due to the fact that we investigated the production of cytokines by PBMCs in response to a panel of stimuli whereas in other studies, the levels of cytokine were quantified in serum and BAL. Secondly, the generally lower cytokine production in patients' PBMCs compared to

**Table 6.11 Summary of ORs with significance differences**

Stimuli	Cytokine	Unadjusted OR (95% CI) <i>p</i>	OR adjusted for age_cat and sex (95% CI) <i>p</i>
<b>PMA</b>	<b>IL-17A</b>	<b>0.36</b> (0.14-0.93) <i>p</i> =0.034	<b>0.36</b> (0.13-1.00) <i>p</i> =0.003
<b>SEB</b>	<b>IL-17A</b>	<b>0.25</b> (0.063-0.66) <i>p</i> =0.006	<b>0.14</b> (0.04-0.50) <i>p</i> =0.003
<b>PPD</b>	<b>IL-17A</b>	<b>0.32</b> (0.12-0.83) <i>p</i> =0.02	<b>0.31</b> (0.11-0.86) <i>p</i> =0.025
<b>PA</b>	<b>IL-17A</b>	<b>0.24</b> (0.09-0.65) <i>p</i> =0.005	<b>0.17</b> (0.02-0.55) <i>p</i> =0.003
<b>PA</b>	<b>IL-10</b>	<b>0.31</b> (0.11-0.82) <i>p</i> =0.018	<b>0.30</b> (0.10-0.80) <i>p</i> =0.03
<b>HDM</b>	<b>IL-13</b>	<b>0.31</b> (0.11-0.82) <i>p</i> =0.018	<b>0.31</b> (0.10-0.8204) <i>p</i> =0.022
<b>PA</b>	<b>IL-13</b>	<b>0.31</b> (0.11-0.82) <i>p</i> =0.0018	<b>0.27</b> (0.09-0.80) <i>p</i> =0.018

healthy controls could be partially explained by the lack of potency of peripheral blood cells, either T-cell differentiation is skewed or the function of antigen-presenting cells was impaired, in response to stimuli. We postulated that the enhanced cytokine production, including IL-13 and IL-17A, in the serum and BAL in patients with IPF might have exhausted the immune cells therefore cannot respond further stimulation. The exhausted immune system thus causes IPF patients more susceptible to exacerbations. The regulation of systemic T cell differentiation upon stimulation might also be deteriorated. A recent transcriptomic study showed that reduced expression of genes that participate in T-cell co-stimulatory signalling including CD28, ICOS (inducible T-cell costimulator, also known as CD278), LCK (lymphocyte-specific protein tyrosine kinase) and ITK (interleukin-2-inducible T cell kinase) were identified in PBMCs from patients with IPF compared with healthy donors (Herazo-Maya et al., 2013). Further, CD4<sup>+</sup>CD28<sup>+</sup> cells were identified to be the cellular compartments with reduced CD28, ICOS, LCK and ITK expression in the replication cohort. ITK expressed in T cells, NKT cells and mast cells is a non-receptor tyrosine kinase which regulates the T cell receptor (TCR), CD28, CD2, chemokine receptor CXCR4, and FcεR-mediated signaling pathways. In T cells, ITK mediates TCR activation via Src and Lck kinase, phosphorylation of PLC $\gamma$  that leads to accumulation of intracellular calcium and activation of MAP, ERK, JNK kinases and the transcription factors NFAT (nuclear factor of activated T-cells) and AP-1 (activating protein 1) (Sahu and August, 2009). ITK in association with CD28, ICOS, and LCK has a pivotal role in the secretion of Th2 cytokines IL-4, IL-5 and IL-13 and regulation of the development of effective Th2 response in allergic asthma and

worm infections that involves in Th2-mediated inflammation. This study partially explains our results that the generally lower levels of cytokines in PBMCs of patients in IPF upon a broad range of antigen stimulations compared with healthy individuals could be attributed to the decreased expression of T cell co-stimulatory signalling. In another study, down-regulation of CD28 in circulating CD4 T cells was implicated with an association with disease severity in patients with IPF (Gilani et al., 2010). T cells develop functional and phenotypic changes upon repetitive chronic antigen stimulations that could have included the loss of co-stimulatory surface protein CD28. Not only the impaired co-stimulatory signalling in CD4<sup>+</sup>CD28<sup>+</sup> T cells might result in insufficient cytokine production upon antigen stimulation, reduced cytokine production in the PBMCs cultures might also attribute to an activation-induced T cell death in circulating cells (Gilani et al., 2010, Herazo-Maya et al., 2013).

IPF has been considered as an autoimmune disease. The study conducted by Kotsianidis et al. demonstrated that Tregs in peripheral blood and BAL from patients with IPF exhibited defective inhibition of Th1 and Th2 cytokine production by T effector cells (CD4<sup>+</sup>CD25<sup>-</sup>) (Kotsianidis et al., 2009). Locally and systemically reduced Tregs displayed a compromised suppressor role in maintaining the balance of Th1 and Th2 response. The theory of globally skewed regulatory role of Tregs in patients with IPF supported our findings that PBMCs from people with IPF have the tendency of lower levels of both Th1 and Th2 cytokine secretion and correlated with mortality. In this regard, IPF patients might suffer an impaired immunity thus are vulnerable to acute exacerbations usually induced by virus infections (Hoo and Whyte, 2012, Wuyts et al., 2012).

In addition to T cells population, we suspect that the antigen-presenting cells (APCs) also play a role in mediating the production of cytokines in the peripheral blood. Macrophages regulate fibrogenesis by secreting chemokines that recruit fibroblasts and other inflammatory cells. Although collagen-secreting myofibroblasts were considered the cellular origin of extracellular matrix components that lead to fibrosis, macrophages in vivo were found co-localise with collagen-producing myofibroblasts and produce profibrotic mediators that directly activate fibroblasts, including TGF- $\beta$ 1 and platelet-derived growth factor (PDGF and TFG- $\beta$  are the master regulators in fibrosis progression and resolution) (Wynn and Barron, 2010, Duffield et al., 2013). Macrophages can be induced by TLR signalling and IFN- $\gamma$  that turn into M1-type (classically activated) macrophages and M2-type macrophages (alternatively activated) that induced by IL-4 and IL-13, although more subtypes of M2 macrophages have also been described (Hussell and Bell, 2014). A positive correlation between the levels of M2-type macrophages in peripheral blood and lung functions was demonstrated in patients with IPF (Prasse and Muller-Quernheim, 2009). A systematic study in order to elucidate the compartmentalization of cell activation showed that the secretion of IL-2 by T cells in PBMCs and BAL of patients with IPF was decreased after steroid treatment whereas BAL macrophages remained activated. It was suggested that macrophages in IPF failed to respond to the surrounding cytokine milieu (Homolka et al., 2003). This result also implicated why anti-inflammatory treatments fail to relieve the symptoms in patients with IPF.

In the present study, the univariate Cox proportional model was used to define a hazard ratio for a cytokine (biomarker) in relation to mortality and



demonstrated a significant correlation between lower levels of cytokine with poor survival (Prasse and Muller-Quernheim, 2009). However, multivariate Cox proportional models are required to adjust for baseline parameters, such as sex, age, smoking habit, etc. Heterogeneity of pulmonary fibrosis in each IPF patient and no consistent patterns could be found between individuals has been a challenge to identify the immunological parameters to predict disease prognosis. Further investigations including cell compositions in PBMCs, cell population in correlation with cytokine production, and the grouping of multiple cytokines using multivariate model are also needed. A signature pathway generated by multivariate model will further our understanding of the underlying mechanism in IPF.

## **6.7. SUMMARY**

This study suggests that PBMCs in patients with IPF were in general less responsive to a variety of stimulations based on the lower production of IL-17A, IL-10 and IL-13 observed.

Lower levels of IL-17A secreted by PBMCs in response to SEB, PPD, HDM and PA correlated with increased mortality (4 fold); lower levels of IL-13 and IFN- $\gamma$  in PBMCs upon HDM and PA extract stimulation also increased the risk of death by 6 and 4 fold respectively. One exception was higher levels of IFN- $\gamma$  in PBMCs stimulated with SEB were associated with poor survival. These results indicate that the ability of circulating immune cells to produce cytokines in response to stimulation could be used as a prognosis marker in IPF.

## 7. GENERAL DISCUSSION AND FUTURE PERSPECTIVES

---

The first project

*Pseudomonas* quinolone signal (PQS) coordinates the expression of virulence factors of *P. aeruginosa*, promotes the formation of biofilms and has been detected in the CF lung (Collier et al., 2002). In parallel with the fact that the PQS QS system is not essential for bacterial survival (Galloway et al., 2011), it is proposed that disruption of PQS can be a promising treatment to replace antibiotics in the attenuation of pathogenesis of *P. aeruginosa* in the CF. However, little was known about how PQS contributes to *P. aeruginosa* pathogenesis during the initial innate recognition by the human airway epithelium. The purpose of the present study was to investigate whether PQS deficiency affects the interaction of *P. aeruginosa* with differentiated human airway epithelium. This was achieved by infecting human differentiated bronchial-epithelial cells (chapter 3) with wild-type *P. aeruginosa* PAO1 Lausanne (PAO1-L) and its isogenic PQS-deficient mutant  $\Delta pqsA_L$ . Due to an intrinsic loss of a 5.8 kb genomic fragment in PAO1-N that might mask the impact of our target of interest AQS, we re-generated an AQS deficient mutant by depletion of gene *pqsA* in the PAO1-L background with a genomic sequence closer to the original PAO1 strain (Chapter 2). The phenotype of  $\Delta pqsA_L$  was characterised in vitro and showed highly reduced production of AQS, decreased secretion of exotoxins pyocyanin and rhamnolipids, and fragile

biofilms; thus  $\Delta pqsA_L$  displayed a phenotype associated with attenuation (Chapter 2). Bacterial pathogenesis and innate immune recognition by diffCalu-3 cells of PQS-competent and PQS-deficient strains were subsequently assessed by determining bacterial growth within cultures, induction of proinflammatory cytokines (mRNA and protein), activation of TLR-mediated signalling pathways and cytotoxicity (Chapter 4). Further, the efficacy of the in vitro differentiated human epithelial infection model was evaluated using a highly virulent CF isolate LESB58 (Chapter 5). The results indicated that Aqs do not contribute to the initial immune recognition of *P. aeruginosa* by human airway epithelium. CF clinical isolate LESB58 displayed slower growth and caused less damage to the airway epithelium compared to PAO1-L.

Our results show that *P. aeruginosa* infection in airway epithelium initiates through the attachment of bacteria to apical protrusions, bacterial accumulation close to cell junctions and a robust activation of pro-inflammatory mediators (mRNA). Degradation of actin and tight junction proteins was detected at 3 hpi whilst no bacteria could be detected across the epithelial layer. Substantial disruption of actin and tight junction proteins along with breach of barrier integrity, as suggested by the detection of bacteria translocation, occurs at 6 hpi.

In the CF lung, the accumulation of abnormally processed CFTR proteins in the endoplasmic reticulum (ER) results in 'ER stress' and impaired mucociliary clearance leading to dysregulation of the innate immune function and persisted and ineffective airway inflammation (Cohen-Cymerknoh et al., 2013). Our findings are in agreement with previous literature describing secretion by

airway epithelial cells of pro-inflammatory mediators able to recruit and activate phagocytic cells in response to bacterial infection (Gomez and Prince, 2008, Pfeifer et al., 2012). The expression of mRNA encoding for GM-CSF, IL-8, TNF- $\alpha$  and IL-17C in diffCalu-3 cells was highly induced by *P. aeruginosa* PAO1-L infection. TNF- $\alpha$  and the recently identified cytokine IL-17C, are of great interest because of their predominant roles in regulating airway inflammation. TNF- $\alpha$  is considered a pleiotropic cytokine. It confers protection against *P. aeruginosa* in mice as depletion of TNF- $\alpha$  in DBA/2 mice and BALB/c mice using anti-TNF- $\alpha$  antibodies increased susceptibility to *P. aeruginosa* lung infection (Morissette et al., 1996, Gosselin et al., 1995, Sadikot et al., 2005). On the other side it was also found to promote inflammation in CF airways (Mukhopadhyay et al., 2006, Maille et al., 2011). IL-17C, produced by epithelial cells and keratinocytes in an autocrine manner, acts as a pro-inflammatory mediator in the mucosal epithelium upon bacterial and viral infections (Bordon, 2011, Ramirez-Carrozzi et al., 2011, Pfeifer et al., 2012). Although the downstream signaling pathways remain mostly unknown, IL-17C has been shown to promote Th17 cell differentiation via the binding of its receptor IL-17RE on Th17 cells (Chang et al., 2011). The binding of IL-17C/IL-17RE induced the expression of I $\kappa$ B $\xi$  to potentiate the Th17 cell response in a mouse model of autoimmune disease: experimental autoimmune encephalomyelitis (EAE) (Chang et al., 2011, Ramirez-Carrozzi et al., 2011). Of note, IL-17C can work synergistically with TNF- $\alpha$  to promote skin inflammation in psoriasis using a IL-17C transgenic mouse model (Johnston et al., 2012). Recent studies defined CF as a ‘Th17 disease’; Th17 cells and the cytokines IL-17A/F, IL-22 and IL-23, which would promote neutrophil

recruitment to the airways, are increased in CF and might lead to a neutrophil-mediated tissue damage in the CF airways (McAllister et al., 2005, Tan et al., 2011, Brodlie et al., 2011, Decraene et al., 2010). We postulate that IL-17C production by airway epithelial cells upon *P. aeruginosa* infection not only synergistically enhances the induction of TNF- $\alpha$  which could perpetuate the airway inflammation, but also plays a role in shaping the subsequent Th17 response in the adaptive immunity. In combination with our preliminary data, we propose several questions that would be of great importance to further our knowledge on IL-17C and its contribution to the modulation of the Th17 response in the CF: (1) which is the underlying signalling mechanism leading to the production of IL-17C alone or in conjunction with TNF- $\alpha$  in airway epithelial cells upon *P. aeruginosa* infection and the contribution of CFTR expression; (2) would an early inhibition of IL-17C in the airways (or CF airways which is still unknown) dampen a Th17 response and protect from perpetuating inflammation? In the scope of designed immunomodulatory therapy, anti-TNF- $\alpha$  therapy has been tested in CF and showed abrupt stabilization with improved forced expiratory volume (FEV1) (Chmiel and Konstan, 2007, Casserly and Donat, 2009). To promote resolution of chronic inflammation in the CF lung, manipulation of the signalling pathways triggered by pro-inflammatory cytokines (TNF- $\alpha$  and IL-17C for instance) could have beneficial consequences for the host response as it might be possible to stimulate sufficient phagocytic cells for bacterial clearance without overwhelming the lung with inflammation that leads to tissue damage.

The signalling pathways induced during *P. aeruginosa* infection in diffCalu-3 cells were investigated. TLR2, TLR5 and asialoGM1 expressed on the apical

surface of airway epithelial cells have been shown essential for the pro-inflammatory activation upon *P. aeruginosa* infection (Zhang et al., 2005, Tseng et al., 2006, Adamo et al., 2004). The binding of flagellin to TLR5, lipoproteins to TLR2 that together with asioloGM1 trigger the downstream signalling activation cascade through the adaptor protein MyD88/TIRAP, and the subsequent MAPK, ERK-1/2, and AKT-dependent translocation of transcription factors NF- $\kappa$ B, p38 and IRFs resulting in the production of pro-inflammatory cytokines (Adamo et al., 2004, Zhang et al., 2005, McNamara et al., 2006, Tseng et al., 2006, Gomez and Prince, 2008). However, the levels of activation of TLR-associated signalling examined in our study including p38, ERK1/2, NF- $\kappa$ B, IRF7, AKT serine/threonine at 3 hpi were less than 2-fold, and thus cannot be considered biologically significant. This could be attributable to the cytotoxic effects of *P. aeruginosa* as actin degradation and disruption of tight junction proteins were observed at the time when the induction of cell signalling was examined (chapter 4 section 4.5.3.-4.5.5.).

We propose a paradigm of initial activation of the airway epithelium in response to *P. aeruginosa* infection from our results in conjunction with previous established knowledge can be tailored as the following sequence of events: (1) apical protrusions in response to *P. aeruginosa* aggregates (Engel and Eran, 2011, Tran et al., 2014) followed by (2) the recruitment of basolateral proteins PIP<sub>3</sub> to the apical side with localised activation of NF- $\kappa$ B signalling and the subsequent (3) alterations of cellular integrity through actin degradation, disruption of tight junctions and disturbance of gap junctions that lead to apoptosis (Engel and Balachandran, 2009, Losa et al., 2014). The above three steps could be mediated by *P. aeruginosa* effectors (1) type IV pili that

bind to N-glycans at the apical surface; (2) the subversion of polarity facilitated by the binding of flagellum to heparan sulfate proteoglycans that are enriched at the basolateral compartment in the epithelium (Bucior et al., 2010, Bucior et al., 2012); (3) disruption of actin cytoskeleton and tight junctions by the T3SS apparatus and the secreted effector proteins ExoS and ExoT that target Rho family proteins Rho, Rac, and Cdc42, etc. via their N-terminal GTPase activity and C-terminal ADP-ribosyltransferase (ADPRT) domain (Engel and Balachandran, 2009).

In contrast to previous studies indicating immunomodulatory properties of AQ QS molecules on PBMCs and airway epithelial cells via inhibition of pro-inflammatory signalling HIP-1 $\alpha$  and NF- $\kappa$ B in vitro through the use of AQ pure compounds or AQs extracts from bacterial culture supernatants (Kim et al., 2010a, Kim et al., 2010b, Legendre et al., 2012), we demonstrated that the activation of pro-inflammatory responses and the cytotoxicity effect in differentiated human airway epithelial cells during *P. aeruginosa* infection are independent of AQS. We postulate that *P. aeruginosa* pathogenesis on airway epithelial cells is initially driven by the flagellum and T3SS (discussed above), thus the impact of PQS to *P. aeruginosa* pathogenesis at early times could be relatively minor in this setting. Interestingly,  $\Delta$ pqsA<sub>L</sub> infection on the murine model was cleared the next day post infection whereas PAO1-L wild-type kept persisting on the site of infection for 5 days until the end of the experiment, indicating the AQS deficient mutant  $\Delta$ pqsA<sub>L</sub> was indeed attenuated compared to the PAO1-L Wt (In collaboration with Dr. James Lazenby, personal communication). This was performed by the infection of lux-labelled PAO1-L and  $\Delta$ pqsA<sub>L</sub> (PAO1attB::[P<sub>K<sub>m</sub>]-luxCDABE and  $\Delta$ pqsA<sub>L</sub>attB::[P<sub>K<sub>m</sub>]-luxCDABE)</sub></sub>



injected subcutaneously on the back neck of BALB/c mice. This is considered an acute in vivo infection model (Personal communication, Dr. Jeni Lockett). Although the above findings seemed to be contradictory, we propose that the AQs deficiency that deprives  $\Delta pqsA_L$  from establishing biofilms for persistence could be the reason why  $\Delta pqsA_L$  was quickly cleared with the aid of professional immune cells that the initial neutrophil recruitment could be of importance in bacterial clearance in the mouse model. In addition, toxins pyocyanin and rhamnolipid, both positively regulated by AQ QS, produced at higher bacterial cell density such as biofilms, were shown to induce neutrophil apoptosis and necrosis in vitro (Prince et al., 2008) and in vivo (Allen et al., 2005, Van Gennip et al., 2009) which also support our hypothesis that AQ QS could be the positive modulator of virulence in *P. aeruginosa* at later stages with biofilm-like growth predominates. A recent study addressed the importance of timing in neutrophil infiltration in relation to the role of PQS in interfering with neutrophil chemotaxis (Hansch et al., 2014). It was shown that low levels of PQS stimulate the chemotaxis of neutrophils via the MAPK and p38 signalling pathways, whereas high levels of PQS, most likely produced by biofilm-like *P. aeruginosa*, do not interfere with neutrophils phagocytic capability and viability (Hansch et al., 2014). The data indirectly supported our hypothesis that PQS enables *P. aeruginosa* to establish prolonged life-style growth by interfering with the ability of neutrophils to clear bacteria; thus the PQS deficient mutant  $\Delta pqsA_L$  would have lost the advantage for persistence. Neutrophils play a vital role in lung defence by facilitating bacteria clearance. The CF airways are characterised by massive neutrophil accumulation that dominates inflammatory process on the respiratory epithelial surface, and

levels of neutrophil elastase are correlated with poor pulmonary functions (Downey et al., 2009, Gifford and Chalmers, 2014). Neutrophil transmigration is facilitated by the cleavage of epithelial junctional proteins, E-cadherin and occludin for instance, that is mediated by calpains (Ca<sup>2+</sup>-dependent cysteine proteases that target cytoskeletal proteins) via the induction of Ca<sup>2+</sup> flux generated by the activation TLR2 in airway epithelial cells upon *P. aeruginosa* PAO1 infection (Chun and Prince, 2009). The sequential events comprising junctional protein degradation, endocytosis, actin re-distribution and the engagement of neutrophils to eradicate bacterial pathogens in the epithelium are suggested to be essential for maintaining membrane homeostasis (Mege et al., 2006, Chun and Prince, 2009). Our results suggest that the impact of PQS on *P. aeruginosa* pathogenicity might be missed in the context of our single cell culture. To build on our preliminary observation that the reactive oxygen species (ROS) production by neutrophils seemed to be altered upon *P. aeruginosa* stimulation in the presence of exogenous PQS molecules despite the donor variations and the side effect from the PQS diluent need further validation. We propose that AQS might interfere with neutrophil migration across bronchial epithelial monolayer. This could be demonstrated in a multicellular model as follows: bronchial epithelial cells (Calu-3 cells) are to be plated on the underside of 3  $\mu$ M transwells to adhere, flipped over and inserted into 24-well plates. 500  $\mu$ l of culture media will be added to the lower chamber (apical surface of the cell in this condition) and 100  $\mu$ l of media to the transwell (basolateral side of the cells). The lower chamber media will be removed when the cells become confluent, therefore cells will be polarised and differentiated at air-liquid interface. Migration assay is to be performed by

inoculating *P. aeruginosa* PAO1-L Wt or  $\Delta pqsA_L$  at the apical surface (lower chamber) for 3 h (suitable time course experiment could be performed) and neutrophils will be added to the basolateral surface for 2 h (Chun and Prince, 2009). The migration can be observed with immunofluorescent staining focusing at bacteria, neutrophils and calpain junctional protein. Alternatively, neutrophils transmigrated to the apical chamber will be collected, centrifuged, and resuspended in PBS for myeloperoxidase (MPO) assay (Chun and Prince, 2009). The number of neutrophils across the epithelial monolayer will be determined accordingly by the MPO activity generated by a standard curve. Meanwhile, the migration assay of neutrophils can be performed toward *P. aeruginosa* and the chemoattractant fMLP (formyl-Methionyl-Leucyl-Phenylalanine, f-Met-Leu-Phe) as positive control in the absence of an epithelial monolayer. The neutrophil migration assay can be modified by replacing Calu-3 cells with Calu-3 CFTR knock-down cells and CF bronchial epithelial cell line with its correspondent CFTR corrected counterpart (for instance IB3-1 and c38 cell lines) to further evaluate the impact of AQs on *P. aeruginosa* pathogenesis in the condition probably happens in the CF lung.

The lack of differences between Wt and  $\Delta pqsA_L$  raised concerns about the efficacy of the diffCalu-3 epithelial infection model, we therefore infected diffCalu-3 cells with a CF highly transmissible isolate LESB58. Unexpectedly, we demonstrated that the CF clinical strain LESB58 causes less cell damage in actin degradation and junction proteins disruption on airway epithelium compared to that of PAO1-L. This finding was in line with the in vivo data showed that LESB58, although overproduced QS molecules, did not develop biofilms and was cleared in the lung demonstrated by an acute murine

respiratory infection (Carter et al., 2010). Interestingly, this paper also showed that the virulence of the QS-overproducer LESB58 and QS deficient isolate LES400 did not differ suggesting that QS does not influence the virulence of CF isolates in this acute infection setting (Carter et al., 2010). Moreover, another type of *P. aeruginosa* LES isolate LESB65 was examined for its persistence via nasopharyngeal inoculation was successfully demonstrated a clinically relevant in vivo chronic infection model up to 28 days (Fothergill et al., 2014). It was presented for the first time that the long-term adaption of *P. aeruginosa* in the upper respiratory tract was the key leads to the persistence in the lung later on. It was found that LESB65 developed its phenotypes including increased resistance to antibiotics and upregulated expression of genes that relevant to biofilm formation in the nasopharynx that will advance to its persistence and migration to the lower respiratory tract (Fothergill et al., 2014). The re-challenge of evolved isolates after persistence also displayed a more rapid colonisation than the initial inoculated strain (Fothergill et al., 2014). We propose that the attenuated phenotype of LESB58 shown in our in vitro model will also exert a privileged adaptation capability thus caused a long-term virulence if it was inoculated in the environment with chronic infection setting. In addition to targeting actin and tight junction proteins, a study indicated that PAO1 also induces airway epithelial apoptosis via binding to the gap junctional protein connexin43 (Cx43) which is involved in the paracellular transfer of small molecules (Losa et al., 2014). Interestingly, decreased Cx43 expression and reduced apoptosis were observed upon CFTR inhibition in Calu-3 cells (Losa et al., 2014) suggesting that the CFTR dysfunction in the CF lung reduces the efficacy of gap junctional proteins to recognise *P. aeruginosa*

resulting in impaired clearance of infected epithelial cells. The pathogenesis mechanism of LESB58 which characterised by minimal actin and junctional protein disruptions on Calu-3 cells requires further investigation by infecting LESB58 on CF epithelial cell lines to be compared with those performed using the PAO1 strain as well as performing LESB58 infections in the chronic murine model described above.

In summary, we demonstrated that PQS is not beneficial for the initial innate recognition of *P. aeruginosa* by in vitro human bronchial epithelial cells based on bacterial growth, cytotoxicity, and activation of pro-inflammatory responses but could facilitate *P. aeruginosa* persistence in vivo. CF clinical strain LESB58, given the high production of AQS and pyocyanin detected in vitro, and its relatively mild infectivity on the human airway epithelium does not induce drastic airway inflammation but rather persist after initial colonisation.

#### The second project

Previous studies have focused on the function of myofibroblasts and fibroblasts as primary 'effector cells' derived from dysregulated apoptosis of airway epithelial cells in tissue remodelling and fibrosis in IPF. However, recent studies showed that Th2, Th17 cells, macrophages, and other myeloid cell populations are of no less importance in regulating disease progression in IPF (Duffield et al., 2013, Wilson et al., 2010). A considerable knowledge in the pathogenesis of IPF was built using the bleomycin-induced pulmonary fibrosis murine model; however, the mouse model has its limitations as it cannot fully recapitulate the complicated heterogeneous disease pattern in IPF. Despite the fact that potential serum and BAL biomarkers have been reported, the

inconsistent correlations with disease severity and variations among studies stress the need for further validation (van den Blink et al., 2010, Richards et al., 2012, Vij and Noth, 2012). The purpose of the current study was to conduct a comprehensive investigation of systemic immune responses in IPF to 1) identify the profile of cytokine production by PBMCs in response to unbiased stimulation and 2) determine potential cytokine biomarkers in relation to disease severity. We hypothesised that the regulation of immune system in IPF is fundamentally altered and the pulmonary fibrogenesis might be attributed to the action of alternatively activated macrophages induced by a Th2-biased environment. Our study revealed for the first time that PBMCs of patient with IPF were less responsive to a broad panel of antigen stimulation than healthy controls, suggesting that IPF patients are not biased to a particular canonical immune status but immunosuppressed. Lower production of cytokines IFN- $\gamma$ , IL-17A and IL-13 by PBMCs in patients with IPF strongly correlated with reduced survival.

The role of T cells in pulmonary fibrosis has been controversial with reports suggesting that could be promoting fibrosis, anti-fibrotic or have no significant impact per se (Luzina et al., 2008). Pro-inflammatory cytokine IL-17A has been considered pro-fibrotic based on the bleomycin-induced fibrotic mice model and enhanced levels of IL-17A were also found in the BAL of patients with IPF (Wilson et al., 2010). A mechanistic study showed that bleomycin-induced IL-17A production by Th17 cells is co-dependent on TGF- $\beta$ 1 signalling, thereby resulting in the promotion of epithelial-mesenchymal transition (EMT) (Wilson et al., 2010). These findings seem to contradict our result showing that PBMCs in patients with IPF were up to 86% less likely to

produce IL-17A than healthy controls (chapter 6, section 6.5.3.). A recent study mapped the distribution of immunomodulatory cells and inflammation-related markers in the lung biopsy of patients with IPF and tissues were grouped by patterns of severity in disease pathology (Nuovo et al., 2012). IL-17 was shown to be produced by macrophages, CD3<sup>+</sup> T cells and epithelial cells based on the co-expression of markers specific to each cell type. However, the pro-inflammatory cytokines, including IL-17, CCR6, retinoid orphan receptor- $\alpha$ ,  $\beta$ ,  $\gamma$  (ROR- $\alpha$ ,  $\beta$ ,  $\gamma$ ) were predominantly expressed by epithelial cells, suggesting that the amounts of IL-17A detected in the BAL of patients with IPF could be mostly secreted from epithelial cells but not recruited CD3<sup>+</sup> T cells, although which IL-17 isotype was not specified in the above study and the fact that IL-17C isotype being predominantly produced by epithelial cells also needs to be considered (Ramirez-Carrozzi et al., 2011). In addition, CD4<sup>+</sup> Th1-associated cytokine IFN- $\gamma$  and Th2-associated cytokines IL-4, IL-5 and IL-13 have been shown to display contrasting activities regarding the promotion of fibrogenesis (refer to Fig. 1.6).

IL-10 was thought to be produced specifically by CD4<sup>+</sup> Th2 cells, but later studies showed that it was secreted by both Th1 and Th2 cells (Moore et al., 2001). IL-10 is also made by CD4<sup>+</sup>CD25<sup>+</sup>Foxp3<sup>+</sup> regulatory T cells (Tregs) and IL-10-induced CD4<sup>+</sup> Tregs (Tr1 cells) (Moore et al., 2001). An imbalance between protective and detrimental subgroups of Tregs in patients with IPF was shown previously (Kotsianidis et al., 2009). The uncontrolled airway inflammation could be caused by a downregulation of suppressor Tregs and a significant correlation between local and systemic Tregs with lung function was found. The numerical and functional deficiency of Treg as well as the fact

that corticosteroids had no effect in increasing the number of Tregs in patients with IPF also indicated that the regulatory Tregs are defective and unable to counterbalance the airway inflammation (Kotsianidis et al., 2009). In accordance with above findings, our data demonstrating that PBMCs from patients with IPF were less likely to secrete IL-10 could be partly due to a reduced number of peripheral Tregs. Further to the dysregulation found in Tregs population, peripheral blood T-cell anergy due to CD4+CD28<sup>null</sup> cell populations that exhibit a downregulation of T-cell co-stimulatory signalling was also reported (Gilani et al., 2010, Herazo-Maya et al., 2013).

In addition to the immunomodulatory effects from T cells in the peripheral blood, we proposed that defective antigen-presenting cells are also involved in the regulation of pulmonary fibrosis (Gabrilovich and Nagaraj, 2009, Wynn and Barron, 2010). The plasticity of macrophage activation plays a pivotal role in the pathophysiology in pulmonary fibrosis (Wynn, 2011, Wynn et al., 2013). It has been demonstrated that the depletion of macrophages during early inflammation in CD11b-DTR (diphtheria toxin receptor) mice partly relieved the fibrosis, whereas scarring persisted if macrophages were removed during the tissue remodelling stage (Duffield et al., 2005). This study indicated that macrophages adjust their functions for wound healing or fibrosis between the inflammatory and remodelling phases. Additionally, a subset of Th2-activated macrophages that express arginase-1 are anti-fibrotic by promoting myofibroblast apoptosis (Pesce et al., 2009), whereas the Th2 cytokines IL-4 and IL-13 induce another macrophage subpopulations to secrete pro-fibrotic cytokine TGF- $\beta$ 1 (Ingram et al., 2004, Wilson et al., 2010). The above evidence showed that macrophages can adopt different activation states



depending on the stimulation and can be anti-fibrotic or pro-fibrotic. As such, the macrophage activation stage could be indicative of the state of disease progression in patients with IPF. To determine the macrophage activation status of patients with IPF compared with healthy controls, experiments will soon be conducted in our laboratory to analyse the profile of cytokine/chemokine secreted by LPS stimulated CD14+ monocytes derived from PBMCs of cases and controls. Furthermore, to understand the clinical meaning of the state of macrophage activation, the correlation between the macrophage activation profile and clinical data including lung functions, survival will also be conducted.

In this study, the association between cytokine production and the disease was analysed individually. From the discussion above, it is unlikely for one single factor to regulate the disease progression in IPF. For biomarkers to become valuable in clinical practice, we proposed that it would be of great interest to analyse the profile of cytokine production by PBMCs of each individual (a combination of cytokine signature including IFN- $\gamma$ , IL-17A, IL-10, and IL-13 of each individual) together with their medical records and disease outcomes. Advanced statistical analyses such as multivariate clustering will be required. The combination with lung samples, such as biomarkers in BAL and histological patterns will also help to elucidate the underlying mechanism of IPF.

## REFERENCES

---

- ABDEL-MAWGOUD, A. M., LEPINE, F. & DEZIEL, E. 2010. Rhamnolipids: diversity of structures, microbial origins and roles. *Appl Microbiol Biotechnol*, 86, 1323-36.
- ADAMO, R., SOKOL, S., SOONG, G., GOMEZ, M. I. & PRINCE, A. 2004. *Pseudomonas aeruginosa* flagella activate airway epithelial cells through asialoGM1 and toll-like receptor 2 as well as toll-like receptor 5. *Am J Respir Cell Mol Biol*, 30, 627-34.
- AENDEKERK, S., DIGGLE, S. P., SONG, Z., HOIBY, N., CORNELIS, P., WILLIAMS, P. & CAMARA, M. 2005. The MexGHI-OpmD multidrug efflux pump controls growth, antibiotic susceptibility and virulence in *Pseudomonas aeruginosa* via 4-quinolone-dependent cell-to-cell communication. *Microbiology*, 151, 1113-25.
- AIRES, J. R., PECHERE, J. C., VAN DELDEN, C. & KOHLER, T. 2002. Amino acid residues essential for function of the MexF efflux pump protein of *Pseudomonas aeruginosa*. *Antimicrob Agents Chemother*, 46, 2169-73.
- ALBER, A., HOWIE, S. E., WALLACE, W. A. & HIRANI, N. 2012. The role of macrophages in healing the wounded lung. *Int J Exp Pathol*, 93, 243-51.
- ALBERTS, B., JOHNSON, A. & LEWIS, J. 2002. *Molecular Biology of the Cell*, Garland Science.
- ALESSANDRI, A. L., SOUSA, L. P., LUCAS, C. D., ROSSI, A. G., PINHO, V. & TEIXEIRA, M. M. 2013. Resolution of inflammation: mechanisms and opportunity for drug development. *Pharmacol Ther*, 139, 189-212.
- ALLEN, L., DOCKRELL, D. H., PATTERY, T., LEE, D. G., CORNELIS, P., HELLEWELL, P. G. & WHYTE, M. K. 2005. Pyocyanin production by *Pseudomonas aeruginosa* induces neutrophil apoptosis and impairs neutrophil-mediated host defenses in vivo. *J Immunol*, 174, 3643-9.
- ALLESEN-HOLM, M., BARKEN, K. B., YANG, L., KLAUSEN, M., WEBB, J. S., KJELLEBERG, S., MOLIN, S., GIVSKOV, M. & TOLKER-NIELSEN, T. 2006. A characterization of DNA release in *Pseudomonas aeruginosa* cultures and biofilms. *Mol Microbiol*, 59, 1114-28.
- ANDERSSON, C., ZAMAN, M. M., JONES, A. B. & FREEDMAN, S. D. 2008. Alterations in immune response and PPAR/LXR regulation in cystic fibrosis macrophages. *J Cyst Fibros*, 7, 68-78.
- ANGUS, A. A., EVANS, D. J., BARBIERI, J. T. & FLEISZIG, S. M. 2010. The ADP-ribosylation domain of *Pseudomonas aeruginosa* ExoS is required for membrane bleb niche formation and bacterial survival within epithelial cells. *Infect Immun*, 78, 4500-10.
- ARMSTRONG, D., BELL, S., ROBINSON, M., BYE, P., ROSE, B., HARBOUR, C., LEE, C., SERVICE, H., NISSEN, M., SYRMIS, M. & WAINWRIGHT, C. Evidence for spread of a clonal strain of *Pseudomonas aeruginosa* among cystic fibrosis clinics. *J Clin Microbiol*. 2003 May;41(5):2266-7.
- ATKINSON, S., CHANG, C. Y., SOCKETT, R. E., CAMARA, M. & WILLIAMS, P. 2006. Quorum sensing in *Yersinia enterocolitica* controls swimming and swarming motility. *J Bacteriol*, 188, 1451-61.
- AZGHANI, A. O. 1996. *Pseudomonas aeruginosa* and epithelial permeability: role of virulence factors elastase and exotoxin A. *Am J Respir Cell Mol Biol*, 15, 132-40.
- B, B. M., LAWSON, W. E., OURY, T. D., SISSON, T. H., RAGHAVENDRAN, K. & HOGABOAM, C. M. 2013. Animal models of fibrotic lung disease. *Am J Respir Cell Mol Biol*, 49, 167-79.
- BACCALA, R., GONZALEZ-QUINTIAL, R., LAWSON, B. R., STERN, M. E., KONO, D. H., BEUTLER, B. & THEOFILOPOULOS, A. N. 2009. Sensors of the innate immune system: their mode of action. *Nat Rev Rheumatol*, 5, 448-56.
- BAKER, M. D. & ACHARYA, K. R. 2004. Superantigens: structure-function relationships. *Int J Med Microbiol*, 293, 529-37.
- BALABAN, N. & RASOOLY, A. 2000. Staphylococcal enterotoxins. *Int J Food Microbiol*, 61, 1-10.
- BALLINGER, M. N., PAINE, R., 3RD, SEREZANI, C. H., ARONOFF, D. M., CHOI, E. S., STANDIFORD, T. J., TOEWS, G. B. & MOORE, B. B. 2006. Role of granulocyte

- macrophage colony-stimulating factor during gram-negative lung infection with *Pseudomonas aeruginosa*. *Am J Respir Cell Mol Biol*, 34, 766-74.
- BARGAGLI, E., PRASSE, A., OLIVIERI, C., MULLER-QUERNHEIM, J. & ROTTOLI, P. 2011. Macrophage-derived biomarkers of idiopathic pulmonary fibrosis. *Pulm Med*, 717130, 29.
- BARKAUSKAS, C. E., CRONCE, M. J., RACKLEY, C. R., BOWIE, E. J., KEENE, D. R., STRIPP, B. R., RANDELL, S. H., NOBLE, P. W. & HOGAN, B. L. 2013a. Type 2 alveolar cells are stem cells in adult lung. *J Clin Invest*, 123, 3025-36.
- BARKAUSKAS, C. E., CRONCE, M. J., RACKLEY, C. R., BOWIE, E. J., KEENE, D. R., STRIPP, B. R., RANDELL, S. H., NOBLE, P. W. & HOGAN, B. L. M. 2013b. Type 2 alveolar cells are stem cells in adult lung. *The Journal of Clinical Investigation*, 123, 3025-3036.
- BARNES, P. J. 2004. Alveolar macrophages as orchestrators of COPD. *Copd*, 1, 59-70.
- BARNES, P. J. 2008. Immunology of asthma and chronic obstructive pulmonary disease. *Nat Rev Immunol*, 8, 183-92.
- BARRILA, J., RADTKE, A. L., CRABBE, A., SARKER, S. F., HERBST-KRALOVETZ, M. M., OTT, C. M. & NICKERSON, C. A. 2010. Organotypic 3D cell culture models: using the rotating wall vessel to study host-pathogen interactions. *Nat Rev Microbiol*, 8, 791-801.
- BARTLING, T. R. & DRUMM, M. L. 2009. Oxidative stress causes IL8 promoter hyperacetylation in cystic fibrosis airway cell models. *Am J Respir Cell Mol Biol*, 40, 58-65.
- BAUM, B. & GEORGIU, M. 2011. Dynamics of adherens junctions in epithelial establishment, maintenance, and remodeling. *J Cell Biol*, 192, 907-17.
- BÉDARD, M., MCCLURE, C. D., SCHILLER, N. L., FRANCOEUR, C., CANTIN, A. & DENIS, M. 1993. Release of Interleukin-8, Interleukin-6, and Colony-stimulating Factors by Upper Airway Epithelial Cells: Implications for Cystic Fibrosis. *American journal of respiratory cell and molecular biology*, 9, 455-462.
- BERUBE, K., PRYTHERCH, Z., JOB, C. & HUGHES, T. 2010. Human primary bronchial lung cell constructs: the new respiratory models. *Toxicology*, 278, 311-8.
- BLOHMKE, C. J., PARK, J., HIRSCHFELD, A. F., VICTOR, R. E., SCHNEIDERMAN, J., STEFANOWICZ, D., CHILVERS, M. A., DURIE, P. R., COREY, M., ZIELENSKI, J., DORFMAN, R., SANDFORD, A. J., DALEY, D. & TURVEY, S. E. 2010. TLR5 as an anti-inflammatory target and modifier gene in cystic fibrosis. *J Immunol*, 185, 7731-8.
- BLUMBERG, P. M. 1988. Protein kinase C as the receptor for the phorbol ester tumor promoters: sixth Rhoads memorial award lecture. *Cancer Res*, 48, 1-8.
- BOLES, B. R., THOENDEL, M. & SINGH, P. K. 2005. Rhamnolipids mediate detachment of *Pseudomonas aeruginosa* from biofilms. *Mol Microbiol*, 57, 1210-23.
- BORDON, Y. 2011. Cytokines: IL-17C joins the family firm. *Nat Rev Immunol*, 11, 805.
- BOUCHERAT, O., BOCZKOWSKI, J., JEANNOTTE, L. & DELACOURT, C. 2013. Cellular and molecular mechanisms of goblet cell metaplasia in the respiratory airways. *Exp Lung Res*, 39, 207-16.
- BRENNAN, S., SLY, P. D., GANGELL, C. L., STURGES, N., WINFIELD, K., WIKSTROM, M., GARD, S. & UPHAM, J. W. 2009. Alveolar macrophages and CC chemokines are increased in children with cystic fibrosis. *Eur Respir J*, 34, 655-61.
- BRINGARDNER, B. D., BARAN, C. P., EUBANK, T. D. & MARSH, C. B. 2008. The role of inflammation in the pathogenesis of idiopathic pulmonary fibrosis. *Antioxid Redox Signal*, 10, 287-301.
- BRODLIE, M., MCKEAN, M. C., JOHNSON, G. E., ANDERSON, A. E., HILKENS, C. M., FISHER, A. J., CORRIS, P. A., LORDAN, J. L. & WARD, C. 2011. Raised interleukin-17 is immunolocalised to neutrophils in cystic fibrosis lung disease. *Eur Respir J*, 37, 1378-85.
- BRYANT, D. M. & MOSTOV, K. E. 2008. From cells to organs: building polarized tissue. *Nat Rev Mol Cell Biol*, 9, 887-901.
- BUCIOR, I., MOSTOV, K. & ENGEL, J. N. 2010. *Pseudomonas aeruginosa*-mediated damage requires distinct receptors at the apical and basolateral surfaces of the polarized epithelium. *Infect Immun*, 78, 939-53.

- BUCIOR, I., PIELAGE, J. F. & ENGEL, J. N. 2012. Pseudomonas aeruginosa Pili and Flagella Mediate Distinct Binding and Signaling Events at the Apical and Basolateral Surface of Airway Epithelium. *PLoS Pathog*, 8, e1002616.
- BURCH, P. M. & HEINTZ, N. H. 2005. Redox regulation of cell-cycle re-entry: cyclin D1 as a primary target for the mitogenic effects of reactive oxygen and nitrogen species. *Antioxid Redox Signal*, 7, 741-51.
- CAI, Z., SCOTT-WARD, T. S., LI, H., SCHMIDT, A. & SHEPPARD, D. N. 2004. Strategies to investigate the mechanism of action of CFTR modulators. *J Cyst Fibros*, 2, 141-7.
- CAIAZZA, N. C., SHANKS, R. M. & O'TOOLE, G. A. 2005. Rhamnolipids modulate swarming motility patterns of Pseudomonas aeruginosa. *J Bacteriol*, 187, 7351-61.
- CALDWELL, C. C., CHEN, Y., GOETZMANN, H. S., HAO, Y., BORCHERS, M. T., HASSETT, D. J., YOUNG, L. R., MAVRODI, D., THOMASHOW, L. & LAU, G. W. 2009. Pseudomonas aeruginosa exotoxin pyocyanin causes cystic fibrosis airway pathogenesis. *Am J Pathol*, 175, 2473-88.
- CAMPODONICO, V. L., GADJEVA, M., PARADIS-BLEAU, C., ULUER, A. & PIER, G. B. 2008. Airway epithelial control of Pseudomonas aeruginosa infection in cystic fibrosis. *Trends Mol Med*, 14, 120-33.
- CAO, H., KRISHNAN, G., GOUMNEROV, B., TSONGALIS, J., TOMPKINS, R. & RAHME, L. G. 2001. A quorum sensing-associated virulence gene of Pseudomonas aeruginosa encodes a LysR-like transcription regulator with a unique self-regulatory mechanism. *Proc Natl Acad Sci U S A*, 98, 14613-8.
- CARTER, M. E., FOTHERGILL, J. L., WALSHAW, M. J., RAJAKUMAR, K., KADIOGLU, A. & WINSTANLEY, C. 2010. A subtype of a Pseudomonas aeruginosa cystic fibrosis epidemic strain exhibits enhanced virulence in a murine model of acute respiratory infection. *J Infect Dis*, 202, 935-42.
- CASSERLY, B. & DONAT, W. 2009. Stabilization of lung function and clinical symptoms in a patient with cystic fibrosis (CF) after institution of infliximab: a monoclonal antibody that binds tumor necrosis factor alpha. *Lung*, 187, 149-52.
- CHANG, M. S., CHEN, B. C., YU, M. T., SHEU, J. R., CHEN, T. F. & LIN, C. H. 2005. Phorbol 12-myristate 13-acetate upregulates cyclooxygenase-2 expression in human pulmonary epithelial cells via Ras, Raf-1, ERK, and NF-kappaB, but not p38 MAPK, pathways. *Cell Signal*, 17, 299-310.
- CHANG, S. H., REYNOLDS, J. M., PAPPU, B. P., CHEN, G., MARTINEZ, G. J. & DONG, C. 2011. Interleukin-17C promotes Th17 cell responses and autoimmune disease via interleukin-17 receptor E. *Immunity*, 35, 611-21.
- CHEN, J. & STUBBE, J. 2005. Bleomycins: towards better therapeutics. *Nat Rev Cancer*, 5, 102-12.
- CHENG, K., SMYTH, R. L., GOVAN, J. R., DOHERTY, C., WINSTANLEY, C., DENNING, N., HEAF, D. P., VAN SAENE, H. & HART, C. A. 1996. Spread of beta-lactam-resistant Pseudomonas aeruginosa in a cystic fibrosis clinic. *Lancet*, 348, 639-42.
- CHMIEL, J. F. & KONSTAN, M. W. 2007. Inflammation and anti-inflammatory therapies for cystic fibrosis. *Clin Chest Med*, 28, 331-46.
- CHRISTMAS, S. E., DE LA MATA ESPINOSA, C. T., HALLIDAY, D., BUXTON, C. A., CUMMERSON, J. A. & JOHNSON, P. M. 2006. Levels of expression of complement regulatory proteins CD46, CD55 and CD59 on resting and activated human peripheral blood leucocytes. *Immunology*, 119, 522-8.
- CHRISTOVA, N., TULEVA, B., LALCHEV, Z., JORDANOVA, A. & JORDANOV, B. 2004. Rhamnolipid biosurfactants produced by Renibacterium salmoninarum 27BN during growth on n-hexadecane. *Z Naturforsch C*, 59, 70-4.
- CHUN, J. & PRINCE, A. 2009. TLR2-induced calpain cleavage of epithelial junctional proteins facilitates leukocyte transmigration. *Cell Host Microbe*, 5, 47-58.
- COHEN-CYMBERKNOH, M., KEREM, E., FERKOL, T. & ELIZUR, A. 2013. Airway inflammation in cystic fibrosis: molecular mechanisms and clinical implications. *Thorax*, 68, 1157-62.
- COHEN, T. S. & PRINCE, A. 2012. Cystic fibrosis: a mucosal immunodeficiency syndrome. *Nat Med*, 18, 509-19.
- COLLIER, D. N., ANDERSON, L., MCKNIGHT, S. L., NOAH, T. L., KNOWLES, M., BOUCHER, R., SCHWAB, U., GILLIGAN, P. & PESCI, E. C. 2002. A bacterial cell to cell signal in the lungs of cystic fibrosis patients. *FEMS Microbiol Lett*, 215, 41-6.

- COOLEY, M., CHHABRA, S. R. & WILLIAMS, P. 2008. N-Acylhomoserine lactone-mediated quorum sensing: a twist in the tail and a blow for host immunity. *Chemistry & Biology*, 15, 1141-1147.
- COWELL, B. A., EVANS, D. J. & FLEISZIG, S. M. 2005. Actin cytoskeleton disruption by ExoY and its effects on *Pseudomonas aeruginosa* invasion. *FEMS Microbiol Lett*, 250, 71-6.
- COZENS, A. L., YEZZI, M. J., KUNZELMANN, K., OHRUI, T., CHIN, L., ENG, K., FINKBEINER, W. E., WIDDICOMBE, J. H. & GRUENERT, D. C. 1994. CFTR expression and chloride secretion in polarized immortal human bronchial epithelial cells. *Am J Respir Cell Mol Biol*, 10, 38-47.
- CROUCH, E. & WRIGHT, J. R. 2001. Surfactant proteins a and d and pulmonary host defense. *Annu Rev Physiol*, 63, 521-54.
- D'ARGENIO, D. A., CALFEE, M. W., RAINEY, P. B. & PESCI, E. C. 2002. Autolysis and autoaggregation in *Pseudomonas aeruginosa* colony morphology mutants. *J Bacteriol*, 184, 6481-9.
- DAS, T., KUTTY, S. K., KUMAR, N. & MANEFIELD, M. 2013. Pyocyanin facilitates extracellular DNA binding to *Pseudomonas aeruginosa* influencing cell surface properties and aggregation. *PLoS One*, 8, 11.
- DASENBROOK, E. C., MERLO, C. A., DIENER-WEST, M., LECHTZIN, N. & BOYLE, M. P. 2008. Persistent methicillin-resistant *Staphylococcus aureus* and rate of FEV1 decline in cystic fibrosis. *Am J Respir Crit Care Med*, 178, 814-21.
- DAVEY, M. E., CAIAZZA, N. C. & O'TOOLE, G. A. 2003. Rhamnolipid surfactant production affects biofilm architecture in *Pseudomonas aeruginosa* PAO1. *J Bacteriol*, 185, 1027-36.
- DECRAENE, A., WILLEMS-WIDYASTUTI, A., KASRAN, A., DE BOECK, K., BULLENS, D. M. & DUPONT, L. J. 2010. Elevated expression of both mRNA and protein levels of IL-17A in sputum of stable Cystic Fibrosis patients. *Respir Res*, 11, 1465-9921.
- DECRAMER, M., JANSSENS, W. & MIRAVITLLES, M. 2012. Chronic obstructive pulmonary disease. *Lancet*, 379, 1341-1351.
- DEGRYSE, A. L. & LAWSON, W. E. 2011. Progress toward improving animal models for idiopathic pulmonary fibrosis. *Am J Med Sci*, 341, 444-9.
- DEKIMPE, V. & DEZIEL, E. 2009. Revisiting the quorum-sensing hierarchy in *Pseudomonas aeruginosa*: the transcriptional regulator RhIR regulates LasR-specific factors. *Microbiology*, 155, 712-23.
- DEMEDTS, M., BEHR, J., BUHL, R., COSTABEL, U., DEKHUIJZEN, R., JANSEN, H. M., MACNEE, W., THOMEER, M., WALLAERT, B., LAURENT, F., NICHOLSON, A. G., VERBEKEN, E. K., VERSCHAKELLEN, J., FLOWER, C. D., CAPRON, F., PETRUZZELLI, S., DE VUYST, P., VAN DEN BOSCH, J. M., RODRIGUEZ-BECERRA, E., CORVASCE, G., LANKHORST, I., SARDINA, M. & MONTANARI, M. 2005. High-dose acetylcysteine in idiopathic pulmonary fibrosis. *N Engl J Med*, 353, 2229-42.
- DENNING, G. M., ANDERSON, M. P., AMARA, J. F., MARSHALL, J., SMITH, A. E. & WELSH, M. J. 1992a. Processing of mutant cystic fibrosis transmembrane conductance regulator is temperature-sensitive. *Nature*, 358, 761-4.
- DENNING, G. M., OSTEDGAARD, L. S., CHENG, S. H., SMITH, A. E. & WELSH, M. J. 1992b. Localization of cystic fibrosis transmembrane conductance regulator in chloride secretory epithelia. *J Clin Invest*, 89, 339-49.
- DERICHS, N. 2013. Targeting a genetic defect: cystic fibrosis transmembrane conductance regulator modulators in cystic fibrosis. *Eur Respir Rev*, 22, 58-65.
- DEVOR, D. C., SINGH, A. K., LAMBERT, L. C., DELUCA, A., FRIZZELL, R. A. & BRIDGES, R. J. 1999. Bicarbonate and chloride secretion in Calu-3 human airway epithelial cells. *J Gen Physiol*, 113, 743-60.
- DEZIEL, E., GOPALAN, S., TAMPKAKAKI, A. P., LEPINE, F., PADFIELD, K. E., SAUCIER, M., XIAO, G. & RAHME, L. G. 2005. The contribution of MvfR to *Pseudomonas aeruginosa* pathogenesis and quorum sensing circuitry regulation: multiple quorum sensing-regulated genes are modulated without affecting lasRI, rhIRI or the production of N-acyl-L-homoserine lactones. *Mol Microbiol*, 55, 998-1014.
- DEZIEL, E., LEPINE, F., MILOT, S. & VILLEMUR, R. 2003. rhIA is required for the production of a novel biosurfactant promoting swarming motility in *Pseudomonas*

- aeruginosa: 3-(3-hydroxyalkanoyloxy)alkanoic acids (HAAs), the precursors of rhamnolipids. *Microbiology*, 149, 2005-13.
- DIAZ, M. R., KING, J. M. & YAHR, T. L. 2011. Intrinsic and extrinsic regulation of type III secretion gene expression in *Pseudomonas aeruginosa*. *Front Microbiol*, 2, 00089.
- DIGGLE, S. P., CORNELIS, P., WILLIAMS, P. & CAMARA, M. 2006a. 4-quinolone signalling in *Pseudomonas aeruginosa*: old molecules, new perspectives. *Int J Med Microbiol*, 296, 83-91.
- DIGGLE, S. P., MATTHIJS, S., WRIGHT, V. J., FLETCHER, M. P., CHHABRA, S. R., LAMONT, I. L., KONG, X., HIDER, R. C., CORNELIS, P., CAMARA, M. & WILLIAMS, P. 2007. The *Pseudomonas aeruginosa* 4-quinolone signal molecules HHQ and PQS play multifunctional roles in quorum sensing and iron entrapment. *Chem Biol*, 14, 87-96.
- DIGGLE, S. P., STACEY, R. E., DODD, C., CAMARA, M., WILLIAMS, P. & WINZER, K. 2006b. The galactophilic lectin, LecA, contributes to biofilm development in *Pseudomonas aeruginosa*. *Environ Microbiol*, 8, 1095-104.
- DIGGLE, S. P., WINZER, K., CHHABRA, S. R., WORRALL, K. E., CAMARA, M. & WILLIAMS, P. 2003. The *Pseudomonas aeruginosa* quinolone signal molecule overcomes the cell density-dependency of the quorum sensing hierarchy, regulates rhl-dependent genes at the onset of stationary phase and can be produced in the absence of LasR. *Mol Microbiol*, 50, 29-43.
- DOCKRELL, H. M., YOUNG, S. K., BRITTON, K., BRENNAN, P. J., RIVOIRE, B., WATERS, M. F., LUCAS, S. B., SHAHID, F., DOJKI, M., CHIANG, T. J., EHSAN, Q., MCADAM, K. P. & HUSSAIN, R. 1996. Induction of Th1 cytokine responses by mycobacterial antigens in leprosy. *Infect Immun*, 64, 4385-9.
- DOSEL, J., MEYER-HOFFERT, U., SCHRODER, J. M. & GERSTEL, U. 2012. *Pseudomonas aeruginosa*-derived rhamnolipids subvert the host innate immune response through manipulation of the human beta-defensin-2 expression. *Cell Microbiol*, 14, 1364-75.
- DOWNEY, D. G., BELL, S. C. & ELBORN, J. S. 2009. Neutrophils in cystic fibrosis. *Thorax*, 64, 81-8.
- DUFFIELD, J. S., FORBES, S. J., CONSTANDINOU, C. M., CLAY, S., PARTOLINA, M., VUTHOORI, S., WU, S., LANG, R. & IREDALE, J. P. 2005. Selective depletion of macrophages reveals distinct, opposing roles during liver injury and repair. *J Clin Invest*, 115, 56-65.
- DUFFIELD, J. S., LUPHER, M., THANNICKAL, V. J. & WYNN, T. A. 2013. Host responses in tissue repair and fibrosis. *Annu Rev Pathol*, 8, 241-76.
- DULCEY, C. E., DEKIMPE, V., FAUVELLE, D. A., MILOT, S., GROLEAU, M. C., DOUCET, N., RAHME, L. G., LEPINE, F. & DEZIEL, E. 2013. The end of an old hypothesis: the *pseudomonas* signaling molecules 4-hydroxy-2-alkylquinolines derive from fatty acids, not 3-ketofatty acids. *Chem Biol*, 20, 1481-91.
- EBERL, L. 2006. Quorum sensing in the genus *Burkholderia*. *Int J Med Microbiol*, 296, 103-10.
- EDENBOROUGH, F. P., STONE, H. R., KELLY, S. J., ZADIK, P., DOHERTY, C. J. & GOVAN, J. R. 2004. Genotyping of *Pseudomonas aeruginosa* in cystic fibrosis suggests need for segregation. *J Cyst Fibros*, 3, 37-44.
- EHRE, C., WORTHINGTON, E. N., LIESMAN, R. M., GRUBB, B. R., BARBIER, D., O'NEAL, W. K., SALLENAVE, J. M., PICKLES, R. J. & BOUCHER, R. C. 2012. Overexpressing mouse model demonstrates the protective role of Muc5ac in the lungs. *Proc Natl Acad Sci U S A*, 109, 16528-33.
- EISELE, N. A. & ANDERSON, D. M. 2011. Host defense and the airway epithelium: frontline responses that protect against bacterial invasion and pneumonia. *J Pathog*, 249802, 22.
- EL SOLH, A. A., AKINNUSI, M. E., WIENER-KRONISH, J. P., LYNCH, S. V., PINEDA, L. A. & SZARPA, K. 2008. Persistent infection with *Pseudomonas aeruginosa* in ventilator-associated pneumonia. *Am J Respir Crit Care Med*, 178, 513-9.
- ENGBRECHT, J. & SILVERMAN, M. 1984. Identification of genes and gene products necessary for bacterial bioluminescence. *Proc Natl Acad Sci U S A*, 81, 4154-8.
- ENGEL, J. & BALACHANDRAN, P. 2009. Role of *Pseudomonas aeruginosa* type III effectors in disease. *Curr Opin Microbiol*, 12, 61-66.
- ENGEL, J. & ERAN, Y. 2011. Subversion of mucosal barrier polarity by *Pseudomonas aeruginosa*. *Front Microbiol*, 2, 26.

- ENGELMAN, J. A. 2009. Targeting PI3K signalling in cancer: opportunities, challenges and limitations. *Nat Rev Cancer*, 9, 550-62.
- ESSAR, D. W., EBERLY, L., HADERO, A. & CRAWFORD, I. P. 1990. Identification and characterization of genes for a second anthranilate synthase in *Pseudomonas aeruginosa*: interchangeability of the two anthranilate synthases and evolutionary implications. *J Bacteriol*, 172, 884-900.
- FAHEY, J. V., SCHAEFER, T. M., CHANNON, J. Y. & WIRA, C. R. 2005. Secretion of cytokines and chemokines by polarized human epithelial cells from the female reproductive tract. *Hum Reprod*, 20, 1439-1446.
- FLETCHER, M. 2007. Biosynthesis and regulation of 2-Alkyl-4-Quinolones in *Pseudomonas aeruginosa*. PhD, University of Nottingham, UK.
- FLETCHER, M. P., DIGGLE, S. P., CAMARA, M. & WILLIAMS, P. 2007. Biosensor-based assays for PQS, HHQ and related 2-alkyl-4-quinolone quorum sensing signal molecules. *Nat Protoc*, 2, 1254-62.
- FLOREA, B. I., CASSARA, M. L., JUNGINGER, H. E. & BORCHARD, G. 2003. Drug transport and metabolism characteristics of the human airway epithelial cell line Calu-3. *Journal of controlled release*, 87, 131-138.
- FOGH, J., FOGH, J. M. & ORFEO, T. 1977. One hundred and twenty-seven cultured human tumor cell lines producing tumors in nude mice. *J Natl Cancer Inst*, 59, 221-6.
- FOLCH, B., DEZIEL, E. & DOUCET, N. 2013. Systematic mutational analysis of the putative hydrolase PqsE: toward a deeper molecular understanding of virulence acquisition in *Pseudomonas aeruginosa*. *PLoS One*, 8.
- FOTHERGILL, J. L., NEILL, D. R., LOMAN, N., WINSTANLEY, C. & KADIOGLU, A. 2014. *Pseudomonas aeruginosa* adaptation in the nasopharyngeal reservoir leads to migration and persistence in the lungs. *Nat Commun*, 5.
- FOTHERGILL, J. L., PANAGEA, S., HART, C. A., WALSHAW, M. J., PITT, T. L. & WINSTANLEY, C. 2007. Widespread pyocyanin over-production among isolates of a cystic fibrosis epidemic strain. *BMC Microbiol*, 7, 45.
- FRANKS, T. M. & HETZER, M. W. 2013. The role of Nup98 in transcription regulation in healthy and diseased cells. *Trends Cell Biol*, 23, 112-7.
- GABRILOVICH, D. I. & NAGARAJ, S. 2009. Myeloid-derived suppressor cells as regulators of the immune system. *Nat Rev Immunol*, 9, 162-74.
- GALLOWAY, W. R., HODGKINSON, J. T., BOWDEN, S. D., WELCH, M. & SPRING, D. R. 2011. Quorum sensing in Gram-negative bacteria: small-molecule modulation of AHL and AI-2 quorum sensing pathways. *Chem Rev*, 111, 28-67.
- GASSE, P., RITEAU, N., VACHER, R., MICHEL, M. L., FAUTREL, A., DI PADOVA, F., FICK, L., CHARRON, S., LAGENTE, V., EBERL, G., LE BERT, M., QUESNIAUX, V. F., HUAUX, F., LEITE-DE-MORAES, M., RYFFEL, B. & COUILLIN, I. 2011. IL-1 and IL-23 mediate early IL-17A production in pulmonary inflammation leading to late fibrosis. *PLoS One*, 6, 16.
- GEIJTENBEEK, TEUNIS B. H. 2012. Actin' as a Death Signal. *Immunity*, 36, 557-559.
- GERSTEL, U., CZAPP, M., BARTELS, J. & SCHRODER, J. M. 2009. Rhamnolipid-induced shedding of flagellin from *Pseudomonas aeruginosa* provokes hBD-2 and IL-8 response in human keratinocytes. *Cell Microbiol*, 11, 842-53.
- GHARAEI-KERMANI, M., ULLENBRUCH, M. & PHAN, S. H. 2005. Animal models of pulmonary fibrosis. *Methods Mol Med*, 117, 251-9.
- GIFFORD, A. M. & CHALMERS, J. D. 2014. The role of neutrophils in cystic fibrosis. *Curr Opin Hematol*, 21, 16-22.
- GILANI, S. R., VUGA, L. J., LINDELL, K. O., GIBSON, K. F., XUE, J., KAMINSKI, N., VALENTINE, V. G., LINDSAY, E. K., GEORGE, M. P., STEELE, C. & DUNCAN, S. R. 2010. CD28 down-regulation on circulating CD4 T-cells is associated with poor prognoses of patients with idiopathic pulmonary fibrosis. *PLoS One*, 5, 0008959.
- GODFREY, R. W. 1997. Human airway epithelial tight junctions. *Microsc Res Tech*, 38, 488-99.
- GOMEZ, M. I. & PRINCE, A. 2008. Airway epithelial cell signaling in response to bacterial pathogens. *Pediatr Pulmonol*, 43, 11-9.
- GONZALEZ-MARISCAL, L., BETANZOS, A., NAVA, P. & JARAMILLO, B. E. 2003. Tight junction proteins. *Prog Biophys Mol Biol*, 81, 1-44.

- GOSSELIN, D., DESANCTIS, J., BOULE, M., SKAMENE, E., MATOUK, C. & RADZIOCH, D. 1995. Role of tumor necrosis factor alpha in innate resistance to mouse pulmonary infection with *Pseudomonas aeruginosa*. *Infect Immun*, 63, 3272-8.
- GRAHAM, A., STEEL, D. M., WILSON, R., COLE, P. J., ALTON, E. W. & GEDDES, D. M. 1993. Effects of purified *Pseudomonas rhamnolipids* on bioelectric properties of sheep tracheal epithelium. *Exp Lung Res*, 19, 77-89.
- GRAINGER, C. I., GREENWELL, L. L., LOCKLEY, D. J., MARTIN, G. P. & FORBES, B. 2006. Culture of Calu-3 cells at the air interface provides a representative model of the airway epithelial barrier. *Pharmaceutical Research*, 23, 1482-1490.
- GRANT, S. G., JESSEE, J., BLOOM, F. R. & HANAHAHAN, D. 1990. Differential plasmid rescue from transgenic mouse DNAs into *Escherichia coli* methylation-restriction mutants. *Proc Natl Acad Sci U S A*, 87, 4645-9.
- GREENE, C. M. & MCELVANEY, N. G. 2005. Toll-like receptor expression and function in airway epithelial cells. *Arch Immunol Ther Exp*, 53, 418-27.
- GUILLOT, L., MEDJANE, S., LE-BARILLEC, K., BALLOY, V., DANIEL, C., CHIGNARD, M. & SI-TAHAR, M. 2004. Response of human pulmonary epithelial cells to lipopolysaccharide involves Toll-like receptor 4 (TLR4)-dependent signaling pathways: evidence for an intracellular compartmentalization of TLR4. *J Biol Chem*, 279, 2712-8.
- GUINA, T., PURVINE, S. O., YI, E. C., ENG, J., GOODLETT, D. R., AEBERSOLD, R. & MILLER, S. I. 2003. Quantitative proteomic analysis indicates increased synthesis of a quinolone by *Pseudomonas aeruginosa* isolates from cystic fibrosis airways. *Proc Natl Acad Sci U S A*, 100, 2771-6.
- HA, D. G., MERRITT, J. H., HAMPTON, T. H., HODGKINSON, J. T., JANECEK, M., SPRING, D. R., WELCH, M. & O'TOOLE, G. A. 2011. 2-Heptyl-4-quinolone, a precursor of the *Pseudomonas* quinolone signal molecule, modulates swarming motility in *Pseudomonas aeruginosa*. *J Bacteriol*, 193, 6770-80.
- HALLSTRAND, T. S., HACKETT, T. L., ALTEMEIER, W. A., MATUTE-BELLO, G., HANSBRO, P. M. & KNIGHT, D. A. 2014. Airway epithelial regulation of pulmonary immune homeostasis and inflammation. *Clin Immunol*, 151, 1-15.
- HAMILTON, J. A. 2008. Colony-stimulating factors in inflammation and autoimmunity. *Nat Rev Immunol*, 8, 533-544.
- HAMS, E., ARMSTRONG, M. E., BARLOW, J. L., SAUNDERS, S. P., SCHWARTZ, C., COOKE, G., FAHY, R. J., CROTTY, T. B., HIRANI, N., FLYNN, R. J., VOEHRINGER, D., MCKENZIE, A. N., DONNELLY, S. C. & FALLON, P. G. 2014. IL-25 and type 2 innate lymphoid cells induce pulmonary fibrosis. *Proc Natl Acad Sci U S A*, 111, 367-72.
- HAN, Z. T., TONG, Y. K., HE, L. M., ZHANG, Y., SUN, J. Z., WANG, T. Y., ZHANG, H., CUI, Y. L., NEWMARK, H. L., CONNEY, A. H. & CHANG, R. L. 1998. 12-O-Tetradecanoylphorbol-13-acetate (TPA)-induced increase in depressed white blood cell counts in patients treated with cytotoxic cancer chemotherapeutic drugs. *Proc Natl Acad Sci U S A*, 95, 5362-5.
- HANCOCK, J. T., DESIKAN, R. & NEILL, S. J. 2001. Role of reactive oxygen species in cell signalling pathways. *Biochem Soc Trans*, 29, 345-50.
- HANSCH, G. M. 2012. Host Defence against Bacterial Biofilms: "Mission Impossible"? *ISRN Immunology*, 2012, 17.
- HANSCH, G. M., PRIOR, B., BRENNER-WEISS, G., OBST, U. & OVERHAGE, J. 2014. The *Pseudomonas* quinolone signal (PQS) stimulates chemotaxis of polymorphonuclear neutrophils. *J Appl Biomater Funct Mater*, 9, 5000204.
- HAO, Y., KUANG, Z., WALLING, B. E., BHATIA, S., SIVAGURU, M., CHEN, Y., GASKINS, H. R. & LAU, G. W. 2012. *Pseudomonas aeruginosa* pyocyanin causes airway goblet cell hyperplasia and metaplasia and mucus hypersecretion by inactivating the transcriptional factor FoxA2. *Cell Microbiol*, 14, 401-15.
- HARCOURT, J. L., CAIDI, H., ANDERSON, L. J. & HAYNES, L. M. 2011. Evaluation of the Calu-3 cell line as a model of in vitro respiratory syncytial virus infection. *J Virol Methods*, 174, 144-9.
- HARTL, D., GRIESE, M., KAPPLER, M., ZISSEL, G., REINHARDT, D., REBHAN, C., SCHENDEL, D. J. & KRAUSS-ETSCHMANN, S. 2006. Pulmonary T(H)2 response in *Pseudomonas aeruginosa*-infected patients with cystic fibrosis. *J Allergy Clin Immunol*, 117, 204-11.



- HAUSER, A. R., JAIN, M., BAR-MEIR, M. & MCCOLLEY, S. A. 2011. Clinical significance of microbial infection and adaptation in cystic fibrosis. *Clin Microbiol Rev*, 24, 29-70.
- HAWS, C., FINKBEINER, W. E., WIDDICOMBE, J. H. & WINE, J. J. 1994. CFTR in Calu-3 human airway cells: channel properties and role in cAMP-activated Cl<sup>-</sup> conductance. *Am J Physiol*, 266, L502-12.
- HAZAN, R., HE, J., XIAO, G., DEKIMPE, V., APIDIANAKIS, Y., LESIC, B., ASTRAKAS, C., DEZIEL, E., LEPINE, F. & RAHME, L. G. 2010. Homeostatic interplay between bacterial cell-cell signaling and iron in virulence. *PLoS Pathog*, 6, 1000810.
- HE, J. Q., SANDFORD, A. J., WANG, I. M., STEPANIANTS, S., KNIGHT, D. A., KICIC, A., STICK, S. M. & PARE, P. D. 2008. Selection of housekeeping genes for real-time PCR in atopic human bronchial epithelial cells. *Eur Respir J*, 32, 755-62.
- HEEB, S., BLUMER, C. & HAAS, D. 2002. Regulatory RNA as mediator in GacA/RsmA-dependent global control of exoproduct formation in *Pseudomonas fluorescens* CHA0. *J Bacteriol*, 184, 1046-56.
- HEEB, S., FLETCHER, M. P., CHHABRA, S. R., DIGGLE, S. P., WILLIAMS, P. & CÁMARA, M. 2011. Quinolones: from antibiotics to autoinducers. *FEMS Microbiology Reviews*, 35, 247-274.
- HEINIGER, R. W., WINTHER-LARSEN, H. C., PICKLES, R. J., KOOMEY, M. & WOLFGANG, M. C. 2010. Infection of human mucosal tissue by *Pseudomonas aeruginosa* requires sequential and mutually dependent virulence factors and a novel pilus-associated adhesin. *Cell Microbiol*, 12, 1158-73.
- HERAZO-MAYA, J. D., NOTH, I., DUNCAN, S. R., KIM, S., MA, S. F., TSENG, G. C., FEINGOLD, E., JUAN-GUARDELA, B. M., RICHARDS, T. J., LUSSIER, Y., HUANG, Y., VIJ, R., LINDELL, K. O., XUE, J., GIBSON, K. F., SHAPIRO, S. D., GARCIA, J. G. & KAMINSKI, N. 2013. Peripheral blood mononuclear cell gene expression profiles predict poor outcome in idiopathic pulmonary fibrosis. *Sci Transl Med*, 5, 3005964.
- HERNAN, M. A. 2010. The hazards of hazard ratios. *Epidemiology*, 21, 13-5.
- HEURLIER, K., WILLIAMS, F., HEEB, S., DORMOND, C., PESSI, G., SINGER, D., CAMARA, M., WILLIAMS, P. & HAAS, D. 2004. Positive control of swarming, rhamnolipid synthesis, and lipase production by the posttranscriptional RsmA/RsmZ system in *Pseudomonas aeruginosa* PAO1. *J Bacteriol*, 186, 2936-45.
- HOGARDT, M. & HEESEMANN, J. 2010. Adaptation of *Pseudomonas aeruginosa* during persistence in the cystic fibrosis lung. *Int J Med Microbiol*, 300, 557-62.
- HOIBY, N., CIOFU, O. & BJARNSHOLT, T. 2010. *Pseudomonas aeruginosa* biofilms in cystic fibrosis. *Future Microbiol*, 5, 1663-74.
- HOLMSKOV, U., THIEL, S. & JENSENIUS, J. C. 2003. Collections and ficolins: humoral lectins of the innate immune defense. *Annu Rev Immunol*, 21, 547-78.
- HOMER, R. J., ELIAS, J. A., LEE, C. G. & HERZOG, E. 2011. Modern concepts on the role of inflammation in pulmonary fibrosis. *Arch Pathol Lab Med*, 135, 780-8.
- HOMOLKA, J., ZIEGENHAGEN, M. W., GAEDE, K. I., ENTZIAN, P., ZISSEL, G. & MULLER-QUERNHEIM, J. 2003. Systemic immune cell activation in a subgroup of patients with idiopathic pulmonary fibrosis. *Respiration*, 70, 262-9.
- HOO, Z. H. & WHYTE, M. K. B. 2012. Idiopathic pulmonary fibrosis. *Thorax*.
- HOOI, D. S., BYCROFT, B. W., CHHABRA, S. R., WILLIAMS, P. & PRITCHARD, D. I. 2004. Differential immune modulatory activity of *Pseudomonas aeruginosa* quorum-sensing signal molecules. *Infect Immun*, 72, 6463-70.
- HOOK, A. L., CHANG, C. Y., YANG, J., LUCKETT, J., COCKAYNE, A., ATKINSON, S., MEI, Y., BAYSTON, R., IRVINE, D. J., LANGER, R., ANDERSON, D. G., WILLIAMS, P., DAVIES, M. C. & ALEXANDER, M. R. 2012. Combinatorial discovery of polymers resistant to bacterial attachment. *Nat Biotechnol*, 30, 868-75.
- HOVENBERG, H. W., DAVIES, J. R. & CARLSTEDT, I. 1996. Different mucins are produced by the surface epithelium and the submucosa in human trachea: identification of MUC5AC as a major mucin from the goblet cells. *Biochem J*, 318, 319-24.
- HUGGETT, J., DHEDA, K., BUSTIN, S. & ZUMLA, A. 2005. Real-time RT-PCR normalisation; strategies and considerations. *Genes Immun*, 6, 279-284.
- HUGHES, C. S., POSTOVIT, L. M. & LAJOIE, G. A. 2010. Matrigel: A complex protein mixture required for optimal growth of cell culture. *PROTEOMICS*, 10, 1886-1890.

- HULBERT, W. C., FORSTER, B. B., MEHTA, J. G., MAN, S. F., MOLDAY, R. S., WALKER, B. A., WALKER, D. C. & HOGG, J. C. 1989. Study of airway epithelial permeability with dextran. *J Electron Microsc Tech*, 11, 137-42.
- HUSSELL, T. & BELL, T. J. 2014. Alveolar macrophages: plasticity in a tissue-specific context. *Nat Rev Immunol*, 14, 81-93.
- INGRAM, J. L., RICE, A. B., GEISENHOFFER, K., MADTES, D. K. & BONNER, J. C. 2004. IL-13 and IL-1beta promote lung fibroblast growth through coordinated up-regulation of PDGF-AA and PDGF-Ralpha. *FASEB J*, 18, 1132-4.
- IRWIN, R. S., AUGUSTYN, N., FRENCH, C. T., RICE, J., TEDESCHI, V. & WELCH, S. J. 2013. Spread the word about the journal in 2013: From citation manipulation to invalidation of patient-reported outcomes measures to renaming the clara cell to new journal features. *CHEST Journal*, 143, 1-4.
- JACQUOT, J., TABARY, O., LE ROUZIC, P. & CLEMENT, A. 2008. Airway epithelial cell inflammatory signalling in cystic fibrosis. *Int J Biochem Cell Biol*, 40, 1703-15.
- JAKUBZICK, C., KUNKEL, S. L., PURI, R. K. & HOGABOAM, C. M. 2004. Therapeutic targeting of IL-4- and IL-13-responsive cells in pulmonary fibrosis. *Immunol Res*, 30, 339-49.
- JELLSBAK, L., JOHANSEN, H. K., FROST, A. L., THOGERSEN, R., THOMSEN, L. E., CIOFU, O., YANG, L., HAAGENSEN, J. A., HOIBY, N. & MOLIN, S. 2007. Molecular epidemiology and dynamics of *Pseudomonas aeruginosa* populations in lungs of cystic fibrosis patients. *Infect Immun*, 75, 2214-24.
- JENSEN, P. O., BJARNSHOLT, T., PHIPPS, R., RASMUSSEN, T. B., CALUM, H., CHRISTOFFERSEN, L., MOSER, C., WILLIAMS, P., PRESSLER, T., GIVSKOV, M. & HOIBY, N. 2007. Rapid necrotic killing of polymorphonuclear leukocytes is caused by quorum-sensing-controlled production of rhamnolipid by *Pseudomonas aeruginosa*. *Microbiology*, 153, 1329-38.
- JIMENEZ, P. N., KOCH, G., THOMPSON, J. A., XAVIER, K. B., COOL, R. H. & QUAX, W. J. 2012. The multiple signaling systems regulating virulence in *Pseudomonas aeruginosa*. *Microbiol Mol Biol Rev*, 76, 46-65.
- JOHNSON, M. K. & BOESE-MARRAZZO, D. 1980. Production and properties of heat-stable extracellular hemolysin from *Pseudomonas aeruginosa*. *Infect Immun*, 29, 1028-33.
- JOHNSTON, A., DAWES, S. M., DIACONU, D., FU, W., RIBLETT, M., ELDER, J. T., GUDJONSSON, J. E., MCCORMICK, T. S. & WARD, N. L. 2012. IL-17C and TNF alpha synergize to produce a psoriasis-like gene signature in human keratinocytes and an inflammatory skin phenotype in K5-IL-17C transgenic mice. *Journal of Investigative Dermatology*, 132, S99-S99.
- JONES, A. M., DODD, M. E., GOVAN, J. R., BARCUS, V., DOHERTY, C. J., MORRIS, J. & WEBB, A. K. 2004. *Burkholderia cenocepacia* and *Burkholderia multivorans*: influence on survival in cystic fibrosis. *Thorax*, 59, 948-51.
- JONULEIT, H., KUHN, U., MULLER, G., STEINBRINK, K., PARAGNIK, L., SCHMITT, E., KNOP, J. & ENK, A. H. 1997. Pro-inflammatory cytokines and prostaglandins induce maturation of potent immunostimulatory dendritic cells under fetal calf serum-free conditions. *Eur J Immunol*, 27, 3135-42.
- KALISH, L. A., WALTZ, D. A., DOVEY, M., POTTER-BYNOE, G., MCADAM, A. J., LIPUMA, J. J., GERARD, C. & GOLDMANN, D. 2006. Impact of *Burkholderia dolosa* on lung function and survival in cystic fibrosis. *Am J Respir Crit Care Med*, 173, 421-5.
- KATKIN, J. P. 2014. Cystic fibrosis: Clinical manifestations and diagnosis [Online]. Available: <http://www.uptodate.com/contents/cystic-fibrosis-clinical-manifestations-and-diagnosis> [Accessed October 26 2014].
- KATO, A. & SCHLEIMER, R. P. 2007. Beyond inflammation: airway epithelial cells are at the interface of innate and adaptive immunity. *Curr Opin Immunol*, 19, 711-20.
- KIERBEL, A., GASSAMA-DIAGNE, A., MOSTOV, K. & ENGEL, J. N. 2005. The phosphoinositol-3-kinase-protein kinase B/Akt pathway is critical for *Pseudomonas aeruginosa* strain PAK internalization. *Mol Biol Cell*, 16, 2577-85.
- KIERBEL, A., GASSAMA-DIAGNE, A., ROCHA, C., RADOSHEVICH, L., OLSON, J., MOSTOV, K. & ENGEL, J. 2007. *Pseudomonas aeruginosa* exploits a PIP3-dependent pathway to transform apical into basolateral membrane. *J Cell Biol*, 177, 21-7.

- KIM, K., KIM, S. H., LEPINE, F., CHO, Y. H. & LEE, G. R. 2010a. Global gene expression analysis on the target genes of PQS and HHQ in J774A.1 monocyte/macrophage cells. *Microb Pathog*, 49, 174-80.
- KIM, K., KIM, Y. U., KOH, B. H., HWANG, S. S., KIM, S.-H., LE PINE, F., CHO, Y.-H. & LEE, G. R. 2010b. HHQ and PQS, two *Pseudomonas aeruginosa* quorum-sensing molecules, down-regulate the innate immune responses through the nuclear factor- $\kappa$ B pathway. *British society of immunology*, 129, 578-588.
- KIM, K. C. 1985. Possible requirement of collagen gel substratum for production of mucin-like glycoproteins by primary rabbit tracheal epithelial cells in culture. *In Vitro Cell Dev Biol*, 21, 617-21.
- KING, T. E., PARDO, A. & SELMAN, M. 2011. Idiopathic pulmonary fibrosis. *The Lancet*, 378, 1949-1961.
- KIPNIS, E., SAWA, T. & WIENER-KRONISH, J. 2006. Targeting mechanisms of *Pseudomonas aeruginosa* pathogenesis. *Médecine et Maladies Infectieuses*, 36, 78-91.
- KIRBY, A. C., COLES, M. C. & KAYE, P. M. 2009. Alveolar Macrophages Transport Pathogens to Lung Draining Lymph Nodes. *J Immunol*, 183, 1983-1989.
- KIRCHNER, S., FOTHERGILL, J. L., WRIGHT, E. A., JAMES, C. E., MOWAT, E. & WINSTANLEY, C. 2012. Use of artificial sputum medium to test antibiotic efficacy against *Pseudomonas aeruginosa* in conditions more relevant to the cystic fibrosis lung. *J Vis Exp*, 5.
- KLEIN WOLTERINK, R. G., KLEINJAN, A., VAN NIMWEGEN, M., BERGEN, I., DE BRUIJN, M., LEVANI, Y. & HENDRIKS, R. W. 2012. Pulmonary innate lymphoid cells are major producers of IL-5 and IL-13 in murine models of allergic asthma. *Eur J Immunol*, 42, 1106-16.
- KLINGER, J. D., TANDLER, B., LIEDTKE, C. M. & BOAT, T. F. 1984. Proteinases of *Pseudomonas aeruginosa* evoke mucin release by tracheal epithelium. *J Clin Invest*, 74, 1669-78.
- KLOCKGETHER, J., MUNDER, A., NEUGEBAUER, J., DAVENPORT, C. F., STANKE, F., LARBIG, K. D., HEEB, S., SCHOCK, U., POHL, T. M., WIEHLMANN, L. & TUMMLER, B. 2010. Genome diversity of *Pseudomonas aeruginosa* PAO1 laboratory strains. *J Bacteriol*, 192, 1113-21.
- KNOWLES, M. R. & BOUCHER, R. C. 2002. Mucus clearance as a primary innate defense mechanism for mammalian airways. *J Clin Invest*, 109, 571-7.
- KOHLER, T., CURTY, L. K., BARJA, F., VAN DELDEN, C. & PECHERE, J. C. 2000. Swarming of *Pseudomonas aeruginosa* is dependent on cell-to-cell signaling and requires flagella and pili. *J Bacteriol*, 182, 5990-6.
- KOHLER, T., EPP, S. F., CURTY, L. K. & PECHERE, J. C. 1999. Characterization of MexT, the regulator of the MexE-MexF-OprN multidrug efflux system of *Pseudomonas aeruginosa*. *J Bacteriol*, 181, 6300-5.
- KONSTAN, M. W., HILLIARD, K. A., NORVELL, T. M. & BERGER, M. 1994. Bronchoalveolar lavage findings in cystic fibrosis patients with stable, clinically mild lung disease suggest ongoing infection and inflammation. *Am J Respir Crit Care Med*, 150, 448-54.
- KOTSIANIDIS, I., NAKOU, E., BOUCHLIOU, I., TZOUVELEKIS, A., SPANOUDAKIS, E., STEIROPOULOS, P., SOTIRIOU, I., AIDINIS, V., MARGARITIS, D., TSATALAS, C. & BOUROS, D. 2009. Global impairment of CD4+CD25+FOXP3+ regulatory T cells in idiopathic pulmonary fibrosis. *Am J Respir Crit Care Med*, 179, 1121-30.
- KOWALSKI, M. P., DUBOUIX-BOURANDY, A., BAJMOCZI, M., GOLAN, D. E., ZAIDI, T., COUTINHO-SLEDGE, Y. S., GYGI, M. P., GYGI, S. P., WIEMER, E. A. & PIER, G. B. 2007. Host resistance to lung infection mediated by major vault protein in epithelial cells. *Science*, 317, 130-2.
- KREDA, S. M., DAVIS, C. W. & ROSE, M. C. 2012. CFTR, mucins, and mucus obstruction in cystic fibrosis. *Cold Spring Harb Perspect Med*, 2.
- KUANG, Z., HAO, Y., WALLING, B. E., JEFFRIES, J. L., OHMAN, D. E. & LAU, G. W. 2011. *Pseudomonas aeruginosa* elastase provides an escape from phagocytosis by degrading the pulmonary surfactant protein-A. *PLoS One*, 6, 1.
- KUCHMA, S. L., BROTHERS, K. M., MERRITT, J. H., LIBERATI, N. T., AUSUBEL, F. M. & O'TOOLE, G. A. 2007. BifA, a cyclic-Di-GMP phosphodiesterase, inversely

- regulates biofilm formation and swarming motility by *Pseudomonas aeruginosa* PA14. *J Bacteriol*, 189, 8165-78.
- KUKAVICA-IBRULJ, I., BRAGONZI, A., PARONI, M., WINSTANLEY, C., SANSCHAGRIN, F., O'TOOLE, G. A. & LEVESQUE, R. C. 2008. In vivo growth of *Pseudomonas aeruginosa* strains PAO1 and PA14 and the hypervirulent strain LESB58 in a rat model of chronic lung infection. *J Bacteriol*, 190, 2804-13.
- KULKARNI, B., MOHAMMED, I., HOPKINSON, A. & DUA, H. S. 2011. Validation of endogenous control genes for gene expression studies on human ocular surface epithelium. *PLoS One*, 6, 3.
- LAMBRECHT, B. N., CARRO-MUINO, I., VERMAELEN, K. & PAUWELS, R. A. 1999. Allergen-induced changes in bone-marrow progenitor and airway dendritic cells in sensitized rats. *Am J Respir Cell Mol Biol*, 20, 1165-74.
- LANSDELL, K. A., KIDD, J. F., DELANEY, S. J., WAINWRIGHT, B. J. & SHEPPARD, D. N. 1998. Regulation of murine cystic fibrosis transmembrane conductance regulator Cl<sup>-</sup> channels expressed in Chinese hamster ovary cells. *J Physiol*, 512, 751-64.
- LASARRE, B. & FEDERLE, M. J. 2013. Exploiting quorum sensing to confuse bacterial pathogens. *Microbiol Mol Biol Rev*, 77, 73-111.
- LAU, G. W., RAN, H., KONG, F., HASSETT, D. J. & MAVRODI, D. 2004. *Pseudomonas aeruginosa* pyocyanin is critical for lung infection in mice. *Infect Immun*, 72, 4275-8.
- LAVOIE, E. G., WANGDI, T. & KAZMIERCZAK, B. I. 2011. Innate immune responses to *Pseudomonas aeruginosa* infection. *Microbes Infect*, 13, 1133-45.
- LAZENBY, J. J., GRIFFIN, P. E., KYD, J., WHITCHURCH, C. B. & COOLEY, M. A. 2013. A quadruple knockout of lasIR and rhlIR of *Pseudomonas aeruginosa* PAO1 that retains wild-type twitching motility has equivalent infectivity and persistence to PAO1 in a mouse model of lung infection. *PLoS One*, 8.
- LE, B. V., KHORSI-CAUET, H., BACH, V. & GAY-QUEHEILLARD, J. 2012. Mast cells mediate *Pseudomonas aeruginosa* lipopolysaccharide-induced lung inflammation in rat. *Eur J Clin Microbiol Infect Dis*, 31, 1983-90.
- LECH, M. & ANDERS, H. J. 2013. Macrophages and fibrosis: How resident and infiltrating mononuclear phagocytes orchestrate all phases of tissue injury and repair. *Biochim Biophys Acta*, 7, 989-97.
- LECHNER, J. & LAVECK, M. 1985. A serum-free method for culturing normal human bronchial epithelial cells at clonal density. *Journal of tissue culture methods*, 9, 43-48.
- LEE, A., CHOW, D., HAUS, B., TSENG, W., EVANS, D., FLEISZIG, S., CHANDY, G. & MACHEN, T. 1999. Airway epithelial tight junctions and binding and cytotoxicity of *Pseudomonas aeruginosa*. *Am J Physiol*, 277, L204-17.
- LEE, C. G., HOMER, R. J., ZHU, Z., LANONE, S., WANG, X., KOTELIANSKY, V., SHIPLEY, J. M., GOTWALS, P., NOBLE, P., CHEN, Q., SENIOR, R. M. & ELIAS, J. A. 2001. Interleukin-13 induces tissue fibrosis by selectively stimulating and activating transforming growth factor beta-1. *J Exp Med*, 194, 809-21.
- LEE, J., WU, J., DENG, Y., WANG, J., WANG, C., WANG, J., CHANG, C., DONG, Y., WILLIAMS, P. & ZHANG, L.-H. 2013. A cell-cell communication signal integrates quorum sensing and stress response. *Nat Chem Biol*, 9, 339-343.
- LEGENDRE, C., REEN, F. J., MOOIJ, M. J., MCGLACKEN, G. P., ADAMS, C. & O'GARA, F. 2012. *Pseudomonas aeruginosa* Alkyl Quinolones Repress Hypoxia-Inducible Factor 1 (HIF-1) Signaling through HIF-1alpha Degradation. *Infect Immun*, 80, 3985-92.
- LEGGE, K. L. & BRACIALE, T. J. 2003. Accelerated migration of respiratory dendritic cells to the regional lymph nodes is limited to the early phase of pulmonary infection. *Immunity*, 18, 265-77.
- LEPANTO, P., BRYANT, D. M., ROSSELLO, J., DATTA, A., MOSTOV, K. E. & KIERBEL, A. 2011. *Pseudomonas aeruginosa* interacts with epithelial cells rapidly forming aggregates that are internalized by a Lyn-dependent mechanism. *Cell Microbiol*, 13, 1212-22.
- LEWIS, D. A., JONES, A., PARKHILL, J., SPEERT, D. P., GOVAN, J. R., LIPUMA, J. J., LORY, S., WEBB, A. K. & MAHENTHIRALINGAM, E. 2005. Identification of DNA markers for a transmissible *Pseudomonas aeruginosa* cystic fibrosis strain. *Am J Respir Cell Mol Biol*, 33, 56-64.

- LIN, T. J., GARDUNO, R., BOUDREAU, R. T. & ISSEKUTZ, A. C. 2002. *Pseudomonas aeruginosa* activates human mast cells to induce neutrophil transendothelial migration via mast cell-derived IL-1 alpha and beta. *J Immunol*, 169, 4522-30.
- LINSEDELL, P. 2013. Functional architecture of the CFTR chloride channel. *Mol Membr Biol*, 17, 17.
- LIPSCOMB, M. F. & MASTEN, B. J. 2002. Dendritic cells: immune regulators in health and disease. *Physiol Rev*, 82, 97-130.
- LOSA, D., KOHLER, T., BELLEC, J., DUDEZ, T., CRESPIAN, S., BACCHETTA, M., BOULANGER, P., HONG, S. S., MOREL, S., NGUYEN, T. H., VAN DELDEN, C. & CHANSON, M. 2014. *Pseudomonas aeruginosa*-Induced Apoptosis in Airway Epithelial Cells Is Mediated by Gap Junctional Communication in a JNK-Dependent Manner. *J Immunol*, 192, 4804-12.
- LU, C., KIRSCH, B., ZIMMER, C., DE JONG, J. C., HENN, C., MAURER, C. K., MUSKEN, M., HAUSSLER, S., STEINBACH, A. & HARTMANN, R. W. 2012. Discovery of antagonists of PqsR, a key player in 2-alkyl-4-quinolone-dependent quorum sensing in *Pseudomonas aeruginosa*. *Chem Biol*, 19, 381-90.
- LUZINA, I. G., TODD, N. W., IACONO, A. T. & ATAMAS, S. P. 2008. Roles of T lymphocytes in pulmonary fibrosis. *J Leukoc Biol*, 83, 237-44.
- LYCZAK, J. B., CANNON, C. L. & PIER, G. B. 2002. Lung infections associated with cystic fibrosis. *Clin Microbiol Rev*, 15, 194-222.
- MACHEN, T. E. 2006. Innate immune response in CF airway epithelia: hyperinflammatory? *Am J Physiol Cell Physiol*, 291, C218-30.
- MADDOCKS, S. E. & OYSTON, P. C. 2008. Structure and function of the LysR-type transcriptional regulator (LTTR) family proteins. *Microbiology*, 154, 3609-23.
- MAILLE, E., TRINH, N. T., PRIVE, A., BILODEAU, C., BISSONNETTE, E., GRANDVAUX, N. & BROCHIERO, E. 2011. Regulation of normal and cystic fibrosis airway epithelial repair processes by TNF-alpha after injury. *Am J Physiol Lung Cell Mol Physiol*, 301, 9.
- MAJIK, M. S. & PARVATKAR, P. T. 2013. Next generation biofilm inhibitors for *Pseudomonas aeruginosa*: synthesis and rational design approaches. *Curr Top Med Chem*, 13, 13.
- MALHOTRA, D., THIMMULAPPA, R. K., MERCADO, N., ITO, K., KOMBAIRAJU, P., KUMAR, S., MA, J., FELLER-KOPMAN, D., WISE, R., BARNES, P. & BISWAL, S. 2011. Denitrosylation of HDAC2 by targeting Nrf2 restores glucocorticosteroid sensitivity in macrophages from COPD patients. *J Clin Invest*, 121, 4289-302.
- MALL, M. A. 2008. Role of cilia, mucus, and airway surface liquid in mucociliary dysfunction: lessons from mouse models. *J Aerosol Med Pulm Drug Deliv*, 21, 13-24.
- MANN, E. E. & WOZNIAK, D. J. 2012. *Pseudomonas* biofilm matrix composition and niche biology. *FEMS Microbiol Rev*, 36, 893-916.
- MANOS, J., HU, H., ROSE, B. R., WAINWRIGHT, C. E., ZABLOTSKA, I. B., CHENEY, J., TURNBULL, L., WHITCHURCH, C. B., GRIMWOOD, K., HARMER, C., ANUJ, S. N. & HARBOUR, C. 2013. Virulence factor expression patterns in *Pseudomonas aeruginosa* strains from infants with cystic fibrosis. *Eur J Clin Microbiol Infect Dis*, 32, 1583-92.
- MARTIN, F. J. & PRINCE, A. S. 2008. TLR2 regulates gap junction intercellular communication in airway cells. *J Immunol*, 180, 4986-93.
- MARTIN, L. D., ROCHELLE, L. G., FISCHER, B. M., KRUNKOSKY, T. M. & ADLER, K. B. 1997. Airway epithelium as an effector of inflammation: molecular regulation of secondary mediators. *Eur Respir J*, 10, 2139-2146.
- MARTINEZ, F. D. & VERCELLI, D. 2013. Asthma. *Lancet*, 382, 1360-1372.
- MATSUI, H., GRUBB, B. R., TARRAN, R., RANDELL, S. H., GATZY, J. T., DAVIS, C. W. & BOUCHER, R. C. 1998. Evidence for periciliary liquid layer depletion, not abnormal ion composition, in the pathogenesis of cystic fibrosis airways disease. *Cell*, 95, 1005-15.
- MATSUI, H., WAGNER, V. E., HILL, D. B., SCHWAB, U. E., ROGERS, T. D., BUTTON, B., TAYLOR, R. M., 2ND, SUPERFINE, R., RUBINSTEIN, M., IGLEWSKI, B. H. & BOUCHER, R. C. 2006. A physical linkage between cystic fibrosis airway surface dehydration and *Pseudomonas aeruginosa* biofilms. *Proc Natl Acad Sci U S A*, 103, 18131-6.

- MCALLISTER, F., HENRY, A., KREINDLER, J. L., DUBIN, P. J., ULRICH, L., STEELE, C., FINDER, J. D., PILEWSKI, J. M., CARRENO, B. M., GOLDMAN, S. J., PIRHONEN, J. & KOLLS, J. K. 2005. Role of IL-17A, IL-17F, and the IL-17 receptor in regulating growth-related oncogene-alpha and granulocyte colony-stimulating factor in bronchial epithelium: implications for airway inflammation in cystic fibrosis. *J Immunol*, 175, 404-12.
- MCCALLUM, S. J., GALLAGHER, M. J., CORKILL, J. E., HART, C. A., LEDSON, M. J. & WALSHAW, M. J. 2002. Spread of an epidemic *Pseudomonas aeruginosa* strain from a patient with cystic fibrosis (CF) to non-CF relatives. *Thorax*, 57, 559-60.
- MCKNIGHT, S. L., IGLEWSKI, B. H. & PESCI, E. C. 2000. The *Pseudomonas* quinolone signal regulates rhl quorum sensing in *Pseudomonas aeruginosa*. *J Bacteriol*, 182, 2702-8.
- MCNAMARA, N., GALLUP, M., SUCHER, A., MALTSEVA, I., MCKEMY, D. & BASBAUM, C. 2006. AsialoGM1 and TLR5 cooperate in flagellin-induced nucleotide signaling to activate Erk1/2. *Am J Respir Cell Mol Biol*, 34, 653-60.
- MEGE, R. M., GAVARD, J. & LAMBERT, M. 2006. Regulation of cell-cell junctions by the cytoskeleton. *Curr Opin Cell Biol*, 18, 541-8.
- MELTZER, E. B. & NOBLE, P. W. 2008. Idiopathic pulmonary fibrosis. *Orphanet J Rare Dis*, 3, 1750-1172.
- MI, S., LI, Z., YANG, H. Z., LIU, H., WANG, J. P., MA, Y. G., WANG, X. X., LIU, H. Z., SUN, W. & HU, Z. W. 2011. Blocking IL-17A promotes the resolution of pulmonary inflammation and fibrosis via TGF-beta1-dependent and -independent mechanisms. *J Immunol*, 187, 3003-14.
- MICHAEL, B., SMITH, J. N., SWIFT, S., HEFFRON, F. & AHMER, B. M. 2001. SdiA of *Salmonella enterica* is a LuxR homolog that detects mixed microbial communities. *J Bacteriol*, 183, 5733-42.
- MICHLEWSKA, S., DRANSFIELD, I., MEGSON, I. L. & ROSSI, A. G. 2009. Macrophage phagocytosis of apoptotic neutrophils is critically regulated by the opposing actions of pro-inflammatory and anti-inflammatory agents: key role for TNF-alpha. *FASEB J*, 23, 844-54.
- MILLER, M. B. & BASSLER, B. L. 2001. Quorum sensing in bacteria. *Annu Rev Microbiol*, 55, 165-99.
- MIRE-SLUIJS, A. R., WICKREMASINGHE, R. G., HOFFBRAND, A. V., TIMMS, A. M. & FRANCIS, G. E. 1987. Human T lymphocytes stimulated by phytohaemagglutinin undergo a single round of cell division without a requirement for interleukin-2 or accessory cells. *Immunology*, 60, 7-12.
- MJOSBERG, J. M., TRIFARI, S., CRELLIN, N. K., PETERS, C. P., VAN DRUNEN, C. M., PIET, B., FOKKENS, W. J., CUPEDO, T. & SPITS, H. 2011. Human IL-25- and IL-33-responsive type 2 innate lymphoid cells are defined by expression of CCR2 and CD161. *Nat Immunol*, 12, 1055-62.
- MOISEEVA, E. P. & BRADDING, P. 2011. Mast cells in lung inflammation. *Adv Exp Med Biol*, 716, 235-69.
- MOORE, K. W., DE WAAL MALEFYT, R., COFFMAN, R. L. & O'GARRA, A. 2001. Interleukin-10 and the interleukin-10 receptor. *Annu Rev Immunol*, 19, 683-765.
- MORISSETTE, C., FRANCOEUR, C., DARMOND-ZWAIG, C. & GERVAIS, F. 1996. Lung phagocyte bactericidal function in strains of mice resistant and susceptible to *Pseudomonas aeruginosa*. *Infect Immun*, 64, 4984-92.
- MOSKWA, P., LORENTZEN, D., EXCOFFON, K. J., ZABNER, J., MCCRAY, P. B., JR., NAUSEEF, W. M., DUPUY, C. & BANFI, B. 2007. A novel host defense system of airways is defective in cystic fibrosis. *Am J Respir Crit Care Med*, 175, 174-83.
- MUIR, A., SOONG, G., SOKOL, S., REDDY, B., GOMEZ, M. I., VAN HEECKEREN, A. & PRINCE, A. 2004. Toll-like receptors in normal and cystic fibrosis airway epithelial cells. *Am J Respir Cell Mol Biol*, 30, 777-83.
- MUKHOPADHYAY, S., HOIDAL, J. R. & MUKHERJEE, T. K. 2006. Role of TNFalpha in pulmonary pathophysiology. *Respir Res*, 7, 125.
- MULCAHY, H., CHARRON-MAZENOD, L. & LEWENZA, S. 2010. *Pseudomonas aeruginosa* produces an extracellular deoxyribonuclease that is required for utilization of DNA as a nutrient source. *Environmental Microbiology*, 12, 1621-1629.
- MURPHY, K. 2011. *Janeway's Immunobiology*, Garland Science.

- MURRAY, L. A., ARGENTIERI, R. L., FARRELL, F. X., BRACHT, M., SHENG, H., WHITAKER, B., BECK, H., TSUI, P., COCHLIN, K., EVANOFF, H. L., HOGABOAM, C. M. & DAS, A. M. 2008. Hyper-responsiveness of IPF/UIP fibroblasts: interplay between TGFbeta1, IL-13 and CCL2. *Int J Biochem Cell Biol*, 40, 2174-82.
- NALYSNYK, L., CID-RUZAFKA, J., ROTELLA, P. & ESSER, D. 2012. Incidence and prevalence of idiopathic pulmonary fibrosis: review of the literature. *European Respiratory Review*, 21, 355-361.
- NATURE.COM. 2014. Cell Adhesion, Cell Communication | Learn Science at Scitable [Online]. Available: <http://www.nature.com/scitable/topicpage/cell-adhesion-and-cell-communication-14050486> [Accessed 20 October 2014].
- NAVARATNAM, V., FLEMING, K. M., WEST, J., SMITH, C. J., JENKINS, R. G., FOGARTY, A. & HUBBARD, R. B. 2011. The rising incidence of idiopathic pulmonary fibrosis in the U.K. *Thorax*, 66, 462-7.
- NAVARATNAM, V., FOGARTY, A. W., MCKEEVER, T., THOMPSON, N., JENKINS, G., JOHNSON, S. R., DOLAN, G., KUMARAN, M., POINTON, K. & HUBBARD, R. B. 2013. Presence of a prothrombotic state in people with idiopathic pulmonary fibrosis: a population-based case-control study. *Thorax*.
- NEALSON, K. H. & HASTINGS, J. W. 1979. Bacterial bioluminescence: its control and ecological significance. *Microbiol Rev*, 43, 496-518.
- NEMBRINI, C., MARSLAND, B. J. & KOPF, M. 2009. IL-17-producing T cells in lung immunity and inflammation. *J Allergy Clin Immunol*, 123, 986-94.
- NIZET, V. & JOHNSON, R. S. 2009. Interdependence of hypoxic and innate immune responses. *Nat Rev Immunol*, 9, 609-17.
- NOBLE, P. W., BARKAUSKAS, C. E. & JIANG, D. 2012. Pulmonary fibrosis: patterns and perpetrators. *J Clin Invest*, 122, 2756-62.
- NOORDMAN, W. H. & JANSSEN, D. B. 2002. Rhamnolipid stimulates uptake of hydrophobic compounds by *Pseudomonas aeruginosa*. *Appl Environ Microbiol*, 68, 4502-8.
- NUOVO, G. J., HAGOOD, J. S., MAGRO, C. M., CHIN, N., KAPIL, R., DAVIS, L., MARSH, C. B. & FOLCIK, V. A. 2012. The distribution of immunomodulatory cells in the lungs of patients with idiopathic pulmonary fibrosis. *Mod Pathol*, 25, 416-33.
- O'MALLEY, Y. Q., RESZKA, K. J., RASMUSSEN, G. T., ABDALLA, M. Y., DENNING, G. M. & BRITIGAN, B. E. 2003. The *Pseudomonas* secretory product pyocyanin inhibits catalase activity in human lung epithelial cells. *Am J Physiol Lung Cell Mol Physiol*, 285, 18.
- O'SULLIVAN, B. P. & FREEDMAN, S. D. 2009. Cystic fibrosis. *Lancet*, 373, 1891-904.
- OPITZ, B., PUSCHEL, A., SCHMECK, B., HOCHE, A. C., ROSSEAU, S., HAMMERSCHMIDT, S., SCHUMANN, R. R., SUTTORP, N. & HIPPENSTIEL, S. 2004. Nucleotide-binding oligomerization domain proteins are innate immune receptors for internalized *Streptococcus pneumoniae*. *J Biol Chem*, 279, 36426-32.
- ORTEGA-GÓMEZ, A., PERRETTI, M. & SOEHNLEIN, O. 2013. Resolution of inflammation: an integrated view. *EMBO Mol Med*, 5, 661-74.
- PALMER, K. L., MASHBURN, L. M., SINGH, P. K. & WHITELEY, M. 2005. Cystic fibrosis sputum supports growth and cues key aspects of *Pseudomonas aeruginosa* physiology. *J Bacteriol*, 187, 5267-77.
- PAPI, A. & JOHNSTON, S. L. 1999. Respiratory epithelial cell expression of vascular cell adhesion molecule-1 and its up-regulation by rhinovirus infection via NF-kappaB and GATA transcription factors. *J Biol Chem*, 274, 30041-51.
- PAPPU, R., RUTZ, S. & OUYANG, W. 2012. Regulation of epithelial immunity by IL-17 family cytokines. *Trends Immunol*, 33, 343-9.
- PARK, S. W., AHN, M. H., JANG, H. K., JANG, A. S., KIM, D. J., KOH, E. S., PARK, J. S., UH, S. T., KIM, Y. H., PARK, J. S., PAIK, S. H., SHIN, H. K., YOUM, W. & PARK, C. S. 2009. Interleukin-13 and its receptors in idiopathic interstitial pneumonia: clinical implications for lung function. *J Korean Med Sci*, 24, 614-20.
- PARKER, D. & PRINCE, A. 2011. Innate immunity in the respiratory epithelium. *Am J Respir Cell Mol Biol*, 45, 189-201.
- PARKER, D. & PRINCE, A. 2013. Epithelial uptake of flagella initiates proinflammatory signaling. *PLoS One*, 8, 20.

- PATRICK, A. E. & THOMAS, P. J. 2012. Development of CFTR Structure. *Front Pharmacol*, 3.
- PATTLE, R. E. 1955. Properties, function and origin of the alveolar lining layer. *Nature*, 175, 1125-6.
- PESCE, J. T., RAMALINGAM, T. R., MENTINK-KANE, M. M., WILSON, M. S., EL KASMI, K. C., SMITH, A. M., THOMPSON, R. W., CHEEVER, A. W., MURRAY, P. J. & WYNN, T. A. 2009. Arginase-1-expressing macrophages suppress Th2 cytokine-driven inflammation and fibrosis. *PLoS Pathog*, 5, 10.
- PESCI, E., MILBANK, J., PEARSON, J., MCKNIGHT, S., KENDE, A., GREENBERG, E. & IGLEWSKI, B. 1999. Quinolone signaling in the cell-to-cell communication system of *Pseudomonas aeruginosa*. *Proc Natl Acad Sci USA*, 96, 11229 - 11234.
- PETIT-BERTRON, A. F., TABARY, O., CORVOL, H., JACQUOT, J., CLEMENT, A., CAVAILLON, J. M. & ADIB-CONQUY, M. 2008. Circulating and airway neutrophils in cystic fibrosis display different TLR expression and responsiveness to interleukin-10. *Cytokine*, 41, 54-60.
- PEZZULO, A. A., TANG, X. X., HOEGGER, M. J., ALAIWA, M. H., RAMACHANDRAN, S., MONINGER, T. O., KARP, P. H., WOHLFORD-LENANE, C. L., HAAGSMAN, H. P., VAN EIJK, M., BANFI, B., HORSWILL, A. R., STOLTZ, D. A., MCCRAY, P. B., JR., WELSH, M. J. & ZABNER, J. 2012. Reduced airway surface pH impairs bacterial killing in the porcine cystic fibrosis lung. *Nature*, 487, 109-13.
- PFEIFER, P., VOSS, M., WONNENBERG, B., HELLBERG, J., SEILER, F., LEPPER, P. M., BISCHOFF, M., LANGER, F., SCHAFERS, H. J., MENGER, M. D., BALS, R. & BEISSWENGER, C. 2012. IL-17C is a Mediator of Respiratory Epithelial Innate Immune Response. *Am J Respir Cell Mol Biol*.
- PLEASS, R. J., LANG, M. L., KERR, M. A. & WOOF, J. M. 2007. IgA is a more potent inducer of NADPH oxidase activation and degranulation in blood eosinophils than IgE. *Mol Immunol*, 44, 1401-8.
- PLOTKOWSKI, M. C., POVOA, H. C., ZAHM, J. M., LIZARD, G., PEREIRA, G. M., TOURNIER, J. M. & PUCHELLE, E. 2002. Early mitochondrial dysfunction, superoxide anion production, and DNA degradation are associated with non-apoptotic death of human airway epithelial cells induced by *Pseudomonas aeruginosa* exotoxin A. *Am J Respir Cell Mol Biol*, 26, 617-26.
- POLITO, A. J. & PROUD, D. 1998. Epithelia cells as regulators of airway inflammation. *J Allergy Clin Immunol*, 102, 714-8.
- PRASSE, A. & MULLER-QUERNHEIM, J. 2009. Non-invasive biomarkers in pulmonary fibrosis. *Respirology*, 14, 788-95.
- PRINCE, L. R., BIANCHI, S. M., VAUGHAN, K. M., BEWLEY, M. A., MARRIOTT, H. M., WALMSLEY, S. R., TAYLOR, G. W., BUTTLE, D. J., SABROE, I., DOCKRELL, D. H. & WHYTE, M. K. 2008. Subversion of a lysosomal pathway regulating neutrophil apoptosis by a major bacterial toxin, pyocyanin. *J Immunol*, 180, 3502-11.
- QUINTON, P. M. 2010. Role of epithelial HCO<sub>3</sub><sup>-</sup> transport in mucin secretion: lessons from cystic fibrosis. *Am J Physiol Cell Physiol*, 299, 6.
- RACKLEY, C. R. & STRIPP, B. R. 2012. Building and maintaining the epithelium of the lung. *J Clin Invest*, 122, 2724-30.
- RADA, B., JENDRYSIK, M. A., PANG, L., HAYES, C. P., YOO, D. G., PARK, J. J., MOSKOWITZ, S. M., MALECH, H. L. & LETO, T. L. 2013. Pyocyanin-enhanced neutrophil extracellular trap formation requires the NADPH oxidase. *PLoS One*, 8, 14.
- RADA, B. & LETO, T. L. 2013. Pyocyanin effects on respiratory epithelium: relevance in *Pseudomonas aeruginosa* airway infections. *Trends in microbiology*, 21, 73-81.
- RAHIM, R., OCHSNER, U. A., OLVERA, C., GRANINGER, M., MESSNER, P., LAM, J. S. & SOBERON-CHAVEZ, G. 2001. Cloning and functional characterization of the *Pseudomonas aeruginosa* rhlC gene that encodes rhamnosyltransferase 2, an enzyme responsible for di-rhamnolipid biosynthesis. *Mol Microbiol*, 40, 708-18.
- RAHMAN, I. & MACNEE, W. 2000. Oxidative stress and regulation of glutathione in lung inflammation. *Eur Respir J*, 16, 534-54.
- RAMIREZ-CARROZZI, V., SAMBANDAM, A., LUIS, E., LIN, Z., JEET, S., LESCH, J., HACKNEY, J., KIM, J., ZHOU, M., LAI, J., MODRUSAN, Z., SAI, T., LEE, W., XU, M., CAPLAZI, P., DIEHL, L., DE VOSS, J., BALAZS, M., GONZALEZ, L., JR., SINGH, H., OUYANG, W. & PAPPU, R. 2011. IL-17C regulates the innate immune function of epithelial cells in an autocrine manner. *Nat Immunol*, 12, 1159-66.



- RAMPIONI, G., PUSTELNY, C., FLETCHER, M. P., WRIGHT, V. J., BRUCE, M., RUMBAUGH, K. P., HEEB, S., CÁMARA, M. & WILLIAMS, P. 2010. Transcriptomic analysis reveals a global alkyl-quinolone-independent regulatory role for PqsE in facilitating the environmental adaptation of *Pseudomonas aeruginosa* to plant and animal hosts. *Environmental Microbiology*, 12, 1659-1673.
- RAN, H., HASSETT, D. & LAU, G. 2003. Human targets of *Pseudomonas aeruginosa* pyocyanin. *Proc Natl Acad Sci U S A*, 100, 14315 - 14320.
- RANDAK, C. O., DONG, Q., VER HEUL, A. R., ELCOCK, A. H. & WELSH, M. J. 2013. ATP and AMP mutually influence their interaction with the ATP-binding cassette (ABC) adenylate kinase cystic fibrosis transmembrane conductance regulator (CFTR) at separate binding sites. *J Biol Chem*, 288, 27692-701.
- RAOUST, E. S., BALLOY, V., GARCIA-VERDUGO, I., TOUQUI, L., RAMPHAL, R. & CHIGNARD, M. 2009. *Pseudomonas aeruginosa* LPS or flagellin are sufficient to activate TLR-dependent signaling in murine alveolar macrophages and airway epithelial cells. *PLoS One*, 4, e7259.
- RATJEN, F. A. 2009. Cystic fibrosis: pathogenesis and future treatment strategies. *Respir Care*, 54, 595-605.
- READ, R. C., ROBERTS, P., MUNRO, N., RUTMAN, A., HASTIE, A., SHRYOCK, T., HALL, R., MCDONALD-GIBSON, W., LUND, V., TAYLOR, G. & ET AL. 1985. Effect of *Pseudomonas aeruginosa* rhamnolipids on mucociliary transport and ciliary beating. *J Appl Physiol*, 72, 2271-7.
- RECINOS, D. A., SEKEDAT, M. D., HERNANDEZ, A., COHEN, T. S., SAKHTAH, H., PRINCE, A. S., PRICE-WHELAN, A. & DIETRICH, L. E. 2012. Redundant phenazine operons in *Pseudomonas aeruginosa* exhibit environment-dependent expression and differential roles in pathogenicity. *Proc Natl Acad Sci U S A*, 109, 19420-5.
- REIS, R. S., PEREIRA, A. G., NEVES, B. C. & FREIRE, D. M. G. 2011. Gene regulation of rhamnolipid production in *Pseudomonas aeruginosa* – A review. *Bioresource Technology*, 102, 6377-6384.
- REJMAN, J., DI GIOIA, S., BRAGONZI, A. & CONESE, M. 2007. *Pseudomonas aeruginosa* infection destroys the barrier function of lung epithelium and enhances polyplex-mediated transfection. *Hum Gene Ther*, 18, 642-52.
- RETZLAFF, M., STAHL, M., EBERL, H. C., LAGLEDER, S., BECK, J., KESSLER, H. & BUCHNER, J. 2009. Hsp90 is regulated by a switch point in the C-terminal domain. *EMBO Rep*, 10, 1147-53.
- REYNOLDS, J. M., MARTINEZ, G. J., NALLAPARAJU, K. C., CHANG, S. H., WANG, Y. H. & DONG, C. 2012. Cutting Edge: Regulation of Intestinal Inflammation and Barrier Function by IL-17C. *J Immunol*, 189, 4226-30.
- REYNOLDS, S. D. & MALKINSON, A. M. 2010. Clara cell: progenitor for the bronchiolar epithelium. *Int J Biochem Cell Biol*, 42, 1-4.
- RICE, S. A., TAN, C. H., MIKKELSEN, P. J., KUNG, V., WOO, J., TAY, M., HAUSER, A., MCDOUGALD, D., WEBB, J. S. & KJELLEBERG, S. 2009. The biofilm life cycle and virulence of *Pseudomonas aeruginosa* are dependent on a filamentous prophage. *ISME J*, 3, 271-82.
- RICHARDS, T. J., KAMINSKI, N., BARIBAUD, F., FLAVIN, S., BRODMERKEL, C., HOROWITZ, D., LI, K., CHOI, J., VUGA, L. J., LINDELL, K. O., KLESEN, M., ZHANG, Y. & GIBSON, K. F. 2012. Peripheral blood proteins predict mortality in idiopathic pulmonary fibrosis. *Am J Respir Crit Care Med*, 185, 67-76.
- ROBINSON, D. S. 2009. Regulatory T cells and asthma. *Clin Exp Allergy*, 39, 1314-23.
- ROBINSON, J. 2008. Reactive oxygen species in phagocytic leukocytes. *Histochemistry and Cell Biology*, 130, 281-297.
- ROSS, M. H., KAYE, G. I. & PAWLINA, W. 2010. *Histology: A Text and Atlas*, Lippincott Williams and Wilkins.
- ROTH, M. 2008. Pathogenesis of COPD. Part III. Inflammation in COPD. *Int J Tuberc Lung Dis*, 12, 375-80.
- ROUM, J. H., BUHL, R., MCELVANEY, N. G., BOROK, Z. & CRYSTAL, R. G. 1993. Systemic deficiency of glutathione in cystic fibrosis. *J Appl Physiol*, 75, 2419-24.
- ROWE, S. M. & VERKMAN, A. S. 2013. Cystic fibrosis transmembrane regulator correctors and potentiators. *Cold Spring Harb Perspect Med*, 3.

- RUBIN, R. & STRAYER, D. S. 2008. Rubin's Pathology: Clinicopathologic foundations of Medicine, Lippincott Williams & Wilkins.
- RYU, J. H., KIM, C. H. & YOON, J. H. 2010. Innate immune responses of the airway epithelium. *Mol Cells*, 30, 173-83.
- SADIKOT, R. T., BLACKWELL, T. S., CHRISTMAN, J. W. & PRINCE, A. S. 2005. Pathogen-host interactions in *Pseudomonas aeruginosa* pneumonia. *Am J Respir Crit Care Med*, 171, 1209-23.
- SAGEL, S. D., WAGNER, B. D., ANTHONY, M. M., EMMETT, P. & ZEMANICK, E. T. 2012. Sputum biomarkers of inflammation and lung function decline in children with cystic fibrosis. *Am J Respir Crit Care Med*, 186, 857-65.
- SAHU, N. & AUGUST, A. 2009. ITK inhibitors in inflammation and immune-mediated disorders. *Curr Top Med Chem*, 9, 690-703.
- SALUNKHE, P., SMART, C. H., MORGAN, J. A., PANAGEA, S., WALSHAW, M. J., HART, C. A., GEFFERS, R., TUMMLER, B. & WINSTANLEY, C. 2005. A cystic fibrosis epidemic strain of *Pseudomonas aeruginosa* displays enhanced virulence and antimicrobial resistance. *J Bacteriol*, 187, 4908-20.
- SCHAIBLE, B., MCCLEAN, S. N., SELFRIDGE, A., BROQUET, A., ASEHNOUNE, K., TAYLOR, C. T. & SCHAFFER, K. 2013. Hypoxia Modulates Infection of Epithelial Cells by *Pseudomonas aeruginosa*. *PLoS One*, 8, e56491.
- SCHUSTER, M., LOSTROH, C. P., OGI, T. & GREENBERG, E. P. 2003. Identification, timing, and signal specificity of *Pseudomonas aeruginosa* quorum-controlled genes: a transcriptome analysis. *J Bacteriol*, 185, 2066-79.
- SEROHIJOS, A. W., HEGEDUS, T., ALEKSANDROV, A. A., HE, L., CUI, L., DOKHOLYAN, N. V. & RIORDAN, J. R. 2008. Phenylalanine-508 mediates a cytoplasmic-membrane domain contact in the CFTR 3D structure crucial to assembly and channel function. *Proc Natl Acad Sci U S A*, 105, 3256-61.
- SHAFIKHANI, S. H., MORALES, C. & ENGEL, J. 2008. The *Pseudomonas aeruginosa* type III secreted toxin ExoT is necessary and sufficient to induce apoptosis in epithelial cells. *Cell Microbiol*, 10, 994-1007.
- SHAH, A. S., BEN-SHAHAR, Y., MONINGER, T. O., KLINE, J. N. & WELSH, M. J. 2009. Motile cilia of human airway epithelia are chemosensory. *Science*, 325, 1131-4.
- SHAN, J., HUANG, J., LIAO, J., ROBERT, R. & HANRAHAN, J. W. 2011. Anion secretion by a model epithelium: more lessons from Calu-3. *Acta Physiol*, 202, 523-31.
- SHARMA, G., RAO, S., BANSAL, A., DANG, S., GUPTA, S. & GABRANI, R. 2013. *Pseudomonas aeruginosa* biofilm: Potential therapeutic targets. *Biologicals*, 2, 00133-4.
- SHEN, B. Q., FINKBEINER, W. E., WINE, J. J., MRSNY, R. J. & WIDDICOMBE, J. H. 1994. Calu-3: a human airway epithelial cell line that shows cAMP-dependent Cl<sup>-</sup> secretion. *Am J Physiol*, 266, L493-501.
- SHEN, K., SAYEED, S., ANTALIS, P., GLADITZ, J., AHMED, A., DICE, B., JANTO, B., DOPICO, R., KEEFE, R., HAYES, J., JOHNSON, S., YU, S., EHRLICH, N., JOCZ, J., KROPP, L., WONG, R., WADOWSKY, R. M., SLIFKIN, M., PRESTON, R. A., ERDOS, G., POST, J. C., EHRLICH, G. D. & HU, F. Z. 2006. Extensive genomic plasticity in *Pseudomonas aeruginosa* revealed by identification and distribution studies of novel genes among clinical isolates. *Infect Immun*, 74, 5272-83.
- SHEPPARD, D. N. & WELSH, M. J. 1999. Structure and function of the CFTR chloride channel. *Physiol Rev*, 79, S23-45.
- SHERWOOD, L. 2007. Human Physiology: From Cells to Systems, Seventh Edition, Yolanda Cossio.
- SIMON, R., PRIEFER, U. & PUHLER, A. 1983. A Broad Host Range Mobilization System for In Vivo Genetic Engineering: Transposon Mutagenesis in Gram Negative Bacteria. *Nat Biotech*, 1, 784-791.
- SIMONIN-LE JEUNE, K., LE JEUNE, A., JOUNEAU, S., BELLEGUIC, C., ROUX, P. F., JAGUIN, M., DIMANCHE-BOITRE, M. T., LECUREUR, V., LECLERCQ, C., DESRUES, B., BRINCHAULT, G., GANGNEUX, J. P. & MARTIN-CHOULY, C. 2013. Impaired functions of macrophage from cystic fibrosis patients: CD11b, TLR-5 decrease and sCD14, inflammatory cytokines increase. *PLoS One*, 8.
- SINGH, G., WU, B., BAEK, M. S., CAMARGO, A., NGUYEN, A., SLUSHER, N. A., SRINIVASAN, R., WIENER-KRONISH, J. P. & LYNCH, S. V. 2010. Secretion of

- Pseudomonas aeruginosa* type III cytotoxins is dependent on *Pseudomonas* quinolone signal concentration. *Microb Pathog*, 49, 196-203.
- SINGH, S. 2012. Innate immune recognition of *Pseudomonas aeruginosa*. PhD, University of Nottingham, UK.
- SKINDERSON, M. E., ZEUTHEN, L. H., BRIX, S., FINK, L. N., LAZENBY, J., WHITTALL, C., WILLIAMS, P., DIGGLE, S. P., FROEKIAER, H., COOLEY, M. & GIVSKOV, M. 2009. *Pseudomonas aeruginosa* quorum-sensing signal molecules interfere with dendritic cell-induced T-cell proliferation. *FEMS Immunol Med Microbiol*, 55, 335-45.
- SMITH, R. S., FEDYK, E. R., SPRINGER, T. A., MUKAIDA, N., IGLEWSKI, B. H. & PHIPPS, R. P. 2001. IL-8 production in human lung fibroblasts and epithelial cells activated by the *Pseudomonas* autoinducer N-3-oxododecanoyl homoserine lactone is transcriptionally regulated by NF-kappa B and activator protein-2. *J Immunol*, 167, 366-74.
- SOONG, G., PARKER, D., MAGARGEE, M. & PRINCE, A. S. 2008. The type III toxins of *Pseudomonas aeruginosa* disrupt epithelial barrier function. *J Bacteriol*, 190, 2814-21.
- SPORTY, J. L., HORALKOVA, L. & EHRHARDT, C. 2008. In vitro cell culture models for the assessment of pulmonary drug disposition. *Expert Opin Drug Metab Toxicol*, 4, 333-45.
- SRIRAMULU, D. D., LUNSDORF, H., LAM, J. S. & ROMLING, U. 2005. Microcolony formation: a novel biofilm model of *Pseudomonas aeruginosa* for the cystic fibrosis lung. *J Med Microbiol*, 54, 667-76.
- SRISKANDAN, S., FAULKNER, L. & HOPKINS, P. 2007. *Streptococcus pyogenes*: Insight into the function of the streptococcal superantigens. *Int J Biochem Cell Biol*, 39, 12-9.
- STEELE, M. P. & SCHWARTZ, D. A. 2013. Molecular mechanisms in progressive idiopathic pulmonary fibrosis. *Annu Rev Med*, 64, 265-76.
- STEVENS, D. A., MOSS, R. B., KURUP, V. P., KNUTSEN, A. P., GREENBERGER, P., JUDSON, M. A., DENNING, D. W., CRAMERI, R., BRODY, A. S., LIGHT, M., SKOV, M., MAISH, W. & MASTELLA, G. 2003. Allergic bronchopulmonary aspergillosis in cystic fibrosis--state of the art: Cystic Fibrosis Foundation Consensus Conference. *Clin Infect Dis*, 1, S225-64.
- STEWART, C. E., TORR, E. E., MOHD JAMILI, N. H., BOSQUILLON, C. & SAYERS, I. 2012. Evaluation of differentiated human bronchial epithelial cell culture systems for asthma research. *J Allergy*, 943982, 11.
- STOLTZ, D. A., MEYERHOLZ, D. K., PEZZULO, A. A., RAMACHANDRAN, S., ROGAN, M. P., DAVIS, G. J., HANFLAND, R. A., WOHLFORD-LENANE, C., DOHRN, C. L., BARTLETT, J. A., NELSON, G. A. T., CHANG, E. H., TAFT, P. J., LUDWIG, P. S., ESTIN, M., HORNICK, E. E., LAUNSPACH, J. L., SAMUEL, M., ROKHLINA, T., KARP, P. H., OSTEDGAARD, L. S., UC, A., STARNER, T. D., HORSWILL, A. R., BROGDEN, K. A., PRATHER, R. S., RICHTER, S. S., SHILYANSKY, J., MCCRAY, P. B., JR., ZABNER, J. & WELSH, M. J. 2010. Cystic fibrosis pigs develop lung disease and exhibit defective bacterial eradication at birth. *Sci Transl Med*, 2, 3000928.
- STOVER, C. K., PHAM, X. Q., ERWIN, A. L., MIZOGUCHI, S. D., WARRENER, P., HICKEY, M. J., BRINKMAN, F. S. L., HUFNAGLE, W. O., KOWALIK, D. J., LAGROU, M., GARBER, R. L., GOLTRY, L., TOLENTINO, E., WESTBROCK-WADMAN, S., YUAN, Y., BRODY, L. L., COULTER, S. N., FOLGER, K. R., KAS, A., LARBIG, K., LIM, R., SMITH, K., SPENCER, D., WONG, G. K. S., WU, Z., PAULSEN, I. T., REIZER, J., SAIER, M. H., HANCOCK, R. E. W., LORY, S. & OLSON, M. V. 2000. Complete genome sequence of *Pseudomonas aeruginosa* PAO1, an opportunistic pathogen. *Nature*, 406, 959-964.
- STOW, J. L., LOW, P. C., OFFENHAUSER, C. & SANGHERMANI, D. 2009. Cytokine secretion in macrophages and other cells: pathways and mediators. *Immunobiology*, 214, 601-12.
- STRATHMANN, M., GRIEBE, T. & FLEMMING, H. C. 2000. Artificial biofilm model--a useful tool for biofilm research. *Appl Microbiol Biotechnol*, 54, 231-7.
- STRIPP, B. R. & REYNOLDS, S. D. 2008. Maintenance and repair of the bronchiolar epithelium. *Proc Am Thorac Soc*, 5, 328-33.
- SUZUKI, T., CHOW, C. W. & DOWNEY, G. P. 2008. Role of innate immune cells and their products in lung immunopathology. *Int J Biochem Cell Biol*, 40, 1348-61.

- TAKEUCHI, O. & AKIRA, S. 2010. Pattern recognition receptors and inflammation. *Cell*, 140, 805-20.
- TAM, A., WADSWORTH, S., DORSCHIED, D., MAN, S. F. & SIN, D. D. 2011. The airway epithelium: more than just a structural barrier. *Ther Adv Respir Dis*, 5, 255-73.
- TAN, H. L., REGAMEY, N., BROWN, S., BUSH, A., LLOYD, C. M. & DAVIES, J. C. 2011. The Th17 pathway in cystic fibrosis lung disease. *Am J Respir Crit Care Med*, 184, 252-8.
- TAN, H. L. & ROSENTHAL, M. 2013. IL-17 in lung disease: friend or foe? *Thorax*, 68, 788-90.
- THANNICKAL, V. J., TOEWS, G. B., WHITE, E. S., LYNCH, J. P., 3RD & MARTINEZ, F. J. 2004. Mechanisms of pulmonary fibrosis. *Annu Rev Med*, 55, 395-417.
- TIELKER, D., HACKER, S., LORIS, R., STRATHMANN, M., WINGENDER, J., WILHELM, S., ROSENAU, F. & JAEGER, K. E. 2005. *Pseudomonas aeruginosa* lectin LecB is located in the outer membrane and is involved in biofilm formation. *Microbiology*, 151, 1313-23.
- TOWBIN, H., STAHELIN, T. & GORDON, J. 1979. Electrophoretic transfer of proteins from polyacrylamide gels to nitrocellulose sheets: procedure and some applications. *Proc Natl Acad Sci U S A*, 76, 4350-4.
- TRAN, C. S., ERAN, Y., RUCH, T. R., BRYANT, D. M., DATTA, A., BRAKEMAN, P., KIERBEL, A., WITTMANN, T., METZGER, R. J., MOSTOV, K. E. & ENGEL, J. N. 2014. Host cell polarity proteins participate in innate immunity to *Pseudomonas aeruginosa* infection. *Cell Host Microbe*, 15, 636-43.
- TRAPNELL, B. C. & WHITSETT, J. A. 2002. Gm-CSF regulates pulmonary surfactant homeostasis and alveolar macrophage-mediated innate host defense. *Annu Rev Physiol*, 64, 775-802.
- TRAVES, S. L. & DONNELLY, L. E. 2008. Th17 cells in airway diseases. *Curr Mol Med*, 8, 416-26.
- TSENG, J., DO, J., WIDDICOMBE, J. H. & MACHEN, T. E. 2006. Innate immune responses of human tracheal epithelium to *Pseudomonas aeruginosa* flagellin, TNF-alpha, and IL-1beta. *Am J Physiol Cell Physiol*, 290, 26.
- TSUCHIYA, M., KUMAR, P., BHATTACHARYYA, S., CHATTORAJ, S., SRIVASTAVA, M., POLLARD, H. B. & BISWAS, R. 2013. Differential regulation of inflammation by inflammatory mediators in cystic fibrosis lung epithelial cells. *J Interferon Cytokine Res*, 33, 121-9.
- TUDER, R. M. & PETRACHE, I. 2012. Pathogenesis of chronic obstructive pulmonary disease. *J Clin Invest*, 122, 2749-55.
- VAN DEN BLINK, B., WIJSENBEK, M. S. & HOOGSTEDEN, H. C. 2010. Serum biomarkers in idiopathic pulmonary fibrosis. *Pulm Pharmacol Ther*, 23, 515-20.
- VAN DER POLL, T. & OPAL, S. M. 2009. Pathogenesis, treatment, and prevention of pneumococcal pneumonia. *Lancet*, 374, 1543-56.
- VAN GENNIP, M., CHRISTENSEN, L. D., ALHEDE, M., PHIPPS, R., JENSEN, P. O., CHRISTOPHERSEN, L., PAMP, S. J., MOSER, C., MIKKELSEN, P. J., KOH, A. Y., TOLKER-NIELSEN, T., PIER, G. B., HOIBY, N., GIVSKOV, M. & BJARNSHOLT, T. 2009. Inactivation of the rhlA gene in *Pseudomonas aeruginosa* prevents rhamnolipid production, disabling the protection against polymorphonuclear leukocytes. *APMIS*, 117, 537-46.
- VAN OOSTERHOUT, A. J. & BLOKSMA, N. 2005. Regulatory T-lymphocytes in asthma. *Eur Respir J*, 26, 918-32.
- VAN WETERING, S., MANNESSE-LAZEROMS, S. P., VAN STERKENBURG, M. A. & HIEMSTRA, P. S. 2002. Neutrophil defensins stimulate the release of cytokines by airway epithelial cells: modulation by dexamethasone. *Inflamm Res*, 51, 8-15.
- VANCE, R. E., ISBERG, R. R. & PORTNOY, D. A. 2009. Patterns of pathogenesis: discrimination of pathogenic and nonpathogenic microbes by the innate immune system. *Cell Host Microbe*, 6, 10-21.
- VIJ, R. & NOTH, I. 2012. Peripheral blood biomarkers in idiopathic pulmonary fibrosis. *Transl Res*, 159, 218-27.
- VOISARD, C., BULL, C. T., KEEL, C., LAVILLE, J., MAURHOFER, M., SCHNIDER, U., DÉFAGO, G. & HAAS, D. 2007. Biocontrol of root diseases by *Pseudomonas fluorescens* CHA0: current concepts and experimental approaches. *Molecular Ecology of Rhizosphere Microorganisms*. Wiley-VCH Verlag GmbH.

- WAGNER, V. E. & IGLEWSKI, B. H. 2008. *P. aeruginosa* Biofilms in CF Infection. *Clin Rev Allergy Immunol*, 35, 124-34.
- WAN, H., WINTON, H. L., SOELLER, C., STEWART, G. A., THOMPSON, P. J., GRUENERT, D. C., CANNELL, M. B., GARROD, D. R. & ROBINSON, C. 2000. Tight junction properties of the immortalized human bronchial epithelial cell lines Calu-3 and 16HBE14o. *Eur Respir J*, 15, 1058-68.
- WANG, J., YU, B., TIAN, D. & NI, M. 2013. Rhamnolipid but not motility is associated with the initiation of biofilm seeding dispersal of *Pseudomonas aeruginosa* strain PA17. *J Biosci*, 38, 149-56.
- WANG, J. Y. 2013. The innate immune response in house dust mite-induced allergic inflammation. *Allergy Asthma Immunol Res*, 5, 68-74.
- WARDLAW, A. J. & HAMID, Q. A. 2002. *Textbook of Respiratory Cell and Molecular Biology* CRC Press.
- WATERS, C. M. & BASSLER, B. L. 2005. Quorum sensing: cell-to-cell communication in bacteria. *Annu Rev Cell Dev Biol*, 21, 319-46.
- WEI, Q. & MA, L. Z. 2013. Biofilm matrix and its regulation in *Pseudomonas aeruginosa*. *Int J Mol Sci*, 14, 20983-1005.
- WEICHHART, T. & SAEMANN, M. D. 2008. The PI3K/Akt/mTOR pathway in innate immune cells: emerging therapeutic applications. *Ann Rheum Dis*, 67, 098459.
- WEST, J. B. 2003. *Pulmonary Pathophysiology: The Essentials*, Lippincott Williams & Wilkins.
- WESTPHALEN, K., GUSAROVA, G. A., ISLAM, M. N., SUBRAMANIAN, M., COHEN, T. S., PRINCE, A. S. & BHATTACHARYA, J. 2014. Sessile alveolar macrophages communicate with alveolar epithelium to modulate immunity. *Nature*, 506, 503-6.
- WHITCHURCH, C. B., TOLKER-NIELSEN, T., RAGAS, P. C. & MATTICK, J. S. 2002. Extracellular DNA required for bacterial biofilm formation. *Science*, 295.
- WIDMAIER, E., RAFF, H. & STRANG, K. 2006. *Vander's Human Physiology: The Mechanisms of Body Function*, McGraw-Hill Higher Education.
- WILLIAMS, P. 2007. Quorum sensing, communication and cross-kingdom signalling in the bacterial world. *Microbiology*, 153, 3923-38.
- WILLIAMS, P. & CÁMARA, M. 2009. Quorum sensing and environmental adaptation in *Pseudomonas aeruginosa*: a tale of regulatory networks and multifunctional signal molecules. *Curr Opin Microbiol*, 12, 182-191.
- WILSON, M. S., MADALA, S. K., RAMALINGAM, T. R., GOCHUICO, B. R., ROSAS, I. O., CHEEVER, A. W. & WYNN, T. A. 2010. Bleomycin and IL-1beta-mediated pulmonary fibrosis is IL-17A dependent. *J Exp Med*, 207, 535-52.
- WINSOR, G. L., LAM, D. K., FLEMING, L., LO, R., WHITESIDE, M. D., YU, N. Y., HANCOCK, R. E. & BRINKMAN, F. S. 2011. *Pseudomonas* Genome Database: improved comparative analysis and population genomics capability for *Pseudomonas* genomes. *Nucleic Acids Res*, 39, 6.
- WINSTANLEY, C. & FOTHERGILL, J. L. 2009. The role of quorum sensing in chronic cystic fibrosis *Pseudomonas aeruginosa* infections. *FEMS Microbiol Lett*, 290, 1-9.
- WINSTANLEY, C., LANGILLE, M. G., FOTHERGILL, J. L., KUKAVICA-IBRULJ, I., PARADIS-BLEAU, C., SANSCHAGRIN, F., THOMSON, N. R., WINSOR, G. L., QUAIL, M. A., LENNARD, N., BIGNELL, A., CLARKE, L., SEEGER, K., SAUNDERS, D., HARRIS, D., PARKHILL, J., HANCOCK, R. E., BRINKMAN, F. S. & LEVESQUE, R. C. 2009. Newly introduced genomic prophage islands are critical determinants of in vivo competitiveness in the Liverpool Epidemic Strain of *Pseudomonas aeruginosa*. *Genome Res*, 19, 12-23.
- WRIGHT, J. R. 2005. Immunoregulatory functions of surfactant proteins. *Nat Rev Immunol*, 5, 58-68.
- WU, M. H., SMITH, S. L. & DOLAN, M. E. 2001. High efficiency electroporation of human umbilical cord blood CD34+ hematopoietic precursor cells. *Stem Cells*, 19, 492-9.
- WU, R., ZHAO, Y. & CHANG, M. 1997. Growth and differentiation of conducting airway epithelial cells in culture. *European Respiratory Journal*, 10, 2398-2403.
- WUYTS, W. A., THOMEER, M., DEMEDTS, M. G. & VERLEDEN, G. M. 2012. New idiopathic pulmonary fibrosis guidelines: some unresolved questions. *Am J Respir Crit Care Med*, 185, 588; author reply 588-9.
- WYNN, T. A. 2004. Fibrotic disease and the Th1/Th2 paradigm. *Nat Rev Immunol*, 4, 583-94.
- WYNN, T. A. 2011. Integrating mechanisms of pulmonary fibrosis. *J Exp Med*, 208, 1339-50.

- WYNN, T. A. & BARRON, L. 2010. Macrophages: master regulators of inflammation and fibrosis. *Semin Liver Dis*, 30, 245-57.
- WYNN, T. A., CHAWLA, A. & POLLARD, J. W. 2013. Macrophage biology in development, homeostasis and disease. *Nature*, 496, 445-455.
- XIAO, G., DEZIEL, E., HE, J., LEPINE, F., LESIC, B., CASTONGUAY, M. H., MILOT, S., TAMPAKAKI, A. P., STACHEL, S. E. & RAHME, L. G. 2006a. MvfR, a key *Pseudomonas aeruginosa* pathogenicity LTTR-class regulatory protein, has dual ligands. *Mol Microbiol*, 62, 1689-99.
- XIAO, G., HE, J. & RAHME, L. G. 2006b. Mutation analysis of the *Pseudomonas aeruginosa* mvfR and pqsABCDE gene promoters demonstrates complex quorum-sensing circuitry. *Microbiology*, 152, 1679-86.
- XIAO, L., LI, Z. H., HOU, X. M. & YU, R. J. 2003. Evaluation of interleukin-13 in the serum and bronchoalveolar lavage fluid of patients with idiopathic pulmonary fibrosis. *Zhonghua Jie He He Hu Xi Za Zhi*, 26, 686-8.
- XU, S. & POWERS, M. A. 2013. In vivo analysis of human nucleoporin repeat domain interactions. *Mol Biol Cell*, 24, 1222-31.
- XUE, J., SCHMIDT, S. V., SANDER, J., DRAFFEHN, A., KREBS, W., QUESTER, I., DE NARDO, D., GOHEL, T. D., EMDE, M., SCHMIDLEITHNER, L., GANESAN, H., NINO-CASTRO, A., MALLMANN, M. R., LABZIN, L., THEIS, H., KRAUT, M., BEYER, M., LATZ, E., FREEMAN, T. C., ULAS, T. & SCHULTZE, J. L. 2014. Transcriptome-based network analysis reveals a spectrum model of human macrophage activation. *Immunity*, 40, 274-88.
- YANG, L., NILSSON, M., GJERMENSEN, M., GIVSKOV, M. & TOLKER-NIELSEN, T. 2009. Pyoverdine and PQS mediated subpopulation interactions involved in *Pseudomonas aeruginosa* biofilm formation. *Mol Microbiol*, 74, 1380-92.
- YE, D., MA, I. & MA, T. Y. 2006. Molecular mechanism of tumor necrosis factor- $\alpha$  modulation of intestinal epithelial tight junction barrier. *Am J Physiol Gastrointest Liver Physiol*, 290, G496-504.
- ZHANG, Z., LOUBOUTIN, J. P., WEINER, D. J., GOLDBERG, J. B. & WILSON, J. M. 2005. Human airway epithelial cells sense *Pseudomonas aeruginosa* infection via recognition of flagellin by Toll-like receptor 5. *Infect Immun*, 73, 7151-60.
- ZHU, Y., CHIDEKEL, A. & SHAFFER, T. H. 2010. Cultured human airway epithelial cells (calu-3): a model of human respiratory function, structure, and inflammatory responses. *Crit Care Res Pract*, 394578, 27.